



A Study of the Molecular and Biological Characteristics of Ovine Interleukin-12

Sarah Jane Swinburne

B.Sc., B.Health.Sci. (Hons)

Transplantation Immunology Laboratory, the Queen Elizabeth Hospital, and
the Department of Medicine, the University of Adelaide.

Submitted in fulfilment of the degree Doctor of Philosophy at the University of
Adelaide, June 2000.

Table of Contents

	Page
List of Figures	9
Summary	11
Declaration	13
Acknowledgements	14
Presentations and Publications	16
Abbreviations	19
Chapter 1 - Literature Review	22
1.1. Introduction	22
1.1.1. Identification of Interleukin-12	22
1.1.2. Cells Producing IL-12	23
1.1.3. Cells Responding to IL-12	23
1.2. Molecular Characteristics of IL-12	23
1.2.1. The p35 Subunit	24
1.2.2. The p40 Subunit	27
1.2.3. Homodimers of the p40 Subunit	28
1.3. The IL-12 Receptor	30
1.4. The Th1 vs Th2 Paradigm	30
1.4.1. The Th1/Th2 Paradigm in Transplantation	31
1.4.2. The Influence of IL-12 on the Th1/Th2 Subsets	32
1.5. IL-12 in Allograft Rejection	35
1.6. Additional Effects of IL-12 that may Mediate Allograft Rejection	37
1.6.1. IL-12 Induction of T and NK Cell Cytotoxicity	37
1.6.2. IL-12 Induction of Allospecific Cytotoxic T Lymphocytes	39
1.6.3. Natural Killer Cell Induction of Cytotoxic T Lymphocytes	39

1.6.4. The Effect of IL-12 on Homing Molecules	40
1.6.5. IL-12 and the Maintenance of T Cell Anergy	41
1.7. Antagonism of IL-12 by IL-12 p40 in Alloimmune Responses	42
<hr/>	
Chapter 2 – Materials and Methods	45
2.1. Materials	45
2.1.1. Antibodies	45
2.1.2. Cell Lines (Cell Culture and Bacterial)	46
2.1.3. Cytokines	46
2.1.4. Radiochemicals	46
2.1.5. Flow Cytometry	46
2.1.6. General Chemicals	47
2.1.7. Tissue Culture Reagents	50
2.1.8. Molecular Biology Reagents	50
2.1.9. Film	51
2.1.10 Plasmid Vectors	51
2.2. Buffers and Solutions	52
2.2.1. Agarose Gel Electrophoresis	52
2.2.2. RNA Extraction	52
2.2.3. Cloning and Transfection	53
2.2.4. SDS-PAGE	55
2.2.5. Tissue Culture	58
2.2.6. Western Blotting	59
2.2.7. Flow Cytometry	61
2.2.8. Isolation of Genomic DNA	61
2.3. Methods	62
2.3.1. Total RNA Extraction	62
2.3.2. Spectrophotometric Nucleic Acid Quantitation	63
2.3.3. Reverse Transcription	63
2.3.4. Polymerase Chain Reaction (PCR)	64

2.3.5. KlenTaq Polymerase PCR for cDNA Cloning	65
2.3.6. Agarose Gel Electrophoresis	65
2.3.7. Purification of PCR and Restriction Products	66
2.3.8. Ligation into Cloning and Expression Vectors	67
2.3.9. Restriction Digestion of DNA	68
2.3.10. Manufacture of Competent <i>E. coli</i> TG1 α	69
2.3.11. Transformation of Competent <i>E. coli</i> TG1 α	69
2.3.12. Isolation and Characterisation of Recombinant Plasmids by PCR and Alkaline Lysis (Mini-Prep)	70
2.3.13. Sequencing of Plasmid cDNA Inserts	72
2.3.14. Transfection of the CHO Cell Line with Human and Ovine p35 and p40 Plasmids	73
2.3.15. ³⁵ S Metabolic Labelling and Immunoprecipitation of IL-12 Proteins	73
2.3.16. Sodium Dodecyl Sulphate-Polyacrylamide Gel Electrophoresis (SDS-PAGE)	74
2.3.17. Isolation of Human and Ovine Peripheral Blood Mononuclear Cells	75
2.3.18. Human and Ovine Activated Mononuclear Cell IL-12 Proliferation Assays	76
Chapter 3 - Characterisation of Ovine Interleukin-12	78
Introduction	78
Aims	79
Cloning Protocol	79
Human and Ovine p35	79
Human and Ovine p40	80
3.1. Results	81
3.1.1. Ovine IL-12 p35 cDNA Sequence Analysis	81
3.1.2. Ovine IL-12 p40 cDNA Sequence Analysis	81
3.1.3. Immunoprecipitation of Ovine and Chimaeric IL-12 Proteins	82

3.1.4. Biological Activity of Ovine and Chimaeric Interleukin-12 Heterodimers	83
Discussion	85
Chapter 4 – The Antagonistic Activity of IL-12 p40 in an Ovine <i>In Vitro</i> Model of the Alloimmune Response	90
4.1. Introduction	90
4.1.1. Dendritic Cell Production of IL-12	92
4.1.2. Dendritic Cells are able to Prime Naïve T Cells for IFN- γ Production	92
4.2. Allograft Rejection and Current Immunosuppressive Therapies	93
4.3. Microchimaerism in Transplantation	94
Aims	97
Cloning Protocol	98
Generation of an Ovine IL-12 p40 Expressing Adenoviral Vector	98
4.4. Methods	99
4.4.1. Generation of Dendritic Cells from Human Monocytes	99
4.4.2. Isolation of Ovine Afferent Lymph Dendritic Cells	99
4.4.3. Cell Surface Marker Analysis Using Flow Cytometry	100
4.4.4. LipofectAMINE [™] -Mediated Adenoviral Transfection of Dendritic Cells	101
4.4.5. Infection of Ovine Fibroblasts with Adenoviral Particles	101
4.4.6. Assessment of Adenoviral Transfection Efficiency by Flow Cytometry	102
4.4.7. Dendritic Cell-Mixed Lymphocyte Reaction (DC-MLR)	102
4.4.8. Ovine Two-Way Mixed Lymphocyte Reaction	103
4.5. Results	103
4.5.1. Phenotype of Ovine Dendritic Cells	103

4.5.2. Immunoprecipitation of the IL-12 p40 Subunit Protein	104
4.5.3. Ovine IL-12 Proliferation Assay with Adenoviral Fibroblast Conditioned Medium	105
4.5.4. Adenoviral Transfection Efficiency of Human and Ovine DCs as Assessed by Flow Cytometry	106
4.5.5. Ovine DC-MLR with Adenovirus-Transfected DCs	107
4.5.6. Ovine DC-MLR with Ovine Adult Fibroblast IL-12 p40 Conditioned Medium	107
4.5.7. Ovine Two-Way MLR with Ovine Adult Fibroblast IL-12 p40 Conditioned Medium	108
4.5.8. Human IL-12 Proliferation Assay with Ovine Adult Fibroblast IL-12 p40 Conditioned Medium	108
4.5.9. Phenotypic Analysis of Human Dendritic Cells	109
4.5.10. Human DC-MLR with IL-12 p40 Adenovirus-Transfected DCs	110
Discussion	110
<hr/>	
Chapter 5 - Characterisation of an IL-12 p35 Subunit mRNA Splice Variant	119
5.1. Introduction	119
5.2. Intron Retention in mRNA Transcripts	120
Definitions	123
Aims	124
Cloning Protocol	124
pRc/CMV Cloning	125
pEGFP-N1 Cloning	125
5.3. Methods	126
5.3.1. Preparation of Genomic DNA	126
5.3.2. Analysis of Enhanced Green Fluorescent Protein in Transfected CHO Cells	126
5.3.3. Western Blot of EGFP-Fusion Protein Transfected CHO Cells	127

5.4. Results	128
5.4.1. Identification of a p35 mRNA Variant	128
5.4.2. Exclusion of Genomic DNA	129
5.4.3. Translation of Human and Ovine Variant p35 Nucleotide Sequence	129
5.4.4. Sequence Similarity of p35 Introns	131
5.4.5. Expression of the p35 Variant mRNA Transcript in Normal Human Peripheral Blood Mononuclear Cells	133
5.4.6. Functional Aspects of the Intron Containing IL-12 p35 Variant – Formation of Heterodimers with the p40 Subunit	133
5.4.7. Immunoprecipitation of Human and Ovine Variant Proteins from CHO Cell Transfectants	134
5.4.8. Detection of Properties Attributable to the Variant p35 Protein	134
5.4.9. Immunoprecipitation of the Truncated Variant p35 Protein Alone and in Combination with p40	135
5.4.10. Western Blot Assessment of Standard and Truncated Variant p35 EGFP-Fusion Protein Expression	135
5.4.11. EGFP-Fusion Protein Cellular Localisation	136
5.4.12. Biological Function of EGFP-Fusion/p40 Proteins	137
5.4.13. Heterodimerisation of p35 EGFP-Fusion Proteins with p40 as Assessed by Immunoprecipitation	138
Discussion	138
Chapter 6 - Final Discussion	152
Appendix I - Pre-mRNA Splicing	158
The Splicing Reaction	158
Protein Splicing Factors	161
Exon Definition in Pre-mRNA Splicing	162
Appendix II - Cloning Primers	165

Appendix III - General Purpose Primers	166
Appendix IV - PCR Conditions	167
Appendix V - Cloning and Expression Vectors	168
Appendix VI - Plasmids used in this Thesis	170
Bibliography	172

Amendments

List of Figures

Chapter 1

Figure 1.1. Disulphide Bonds of IL-12

Figure 1.2. Generation of CD4⁺ Th1 and Th2 T Cells

Figure 1.3. The Involvement of IL-12 in Allograft Rejection

Chapter 3

Figure 3.1. Cloning Diagram for Human and Ovine p35

Figure 3.2. Cloning Diagram for Human and Ovine p40

Figure 3.3. Ovine p35 Nucleotide and Protein Sequence

Figure 3.4. Ovine p40 Nucleotide and Protein Sequence

Figure 3.5. Autoradiograph of Ovine, Human and Chimaeric Proteins

Figure 3.6. Ovine Con A Assay with IL-12 Conditioned Medium and Antibody

Figure 3.7. Human PHA Assay with IL-12 Conditioned Medium and Antibody

Chapter 4

Figure 4.1. Transmission and Scanning Electron Micrographs of Ovine DCs

Figure 4.2. Generation of a Replication-Deficient Adenovirus Expressing Ovine
IL-12 p40

Figure 4.3. Phenotypic Analysis of Ovine DCs by Flow Cytometry

Figure 4.4. Autoradiograph of Ovine IL-12 p40 Proteins from Ovine and Human
DCs Transfected with Adenovirus

Figure 4.5. Inhibition of the Ovine Con A Assay by Ovine IL-12 p40

Figure 4.6. Phenotypic Analysis of Human DCs by Flow Cytometry

Figure 4.7. Adenoviral Transfection Efficiency of Human DCs

Figure 4.8. Ovine DC-MLR with Adenovirus-Transfected DCs and IL-12 p40
Fibroblast Conditioned Medium

Figure 4.9. Ovine Two-Way MLR with IL-12 p40 Fibroblast Conditioned Medium

Figure 4.10. Inhibition of the Human PHA Assay by Ovine IL-12 p40

Figure 4.11. Human DC-MLR with Adenovirus-Transfected DCs

Chapter 5

Figure 5.1. Overview of the Pre-mRNA Splicing Reaction

Figure 5.2. Cloning Diagram for Truncated Variant p35 in pRc/CMV

Figure 5.3. Cloning Diagram for Standard and Truncated Variant p35 in pEGFP-N1

Figure 5.4. Western Blot Assembly using a Mini PROTEAN[®] Apparatus

Figure 5.5. Alignment of Human and Ovine Variant p35 Nucleotide Sequences

Figure 5.6. Amplification of Genomic DNA using an Intron 4-Specific Primer

Figure 5.7. Alignment of Human Standard and Variant p35 Amino Acid Sequences

Figure 5.8. Alignment of Ovine Standard and Variant p35 Amino Acid Sequences

Figure 5.9. Prediction of p35 Intron 4 Polypyrimidine Tract and Branch Site Sequences

Figure 5.10. Amplification of Variant p35 from Human cDNA

Figure 5.11. Immunoprecipitation of Variant p35/p40 Proteins from CHO Cell Transfectants

Figure 5.12. Human PHA Assay with Truncated Variant p35/p40 Conditioned Medium

Figure 5.13. Autoradiograph of Truncated Variant p35/p40 Proteins from CHO Cell Transfectants

Figure 5.14. Western Blot of p35 EGFP-Fusion Proteins

Figure 5.15. Cellular Localisation of p35 EGFP-Fusion Proteins

Figure 5.16. Human PHA Assay with p35 EGFP-Fusion/p40 Conditioned Medium

Figure 5.17. Autoradiograph of p35 EGFP-Fusion/p40 Proteins from CHO Cell Transfectants

Appendix I

Figure A.1. Assembly of the Spliceosome

Figure A.2. U5 snRNA Loop Interaction with Exonic Sequence

Figure A.3. Exon Definition Model of Splice Site Selection

Summary

Interleukin-12 (IL-12) is a heterodimeric cytokine composed of two disulphide-linked subunits, p35 and p40, which form biologically active p70. IL-12 is able to induce IFN- γ production from T and NK cells, and promote the proliferation of mitogen-activated T cells.

Chapter 3 describes the characterisation of ovine IL-12. The ovine p35 cDNA was cloned and sequenced, and the biological activity of the ovine heterodimer was assessed. Ovine p35 and p40 showed conservation of protein motifs, including the cysteine residues in the mature proteins. The ovine IL-12 heterodimer was detected as two proteins of approximately 60 and 66 kDa, suggested to result from differential glycosylation. Ovine IL-12 enhanced the proliferation of activated mononuclear cells, demonstrating biological activity. Thus, the ovine IL-12 heterodimer has similar sequence features and biological properties to those described for human and murine IL-12 p70.

The IL-12 p40 subunit protein can inhibit IL-12 heterodimer activity. Modification of dendritic cells (DCs) with IL-12 p40 may provide a useful vehicle for delivery of this immunomodulatory protein to sites of antigen presentation, and allograft acceptance may be induced by inhibition of IL-12.

Chapter 4 describes experiments in which ovine and human DCs were characterised, revealing high level MHC Class I and II expression, and the characteristic DC morphology. The ovine IL-12 p40 subunit was shown to inhibit ovine and human IL-12-specific activity. However, ovine IL-12 p40 transfected DCs and IL-12 p40 conditioned medium, were unable to inhibit proliferation of ovine or

human dendritic cell-mixed lymphocyte reactions (MLR), or the ovine two-way MLR.

Chapter 5 describes the identification and characterisation of an IL-12 p35 mRNA variant shown to result from the retention of intron 4. Translation of the protein results in premature protein truncation due to an in-frame STOP codon. The ability of this transcript to be translated, and the localisation of standard and truncated variant p35 EGFP (enhanced green fluorescent protein)-fusion proteins in CHO cell transfectants was determined. Standard and variant EGFP-fusion proteins showed a cytoplasmic location. The variant p35 protein was assessed for its ability to form intermolecular disulphide bonds with the IL-12 p40 subunit, as the formation of this heterodimer may effectively antagonise normal IL-12 heterodimer. Competition for the IL-12 receptor or transduction of a negative regulatory signal may have provided an antagonist for use in the prevention of allograft rejection. Neither disulphide bonding of the truncated variant protein to p40 or IL-12 p70-like activity could be demonstrated.

Declaration

This thesis contains no material which has been previously been accepted for the award of any other degree or diploma in any university and, to the best of my knowledge and belief, this thesis contains no material previously published or written by another person, except where due reference has been made in the text.

I consent for this thesis to be made available for photocopying and loan in the University Library.

Sarah Swinburne,
June 2000.

Acknowledgements

The production of a body of work such as that which forms the basis of a Ph.D. is dependent on the individual student for completion of experimental work and the final written thesis. However, neither is possible without the contributions of others whether this be in the form of technical, literary or emotional support.

Firstly I would like to thank my supervisors, Ravi and Graeme, for allowing me to work in their laboratory and learn the skills I have used to perform the work presented in this thesis. To Ravi for his help and advice in the general day to day running of the project, and for the time that he has contributed to writing papers and reading drafts of the thesis. To Graeme for his incisive thoughts and contributions to both thesis drafts and papers.

Thanks to all of the gang in the laboratory, past and present, for their help and patience over the last 3 years - Julie, Svjetlana, Antiopi, Toby, Warwick, Peter and Guy.

To 'The Ant' who has converted me to the fine art of coffee drinking! For sharing my passion for drinking good wine and eating out, and most importantly for her friendship and support.

To Julie for helping me wherever she was able, for being a good listener, as well as being easy to talk to. Also, for her excellent technical skills. To her other half Adrian who helped me with the computer equipment on which the thesis was written.

To Svjetlana for her cheerful and caring nature, for providing help around the lab and for the unexpected moments of mischievous behaviour! In addition, for her technical expertise with the adenoviral vectors.

To Toby for his cheerful and enthusiastic nature! For his blood taking skills, which I have made use of on more than one occasion! For helping me with the dendritic cell work by allowing me to use dendritic cells from his sheep and for providing pictures which I have included in the thesis.

To Tina for her most entertaining and comfortable conversation (which I have spent many hours appreciating!), as well as her concern for my well being. For listening to the problems both scientific and otherwise and for the time that she has given to reading drafts of my thesis. I am most grateful – the favour shall be returned.

To Lor-Wai who has provided much entertaining conversation over good wine and coffee! For her most valuable contributions to the thesis by proof-reading and providing critical scientific comment, and for giving up her free time to do so. Hard to put a value on such help – thanks.

To Damian for his help whenever it was requested, for uncountable useful scientific discussions, and for his good nature and sense of humour.

To Terence G, a man of many skills who has mastered the art of coffee drinking, dining and providing great conversation - all at the same time! A major contribution to the maintenance of my sanity!

To my good friend Ruth who has listened to many hours on the topic of my Ph.D. without complaint! Much appreciated. Also, for using her power and influence in the TQEH Pharmacy Department to ensure service with a smile! Particularly for introducing me to the infamous John who has been instrumental in providing the lab with ordered items and going out of his way to help with that task.

To my family who have endured my conversations and discussions about a project, it's problems and solutions (including all of the scientific jargon!). For tolerating the paper and debris around the computer and in my room while the thesis was being written, and for providing love and support - my heartfelt thanks.

To David Turner who gave up some of his own time to read a draft of the thesis and provide critical opinion. Very much appreciated.

Thanks to the animal house staff, Ken, Adrian, Bronwyn and Carlien, for taking blood from the sheep and looking after them. Thanks also to the sheep themselves (in no particular order), Q, R, S, T, O, M and N.



To all of the staff and students in other TQEH departments – the Haematologists of the 6th and 4th floor, the Surgery gang on the 2nd floor, Gwenda and Natalie of the Research Secretariat.

To the people who have contributed to the scientific side of things - Sonja Klebe (who has also provided general help and support!) and Peter Kolesik.

Thanks also to the TQEH Research Foundation who have provided the post-graduate scholarship that has supported me financially for the past 3 years.

And finally, special thanks to all of the CHO cells and *E. coli* bacteria who gave their lives selflessly in the pursuit of scientific discovery!

Presentations and Publications

Presentations

The Queen Elizabeth Hospital Research Day, Adelaide, 1998.

“Biological Activity of Human and Ovine Recombinant Interleukin-12 and the Identification of a Variant IL-12 p35 Subunit”

SWINBURNE, SJ, Krishnan, R and Russ, GR.

Australian Society for Medical Research, Hobart, 1998.

“Human Interleukin-12 is Biologically Active on Ovine Con A-Stimulated Mononuclear Cells”

SWINBURNE, SJ, Krishnan, R and Russ, GR.

Australasian Society of Immunology, Melbourne, 1998.

“Human Interleukin-12 is Biologically Active on Ovine Con A-Stimulated Mononuclear Cells”

SWINBURNE, SJ, Krishnan, R and Russ, GR.

Transplantation Society of Australia and New Zealand, Canberra, 1999.

“Human Interleukin-12 is Biologically Active on Ovine Con A-Stimulated Mononuclear Cells”

SWINBURNE, SJ, Krishnan, R and Russ, GR.

The Queen Elizabeth Hospital Research Day, Adelaide, 1999.

“Characterisation of an Interleukin-12 p35 mRNA Variant”

SWINBURNE, SJ, Krishnan, R and Russ, GR.

XVIII International Congress of the Transplantation Society, Rome, 2000.

“Dendritic Cell Th2 Cytokine Gene Therapy in Sheep”

COATES, T, Krishnan, R, Swinburne, SJ, Klebe, S, Kanchanabat, B, Kireta, S, Russ, GR.

6th International Symposium on Dendritic Cells, Port Douglas, 2000.

“Dendritic Cell Th2 Cytokine Gene Therapy in Sheep”

COATES, T, Krishnan, R, Swinburne, SJ, Klebe, S, Kanchanabat, B, Kireta, S, Russ, GR.

Transplantation Society of Australia and New Zealand, Canberra, 2000.

“Dendritic Cell Th2 Cytokine Gene Therapy in Sheep”

COATES, T, Krishnan, R, Swinburne, SJ, Klebe, S, Kanchanabat, B, Kireta, S, Russ, GR.

Inflammation, Infection and Immunology Seminar Series, Flinders Medical Centre, Adelaide, 2000.

“Characterisation of Ovine Interleukin-12 - Using IL-12 p40 for Dendritic Cell Gene Therapy”

SWINBURNE, SJ, Russ, GR and Krishnan, R.

Department of Ophthalmology Seminar Series, Flinders Medical Centre, Adelaide, 2000.

“Characterisation of Ovine Interleukin-12 - Using IL-12 p40 for Dendritic Cell Gene Therapy”

SWINBURNE, SJ, Russ, GR and Krishnan, R.

Prizes

Winner of Higher Degrees Basic Science Category

The Queen Elizabeth Hospital Research Day, 1998

Winner of a Young Investigator Award

Australian Society for Medical Research, Hobart, 1998.

Publications

“Human Interleukin-12 is Biologically Active on Ovine Con A-Stimulated Mononuclear Cells”

SWINBURNE, SJ, Krishnan, R and Russ, GR.

Abstract published in Immunology and Cell Biology, 1998.

“Ovine Interleukin-12 has Biological Activity on Ovine and Human Activated Peripheral Blood Mononuclear Cells”

SWINBURNE, SJ, Russ, GR and Krishnan, R.

Submitted to ‘Cytokine’ and accepted for Publication, January 2000.

“Gene Therapy using Ovine Afferent Lymph Dendritic Cells Modified by Th2 Cytokine Antagonists for the Prevention of Allograft Rejection”

COATES, PTH, Swinburne, SJ, Kireta, S, Klebe, S, Kanchanabat, B, Krishnan, R and Russ, GR.

Manuscript in Preparation.

“Characterisation of an Interleukin-12 p35 Subunit mRNA Variant”

SWINBURNE, SJ, Russ, GR and Krishnan, R.

Manuscript in Preparation.

Abbreviations

aa	Amino Acid
Adv	Adenovirus
APC	Antigen Presenting Cell
ATP	Adenosine Triphosphate
bGH	Bovine Growth Hormone
bp	Base Pair
cDNA	Complementary DNA
CHO	Chinese Hamster Ovary
Ci	Curie
Con A	Concanavalin A
CPM	Counts Per Minute
CTL	Cytotoxic T Lymphocyte
DC	Dendritic Cell
DNA	Deoxyribonucleic Acid
E.	Escherichia
EBV	Epstein-Barr Virus
EGFP	Enhanced Green Fluorescent Protein
FACS	Fluorescence Activated Cell Scan
FCS	Foetal Calf Serum
FITC	Fluorescein Isothiocyanate
gDNA	Genomic DNA
GFP	Green Fluorescent Protein
GM-CSF	Granulocyte Macrophage-Colony Stimulating Factor
hnRNP	Heterogeneous Nuclear Ribonucleoprotein
H ₂ O	Water
Hu	Human
IFN- γ	Interferon- γ
IL	Interleukin
IU	International Units
kDa	Kilodaltons

L	Ligand
LB	Luria Broth
LPS	Lipopolysaccharide
M	Molar
mA	Milliamp
MHC	Major Histocompatibility Complex
min	Minute
μl	Microlitre
ml	Millilitre
MLR	Mixed Lymphocyte Reaction
mm	Millimetre
MOI	Multiplicity Of Infection
mRNA	Messenger RNA
NF-κB	Nuclear Factor κB
NK	Natural Killer
nm	Nanometre
OD	Optical Density
O/N	Overnight
Ov	Ovine
PBMNC	Peripheral Blood Mononuclear Cells
PCR	Polymerase Chain Reaction
PHA	Phytohaemagglutinin
r	Recombinant
RNA	Ribonucleic Acid
rpm	Revolutions Per Minute
RT	Reverse Transcription
SDS-PAGE	Sodium Dodecyl Sulphate-Polyacrylamide Gel Electrophoresis
sec	Second
S/N	Supernatant
snRNA	Small Nuclear Ribonucleic Acid
snRNP	Small Nuclear Ribonucleoprotein
SR	Serine/Arginine
TCR	T Cell Receptor

TGF- β	Transforming Growth Factor β
TNF- α	Tumour Necrosis Factor α
U	Units
UV	Ultra Violet
vs	Versus

The background of the page is a repeating pattern of stylized, light-colored figures. Each figure is enclosed within a circular frame and appears to be a simplified representation of a person or a character, possibly from a historical or literary context. The figures are arranged in a grid-like pattern across the entire page.

Chapter 1

Literature Review



Chapter 1

Literature Review

1.1. Introduction

1.1.1. Identification of Interleukin-12

IL-12 was initially isolated from the supernatant of the Epstein-Barr Virus (EBV)-transformed cell line, RPMI 8866, and designated Natural Killer Cell Stimulatory Factor (NKSF, (1)). IL-12 was also independently isolated by another group and called Cytotoxic Lymphocyte Maturation Factor (CLMF, (2)). The biological activities of IL-12 include the ability to induce interferon- γ (IFN- γ) production from freshly isolated peripheral blood lymphocytes and synergise with IL-2 in this activity; augment the cytotoxic capabilities of natural killer (NK) cells; and enhance the response of T cells to mitogenic lectins and phorbol diesters (1). The biological activities mediated by this cytokine have been reported at picomolar concentrations (1-3).

The biologically active form of IL-12 was shown to be a heterodimer of 70 kDa. Under reducing conditions two new polypeptides of 35 and 40 kDa were apparent, suggesting that IL-12 was composed of two disulphide-linked subunits (1). The cysteine residues involved in the disulphide linkage between the two subunits of the human heterodimer have been identified and are shown in **Figure 1.1**. A single intermolecular bond exists between cysteine 74 in p35 and cysteine 177 in p40. The remaining cysteine residues, except for cysteine 252 of p40, which is modified with thioglycolic acid, or cysteine, participate in intramolecular disulphide bonding

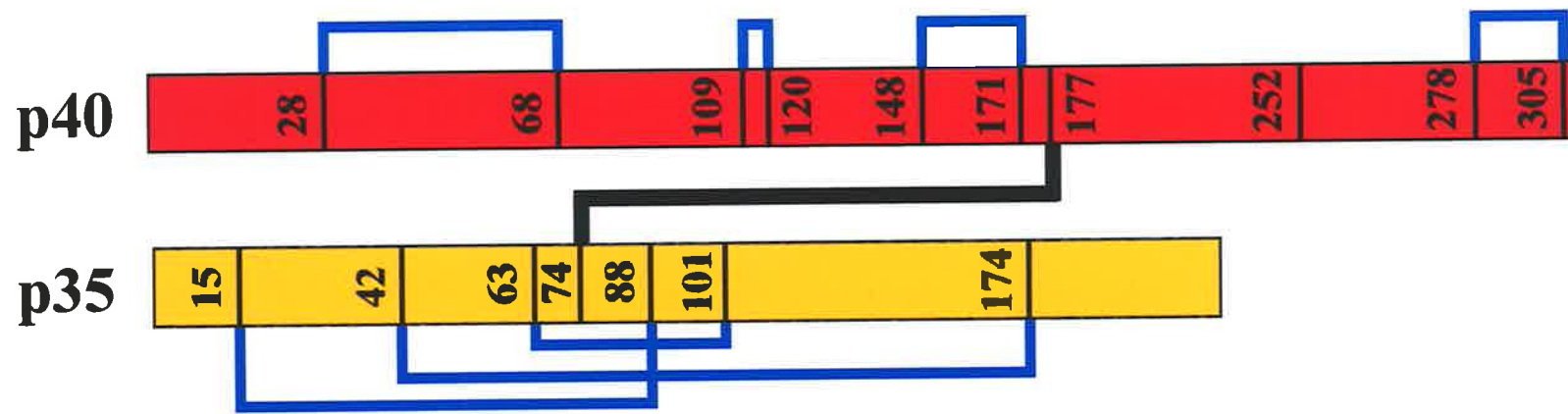


Figure 1.1. Disulphide bonds of IL-12. Positions of the cysteine residues involved in intramolecular disulphide bonds are marked in each subunit and refer to the position in the mature protein. The intermolecular disulphide bond between cysteine 74 (p35) and 177 (p40) is represented by the black line between the two subunits. Diagram modified from Tangarone, 1995 (4).

within the mature protein and contribute to the unique conformation of each subunit (4). Formation of the biologically active heterodimer required both subunits to be expressed within a single cell. Culture supernatant from cells transfected with either subunit alone, or mixing of culture supernatants from p35 and p40 single transfectants did not reconstitute p70-like biological activity (5).

1.1.2. Cells Producing IL-12

A wide range of cell types are capable of IL-12 production. These include monocytes and macrophages (6-8), keratinocytes (9), neutrophils (10) and Kupffer cells (11). In addition, dendritic cells have also been shown to produce the IL-12 p70 heterodimer (12).

1.1.3. Cells Responding to IL-12

IL-12 induces the production of IFN- γ from T cells and NK cells as well as enhancing NK cytotoxic activity (1, 13, 14). The response of mitogen-activated CD4⁺ and CD8⁺ T cells, and IL-2-activated CD56⁺ NK cells, to IL-12 correlates with upregulation of the IL-12 receptor on these cells (15). More recently, IL-12 receptors have also been identified on murine dendritic cells. These cells respond to IL-12 by production of this same cytokine and upregulation of MHC (major histocompatibility complex) Class II expression (16).

1.2. Molecular Characteristics of IL-12

As described in 1.1.1, biologically active IL-12 p70 is heterodimeric in structure, and co-expression of both genes within a single cell is required to generate functional p70 (5, 17, 18). Formation of the IL-12 heterodimer is further complicated

by the independent genetic control required for expression of each subunit. The genes for p35 and p40 are present on separate chromosomes (p35 – human, chromosome 3p12-3q13.2 (19); mouse, chromosome 6C (20) or chromosome 3 (21, 22); p40 – human, chromosome 5q31-q33 (19); mouse, chromosome 11 (20-22)). The regulation of each gene is discussed below.

1.2.1. The p35 Subunit

Expression of p35 mRNA was initially described as constitutive, as p35 mRNA could be detected in both primary cells and cell lines derived from a range of tissue origins (6, 23). p35 mRNA could also be detected using Northern blot analysis in tissue of non-haematopoietic lineage, including lung and brain, although the physiological relevance of this observation was not determined (18). However, the inducible nature of p35 mRNA expression has been demonstrated in unstimulated purified human monocytes. The monocytes required priming with IFN- γ followed by treatment with lipopolysaccharide (LPS) as p35 mRNA was not detected in unstimulated cells. This demonstrated that for monocytes at least, p35 mRNA expression was not constitutive (8, 24).

Expression of p35 mRNA appears to be the limiting factor for p70 production. Whereas p40 protein is generally overexpressed (2, 6, 24), increases in p70 production can still be detected at maximum levels of p40 production, implying that p35 expression is limiting for bioactive p70 production (8, 24).

Analysis of the p35 gene sequence in the mouse predicted multiple transcription start sites for p35 (20, 22), and potential regulatory sites within the mouse promoter region included nuclear factor (NF)- κ B (20, 22) and AP1 (22) transcription factor binding sites. Subsequently, transcripts with alternative

transcription start sites have been identified for both human and mouse p35 (25, 26). The human p35 cDNA initially identified for NKSF (17) and CLMF (5) vary in sequence at the 5' end by 41 bp. In monocytes a p35 mRNA transcript differing from the mRNA transcript identified in lymphoblastoid cells was isolated (25). This transcript began downstream of the TATA box starting from the second methionine (as it appeared in the lymphoblastoid cDNA), and lacked the first 34 aa encoded by the lymphoblastoid transcript. This mRNA species was only present in the monocytes after IFN- γ priming and LPS treatment, but not after LPS treatment alone (25).

Alternative p35 transcripts have also been identified in mice from the A20 B lymphoma cell line and bone marrow-derived dendritic cells, with four different p35 mRNA transcripts isolated (labelled I through to IV) (26). Transcripts II and IV were present in unstimulated cells and translation resulted in premature truncation of the protein. Transcripts I and III were increased upon LPS stimulation of the cells and translation resulted in the generation of the complete p35 protein (with the type III transcript encoding an additional 21 amino acids). Thus, functional p35 protein was dependent on the type of mRNA isoform transcribed and the subsequent ability to translate the mRNA transcript into functional protein. Stimulation of the cell, with LPS for instance, overcame the negative translational control by changing the transcription initiation site (26). As such, IL-12 p35 mRNA expression is extremely complex and detection of a p35 transcript does not necessarily imply that functional p35 protein will be generated.

The p35 protein has a signal peptide sequence at the N-terminal end, which suggests that this protein is secreted. However, minimal p35 protein has been detected in the supernatant of peripheral blood mononuclear cells (PBMNC), cell

lines (6) or p35 plasmid transfected cells (17). Recently, Murphy *et al* suggested that cleavage of the p35 signal peptide required two separate reactions and was processed via an alternative pathway to the signal peptide of p40. The first cleavage of the p35 signal peptide occurred within the endoplasmic reticulum, with the remainder of the signal peptide removed in a second reaction thought to involve a metalloprotease (27). Efficient secretion of the p35 protein was also dependent on glycosylation, as inhibition of this process resulted in minimal p35 protein secretion (27).

It has been suggested that the p35 subunit may form intermolecular disulphide bonds with other p35 molecules or with other unrelated proteins (17). The basis for this suggestion was the observation that in cells transfected with p35 alone two bands, at 30 and 33 kDa, could be detected under reducing conditions. However, under non-reducing conditions no distinct band for p35 was detected. This was suggested to be due to the formation of p35 homodimers or multimers, or due to the interaction of p35 with another molecule unrelated to IL-12 (17). Recently, an IL-12 p40-like protein induced by the infection of B lymphocytes with EBV was identified, and this protein showed 27% similarity to the human p40 subunit amino acid sequence (28). The similarity to p40 suggested that EBI3 (for Epstein-Barr Virus-induced gene 3) might be capable of interacting with IL-12 p35 (28). Further work by the same group confirmed that p35 was capable of associating with EBI3 via a non-covalent interaction, and was not mediated by disulphide bonding. Unlike the p35/p40 interaction, formation of this EBI3/p35 heterodimer occurred when culture supernatants from single transfectants were mixed (29). Co-expression of EBI3 and p35 within a cell line lead to enhanced secretion of both proteins, and the p35/EBI3 complex was shown to exist in normal tissues as it could be immunoprecipitated from full term human placental trophoblasts. Preliminary experiments suggested that

the p35/EBI3 heterodimer could not compete with IL-12 for the IL-12 receptor and a functionally distinct receptor may exist. The existence of an alternative partner for p35 (that is other than p40) is unusual, and was suggested by these authors to be “exceptional” (29).

1.2.2. The p40 Subunit

Primary cells and cell lines have been demonstrated to generate IL-12 p40 in excess (6, 10, 24). Immunoprecipitation of p40 protein from transfected cells resulted in the detection of multiple bands with molecular weights of approximately 40 kDa, proposed to result from differential glycosylation of the p40 protein (17). Subsequently, multiple forms of the p40 protein have been reported from p40 transfected COS cells. After treatment of the proteins with N-glycosidase to remove glycosylation only a single p40 band was detected (30). Posttranslational modification of the human p40 protein at the WSEW amino acid motif has been demonstrated (31). This motif at the C-terminal end can be C-mannosylated, with human IL-12 only the second protein shown to have this modification (31).

Expression of p40 mRNA can be induced by IFN- γ treatment and exposure to LPS or a bacterial source (8, 23, 24), and some functional regulatory elements in the p40 promoter have been defined for both mouse and human p40. In the murine p40 promoter a TATA box 30 bp upstream of the transcription initiation site has been identified (20, 32) and appears to be the only transcription start site present for IL-12 p40 (20). Also present within the promoter region are transcription factor binding sites including a NF- κ B half site (22, 32), an Ets motif (33) and a C/EBP (CCAAT Enhancer Binding Protein (34)) binding site (35). Functional analyses of several motifs within the promoter region have been performed. Proteins from the NF- κ B

family of transcription factors have been shown to interact with the p40 promoter, including p50 homodimers (33) and the p50/c-Rel heterodimer (32, 36). The C/EBP binding site appears to be a critical element, and interacts synergistically with the Rel protein binding site to induce p40 mRNA expression (35). In addition, the human p40 promoter can confer cell type specificity when included in a reporter construct. This is evidenced by a lack of expression in T cell lines, constitutive expression in EBV-transformed B lymphoblastoid cells and inducible expression in the monocyte Thp-1 and RAW264.7 cell lines (33).

1.2.3. Homodimers of the p40 Subunit

The overproduction of p40 from different cell types raised the question of a physiological role for the p40 subunit. Subsequently, an *in vitro* and an *in vivo* role for p40 as an antagonist of IL-12 p70 has been identified (37, 38). Specific inhibition of IL-12 heterodimer mediated activities has been demonstrated for murine p40 (from the culture supernatant of p40 transfected cells). IL-12 p40 was shown to inhibit aggregation of Th1 cells in response to IL-12, inhibit the proliferation of PMA + IL-12 activated splenocytes, and inhibit production of IFN- γ from anti-CD3 monoclonal antibody + IL-12 activated CD4⁺ T cells (37). Characterisation of the p40 subunit from cells transfected with either mouse (39) or human (30) p40 cDNA identified two species of p40 protein. The expected 40 kDa molecular weight protein was present, however, a second protein with a higher molecular weight of approximately 80 kDa was also observed. Reduction of this 80 kDa protein resulted in the migration of a protein with a molecular weight of 40 kDa, and was subsequently shown to be a disulphide linked homodimer of the p40 subunit (30, 39).

Homodimers of p40 (and to a lesser extent the p40 monomer) have the ability to compete with p70 heterodimer for IL-12 receptor binding sites, and are also capable of inhibiting IL-12-dependent proliferation of human PHA-activated PBMNC (30) or mouse Con A blasts (39). Mouse homodimer is formed via a single intermolecular disulphide bond between the two p40 subunits involving the cysteine residue at position 175 (40). For human p70, heterodimer formation is mediated by the interaction of cysteine 177 in p40 with the p35 subunit (4). As such, human p40 homodimers would be expected to be formed via a disulphide linkage between cysteine 177 of each p40 subunit.

An *in vivo* role for the p40 homodimer as an antagonist has also been demonstrated. Mice treated with LPS had p40 homodimer constituting 20-40% of the p40 present in serum. Pretreatment of these mice with homodimer before LPS administration decreased serum IFN- γ levels, indicating that the p40 homodimer was capable of acting as an *in vivo* cytokine antagonist (38).

IL-12 p40 may also function as an effector molecule by acting as a chemotactic agent for macrophages. BUF/N rats injected with RH7777 hepatoma cells engineered to secrete p40 (RH7777/p40) developed inflammation at the injection site, which was not present in rats receiving control tumour cells. Growth of established tumours in RH7777/p40 rats was retarded and followed by complete regression. Inflammation was associated with macrophage infiltration at 3 days post-injection followed by CD8⁺, CD4⁺ T cells and NK cells by day 14 (41). *In vitro* evidence of the chemotactic activity of p40 was demonstrated by the migration of peritoneal macrophages across a membrane toward p40 containing medium in a concentration-dependent manner (41).

1.3. The IL-12 Receptor

PHA-activated blasts proliferate in response to IL-12 and this correlates with upregulation of the IL-12 receptor (IL-12R) on the cell surface (15). The IL-12R components are closely related to granulocyte-colony stimulating factor and leukaemia inhibitory factor receptors (42, 43), and the receptor complex is composed of two separate subunits, designated IL-12R β 1 and IL-12R β 2 (43). Expression of both subunits is required to generate high affinity binding sites with expression of IL-12R β 1 or IL-12R β 2 alone capable of only low affinity IL-12 binding (42, 43). Co-transfection of Ba/F3 cells with IL-12R β 1 and IL-12R β 2 enabled the cells to proliferate in response to IL-12 (44). Co-transfection of the epidermal growth factor (EGF) receptor extracellular domain fused to the transmembrane and cytoplasmic portions of IL-12R β 1 and IL-12R β 2 subunits gave similar results, with cells able to proliferate in response to EGF (45). Another protein, p85, associated with the IL-12R β 1 subunit, is rapidly phosphorylated upon stimulation of IL-12R β 1 Jurkat cell transfectants and PHA-activated T cells. However, the role of this protein in signal transduction has not yet been elucidated (46). In addition, an alternative IL-12R β 1 isoform from murine dendritic cells has been identified which retains the extracellular, transmembrane and cytoplasmic regions up to at least nucleotide 1865 of the coding sequence (of a possible 2217 bp) (16). The functional significance of this finding, and complete cDNA sequence still remain to be determined.

1.4. The Th1 vs Th2 Paradigm

The classification of T cells and T cell clones into two subsets based on their cytokine secretion profile has significantly influenced the study of immunology.

These subsets were initially described for mouse CD4⁺ T cell clones (47) and later for human CD4⁺ T cells (48). CD4⁺ T cells producing the cytokines IFN- γ and IL-2 (47) are designated T helper 1 (Th1) and are associated with the development of cell mediated responses such as delayed type hypersensitivity (49). Th2 T cells produce the cytokines IL-4 (47), IL-10 (50), IL-5 and IL-6 (51) and are associated with the development of humoral responses (49). More recently, a third T helper subset has been described (52). T cells in this Th3 subset produce predominantly transforming growth factor (TGF)- β (52). These cytokine secretion phenotypes are thought to result when a precursor cell, with a Th0 phenotype, and able to produce all cytokines, receives appropriate signals which then limit production to a more specialised range of cytokines (**Figure 1.2**) (49). This paradigm provides a useful framework around which therapeutic strategies can be developed, however, some caution must be exercised. Individual T cells and clones have been isolated which cannot be classified into the aforementioned T helper subsets, with a broad range of cytokine secretion profiles suggested to exist (54).

1.4.1. The Th1/Th2 Paradigm in Transplantation

With regard to transplantation the predominance of Th1-type cytokines has been associated with graft loss, whereas the expression of Th2-type cytokines has been associated with graft survival (55, 56). In mice treated with anti-CD4 antibodies (55, 57) or CTLA4-Ig (CTLA4 extracellular domain fused to the immunoglobulin heavy chain to inhibit the CD80/CD86 costimulatory pathway) (56), cardiac allograft survival correlated with low level intragraft IL-2 and IFN- γ , and enhanced IL-4 and IL-10 expression. However, this pattern of cytokine expression does not always hold, although in some cases only a limited number of cytokines have been assessed. The

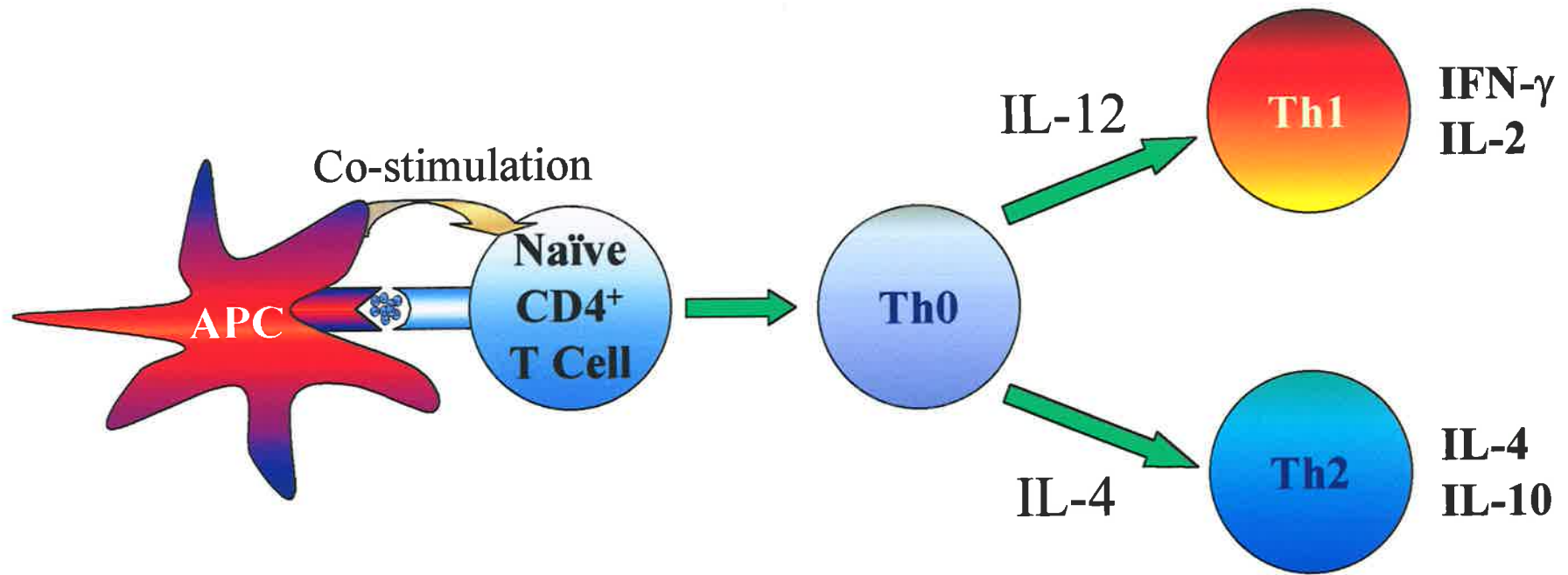


Figure 1.2. Generation of CD4⁺ T cells of the Th1 and Th2 phenotypes via the actions of IL-12 and IL-4 on a 'Th0' precursor cell. Modified from Nickerson *et al*, 1994 (53).

Th1/Th2 paradigm is also unable to explain the failure of Th2 cytokine expression to prolong graft survival in some models (58, 59). The true pattern of cytokine expression may be a combined Th1 and Th2 response. This was demonstrated in a murine intestinal allograft model in which transcripts for intercellular adhesion molecule-1, MHC Class II, IL-2, IL-4, IL-5, IL-6, IL-10 and IFN- γ were present in unmodified rejection, although IFN- γ showed prolonged expression within the graft (60). Similarly, in sensitised recipients of murine orthotopic liver transplants (where normal transplantation leads to spontaneous acceptance) IL-2, IL-4, IL-6, IFN- γ and IL-10 were detected in rejecting allografts. Transient expression of these cytokines was also observed in the spontaneously accepted allografts. The most apparent feature of the rejection was high level IFN- γ expression relative to the other cytokines, which correlated with other features of the rejection process such as IgG2a antibody deposition (61). A proposal has been put forward which suggests that it is the relative levels of IL-4 and IFN- γ which determine graft rejection or acceptance, with high levels of IFN- γ associated with graft loss (62).

1.4.2. The Influence of IL-12 on the Th1/Th2 Subsets

The suggestion that the Th1 cytokines, in particular IFN- γ , are associated with allograft loss, and Th2 with allograft acceptance, prompts the question of how this Th1 response is initiated. One cytokine with the potential to initiate T cell production of IFN- γ is IL-12. IL-12 has been shown to influence the development of the Th1 response by promoting the secretion of IFN- γ from CD4⁺ T cells *in vitro* (7, 63). The ability of IL-12 to drive T cells toward production of IFN- γ has been clearly demonstrated by Hsieh *et al* (7). Using CD4⁺ naïve, ovalbumin-specific T cells, the soluble factor capable of inducing IFN- γ production from the CD4⁺ T cells in

response to heat-killed *Listeria monocytogenes* was identified as IL-12, produced by activated macrophages (7).

IL-12 and IL-4 can promote the development of CD4⁺ T cells toward a Th1 or Th2 phenotype, respectively (64, 65). CD4⁺ T cell clones derived from human PBMNC stimulated with IL-12 and antigen produced low levels of IL-4. When IL-12 was not present high levels of IL-4 could be detected, and the addition of anti-IL-12 antibodies during derivation of the clones correlated with a higher level of IL-4 production. This suggested that IL-12 had an inhibitory effect on the generation of the Th2 phenotype (66). By contrast, differentiation towards a Th2 phenotype has been associated with the loss of IL-12 responsiveness, which can be explained through the effects of IL-4 and IFN- γ on the IL-12 receptor complex. Analysis of the expression of mRNA transcripts in human Th1 and Th2 T cells revealed that, whereas IL-12R β 1 transcripts were present in cells of both phenotypes, IL-12R β 2 transcripts were present only in the Th1 cells. The presence of high affinity binding sites on Th1 and not Th2 cells was evidence of the presence of both IL-12R subunits (67). This response was due to the actions of IL-4, which inhibited expression of the IL-12R β 2 subunit in Th2 cells leading to loss of IL-12 signalling. This inhibition could be reversed during the early stages of Th2 cell development by treatment with IFN- γ , which upregulated IL-12R β 2 and restored IL-12 signalling (68). A similar response has been observed in human T cells activated with PHA and treated with IL-4 or IFN- γ , where loss of IL-12 responsiveness in IL-4-treated cells was associated with changes in IL-12R expression (69).

IL-12 can also generate Th1 effectors in *in vivo* models. IL-12 plays an integral role in the protection against a variety of infectious agents including

parasites, bacteria, viruses and fungi. The protective effect of IL-12 is mediated in most circumstances via IL-12-induced production of IFN- γ (70-75).

C57BL/6 mice show a genetic predisposition towards the development of Th1-type immune responses, whereas BALB/c mice are predisposed to a Th2-type response. The resolution or progress of leishmaniasis is associated with the production of IFN- γ or IL-4, respectively (70). Administration of recombinant (r) IL-12 to mice infected with *Leishmania major* results in a significant decrease in the parasite burden in susceptible BALB/c mice concomitant with increased IFN- γ production. However, treatment of resistant C57BL/6 mice with anti-IL-12 antibody results in exacerbation of the disease and a decrease in IFN- γ production (71). The necessity for IL-12 in host resistance to this parasite by induction of IFN- γ has also been shown by other groups (75, 76).

IL-12 is also required for the protection of mice against other infectious agents such as *Cryptococcus neoformans*, as IL-12 p35 (-/-) and IL-12 p40 (-/-) knockout mice died earlier than wild-type mice and produced minimal amounts of IFN- γ . Administration of recombinant IL-12 to wild type mice was able to prolong the survival of these animals for the duration of the IL-12 treatment (72). IL-12 induction of IFN- γ is also associated with protection against *Mycobacterium tuberculosis* (74) and murine cytomegalovirus (73). In addition, IL-12 has also been demonstrated to be important in the clearance of infection in humans. A natural deletion in the human p40 gene was identified in a child with *Mycobacterium* and *Salmonella* infections, leading to a lack of heterodimer and p40 expression from the patient's PBMNC. The underlying cause was shown to be a homozygous 373 bp deletion in the p40 gene, resulting a frameshift. *In vitro* stimulation of the PBMNC

from this patient with *Mycobacterium* and recombinant IL-12 restored IFN- γ production (77).

IL-12 can also exacerbate infection by abrogating the protective Th2-type response required for resolution of infection with *Trichuris muris*, an intestinal parasite. Administration of recombinant IL-12 resulted in chronic infection of BALB/K mice associated with Th1-type IgG2a that was parasite-specific. These effects, dependent on IFN- γ production, could be abrogated using an anti-IFN- γ antibody (78).

1.5. IL-12 in Allograft Rejection

The ability of IL-12 to drive IFN- γ production *in vitro* and *in vivo*, and the inferred role of IFN- γ in allograft rejection through the Th1 response, suggests that IL-12 may be an important cytokine in the initiation and progression of allograft destruction. The presence of IL-12 within allografts that are subsequently rejected can be demonstrated.

In a rat model of accelerated cardiac allograft rejection, transfusion of donor spleen cells was able to extend graft survival time and this correlated with low-level intragraft IFN- γ and IL-12 heterodimer, as detected by immunohistology. In comparison, rejecting grafts showed increased expression of IL-12 p70 heterodimer (79). Similarly, murine cardiac allograft recipients receiving donor splenocytes plus anti-CD40L (ligand) antibody showed long-term graft survival associated with undetectable IFN- γ and low level IL-12 (80). IL-12 may also contribute to chronic allograft rejection, as rats receiving cardiac allografts and the immunosuppressive drug rapamycin showed delayed onset of IL-12 p70 expression. Strong staining for

IL-12 p70 could be demonstrated on infiltrating mononuclear cells at day 35 when grafts began showing signs of chronic rejection (81).

Administration of recombinant IL-12 to murine liver allograft recipients is also able to induce rejection of grafts that are normally spontaneously accepted. Rejection in this model was characterised by the expression of IFN- γ , macrophage infiltration and the presence of cytotoxic antibodies (82). Alternatively, inhibition of IL-12 using a neutralising antibody can enhance graft survival. In an islet allograft model where multiple minor antigen mismatches were present (but MHC was matched) neutralising IL-12 resulted in prolonged or indefinite allograft survival, dependent on the donor mouse strain. In a further model where donor alloantigen was presented to CD4⁺ T cells by the host antigen presenting cells, anti-IL-12 treatment also significantly prolonged graft survival (83). Thus IL-12 appears to be associated with allograft rejection and the production of IFN- γ within the graft, and recombinant cytokine can induce rejection of accepted grafts.

IL-12 expression would be expected as a result of transplantation due to injury sustained by the graft. In a process called ischaemia/reperfusion injury, removal of the blood supply (ischaemia) and the subsequent re-connection (reperfusion) is known to cause injury to tissues (84). Although the analysis of IL-12 expression has only been assessed in a couple of models, IL-12 does appear to be upregulated after ischaemic injury. In a mouse model of kidney ischaemia, IL-12 p40 mRNA expression was detectable in ischaemic tissue at 6 days post-injury. Combined administration of anti-IL-12 and anti-IL-18 antibodies prevented upregulation of MHC Class I, MHC Class II and IFN- γ mRNA expression (85). In a model of hepatic ischaemia, staining for IL-12 was observed in liver sections from animals affected by ischaemia/reperfusion, and not in the untreated control animals.

Reduced neutrophil recruitment and serum IFN- γ levels were observed in animals treated with anti-IL-12, or in IL-12 p40 knockout mice, and this was associated with decreased injury of the liver (86).

The actual mechanism(s) by which IL-12 contributes to the process of allograft rejection, either by direct effects on the graft or through the activation of effector cells, are less well defined. A role for IL-12 outside the generation of a Th1 response in allograft rejection is considered in the following sections.

1.6. Additional Effects of IL-12 that may Mediate Allograft Rejection

While high levels of IFN- γ are associated with graft rejection and IL-12 is able to initiate IFN- γ production from T cells and NK cells, the biological activities of IL-12 may result in a number of different effector functions capable of mediating allograft destruction. These may include the induction of cytotoxic NK and CD8⁺ T cells that are able to damage the graft, or by the prevention of tolerance toward the allograft.

1.6.1. IL-12 Induction of T and NK Cell Cytotoxicity

IL-12 was originally designated as Natural Killer Cell Stimulatory Factor (1) and Cytotoxic Lymphocyte Maturation Factor (2) reflecting the important role of IL-12 in the generation of cytotoxic effectors. IL-12 appears to act directly on natural killer cells (87), and this is evidenced by the effect of IL-12 on peripheral blood lymphocytes where the cytotoxic activity of the natural killer cells can be augmented (1). IL-12 can enhance the cytotoxic activity of CD16⁺CD5⁻ NK cells (88) and

induce non-MHC-restricted lymphokine-activated killer cell activity in CD56⁺ NK cells (89). In addition, administration of a plasmid expressing recombinant IL-12 to mice has been shown to induce a 10-fold increase in the natural killer cell activity (90). The enhanced cytotoxic capacity of the NK cells is concurrent with an increase in mRNA expression for the cytolytic effector molecules granzyme B (91) and perforin (a pore-forming protein (92)) which are able to kill target cells (13). Granzyme B and perforin mRNA expression has been linked with acute renal allograft rejection (93).

In addition to its ability to induce cytotoxic activity, IL-12 can also act as a chemoattractant for resting NK cells, and neutrophils, recruiting them to the site of expression. This chemotactic ability was also noted for T cells, however, activation was required prior to recruitment (94).

IL-12 is also able to augment the *in vitro* proliferation and cytotoxic capacity of activated CD8⁺ T cells (95, 96). Evidence for the *in vivo* ability of IL-12 to generate cytotoxic effectors is apparent in rodent tumour models. When IL-12 was administered to mice bearing renal carcinomas, enhanced tumour regression was associated with the infiltration of CD8⁺ T cells, NK cells and macrophages. This was again associated with granzyme B and perforin mRNA expression (97). Mice carrying tumours engineered to express IL-12 also showed enhanced tumour regression associated with CD8⁺ T cell cytotoxic activity (98). In addition, viral immunity can also be significantly enhanced after intramuscular injection of plasmid vectors expressing IL-12. The resulting antigen-specific CTL response generated against the influenza virus nucleoprotein antigen was increased in the IL-12-treated mice, as assessed by the specific lysis of target cells (99).

1.6.2. IL-12 Induction of Allospecific Cytotoxic T Lymphocytes

The allogeneic nature of a transplanted organ is likely to result in the generation of alloantigen-specific cytotoxic effectors, and IL-12 may contribute significantly to the development of these cytotoxic cells. The mixed lymphocyte reaction (MLR), is an *in vitro* model of the alloimmune response (100), and the addition of exogenous IL-12 can significantly enhance the resulting CTL activity (101). In this same model, IL-12 was also able to induce granzyme B and perforin mRNA accumulation in major histocompatibility complex Class I-primed lymphocytes (101). Addition of exogenous IL-12 at the initiation of the mixed lymphocyte reaction can augment both MHC-restricted and unrestricted cytotoxicity in response to stimulation with alloantigen. Here the effector cells were CD8⁺ T cells as depletion of this cell population resulted in significantly reduced killing of target cells (102). *In vivo*, mice receiving allogeneic splenocytes plus recombinant IL-12 have an increased cytolytic CD8⁺ T cell response to alloantigen, but not to third party target cells (103). In addition to the biological activity of IL-12 alone, an additive or synergistic effect of IL-12 plus IL-2 (dependent on the IL-2 concentration) can be observed in the induction of CD8⁺ cytotoxic activity (95, 104). This further increases the potential for damage to grafts due to cytotoxic effectors.

1.6.3. Natural Killer Cell Induction of Cytotoxic T Lymphocytes

As described above, IL-12 can act directly on NK cells, whereas cytotoxic T cell development requires additional help and activation. CD4⁺ T cells can provide help for the induction of cytotoxic T cells, but they do not appear to be an absolute requirement for CTL generation, with depletion of CD4⁺ T cells and exposure of CD8⁺ cells to alloantigen still resulting in CTL generation (105). However, depletion

of CD56⁺ NK cells or the addition of anti-CD56 antibody to the mixed lymphocyte reaction has been demonstrated to prevent cytotoxic T cell generation. Soluble mediators did not appear to be required for this response, instead a physical interaction between NK and CD8⁺ T cells was necessary (105). CTL and NK cells are also involved in a two-way regulation process in which NK cells play a role in CTL induction (105) and CD8⁺ CTL can downregulate NK cell activity (106, 107). Thus an additional role for IL-12 in allograft destruction may be mediated by direct activation and recruitment of NK cells and the subsequent generation of allospecific CTL via interaction of the two cell types.

1.6.4. The Effect of IL-12 on Homing Molecules

In addition to the induction of cytotoxic effectors, more recent evidence suggests that expression of IL-12 at a site of inflammation may lead to the recruitment of inflammatory cells by the upregulation of homing molecules. Recirculation of naïve CD4⁺ T cells from the blood to the peripheral lymph nodes involves the lymphocyte homing receptor L-selectin (108). L-selectin can be detected on Th1 cells and not Th2 cells when these cells are stimulated with antigen, and IL-12 can prolong the expression of this molecule on the cell surface (109). IL-12 can also promote the expression of other selectin ligands such as E-selectin and P-selectin on T cells, with Th1 cells derived in the presence of IL-12, and expressing these molecules, showing preferential migration to sites of peripheral inflammation (110). In the case of allograft rejection, production of IL-12 and subsequent upregulation of homing molecules may result in recruitment of cells into the grafted organ, where activated cells may inflict damage to the graft.

1.6.5. IL-12 and the Maintenance of T Cell Anergy

Acceptance of the allograft by the immune system is a requirement for long-term graft survival, and factors that disrupt tolerance are likely to pose a significant risk to the allograft. T cell anergy (functional unresponsiveness) to protein antigens can be induced in experimental models, and IL-12 can provide critical help in the reversal of the anergic state. Tolerance toward a given antigen can be enhanced by neutralising endogenous IL-12. Administration of anti-IL-12 antibody in combination with ovalbumin can induce peripheral unresponsiveness to antigen as shown by suppression of proliferative responses in Peyer's patches and mesenteric lymph nodes, associated with cell apoptosis (111). The tolerogenic mechanism in this model appears to result from Fas-mediated cell apoptosis suggesting that IL-12 provides survival signals to cells differentiating toward a Th1 phenotype (112). In another mouse model, neutralising IL-12 before injection of dendritic cells pulsed with two peptide antigens resulted in the failure to mount a delayed type hypersensitivity response upon rechallenge with the same antigens. The state of tolerance was shown to be specific, as reactivity was maintained toward an unrelated peptide, and treatment of these tolerant mice with recombinant IL-12 was able to reverse the tolerogenic state (113).

Two signals appeared to be required to generate complete reversal of the anergic state and involve both IL-12 and costimulatory molecules. IL-12 can reverse established tolerance *in vitro* and *in vivo*, through a mechanism that shows minimal dependence on the production of IFN- γ (114). The reversal of tolerance by IL-12 can be antagonised by antibodies toward CD80 and CD86, suggesting that the reversal mechanism involves both IL-12 and cell surface costimulatory molecules (114, 115). Exposure of anergic T cells to IL-12 and costimulatory molecules on the surface of

an antigen presenting cell may lead to a reversal of allograft tolerance. Such an environment may be generated upon injury or infection, resulting in inflammatory processes.

1.7. Antagonism of IL-12 by IL-12 p40 in Alloimmune

Responses

As described in the preceding sections, the IL-12 heterodimer is able to induce naïve CD4⁺ T cells to produce IFN- γ (a Th1-type response), generate cytotoxic CD8⁺ T lymphocytes and NK cells, upregulate the expression of homing molecules and prevent or reverse T cell anergy. A schematic diagram for the potential involvement of IL-12 in graft destruction is depicted in **Figure 1.3**. As such, antagonising the *in vivo* activity of IL-12 may provide significant long-term protection of allografts. As described in section 1.2.3, the IL-12 p40 subunit is capable of forming homodimers that are able to inhibit the activity of the heterodimer both *in vitro* (30, 37, 39) and *in vivo* (38). This ability makes the p40 subunit a potential therapeutic candidate for the prevention of allograft rejection.

There is conflicting evidence for a role of IL-12 p40 as an effective inhibitor of allogeneic immune responses. Administration of the p40 homodimer or an anti-IL-12 antibody to murine cardiac allograft recipients resulted in accelerated graft rejection when compared to unmodified recipients (116). In the anti-IL-12 treated groups, IFN- γ mRNA expression was not inhibited although the antagonism resulted in a reduced number of activated donor-specific CTL in the graft. Accelerated rejection was also observed in IL-12 p40 knockout mice (116) and it has been suggested that p40 may enhance the development of alloreactive Th1 cells (117). These authors have extended this study through the use of an *in vitro* model, the

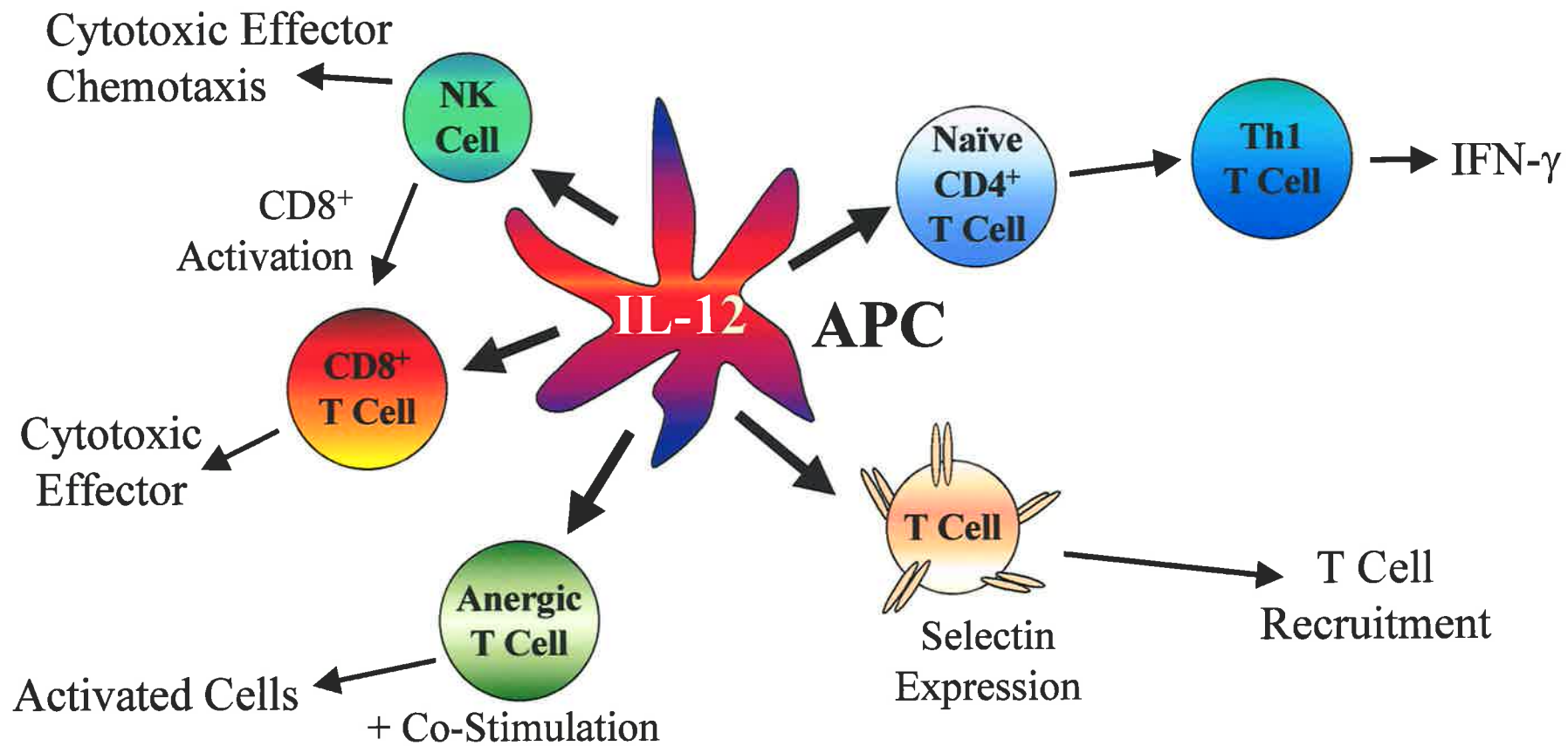


Figure 1.3. Potential modes of IL-12 involvement in allograft destruction.

mixed lymphocyte reaction. Addition of anti-IL-12 antibody to the primary MLR did not significantly affect IFN- γ production, and the addition of p40 homodimer actually enhanced IFN- γ production upon restimulation of the cells. Depletion of the CD8⁺ T cell population in an unmodified MLR resulted in CD4⁺ T cell production of IFN- γ at levels similar to the total cell population. However, depletion of CD8⁺ T cells and addition of p40 homodimer abrogated IFN- γ production, although, depletion of CD4⁺ T cells with addition of homodimer resulted in only a 50% decrease in IFN- γ . *In vivo*, cardiac allograft recipients depleted of CD8⁺ T cells and receiving p40 homodimer had prolonged graft survival. This suggested that while CD4⁺ T cell responses could be inhibited, CD8⁺ T cells were actually stimulated by p40 homodimer (117).

The above work suggests that antagonising the IL-12 heterodimer using IL-12 p40 may not be an effective therapy for organ transplantation. However, there is evidence to suggest that localisation of p40 gene expression to the allograft itself, in contrast to the systemic administration or gene deletion described above, may prolong graft survival (118, 119).

Murine myoblast C₂C₁₂ cells transplanted into allogeneic recipients showed prolonged survival when transduced with a retroviral vector expressing IL-12 p40, despite the infiltration of mononuclear cells (119). Cytotoxic T lymphocyte induction, production of IL-2 and IFN- γ and the delayed-type hypersensitivity response against the C₂C₁₂ cells were also decreased in IL-12 p40 recipients compared to controls, suggesting that the cell mediated immune response was suppressed. The antigen-specific nature of the p40 suppression could be demonstrated by the active response to third party antigen, which remained intact (119).

In a murine pancreatic islet model, islets were transfected with an adenoviral vector expressing IL-12 p40 and transplanted under the renal capsule of syngeneic NOD (non-obese diabetic) mice. Recipients of IL-12 p40 modified cells maintained normoglycaemia and cellular infiltration of islets was minimal, with expression of IFN- γ mRNA not apparent in these grafts. In contrast, IL-10 adenovirus-modified islets showed significant graft destruction associated with cell infiltration and the return of the diabetic state (118).

Thus, IL-12 antagonism using IL-12 p40, when directed to a local environment, can provide significant graft protection. However, prolonged graft survival using IL-12 p40 appears to be dependent on the model in which this antagonist is tested, and the method of delivery.

The aims of the work performed in this thesis were:

- i. to clone the ovine p35 gene and characterise the biological activity of the ovine IL-12 heterodimer;
- ii. to assess the IL-12 antagonistic property of ovine IL-12 p40 and the subsequent ability of IL-12 p40 to inhibit the alloimmune response, and
- iii. to characterise an IL-12 p35 subunit mRNA variant and determine the potential of this molecule for transplantation gene therapy.



Chapter 2

Materials and Methods

Chapter 2

Materials and Methods

2.1. Materials

2.1.1. Antibodies

Polyclonal Rabbit anti-Human IL-12	Genzyme, USA
Living Colors [®] Peptide Antibody	Clontech, USA
CD80 (Mouse anti-Human, IgG1)	Serotec, UK
CD86 (Mouse anti-Human, IgG1)	Serotec, UK
MY-4 FITC-Conjugated (CD14, IgG2b)	Coulter Corporation, USA
CD1a (Mouse anti-Human, IgG1)	Serotec, UK
CD40 (Mouse anti-Human, IgG1)	Serotec, UK
CD33 (Mouse anti-Human, IgG1)	Serotec, UK
CD83 (Mouse anti-Human, IgG2b)	Serotec, UK
X63 (Negative Control, IgG1)	Overgrown S/N
W6/32 (MHC Class I, IgG2b)	Overgrown S/N
3.54 (MHC Class II, IgG2a)	Overgrown S/N
ID4.5 (Negative Control, IgG2a)	Overgrown S/N
SBU I (Ovine MHC Class I, IgG1)	Culture S/N, University of Melbourne, School of Veterinary Science, Australia
SBU II (Ovine MHC Class II, IgG1)	Culture S/N, as above
SBU T6 (Ovine CD1a, IgG1)	Culture S/N, as above
MCTLA4 (Ovine B7.1/7.2 [CD80/86])	Culture S/N (120)
MCD40 (CTLA4-Ig Negative Control)	Culture S/N (120)
Ovine CD14 (Mouse anti-Ovine, IgG1)	Serotec, UK

Biotinylated Goat anti-Rabbit IgG (H&L)	Vector Laboratories, USA
Normal Rabbit Serum (Heat Inactivated)	ICN, USA
Sheep anti-Mouse IgG FITC-Conjugated Fab ₂ Fragments	Silenus Laboratories, Australia

2.1.2. Cell Lines (Cell Culture and Bacterial)

293 – Adenovirus packaging cell line generated by transformation of a human kidney cell line with adenovirus type 5 DNA (121).

CHO - Chinese Hamster Ovary. Biopsy-derived cell line from the ovary of an adult Chinese hamster (122).

Ovine Adult Fibroblasts – generated in the laboratory from skin obtained from adult sheep.

<i>Escherichia coli</i> TG1 α	IMVS, Adelaide
<i>E. coli</i> BJ5183	Dr T-C He (123)
<i>E. coli</i> DH10B	IMVS, Adelaide

2.1.3. Cytokines

Recombinant Human Interleukin-4 (IL-4)	Peptotec, USA
Recombinant Human Granulocyte-Macrophage Colony Stimulating Factor (GM-CSF)	Schering-Plough, Australia
Recombinant Human Tumour Necrosis Factor α (TNF- α)	R&D Systems, USA

2.1.4. Radiochemicals

³⁵ S-labelled Methionine/Cysteine	ICN, USA
³ H-labelled Thymidine	Amersham Pharmacia Biotech, Australia

2.1.5. Flow Cytometry

FACS Lysing™ Solution	Becton Dickinson, USA
EMA (Ethidium Monoazide Bromide)	Molecular Probes, USA
Sodium Azide	Ajax Chemicals, Australia

2.1.6. General Chemicals

Acrylamide (40%) 36:1 Acrylamide:Bis Acrylamide	Bio-Rad, USA
Agar Bacteriological	Oxoid, UK
Ammonium Persulphate (APS)	Bio-Rad, USA
Ampicillin	Boehringer Mannheim, Germany
Amplify™	Amersham International, UK
Apal Restriction Enzyme	New England Biolabs, USA
BamHI Restriction Enzyme	Boehringer Mannheim, Germany
Benchmark™ Prestained Protein Marker	Life Technologies, USA
Bromophenol Blue	Bio-Rad, USA
Calcium Chloride (CaCl ₂ .2H ₂ O)	Ajax Chemicals, Australia
Chloroform	Ajax Chemicals, Australia
Con A (Concanavalin A Type IV)	Sigma, USA
Coomassie Brilliant Blue R-250	Bio-Rad, USA
D-Glucose	BDH, Australia
Diethylpyrocarbonate (DEPC)	Sigma, USA
Dimethylformamide (DMF)	BDH, Australia
Dimethyl Sulphoxide (DMSO)	Ajax Chemicals, Australia
Dithiothreitol (DTT)	Boehringer Mannheim, Germany
EcoRI Restriction Enzyme	New England Biolabs, USA
EDTA (Ethylenediamine Tetraacetic Acid)	Sigma, USA
Ethanol	BDH, Australia
Ethidium Bromide	Sigma, USA
Glacial Acetic Acid	BDH, Australia

Glycerol	Ajax Chemicals, Australia
Guanidine Thiocyanate Salt	Sigma, USA
HEPES (N-[2-Hydroxyethyl] Piperazine- N'-[2-Ethanesulphonic Acid])	Sigma, USA
HindIII Restriction Enzyme	Progen, Australia
Hydrochloric Acid (HCl)	Ajax Chemicals, Australia
8-Hydroxyquinoline	Sigma, USA
Igepal CA 630 (NP-40 Replacement)	Sigma, USA
IPTG (Isopropyl- β -D-Thiogalactopyranoside)	Boehringer Mannheim, Germany
Isoamyl Alcohol	Sigma, USA
Isopropanol	Sigma, USA
Kanamycin	Life Technologies, USA
N-Lauroylsarcosine	Sigma, USA
LipofectAMINE™	Life Technologies, USA
Low Molecular Weight SDS-PAGE Protein Standards	Bio-Rad, USA
Magnesium Chloride (MgCl ₂ .6H ₂ O)	Sigma, USA
2-Mercaptoethanol (β -Mercaptoethanol)	Sigma, USA
Methanol	Ajax Chemicals, Australia
L-Methionine	Sigma, USA
NBT (4-Nitro Blue Tetrazolium Chloride)	Boehringer Mannheim, Germany
NotI Restriction Enzyme	New England Biolabs, USA
Nonidet P-40 (NP-40)	Sigma, USA
Ovalbumin	Sigma, USA
PacI Restriction Enzyme	New England Biolabs, USA
Pansorbin®	Calbiochem, USA
Patent Blue V Dye	Sigma, USA

PHA (Phytohaemagglutinin)	Wellcome, UK
Phenol (RNA), Water Saturated, pH 4.5	Amresco, USA
Phenol (DNA), Water Saturated, pH 6.6/7.9	Amresco, USA
PmeI Restriction Enzyme	New England Biolabs, USA
Potassium Acetate	BDH, Australia
Potassium Chloride (KCl)	Ajax Chemicals, Australia
Potassium di-Hydrogen Orthophosphate (KH ₂ PO ₄)	Ajax Chemicals, Australia
Proteinase K	Merck, Germany
PstI Restriction Enzyme	Boehringer Mannheim, Germany
SacI Restriction Enzyme	New England Biolabs, Germany
Skim Milk Powder	Dairy Vale, Australia
Sodium Acetate	Ajax Chemicals, Australia
Sodium Chloride (NaCl)	M & B, Australia
Sodium Citrate (Na ₃ C ₆ H ₅ O ₇ .2H ₂ O)	BDH, Australia
Sodium Deoxycholate	BDH, Australia
Sodium Dodecyl Sulphate (SDS)	BDH, Australia
Sodium di-Hydrogen Orthophosphate (NaH ₂ PO ₄ .2H ₂ O)	Ajax Chemicals, Australia
Sodium Hydrogen Carbonate (NaHCO ₃)	BDH, Australia
di-Sodium Hydrogen Orthophosphate (Na ₂ HPO ₄ , Anhydrous)	Ajax Chemicals, Australia
Sodium Hydroxide (NaOH)	Ajax Chemicals, Australia
TEMED (N, N, N', N'-Tetramethylethylenediamine)	Bio-Rad, USA
Triton X-100	Bio-Rad, USA
Tris Hydrochloride (Tris [Hydroxymethyl] Aminomethane Hydrochloride) (Tris-HCl)	Sigma, USA
Trizma Base (Tris [Hydroxymethyl] Aminomethane)	Sigma, USA

Tryptone	Oxoid, UK
Tween-20	Bio-Rad, USA
Yeast Extract	Oxoid, UK
XbaI Restriction Enzyme	Promega, USA
X-Gal (5-Bromo-4-Chloro-3-Indolyl- β-D-Galactopyranoside)	Progen Industries Pty Ltd, Australia
XPO ₄ (5-Bromo-4-Chloro-3-Indolyl Phosphate)	Boehringer Mannheim, Germany

2.1.7. Tissue Culture Reagents

BetaPlate Scintillation Fluid	Wallac, Finland
Foetal Calf Serum (FCS)	CSL, Australia
Geneticin [®] (G418)	Life Technologies, USA
L-Glutamine	Multicel, Australia
Lymphoprep [™]	Nycomed, Norway
Metrizamide	Nycomed, Norway
Minimal Essential Medium (MEM)	ICN, USA
Penicillin/Streptomycin	Multicel, Australia
RPMI 1640 Powdered Medium	Sigma, USA
RPMI 1640, Methionine/Cysteine Deficient	ICN, USA
Sodium Pyruvate	ICN, USA
Trypsin	Sigma, USA

2.1.8. Molecular Biology Reagents

Agarose	Progen Industries Pty Ltd, Australia
AmpliTaq [®] Polymerase	Perkin-Elmer, USA
BigDye [™] Terminator Ready Reaction Mix	PE Applied Biosystems, USA
BRESA-CLEAN DNA Purification Kit	Geneworks, Australia
Dye Terminator Ready Reaction Mix	PE Applied Biosystems, USA

JETSTAR Midi Prep Plasmid Kit	Genomed, USA
KlenTaq Polymerase Mix	Clontech, USA
Low Melting Point Agarose	Scot Scientific, Australia
Mineral Oil	Sigma, USA
MMLV Reverse Transcriptase	Life Technologies, USA
dNTPs	Promega, USA
Oligo dT	Amersham Pharmacia
	Biotech, Australia
Oligonucleotides	Life Technologies, USA
Oligonucleotides	Geneworks, Australia
pUC19/HpaII Molecular Marker	Geneworks, Australia
Qiagen Midi Prep Plasmid Kit	Qiagen Inc., USA
RNase A	Sigma, USA
RNasin	Promega, USA
SPP1/EcoRI Molecular Marker	Geneworks, Australia
T4 Ligase	Promega, USA

2.1.9. Film

667 Positive	Polaroid, UK
Kodak X-Omat AR	Kodak, USA

2.1.10. Plasmid Vectors

pBluescript [®] II KS ⁺	Stratagene, USA
pGEM [®] -T Vector (System I Kit)	Promega, USA
pGEM [®] -T Easy Vector (System I Kit)	Promega, USA
pRc/CMV Expression Vector	Invitrogen, USA
Living Colors [®] pEGFP-N1 Expression Vector	Clontech, USA

2.2. Buffers and Solutions

NOTE: Abbreviations for chemicals can be found in section 2.1. **Materials.**

2.2.1. Agarose Gel Electrophoresis

Ethidium Bromide Stain

Compound	Concentration	Quantity
10 mg/ml Ethidium Bromide	1.25 µg/ml	50 µl
H ₂ O		Total 400 ml

6X Loading Buffer

Compound	Concentration	Quantity
50X TAE	1X	50 µl
Glycerol	50%	1.25 ml
Bromophenol Blue	24%	600 µl
H ₂ O		Total 2.5 ml

50X TAE (Electrophoresis Buffer)

Compound	Concentration	Quantity
Trizma Base	~1.6 M	193.8 g
Sodium Acetate	~ 800 mM	65.6 g
EDTA	40.27 mM	14.9 g
H ₂ O		Total 100 ml

Adjust to pH 7.2. Autoclave. Dilute to 1X working concentration.

2.2.2. RNA Extraction

DEPC-Treated Water

Compound	Concentration	Quantity
DEPC	0.1% v/v	100 µl
H ₂ O		Total 100 ml

Stir for 3 hours in fume hood and autoclave.

2 M Sodium Acetate (pH 4.0)

Compound	Concentration	Quantity
Sodium Acetate	2 M	8.204 g
H ₂ O		Total 50 ml

Adjust to pH 4.0. Autoclave.

0.75 M Sodium Citrate

Compound	Quantity
Sodium Citrate	11.029 g
H ₂ O	Total 50 ml
Adjust to pH 7.0. Autoclave.	

Solution D

Compound	Concentration	Quantity
Guanidine Thiocyanate Salt	4 M	12.5 g
0.75 M Sodium Citrate (pH 7.0)	25 mM	0.88 ml
10% N-Lauroylsarcosine	0.5%	1.32 ml
H ₂ O		Total 25 ml
Dissolve at 65°C. Add 180 µl of β-mercaptoethanol.		

2.2.3. Cloning and Transfection***Ampicillin Stock***

Compound	Concentration	Quantity
Ampicillin	50 mg/ml	50 mg
H ₂ O		Total 50 ml
Filter sterilise. Aliquot and store at -20°C.		

Agar Plates (with Ampicillin)

Compound	Concentration	Quantity
Agar Bacteriological		3 g
Luria Broth		300 ml
50 mg/ml Ampicillin	166.67 µg/ml	1 ml
0.1 M IPTG	300 µM	900 µl
20 mg/ml X-Gal	20 µg/ml	300 µl
Heat luria broth until all of agar has dissolved. In Biohazard hood, allow agar to cool to 55°C before adding ampicillin, IPTG and X-Gal. Pour quickly into petri dishes, flame with Bunsen burner to remove bubbles and allow to set. Makes 8-10 plates.		

1 M Calcium Chloride

Compound	Concentration	Quantity
CaCl ₂ .2H ₂ O	1 M	7.351 g
H ₂ O		Total 50 ml
Autoclave.		

0.5 M EDTA

Compound	Concentration	Quantity
EDTA	0.5 M	9.305 g
H ₂ O		Total 50 ml
Adjust to pH 8.0. Autoclave.		

0.1 M IPTG

Compound	Concentration	Quantity
IPTG	0.1 M	1.2 g
H ₂ O		Total 50 ml

Filter sterilise. Aliquot and store at -20°C.

2 M D-Glucose

Compound	Concentration	Quantity
D-Glucose	2 M	18.008 g
H ₂ O		Total 50 ml

Autoclave.

Luria Broth

Compound	Quantity
Yeast Extract	2.5 g
Tryptone	5 g
NaCl	5 g
1 M NaOH	500 µl
H ₂ O	Total 500 ml

Autoclave.

Luria Broth + Ampicillin

Compound	Concentration	Quantity
Luria Broth		100 ml
50 mg/ml Ampicillin	50 µg/ml	100 µl
		Total 100 ml

Store away from the light. Do not autoclave.

Luria Broth + D-Glucose

Compound	Concentration	Quantity
2 M D-Glucose	20 mM	200 µl
H ₂ O		Total 10 ml

1 M MgCl₂

Compound	Concentration	Quantity
MgCl ₂ .6H ₂ O	1 M	10.165 g
H ₂ O		Total 50 ml

Autoclave.

Mini-Prep Solution 1

Compound	Concentration	Quantity
D-Glucose	50 mM	0.9 g
Tris-HCl	25 mM	0.934 g
0.5 M EDTA	10 mM	2 ml
H ₂ O		Total 100 ml

Adjust to pH 8.0. Autoclave.

Mini-Prep Solution 2

Compound	Concentration	Quantity
1 M NaOH	0.2 M	4 ml
20% SDS	1%	1 ml
H ₂ O		Total 20 ml

Mini-Prep Solution 3

Compound	Concentration	Quantity
Potassium Acetate	~ 3 M	29.4 g
Glacial Acetic Acid		11.5 ml
H ₂ O		Total 100 ml
Adjust to pH 4.6. Autoclave.		

20% SDS

Compound	Concentration	Quantity
SDS	20% w/v	4 g
H ₂ O		Total 20 ml
Dissolve at 60°C.		

X-Gal

Compound	Concentration	Quantity
X-Gal	20 mg/ml	0.2 g
DMF		Total 10 ml
Avoid DMF sensitive plastics. Does not require sterilising.		

2.2.4. SDS-PAGE***Acrylamide 10% Resolving Gel***

Compound	Quantity
40% Acrylamide (36:1 Acrylamide:Bis Acrylamide)	1735 µl
H ₂ O	4135 µl
Solution A	1000 µl
10% SDS	70 µl
10% APS	45 µl
TEMED	10 µl
Add TEMED and APS, mix and pour into gel apparatus immediately.	Total 6995 µl

Acrylamide 3% Stacking Gel

Compound	Quantity
40% Acrylamide (36:1 Acrylamide:Bis Acrylamide)	200 μ l
H ₂ O	1800 μ l
Solution B	640 μ l
10% SDS	21 μ l
10% APS	15 μ l
TEMED	5 μ l
Add TEMED and APS, mix and pour into gel apparatus immediately.	Total 2681 μ l

10% APS

Compound	Concentration	Quantity
APS	10% w/v	0.075 g
H ₂ O		Total 75 μ l

Destaining Solution

Compound	Concentration	Quantity
Methanol	45% v/v	450 ml
Glacial Acetic Acid	10% v/v	100 ml
H ₂ O		Total 1000 ml

Electrophoresis Buffer

Compound	Concentration	Quantity
Trizma Base	0.05 mM	0.006 g
Glycine	0.37 mM	0.028 g
SDS	0.1% w/v	1 g
H ₂ O		Total 1000 ml

Loading Buffer

Compound	Concentration	Quantity
2X SDS Sample Buffer	50% v/v	500 μ l
2X Lysis Buffer	50% v/v	500 μ l
Add β -Mercaptoethanol (10% v/v) for reducing gels.		Total 1 ml

2X Lysis Buffer

Compound	Concentration	Quantity
Trizma Base	10 mM	0.012 g
10% Triton X-100	1% v/v	1 ml
10% SDS	0.1% v/v	100 μ l
NaCl	150 mM	0.088 g
H ₂ O		Total 10 ml
Adjust to pH 7.6.		

RIPA Buffer

Compound	Concentration	Quantity
1 M NaCl	0.15 M	15 ml
10% Sodium Deoxycholate	0.5%	5 ml
10% SDS	0.1%	1 ml
NP-40 (or Igepal)	1%	1 ml
1 M Tris-Cl (pH 8.0)	0.05 M	5 ml
L-Methionine	2 mM	0.03 g
H ₂ O		Total 100 ml

2X SDS Sample Buffer

Compound	Concentration	Quantity
Trizma Base	12 mM	0.0726 g
SDS	6% w/v	3 g
Glycerol	20%	10 ml
Bromophenol Blue	0.03%	0.015 g
H ₂ O		Total 50 ml
Adjust to pH 6.8.		

Solution A

Compound	Concentration	Quantity
Trizma Base	3 M	36.33 g
H ₂ O		Total 100 ml
Adjust to pH 8.8. Autoclave.		

Solution B

Compound	Concentration	Quantity
Trizma Base	500 mM	6.055 g
H ₂ O		Total 100 ml
Adjust to pH 6.8. Autoclave.		

10X Staining Solution

Compound	Concentration	Quantity
Coomassie Brilliant Blue R-250	2.5%	12.5 g
Methanol	45%	225 ml
Glacial Acetic Acid	10%	50 ml
H ₂ O		Total 500 ml
Dilute to 1X working concentration with Destain Solution.		

1 M Tris-Cl

Compound	Concentration	Quantity
Tris-Cl	1 M	7.88 g
H ₂ O		Total 50 ml
Adjust to pH 8.0. Autoclave.		

2.2.5. Tissue Culture

Electroporation Medium

Compound	Concentration	Quantity
100 mM D-Glucose	10 mM	1 ml
0.1 M DTT	1 mM	100 µl
RPMI 1640		Total 10 ml

MEM

Compound	Concentration	Quantity
MEM Powdered Medium	-	1 sachet
Penicillin/Streptomycin	50 IU/ml	10 ml
NaHCO ₃	44.04 mM	2.2 g
H ₂ O		Total 1000 ml
Adjust to pH 6.5. Filter sterilise.		

14.5% Metrizamide

Compound	Concentration	Quantity
Metrizamide	14.5% w/v	7.25 g
RPMI		Total 50 ml
Filter sterilise.		

10X PBS (Phosphate Buffered Saline)

Compound	Concentration	Quantity
Na ₂ HPO ₄	161 mM	22.85 g
NaH ₂ PO ₄ .2H ₂ O	40.1 mM	6.25 g
NaCl	1.2 M	70 g
H ₂ O		Total 1000 ml
Dilute to 1X working concentration and autoclave.		

RPMI 1640

Compound	Concentration	Quantity
RPMI 1640 Powdered Media	-	1 sachet
Sodium Pyruvate	1 mM	10 ml
Penicillin/Streptomycin	50 IU/ml	10 ml
NaHCO ₃	23.81 mM	2 g
HEPES	9.99 mM	2.38 g
H ₂ O		Total 1000 ml
Acidify with CO ₂ and filter sterilise.		

s10g

Compound	Concentration	Quantity
FCS	10%	10 ml
L-Glutamine	1%	1 ml
RPMI 1640		Total 100 ml

2.2.6. Western Blotting

5% Blotto

Compound	Concentration	Quantity
Skim Milk Powder	5%	2.5 g
PBS (pH 7.2)		Total 50 ml
Prepare fresh weekly.		

2X Laemmli Sample Buffer

Compound	Quantity
0.5 M Tris-HCl (pH 6.8)	1.25 ml
10% SDS	2 ml
10% Glycerol	2 ml
10X Protease Inhibitor Cocktail Mix	1 ml
0.05% Bromophenol Blue	500 μ l
H ₂ O	Total 10 ml
Add β -mercaptoethanol (10% v/v) for reducing gels.	

NBT

Compound	Concentration	Quantity
NBT	75 mg/ml	75 mg
70% DMF		Total 1 ml
Store away from light in foil at -20°C.		

PBS-FT Antibody Buffer

Compound	Quantity
PBS (pH 7.2)	45 ml
FCS	5 ml
Tween-20	25 μ l
	Total 50 ml

PBS

Compound	Quantity
NaCl	8 g
Na ₂ HPO ₄	1.44 g
KCl	0.2 g
KH ₂ PO ₄	0.24 g
H ₂ O	Total 1000 ml
Adjust to pH 7.2. Autoclave.	

1 M NaCl

Compound	Concentration	Quantity
NaCl	1 M	5.844 g
H ₂ O		Total 100 ml
Autoclave.		

TBS (Tris Buffered Saline)

Compound	Quantity
Tris-HCl	2.42 g
NaCl	29.22 g
H ₂ O	Total 1000 ml
Adjust to pH 7.5.	

Transfer Buffer

Compound	Quantity
Trizma Base	6.06 g
Glycine	28.8 g
Methanol	400 ml
H ₂ O	Total 2000 ml

1 M Trizma

Compound	Concentration	Quantity
Trizma Base	1 M	12.114 g
H ₂ O		Total 100 ml
Adjust to pH 9.5. Autoclave.		

Western Substrate Buffer

Compound	Quantity
1 M Trizma Base (pH 9.5)	5 ml
1 M NaCl	5 ml
1 M MgCl ₂	5 ml
H ₂ O	Total 50 ml
Prepare fresh on day.	

Western Substrate Solution

Compound	Quantity
XPO ₄	35 µl
NBT	45 µl
Western Substrate Buffer	Total 10 ml
Prepare fresh on day.	

XPO₄

Compound	Concentration	Quantity
XPO ₄	50 mg/ml	50 mg
DMF		Total 1 ml
Store away from light in foil at -20°C.		

2.2.7. Flow Cytometry

FACS Lysing™ Solution

Compound	Quantity
FACS Lysing™ Solution	10 ml
H ₂ O	Total 100 ml

FACS Wash Buffer

Compound	Quantity
Sodium Azide	2 g
FCS	10 ml
PBS	Total 500 ml

2.2.8. Isolation of Genomic DNA

Proteinase K

Compound	Concentration	Quantity
Proteinase K	10 mg/ml	100 mg
H ₂ O		Total 10 ml
Store at - 20°C.		

TES

Compound	Concentration	Quantity
1 M Tris-HCl (pH 8.0)	10 mM	100 µl
1 M EDTA	1 mM	10 µl
1 M NaCl	100 mM	1 ml
H ₂ O		Total 10 ml

2.3. Methods

2.3.1. Total RNA Extraction

This protocol is based on the RNA extraction method developed by Chomczynski and Sacchi (124). All steps were carried out in the fume hood, and the RNA samples kept on ice to prevent degradation of RNA.

To each 1.5 ml tube containing cell lysate ($1-5 \times 10^6$ cells in 500 μ l of solution D), 50 μ l of 2 M sodium acetate (pH 4.0), 500 μ l of water saturated phenol (RNA phenol) and 200 μ l of 49:1 chloroform:isoamyl alcohol were added. The solution was vortexed and the tubes were incubated on ice for 15 min before microfuging at 13,000 rpm for 30 min at 4°C.

RNA, in upper aqueous layer, was transferred to a new 1.5 ml tube and 500 μ l of isopropanol was added. The tubes were vortexed and placed at -70°C for 15 min before a 30 min spin at 4°C was performed. The supernatant was then decanted in the fume hood, and the RNA pellet was dissolved in 300 μ l of solution D and 300 μ l of isopropanol. The samples were then vortexed and placed at -70°C for 15 min.

The tubes were microfuged for 10 min at 4°C, and the isopropanol/solution D was decanted. The pellet was then washed with 2 x 10 min washes in 1 ml of cold 75% ethanol. The ethanol was then decanted and the tubes were microfuged briefly. Remaining ethanol was removed using a pipette and the RNA was left to dry.

The RNA pellet was then resuspended in 10 μ l of DEPC-treated water and heated at 65°C for 10 min. The tubes were microfuged briefly and the RNA was then quantitated spectrophotometrically.

2.3.2. Spectrophotometric Nucleic Acid Quantitation

Samples were diluted 1/50 in Milli-Q water for DNA, and DEPC-treated water for RNA. Fifty microlitres of sample was then analysed using a Beckman DU-600 spectrophotometer. The concentration of nucleic acid was calculated using the following formula:

concentration = optical density x dilution factor x conversion factor

An example for an RNA solution with an OD = 0.1259:

$$\frac{0.1259 \times 50 \times 40}{1000} = 0.252 \mu\text{g}/\mu\text{l}$$

Conversion factors: OD_{260 nm} = 1 for DNA = 50 µg/ml

for RNA = 40 µg/ml

NOTE: Milli-Q water is ultrapure water produced using a Millipore Milli-Q Ultrapure Water System.

2.3.3. Reverse Transcription

Master mix was prepared on ice in the PCR room, adding reagents in the order shown:

	Per reaction
Milli-Q H ₂ O	21 µl*
5X 1st Strand Buffer	8 µl
10 mM dNTPs	4 µl
RNAsin (40 U/µl)	1 µl
MMLV Reverse Transcriptase (200 U/µl)	<u>1 µl</u>
	35 µl

***NOTE:** When RNA was not 1 $\mu\text{g}/\mu\text{l}$ the volume of water was adjusted for each tube to give a final volume of 40 μl in the RT reaction.

Oligo dT (1 $\mu\text{g}/\mu\text{l}$) was aliquoted at 4 μl per tube, and in the main laboratory 1 μg of RNA was added to each tube, keeping tubes on ice. Oligo dT and RNA were mixed gently and incubated in a waterbath at 60°C for 5 min. The tubes were microfuged briefly and transferred to ice. Master mix was added at 35 μl per tube, mixed in gently, and the tubes were briefly microcentrifuged. Tubes were then incubated in a waterbath at 37°C for 1 hour.

At the end of this time the tubes were transferred to a second waterbath and incubated at 70°C for 10 min to inactivate the enzymes. The tubes were transferred directly to ice and microfuged briefly before opening. Sterile water was then added (60 μl per tube) to give a final volume of 100 μl .

2.3.4. Polymerase Chain Reaction (PCR)

A master mix was made with addition of the reagents in the order given. In a 0.5 ml tube, for each 25 μl reaction:

Milli-Q H ₂ O	16.4 μl
10X PCR Buffer	2.5 μl
25 mM MgCl ₂	2.5 μl
Primer 1 (100 μM)	0.25 μl
Primer 2 (100 μM)	0.25 μl
10 mM dNTPs	0.5 μl
AmpliTaq [®] Polymerase (5 U/ μl)	<u>0.1 μl</u>
	22.5 μl

In the main laboratory, 2.5 μl of cDNA was added per tube and 1 drop of mineral oil was overlaid on the mixture to prevent evaporation. The tubes were vortexed to mix and then microfuged briefly before placing them into a Perkin-Elmer

TC1 Thermal Cycler. Cycling conditions for the different types of PCR are given in **Appendix IV**.

2.3.5. KlenTaq Polymerase PCR for cDNA Cloning

The KlenTaq polymerase mix contains a modified Taq polymerase enzyme and a proofreading polymerase, and is specifically designed for use in cloning.

The amplification of all cDNAs for cloning was carried out using the conditions cited in **Appendix IV**. The master mix was prepared as follows:

Milli-Q H ₂ O	36 μ l
10X PCR Reaction Buffer	5 μ l
10 mM dNTPs	1 μ l
Primer 1 (100 μ M)	1 μ l
Primer 2 (100 μ M)	1 μ l
KlenTaq Polymerase Mix	<u>1 μl</u>
	45 μ l

Human or ovine cDNA (5 μ l) was added as appropriate and the reactions overlaid with 2 drops of mineral oil. The tubes were vortexed to mix and then microfuged briefly before placing them into a Perkin-Elmer TC1 Thermal Cycler.

2.3.6. Agarose Gel Electrophoresis

DNA grade agarose was used to make 1.5% w/v gels for PCR and restriction digest products, or 1% w/v gels for analysis of DNA plasmid preparations. Agarose was dissolved in an appropriate volume of 1X TAE buffer by heating in the microwave.

In general, 15 μ l of sample was loaded into each well. For markers this consisted of 2.5 μ l of marker, 2.5 μ l of 6X loading buffer and 10 μ l of H₂O. For PCR

products 12.5 μl of product was mixed with 2.5 μl of 6X loading buffer. When electrophoresing restriction fragments 20 μl of restricted product was loaded per well with 2.5 μl of 6X loading buffer. Electrophoresis was carried out at 100 V until the dye front had migrated two thirds of the length of the gel. All gels were then stained in ethidium bromide solution until molecular weight marker bands were clearly visible on the UV transilluminator. A photograph was then taken of the gel using Polaroid 667 film.

2.3.7. Purification of PCR and Restriction Products

Purification of the DNA is commonly necessary to remove salts, dNTPs and residual primers, which may interfere with ligase enzyme activity during the ligation of DNA into plasmid vectors.

Samples were loaded onto a 1.2% low melting point agarose Mini Gel with four lanes in the following manner:

Lane 1 – 3 μl of SPP1, 3 μl of 6X loading buffer, and 14 μl of water

Lane 2 – 3 μl of 6X loading buffer and 10 μl of PCR or 20 μl of restriction digest product

Lane 3 – 3 μl of 6X loading buffer and 20 μl of water

Lane 4 – 3 μl of 6X loading buffer and either 40 μl of PCR product or 60-80 μl of restriction product.

PCR/restriction products were electrophoresed until they had migrated approximately half of the length of the gel (dependent on the product size). Electrophoresis was carried out at approximately 75V to prevent the buffer temperature becoming too high and re-dissolving the gel. The portion of the gel with lanes 1 and 2, and half of lane 3 were removed and stained in ethidium bromide. The

remaining portion of the gel was not stained, and was covered with plastic wrap to prevent drying out. This section of the gel, with the band of interest to be purified, was not stained by ethidium bromide and exposed to UV light to minimise DNA damage.

The stained portion of the gel was visualised under UV light and a scalpel was used to make an incision in the gel on either side of the band of interest. The stained gel was then accurately aligned with the unstained section and the DNA band was then cut out and placed in a 1.5 ml tube. DNA purification was then carried out according to instructions provided with the BRESA-CLEAN kit.

When DNA was purified directly from solution the PCR product was transferred directly to a clean 1.5 ml tube, avoiding the mineral oil. The clean up was then carried out according to the BRESA-CLEAN kit instructions. Product recovery was analysed by loading 3 μ l and 5 μ l of recovered product onto a 1.5% gel and electrophoresing the samples.

2.3.8. Ligation into Cloning and Expression Vectors

DNA purified as per 2.3.7 was used in the ligation reactions. A rough estimate of DNA recovery was based on the intensity of the band under UV light and approximately 50 ng was used (1:1 ratio with cloning vector). All reactions were carried out in a 0.5 ml reaction tube.

In the main lab:

Milli-Q H ₂ O	x μ l to final volume of 20 μ l
10X Reaction Buffer	2 μ l

In the PC2 laboratory:

DNA	x μ l
T4 Ligase (3 U/ μ l)	1 μ l
pGEM [®] -T Vector (50 ng/ μ l) (or pRc/CMV or pEGFP-N1)	1 μ l

The components were mixed gently by pipette and allowed to incubate O/N (overnight) at 4-8°C.

2.3.9. Restriction Digestion of DNA

In general, 0.5-1 μ g of DNA was restriction digested per reaction. For mini-prep plasmid DNA, 10-12 μ l was generally digested.

Single restriction digestion:

DNA	x μ l
10X Buffer	2 μ l
Enzyme	1 μ l
Milli-Q H ₂ O	to 20 μ l

Double restriction digestion:

DNA	x μ l
10X Buffer 1	1 μ l
10X Buffer 2	1 μ l
Enzyme 1	0.5 μ l
Enzyme 2	0.5 μ l
Milli-Q H ₂ O	to 20 μ l

The reaction was then mixed gently by pipette and microfuged briefly before incubation for a minimum of 3 hours at 37°C. For practicality, some incubations were carried out O/N at the same temperature.

2.3.10. Manufacture of Competent *E. coli* TG1 α

A stock flask of TG1 α bacteria was initially prepared by inoculation of 5 μ l of glycerol stock into 100 ml of luria broth (LB). Flasks were incubated in a shaking waterbath at 37°C O/N. Fifty microlitres of the overnight culture was then inoculated into a further 100 ml of LB and the flasks incubated for approximately 4-5 hours (or until cloudy) at 37°C in a shaking waterbath to allow log phase of growth to be reached.

Bacteria were decanted into 2 x 50 ml Oakridge tubes and kept on ice for 5 min. Tubes were then centrifuged for 5 min at 5000 rpm in a SORVALL[®] centrifuge at 4°C. The supernatant was decanted and the bacterial pellet loosened by vortexing. Ice cold 50 mM CaCl₂/20 mM MgCl₂ (2.5 ml) was then added to each tube and vortexed to mix. Cells were transferred to a single tube and incubated on ice for 1 hour prior to transformation. Competent cells were always prepared fresh before each transformation.

2.3.11. Transformation of Competent *E. coli* TG1 α

A positive control plate was always included using an equivalent amount of plasmid DNA in the place of ligation mix. pBluescript[®] II KS⁺ was used as a control to indicate successful transformation. This plasmid also provided a control for the blue colour change expected of non-recombinant colonies by virtue of the β -galactosidase gene present in the plasmid.

Competent bacterial cells were transferred into 1.5 ml tubes with 200 μ l of cells added to 5 μ l of ligation mixture and mixed gently. The cells were incubated on ice for 40 min before exposed to heat shock at 42°C for 2 min and subsequently

transferred to ice for 2 min. LB containing 20 mM glucose (900 μ l) was then added to each tube, and the bacteria incubated in a shaking waterbath at 37°C for 1 hour to recover.

The tubes were then microfuged for 10 sec to pellet the bacteria and all but 150-200 μ l of the supernatant was removed carefully using a pipette. Bacteria were resuspended by gently pipetting up and down and plated onto ampicillin selective plates using a sterile alcohol-flamed spreader (cool on plate before spreading bacteria). The plates were refrigerated until ready for O/N incubation at 37°C.

NOTE: Due to the rapid growth of TG1 α bacteria the 1 hour recovery step was omitted and the bacteria were plated directly after heat shock/ice step. Plates were stored at 4°C until ready for O/N incubation. Only 11-12 hours incubation at 37°C was required as longer times resulted in overgrowth and the loss of individual colonies.

For pEGFP-N1 transformed bacteria, selective plates containing kanamycin at 30 μ g/ml were used.

2.3.12. Isolation and Characterisation of Recombinant Plasmids by PCR and Alkaline Lysis (Mini-Prep)

For pGEM[®]-T and pGEM[®]-T Easy blue (non-recombinant) and white (recombinant) colonies were observed on the plates. Disruption of the β -galactosidase gene by the ligation of the cDNA insert prevents the metabolism of the X-Gal present in the plate, resulting in white colonies. As the expression vectors pRc/CMV and pEGFP-N1 do not have the β -galactosidase gene both recombinant and non-recombinant colonies are white.

White colonies were chosen at random and inoculated into 2 ml of LB + Amp (or LB + kanamycin for pEGFP-N1 transformed bacteria) in a 10 ml yellow top tube. The bacterial culture was derived by incubation of the tubes at 37°C O/N in a shaking waterbath. One blue colony was always chosen as a negative control. The bacterial cultures used for plasmid DNA preparation were first screened by PCR for 35 cycles of amplification for the presence of the correct insert. Bacterial culture was used in place of cDNA with 2.5 µl per tube.

Approximately 1.5 ml of positive culture was decanted into a 1.5 ml tube and the remaining culture stored at 4°C. Bacteria were pelleted by microfuging for 2 min at 13,000 rpm, and the supernatant was aspirated using a pipette. The bacterial pellet was loosened by vortexing and 100 µl of cold Mini-Prep Solution 1 was added. The tubes were vortexed again and 200 µl of Mini-Prep Solution 2 at ambient temperature was added. The contents of the tubes were mixed gently by inversion, to prevent shearing of genomic DNA, and placed on ice for 10 min.

After incubation on ice, 125 µl of Mini-Prep Solution 3 was added and the tubes mixed by inversion, before a further incubation on ice for 10 min.

Samples were then microfuged for 5 min, to pellet the white precipitate, and the supernatant was transferred to a fresh 1.5 ml tube to which 2 µl of RNase A (10 mg/ml) had been added. The tubes were then incubated at 37°C for 30 min.

DNA phenol (200 µl) and chloroform (200 µl) were added to each tube and mixed in thoroughly by vortexing the tubes, before microfuging the tubes for 5 min. The upper aqueous phase was then transferred to a fresh tube and extracted with one volume (400 µl) of chloroform to remove traces of phenol. The tubes were then vortexed before microfuging for 2 min. The aqueous phase was transferred to a clean

tube and 900 μ l of 100% ethanol was added. The samples were then vortexed and incubated at -70°C for 20 min.

The DNA was pelleted by microfuging at 13,000 rpm for 10 min, and a 10 min wash in 70% ethanol was performed. The ethanol was decanted and the excess removed by pipette. DNA was allowed to dry before resuspending in 40 μ l of Milli-Q H_2O . DNA was analysed by running 10 μ l of sample on a 1% agarose gel. Three bands should be observed in all lanes indicating the different plasmid forms. Lowest band is that of supercoiled plasmid.

NOTE: Confirmation of the appropriate insert, as seen by PCR analysis, was carried out by restriction digestion of plasmid preps. For clones showing the correct insert and orientation, the bacteria were streaked on selective plates to ensure that the final plasmid was isolated from a single bacterial colony. Screening procedures were repeated and large scale, high quality plasmid preps were generated using either Qiagen or JETSTAR columns. Only plasmids with supercoiled form were chosen for final quality preps and used for sequencing and transfection.

2.3.13. Sequencing of Plasmid cDNA Inserts

DNA template was sequenced using Dye Terminator (or Big Dye™) chemistry using a Perkin-Elmer TC1 Thermal Cycler. Only one primer (3.2 picomole) per reaction was required. Sequencing results in a linear amplification of product, and 500 ng of plasmid template was used. The amplification conditions are shown in **Appendix IV**.

PCR product was transferred to a 1.5 ml tube containing 50 μ l of 95% ethanol and 2 μ l of 3 M sodium acetate (pH 5.5), vortexed and incubated on ice for 10 min. Tubes were then microfuged for 30 min at 13,000 rpm and the ethanol

removed by pipette. Pellets were washed with 70% ethanol (prepared fresh each time) and microfuging was not required. Ethanol was aspirated by pipette and samples left to air dry. **Samples should be thoroughly dry.** Sequencing gels and results were prepared by the Molecular Pathology Department, Institute of Medical and Veterinary Science, Adelaide.

2.3.14. Transfection of the CHO Cell Line with Human and Ovine p35 and p40 Plasmids

CHO cells were split 24 hours prior to transfection to ensure log phase of growth (approximately 50-70% confluent). Adherent cells were detached from the plastic flask using 2 mM EDTA, washed once with PBS and resuspended at 10^7 cells/ml in electroporation medium. Cells were mixed with 5 μ g of plasmid (5 μ g of each in double transfections) and transferred to the electroporation cuvette. Transfection was performed using a Bio-Rad Gene Pulser II Electroporator set to 0.3 kV, 950 μ F. The cells were aspirated from the cuvettes gently and transferred to 25 cm² flasks containing 6 ml of s10g. Culture supernatant ('conditioned medium') was collected at 48 hours post-transfection.

2.3.15. ³⁵S Metabolic Labelling and Immunoprecipitation of IL-12

Proteins

Cells were transiently transfected as described in 2.3.14. and allowed to become confluent. The cell monolayer was washed with PBS and then incubated for 30 min at 37°C/5% CO₂ with methionine/cysteine deficient RPMI supplemented with 1% FCS and 2% L-glutamine. Medium was then removed and deficient medium

further supplemented with 100 $\mu\text{Ci/ml}$ ^{35}S methionine/cysteine, in addition to FCS and L-glutamine, was then added and the cells incubated O/N (1.5 ml in 25 cm^2 flask). Medium was collected and 10X protease inhibitors were added. Samples were stored at -70°C until use. Each sample was pre-cleared by addition of 25 μl of heat inactivated normal rabbit serum to 500 μl of metabolically labelled culture supernatant. Pansorbin[®] (200 μl) was microfuged for 5 min. The supernatant was discarded and the pellet resuspended with the labelled culture supernatant. Samples were placed on a rotating wheel for 30 min at 4°C . Samples were microfuged for 10 min and the supernatants added to a second Pansorbin[®] pellet, prepared as above. The pre-clearing step was carried out to remove non-specific proteins. Rabbit anti-human IL-12 polyclonal antibody (25 μl) was added to each sample and incubated at 4°C O/N with rotation. Pansorbin[®] (100 μl) supplemented with 1 mg/ml ovalbumin was then added to each sample for 1 hour with rotation at 4°C . The sample pellet was washed by 2 x 15 min washes in RIPA buffer and the tubes microfuged at 6,500 rpm at 4°C . Samples were resuspended in SDS-PAGE loading buffer (50 μl) in preparation for SDS-PAGE analysis.

2.3.16. Sodium Dodecyl Sulphate-Polyacrylamide Gel Electrophoresis (SDS-PAGE)

SDS-PAGE was performed based on the method of Laemmli (125) using a Bio-Rad Mini-PROTEAN[®] II System. A 3% stacking gel and either a 10% or 12.5% resolving gel were used. Samples from the immunoprecipitation resuspended in loading buffer were boiled for 10 min and then microfuged for 5 min. Samples (25 μl /well) were then loaded onto the gel with a marker lane (commercial protein

standards in loading buffer). Each sample was overlaid with approximately 30 μ l of electrophoresis buffer to prevent eddy currents removing sample when the wells were completely covered by buffer. The electrophoresis buffer was poured into the gel tank to approximately 5 mm above the smaller glass plate.

Gels were run at 30 mA until all samples had moved to the stacking/resolving gel interface. The current was then increased to 60 mA, and the gel run until the dye front had run off the end, where electrophoresis was deemed complete.

Gels were stained in staining solution for 45 min. The stain was removed and destaining solution was added. Destain was changed approximately every 30 min until the marker became visible.

Gels were incubated for 30 min in the fluorographic signal enhancer, Amplify™, before drying. Gels were exposed to X-OMAT AR radiography film at -70°C for 7-10 days.

NOTE: Amplify™ further destains gels.

2.3.17. Isolation of Human and Ovine Peripheral Blood Mononuclear Cells

Peripheral blood was collected in 10 ml lithium-heparin tubes to prevent coagulation. Blood was then centrifuged in the tubes for 10 min and the plasma layer discarded (human - 600 rpm, ovine - 1000 rpm). Each 10 ml of blood was divided equally between four 10 ml tubes, topped up to approximately 7.5 ml with PBS and mixed. Approximately 2 ml of room temperature Lymphoprep™ was then underlaid in each tube and centrifugation was performed (human – 20 min @ 2000 rpm, ovine – 25 min @ 2400 rpm). The rotor was permitted to come to rest without active braking. The buffy cell layer was then collected and a 10 min wash in PBS at 1800

rpm was carried out. Cells were resuspended in PBS and counted using a haemocytometer. Cells were then centrifuged at 1800 rpm, the supernatant decanted, and resuspended in s10g at the appropriate density.

2.3.18. Human and Ovine Activated Mononuclear Cell IL-12

Proliferation Assays

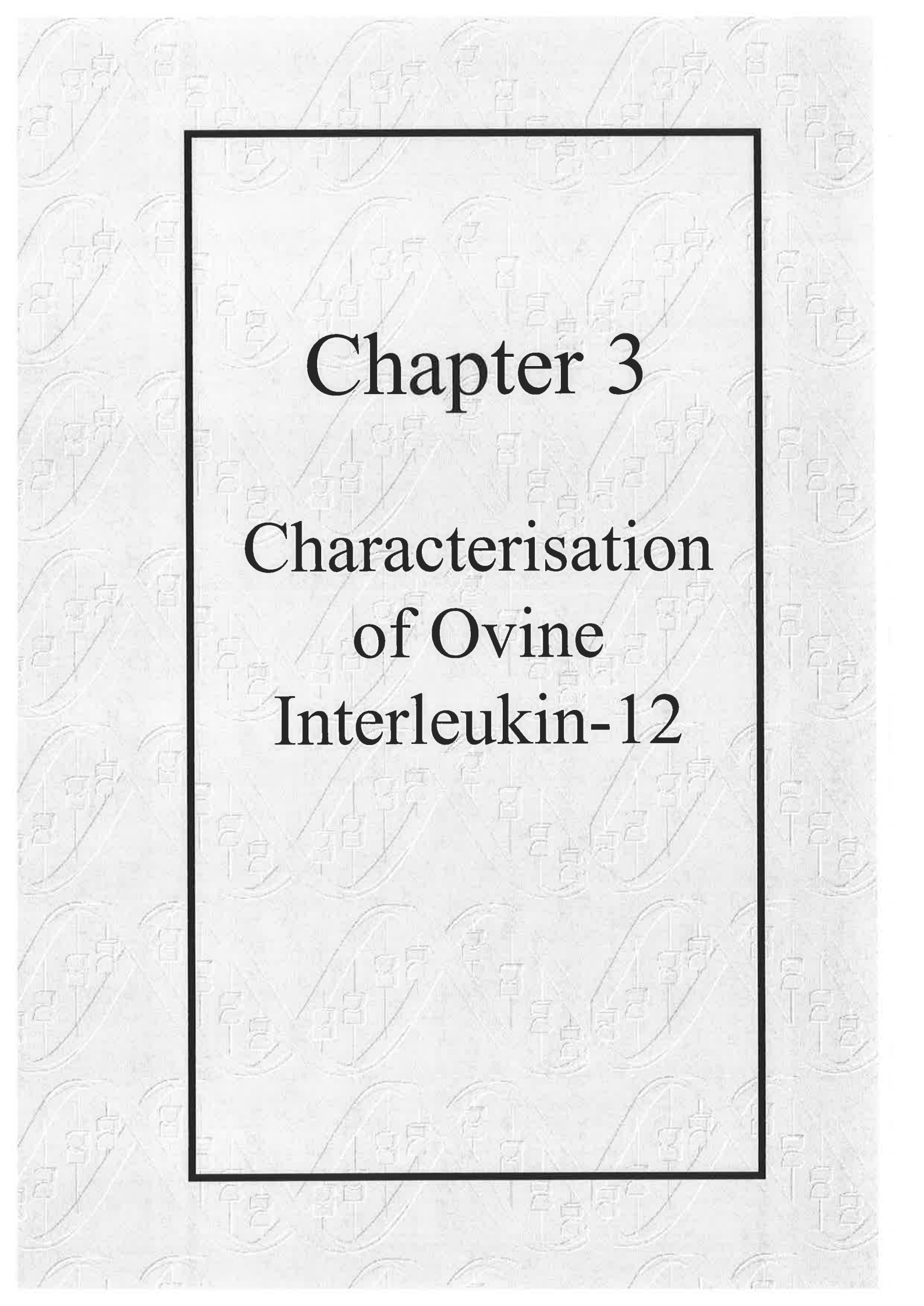
Human peripheral blood mononuclear cells were activated with PHA according to the method of Stern *et al* (2). Briefly, mononuclear cells were isolated and stimulated for 72 hours with 10 µg/ml PHA at 5×10^5 cell/ml in s10g. Cells were washed and resuspended at 4×10^5 cells/ml in s10g, and 50 µl of the cell suspension was aliquoted per well, into a 96 well plate, with or without conditioned medium as appropriate. Assay was performed in a total well volume of 100 µl. At 24 hours plates were pulsed with 50 µl of 10 µCi/ml tritiated thymidine in s10g, and incubated for a further 18 hours.

Ovine mononuclear cells were obtained from peripheral blood collected in 10 ml heparinised tubes and isolated using a Lymphoprep™ density gradient (2.3.17). The PBMNC were resuspended in s10g culture medium at 10^6 cells/ml and stimulated with 1 µg/ml Con A for 48 hours. Cells were washed, counted and resuspended at 10^6 cells/ml in s10g, and 50 µl of the cell suspension was aliquoted into each well of a 96 well plate. (NOTE: Only large blast cells were counted). Culture supernatant from CHO cell transfectants was added at a final concentration of 1.25%, 5% or 20%. The plates were incubated for 30 hours before addition of 40 µl per well of tritiated thymidine (25 µCi/ml in s10g) for a further 18 hours.

Cells were harvested using a Tomtec harvester and filters counted using a Wallac MicroBeta[®] Scintillation Counter. All samples were performed in triplicate.

Inhibition of IL-12 proliferation assays was performed using a final dilution of 1/100 of the rabbit anti-human IL-12 polyclonal antibody. An equivalent concentration of normal rabbit serum was used as a negative control.

The results are from a representative experiment with proliferation expressed as counts per minute. Students T test was performed to determine the p value.



Chapter 3
Characterisation
of Ovine
Interleukin-12

Chapter 3

Characterisation of Ovine Interleukin-12

Introduction

As described in the **Literature Review**, IL-12 is a heterodimeric cytokine composed of two disulphide-linked subunits, p35 and p40, which generate the active molecule, p70 (1). The ability of IL-12 to augment the proliferation of T cells activated by mitogenic lectins and phorbol diesters (1, 2) forms the basis of the proliferation assays used in this chapter to assess ovine and human IL-12 biological activity.

The expression of the IL-12 p70 molecule is generally determined by the expression of p35 (8, 24), and other researchers have shown that the p35 subunit provides species specificity for the human p70 heterodimer. Whereas murine IL-12 p70 is biologically active on human PHA-activated lymphoblasts, human IL-12 p70 does not show biological activity on murine Con A-stimulated splenocytes (18). Co-transfection of human p35 and murine p40 to generate chimaeric p70 showed that the p35 subunit was responsible for the IL-12 p70 species specificity (18, 126).

The principal aim of this chapter was to sequence and characterise the ovine IL-12 p35 cDNA. This follows from a previous study where the ovine p40 sequence was determined (S. Swinburne, Honours Thesis).

Aims

To characterise the structural and biological activity of ovine IL-12 by:

- i. comparing the sequence similarities of cloned ovine p35 and p40 subunits against their respective human and bovine sequences;
- ii. determining the molecular weights of each subunit, and the ovine heterodimer, by immunoprecipitation of proteins from the supernatants of CHO cells transfected with plasmids containing the ovine p35 and p40 cDNAs;
- iii. assessing the biological activity of ovine p35 and p40 subunits, and the ovine heterodimer, by enhancement of proliferation of activated peripheral blood mononuclear cells, and
- iv. characterising chimaeric heterodimers from CHO cells co-transfected with human p35/ovine p40 or ovine p35/human p40 by SDS-PAGE analysis of immunoprecipitated proteins and assessing functional activity in IL-12 proliferation assays.

Cloning Protocol

The forward primers used in PCR reactions for all cloning experiments were modified at the 5' end to include the consensus sequence GCCACC (127) to enhance mRNA translation. All cloning primer sequences are provided in **Appendix II**.

Human and Ovine p35

Human IL-12 p35 primers were designed using the sequence published by Wolf *et al* (17). Ovine p35 primers were designed based on the multiple alignment of published cDNA sequences from closely related species (bovine, goat, and deer).

Primers were designed from the resulting consensus sequence, incorporating degenerate bases where differences existed between species.

Amplification of the PCR products was performed using human or ovine cDNA and the purified products were ligated into the pGEM[®]-T cloning vector (**Figure 3.1**). Orientation of the p35 cDNA was determined using the ApaI/HindIII restriction enzymes. The PCR fragments were excised using the NotI/ApaI restriction enzymes and ligated into the pRc/CMV expression vector restricted with the corresponding enzymes.

Human and Ovine p40

The sequence of the ovine p40 cDNA was determined previously by S Swinburne (Honours Thesis, 1996), Genbank Accession number AF004024. Primers were designed by applying the strategy used for p35, that is, based on multiple alignment of p40 sequences from closely related species.

Primers to human p40 were designed based on the published sequence (17). The reverse p40 primers for ovine and human cloning were modified to include an XbaI restriction enzyme site at the 5' end of the primer to assist in further subcloning procedures. Orientation of the PCR products in the pGEM[®]-T cloning vector was determined by restriction digestion with ApaI/EcoRI (**Figure 3.2**). PCR fragments were excised using NotI/XbaI and ligated into the pRc/CMV vector cut with the corresponding enzymes.

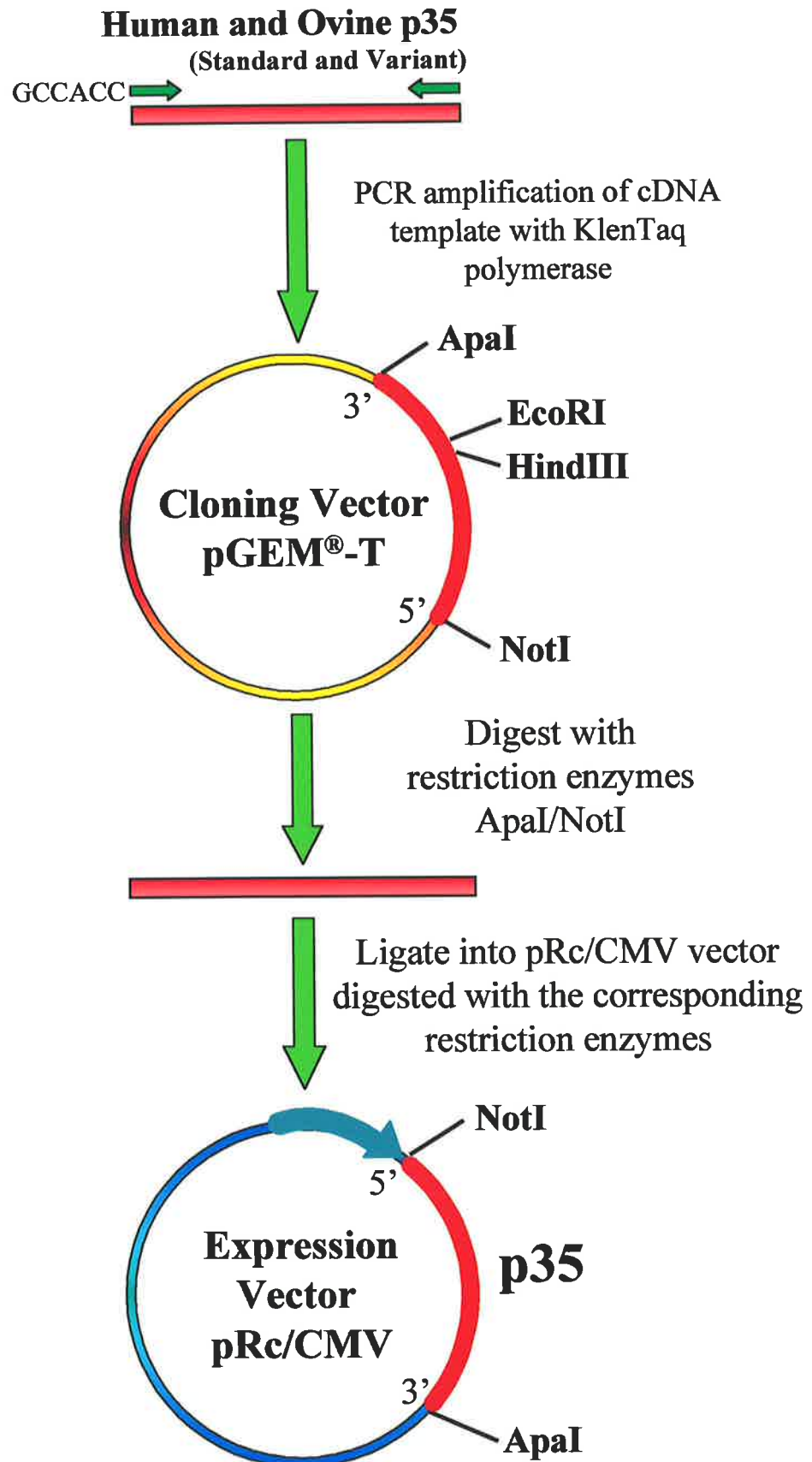


Figure 3.1. Schematic diagram of the steps required to clone the p35 cDNA into the pRc/CMV expression vector for transfection-based studies. This diagram is also relevant to cloning performed in **Chapter 5** for the variant p35 clones.

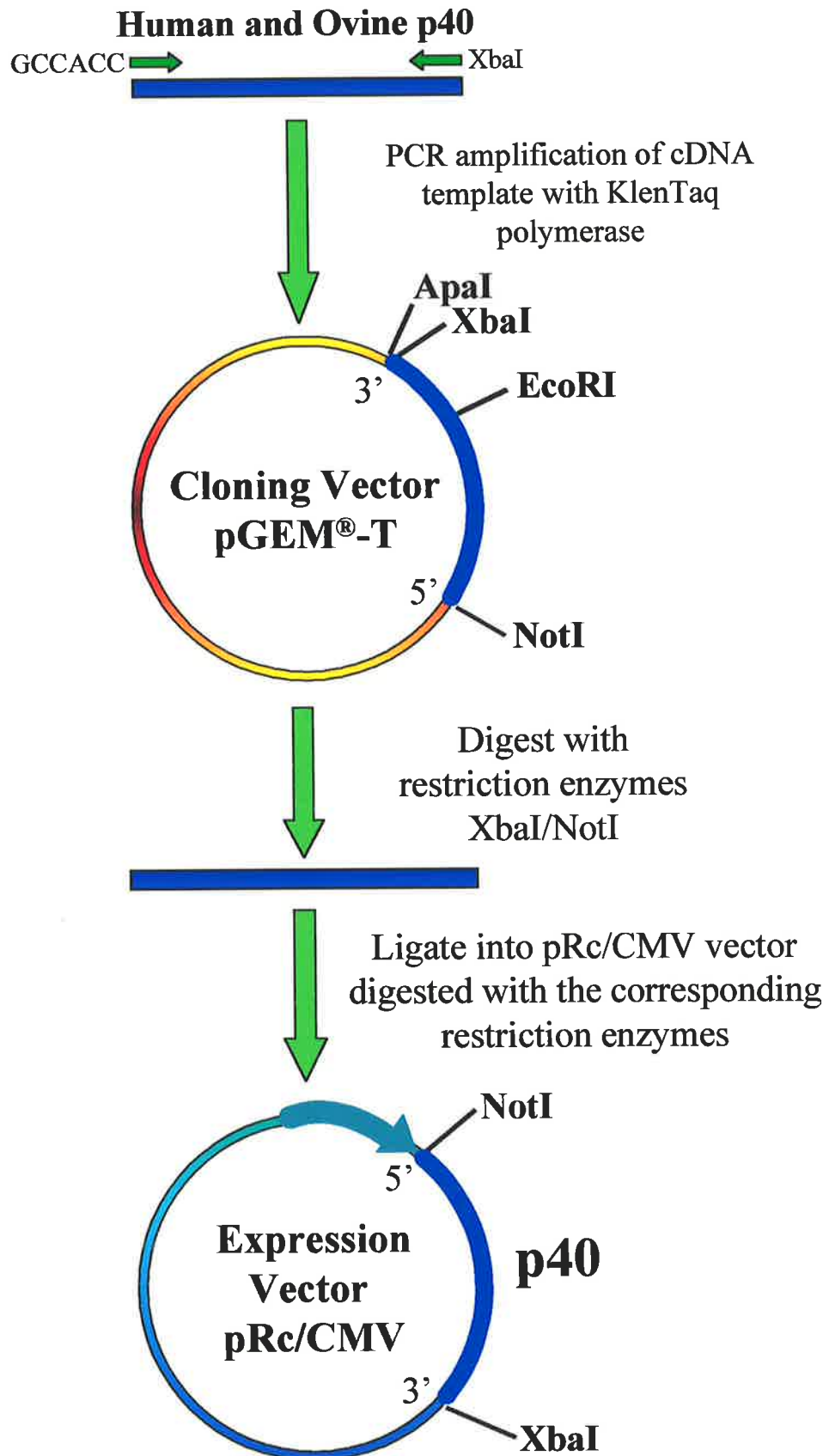


Figure 3.2. Schematic diagram of the steps required to clone the p40 cDNA into the pRc/CMV expression vector for transfection-based studies.

3.1. Results



3.1.1. *Ovine IL-12 p35 cDNA Sequence Analysis*

Complete ovine p35 cDNA sequence was obtained by sequence analysis of multiple independently isolated clones (Genbank Accession number AF173557). The open reading frame was determined to be 666 bp in length, with translation of the nucleotide sequence generating a putative ovine IL-12 p35 protein of 221 aa (**Figure 3.3**). The predicted ovine p35 protein showed 96.4% similarity to bovine p35 and 69.1% similarity to human p35 amino acid sequences. In addition, a single N-linked glycosylation site and two leucine zipper motifs were identified (128). The protein is predicted to be cleaved between positions 25-26 to yield a signal peptide (129), with 7 cysteine residues present in the mature protein. The position and number of these cysteine residues are also conserved between species. In particular, cysteine 73 is likely to participate in intermolecular disulphide bonding, a role previously ascribed to cysteine 74 in the human p35 protein sequence (4).


3.1.2. *Ovine IL-12 p40 cDNA Sequence Analysis*


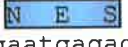

The consensus sequence for ovine p40 of 984 bp (Genbank Accession number AF004024) is shown in **Figure 3.4**. A signal peptide cleavage site is predicted between amino acids 22 and 23 with 10 cysteine residues present in the mature protein. When compared to the known protein sequences of human and bovine p40 the number of cysteine residues are conserved. In particular, the cysteine residue at position 178 of ovine p40 is predicted to play an equivalent role in intermolecular disulphide bonding with ovine p35 to cysteine 177 in human p40, which has been assigned this function (4). A single N-glycosylation site is also present.


M C P L R S L L L I S T L V L L H H L P
atgtgcccgcttcgcagcctcctcctcatatccaccctggttctcctccaccacctgccc
1


H L S L G  R S L P T T T A G P G T S  L
cacctcagtttgggcaggagcctgcccaccaccacagcaggcccaggaacgagttgcctt
61

D Y S Q N L L R A V S N T L Q K A R Q T
gactactccaaaacctgctgagggccgtcagcaacacgctgcagaaggccagacaaacc
121

L E F Y S  T S E E I D H E D I T K D K
ctagaattttactcctgcacttctgaggagattgatcatgaagatatcacciaagataaa
181


T S T V E A  L P L E L A T  ⁷³ L A
accagcacagtgaggcctggtttaccactggaattagccacgaatgagagttgcctggct
241

S R E T S L I T N G H  L S S G K T S F
tccagagagacctcttaataactaatgggcattgtctgtcttctggaagacctctttt
301

M T T L  L R S I Y K D L K M Y H M E F
atgacaaccctgtgccttagaagtatctacaaggacttgaagatgtatcacatggagttc
361

Q A M N A K L L M D P K R Q V F L D Q N
caggccatgaatgcaaagcttctgatggatcctaagaggcaagtctttctagaccagaac
421

M L A A I A E L M Q A L N F D S E T V P
atgctggcagctattgctgagctaatgcaggccctgaatttcgacagtgagactgtgcca
481

Q K P S L E E L D F Y K T K V K L  I L
cagaaaccctccctggaagaactggattttataagacaaaagtcaagctctgcacccct
541

L H A F R I R A V T I D R M M S Y L S S
cttcacgccttcagaattcgtgcggtgaccatcgacagaatgatgagctatctgagttct
601


S 
tcctag
661

Figure 3.3. Ovine p35 nucleotide and protein sequence. The signal peptide cleavage site is shown by the **red** arrow between amino acids 25 and 26. All cysteine residues in the mature protein are marked with **yellow** circles. Cysteine 73 (mature protein position) is marked with a **green** circle and is adjacent to the **blue** boxed N-glycosylation site. The two leucine zipper motifs (40-61 and 92-113) are marked with **dark red** italic text.

M H P Q Q L V V S W F S L V L L A S P I
 atgcaccctcagcagttggcgttttccctggtttctgctggcatcgccatc
1
 V **A** I W E L E K N V Y V V E L D W Y P N
 gtggccatattgggaactggagaaaaatgtttatgtttagaattggattggtatccta
61
 A P G E T V V L T **C** D T P E E D G I T W
 gctcctggagaaacagtggcctcactgtgacactcctgaagaagacggcatcacctgg
121
 T S D Q S S E V L G S G K T L T I Q V K
 acctcagaccagagcagtgaggtcctgggctctggcaaaccttgaccatccaagtcaa
181
 E F G D A G Q Y T **C** H K G G E V L S R S
 gagtttgagatgctgggcagtcacactgtcacaaggaggcaggttctgagtcgttca
241
 L L L L H K K E D G I W S T D I L K D Q
 ctctcctgctgcacaaaaggaagatggaatttggccactgatattttaaggatcag
301
 K E P K A K S F L K **C** E A K D Y S G H F
 aaagaacccaagctaagagtttttaaaatgtgaggcaaaggattattctggacacttc
361
 T **C** S W L T A I S T N L K F S V K S S R
 acctgctcgtggctgacagcaatcagtactaatctgaaattcagtggtcaaaagcagcaga
421
 G S S D P R G V T **C** G A A S L S A E K V
 ggctcctctgacccccgaggggtgacgtgaggagcagcgtccctctcagcagagaaggtc
481
 S M D H R E Y N K Y T V E **C** Q E G S A **C** **178**
 agcatggaccacagggagtataacaagtacacagtgagggtgtcaggagggcagtgctgc
541
 P A A E E S L P I E V V M E A V H K L K
 ccggccgagagagagcctgccattgaggtcgtgatggaagctgtgcacaagctcaag
601
 Y E **N Y T** S S F F I R D I I K P D P P K
 tatgaaaactacaccagcgttcttcatcaggacatcatcaaaccagaccaccaag
661
 N L Q L R P L K N S R Q V E V S W E Y P
 aacctgcaactgagaccactaaagaattctcggcaggtggaagtcagctgggagtagcct
721
 D T W S T P H S Y F S L T F **C** V Q V Q G
 gacacgtggagacccccacattcctacttctccctgacgttttgtgttcaggtccagga
781
 K N K R E K K L F T D Q T S A K V T **C** H
 aagaacaagagagaaaagaactcttcacagaccaaactcagccaaagtcacatgccac
841
 K D A N I R V Q A R D R Y Y S S F **W S E**
 aaggatgccaacatccgctgcaagcccggaccgctactacagctcattctggagtgaa
901
W A S V S **C** S **STOP**
 tgggcatctgtgtcctgcagttag
961

Figure 3.4. Ovine p40 nucleotide and protein sequence. The signal peptide cleavage site is shown by the red arrow between amino acids 22 and 23. All cysteine residues in the mature protein are marked with yellow circles. Cysteine 178 (mature protein) is marked with an orange circle and the N-glycosylation site is marked by a blue box. The green boxes indicate the WSEW C-mannosylation site. Sequence as determined by S Swinburne, Honours Thesis, "Cloning and Characterisation of the Ovine Interleukin-12 p40 Subunit", 1996.

Recently human IL-12 was shown to be the second example of a C-mannosylated protein (31). The C-mannosylation occurred at positions 319-322 with the amino acid sequence WSEW. Analysis of the ovine p40 amino acid sequence revealed this same WSEW motif at positions 318-321, suggesting that the ovine p40 subunit may undergo C-mannosylation.

3.1.3. Immunoprecipitation of Ovine and Chimaeric IL-12 Proteins

CHO cells were co-transfected with plasmids containing the ovine p35 and p40 cDNA inserts to generate ovine IL-12 heterodimer. In addition, transfection of cells with p40 and p35 plasmids alone was performed. Ovine p35 protein could not be immunoprecipitated from the culture supernatant of the p35 single transfectant using the rabbit anti-human polyclonal antibody (**Figure 3.5A i and ii**). This was consistent with the observation that human p35 subunit protein could not be precipitated from either cell lysate or supernatant using this same antibody (data not shown). This result is not unexpected as poor recognition of the p35 subunit by antibodies has been reported (6, 29).

A protein of 40-45 kDa was precipitated from the ovine p40 transfectant, although homodimers of ovine p40 were not detected in the supernatant of CHO cell transfectants (**Figure 3.5A i and ii**). This was also consistent with the observation that human p40 homodimers could not be detected from human p40 transfected cells (data not shown). Immunoprecipitation of co-transfected cells showed the presence of two bands at approximately 70 kDa as well as bands corresponding to dissociated p35 and p40. When the ovine IL-12 heterodimer was resolved on a 10% SDS-PAGE gel the two bands were more apparent, having estimated molecular weights of 60 and

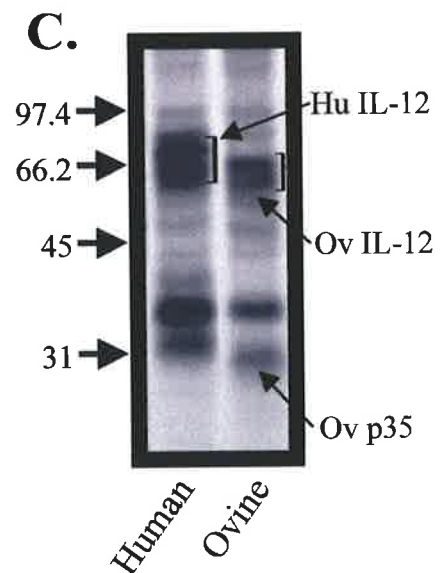
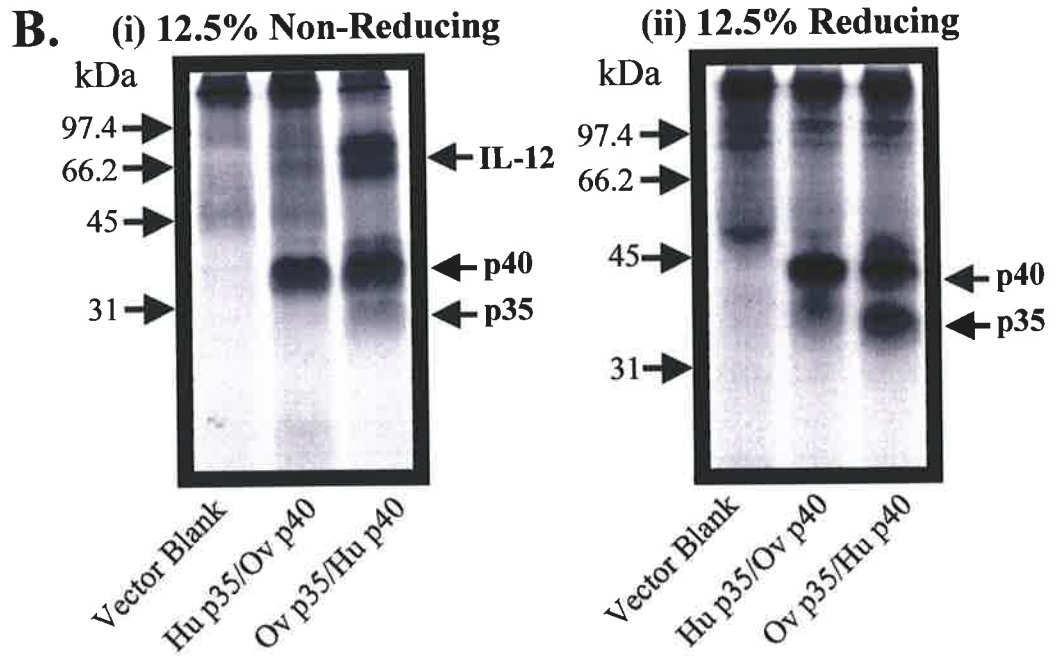
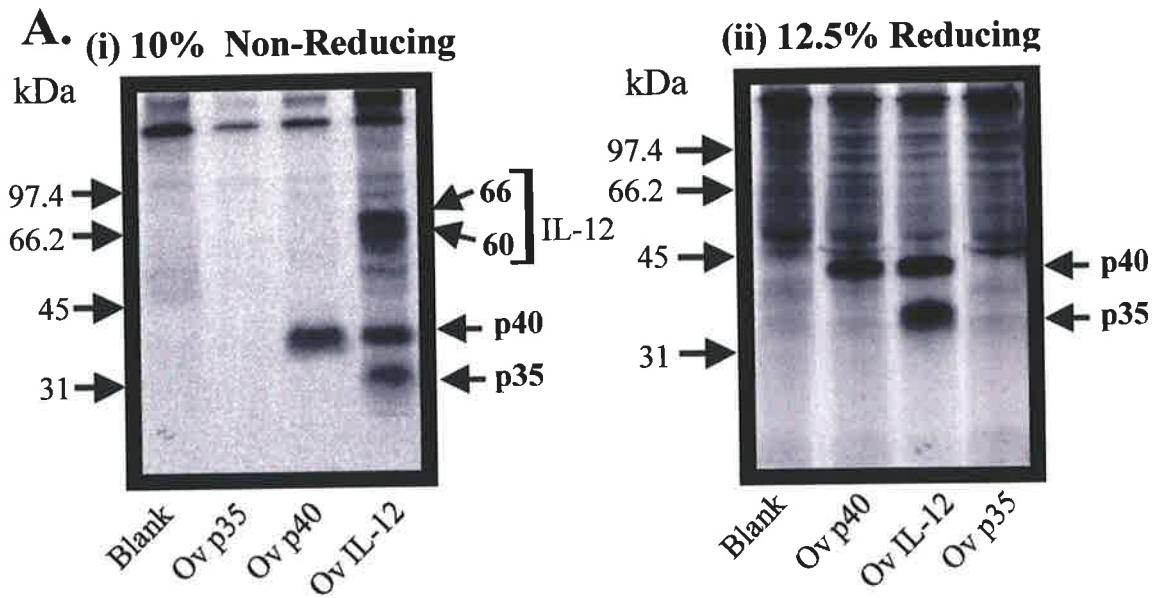


Figure 3.5. Autoradiograph of IL-12 proteins from CHO cell transfectant supernatant. Recombinant proteins were labelled with ^{35}S -methionine/cysteine and immunoprecipitated using a rabbit anti-human IL-12 polyclonal antibody. **A.** Ovine IL-12 proteins. **B.** Chimaeric IL-12 heterodimers. **C.** Comparison of human and ovine IL-12 heterodimers under non-reducing conditions shows the lower molecular weight of ovine p35 and heterodimer.

66 kDa. Under reducing conditions, the heterodimer dissociated into the two subunits of 29 ('p35') and 40 kDa (**Figure 3.5A ii**).

Human/ovine chimaeric heterodimers were also immunoprecipitated using the polyclonal antibody (**Figure 3.5B i and ii**). Both chimaeric co-transfectants precipitated a heterodimeric doublet, as well as the expected p35 and p40 subunits. Under reducing conditions the heterodimer dissociated into two bands corresponding to p35 and p40 (**Figure 3.5B ii**).

Comparison of the human and ovine IL-12 heterodimers revealed that the human heterodimer also resolved into two discrete bands, although the proteins were of higher molecular weights (65 and 70 kDa) than those of the ovine heterodimer (**Figure 3.5C**). This difference was due to the lower molecular weight of the ovine 'p35' protein.

3.1.4. Biological Activity of Ovine and Chimaeric Interleukin-12 Heterodimers

Freshly isolated PBMNC were stimulated with the appropriate mitogen (ovine - Con A, human - PHA) and incubated with culture supernatants from the transfected cells (hereafter referred to as conditioned medium). Con A was chosen as the agent for stimulation of ovine PBMNC. Ovine cells were more responsive to ovine and human IL-12 conditioned medium in the proliferation assays when activated with Con A compared to PHA (data not shown). Furthermore, Con A has been used to activate cells in murine IL-12 proliferation assays (18, 126).

Conditioned medium from CHO cells transfected with expression vector plasmids containing either p35 or p40, but not both, did not enhance the proliferation of activated PBMNC. This was the case whether the expression vectors contained

human or ovine cDNA inserts. A similar response to that of the vector blank transfectant medium was observed (data not shown). Ovine IL-12 heterodimer from co-transfected cells enhanced the proliferation of ovine Con A-stimulated PBMNC (**Figure 3.6A**). Correspondingly, human IL-12 augmented ovine PBMNC proliferation. In both instances a similar level of proliferation was achieved for the cross-species and the native IL-12 heterodimer. To confirm this observation, hu p35/ov p40 and ov p35/hu p40 chimaeric heterodimers were generated and tested in the proliferation assays. As shown in **Figure 3.6A**, conditioned medium from both chimaeric heterodimers was active on mitogen-activated ovine PBMNC.

Specificity of the proliferative response induced by the IL-12 heterodimers was confirmed by blockade with the rabbit anti-IL-12 polyclonal antibody (**Figure 3.6B**). The anti-IL-12 polyclonal antibody was able to significantly inhibit ($p < 0.05$) human IL-12-enhanced ovine cell proliferation, reducing the counts to vector blank levels. The antibody was equally effective in reducing the proliferation induced by both hu p35/ov p40 and ov p35/hu p40 chimaeric molecules, however minimal inhibition of conditioned medium from the ovine co-transfectant was observed.

Ovine, human and chimaeric IL-12 heterodimers were all capable of enhancing the proliferation of human PHA-activated PBMNC (**Figure 3.7A**). The polyclonal antibody was also able to inhibit cellular proliferation when human or chimaeric (hu p35/ov p40 or ov p35/hu p40) conditioned medium was used in the assay (**Figure 3.7B**). Minimal inhibition, using the polyclonal antibody, was observed for ovine IL-12-enhanced proliferation of human PHA-activated cells. This was consistent with the result observed for the ovine Con A-activated cells.

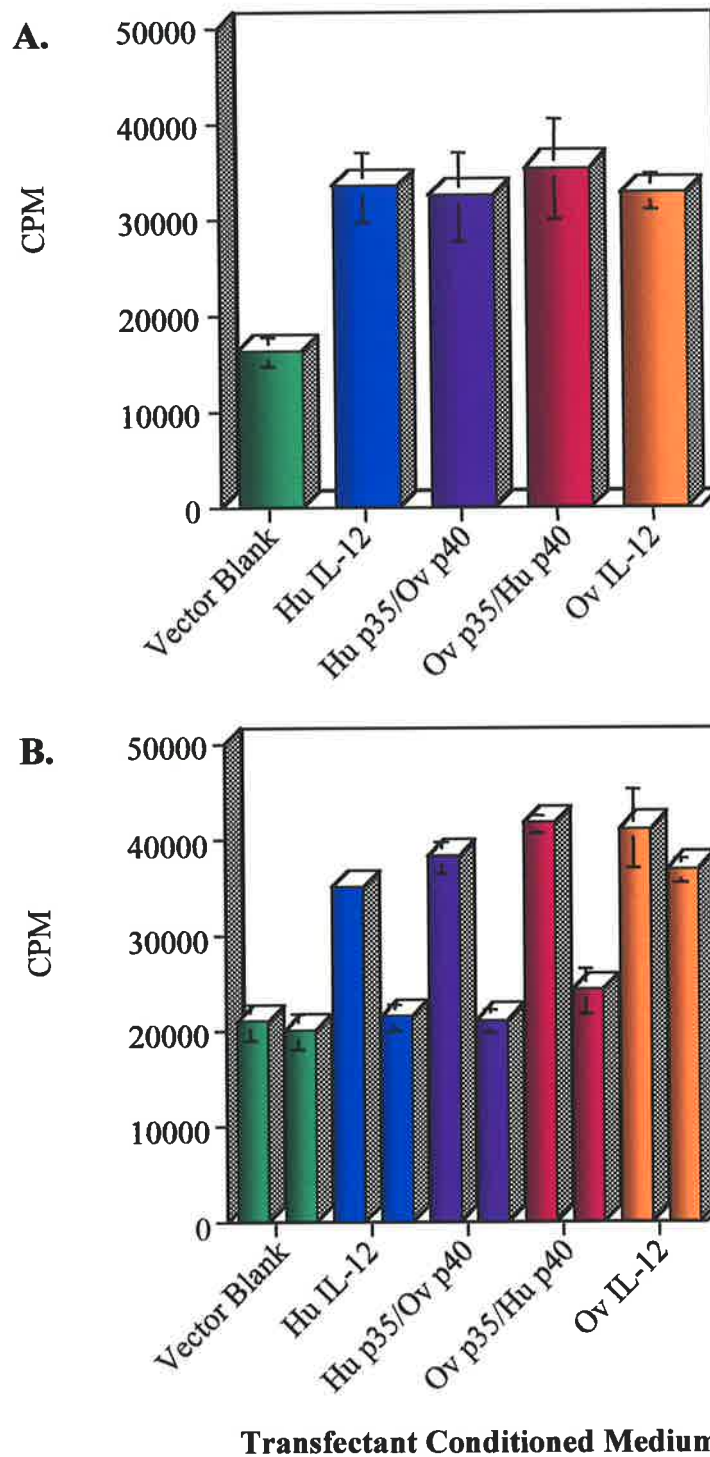
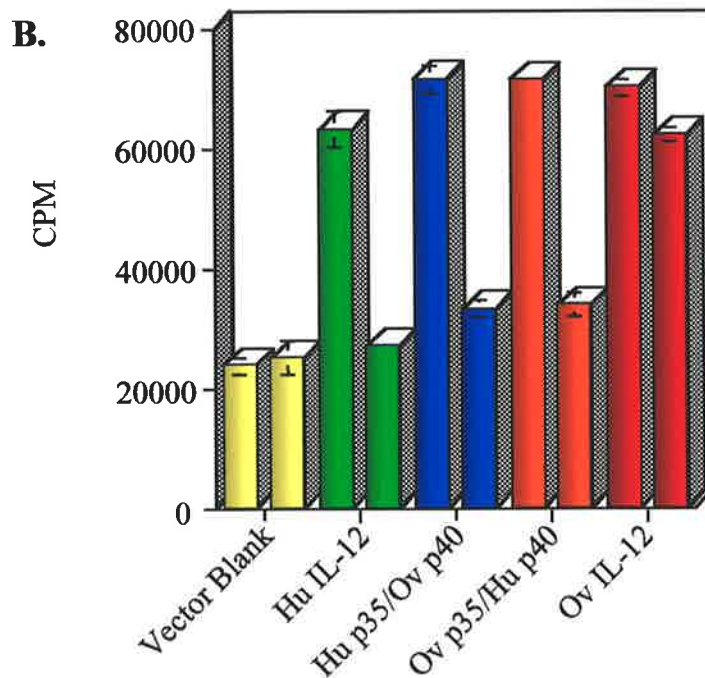
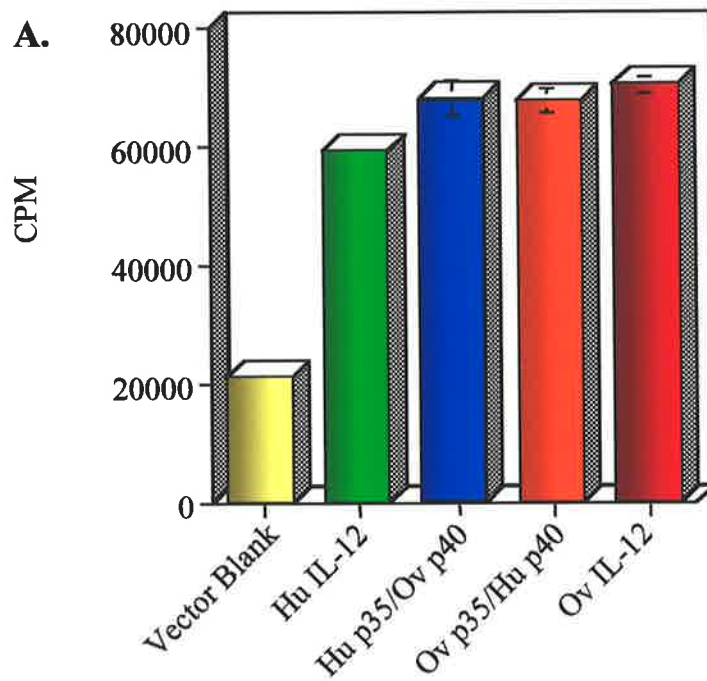


Figure 3.6. Ovine Con A proliferation assay. Conditioned medium was collected from IL-12 transient co-transfectants, with vector blank transfected CHO cell conditioned medium used as a negative control. **A.** A representative experiment using 1.25% conditioned medium is shown (each treatment performed in triplicate). **B.** Left columns indicating normal rabbit serum control and right columns showing inhibition of proliferation with addition of the rabbit anti-human IL-12 polyclonal antibody.



Transfectant Conditioned Medium

Figure 3.7. Human PHA proliferation assay. Conditioned medium from IL-12 transient CHO cell co-transfectants was used, with vector blank conditioned medium as a negative control for the assays. **A.** A representative experiment using 1.25% conditioned medium is shown (each treatment performed in triplicate). **B.** Left columns indicating normal rabbit serum control and right columns showing inhibition of proliferation with addition of the rabbit anti-human IL-12 polyclonal antibody.

Discussion

As described in the **Literature Review** IL-12 may actively participate in allograft rejection. The main aim of characterising ovine IL-12 lies in the ultimate use of IL-12 antagonists to inhibit allograft rejection in a sheep model of renal transplantation, with particular emphasis on utilising the antagonistic properties of the p40 subunit. Although the biological activities of human and murine IL-12 are well established, characterisation of ovine IL-12 is necessary to demonstrate an equivalent biological function of both ovine heterodimer and IL-12 p40. The ovine renal allograft model employed by our laboratory has distinct advantages over mouse models. Sheep are of a similar physical size allowing greater ease of manipulation for surgical procedures and sample collection (G. Patrick, Ph.D. Thesis). In addition, modifying agents such as cytokine antagonists can be tested in an outbred model that mimics the human transplant situation, as compared to transgenic or highly inbred mouse strains (130). To demonstrate the biological activity of ovine IL-12 an *in vitro* assay, the Con A proliferation assay, was developed. As ovine IL-12 heterodimer was not commercially available, cloning and sequencing of ovine p35 and p40 became necessary. For comparison, human IL-12 p35 and p40 were also cloned and recombinant protein generated by transfection of the CHO cell line.

Translation of the ovine p35 cDNA sequence predicted a protein of 221 amino acids in length. Signal cleavage is predicted to occur between amino acids 25-26 with 7 cysteine residues then expected to be present in the mature protein. The length of the nucleotide sequence was consistent with that of closely related species. However, human and murine mRNA transcripts with alternative transcription start sites have been identified (25, 26). This suggests that the ovine transcript identified here may be only one of several possible transcripts. Other mRNA species may be

identified with cDNA generated from different cell types or cells such as macrophages stimulated with LPS. Construction of ovine cDNA libraries from cells stimulated with different activators such as LPS or PHA would aid in the isolation of such transcripts.

A single N-linked glycosylation site is present in ovine p35, and this site is adjacent to the cysteine residue at position 73 (**Figure 3.3**). This cysteine is in the equivalent position to cysteine 74 of the human p35 protein and is likely to be involved in intermolecular disulphide bonding. This glycosylation site is conserved across multiple divergent species (human, murine, deer, feline and ovine as determined by sequence analysis using the ScanProsite program (128)) suggesting that glycosylation at this site is necessary for the function of IL-12 p35. As this site is adjacent to the cysteine residue involved in the formation of the intermolecular disulphide bond, glycosylation may be required for bond formation. That is, appropriate confirmation of the molecule may be acquired upon glycosylation at this site, aiding the interaction of p40 with this cysteine residue. Equally, glycosylation of this site may be required for effective secretion of the p35 protein (27). The importance of this site could be assessed by site directed mutagenesis of the nucleotide sequence to destroy the N-glycosylation site. The effect of the loss of this site on the ability to form heterodimers or to secrete p35 protein from the cells could then be ascertained.

Likewise, the ovine p40 cDNA shows a high degree of similarity to bovine and human IL-12 p40 including conservation of protein motifs such as an N-glycosylation site. The most relevant feature is the conservation of the cysteine residue at position 178. This is the equivalent position to the human cysteine residue responsible for intermolecular disulphide bond formation of the human p70

heterodimer (4). The conservation of these cysteine residues in ovine p35 and p40 suggests that ovine heterodimer formation occurs in a similar manner. Furthermore, conservation of all other cysteine residues between species would predict similar protein folding. This is supported by the cross-species biological activity of human and ovine heterodimers, and further corroborated by the functional activity of human/ovine chimaeric heterodimers on both human and ovine activated PBMNC. Although the p35 subunit has previously been shown to account for the inability of human IL-12 heterodimers to show functional activity on murine Con A-activated splenocytes, human and ovine subunits have an overall higher degree of similarity than do human and murine. This level of similarity is likely to result in the conservation of amino acids in regions involved in the receptor/heterodimer interaction, resulting in signal transduction and the subsequent proliferative response observed.

The availability of both human and ovine p35 and p40 genes in an expression vector allowed the assessment of protein molecular weights and biological activity of ovine and human heterodimers on activated ovine and human PBMNC. This also allowed the generation of chimaeric heterodimers, which could be tested in a similar manner.

Analysis of the proteins precipitated from the ovine p35 transfectant supernatant or lysate using the rabbit anti-human antibody failed to reveal a 35 kDa protein, a finding that was consistent with that of human p35. However, the inability to generate antibodies which effectively recognise the p35 protein alone has been noted (6, 29). The presence of this lower molecular weight p35 band in co-transfected cells is likely to result from the dissociation of the IL-12 heterodimer. This observation is substantiated by the p35 EGFP-fusion studies described in

Chapter 5. Autoradiographs of immunoprecipitated proteins from co-transfected cells revealed bands corresponding to p35, p40 and the IL-12 heterodimer. The ovine heterodimeric proteins migrate to lower molecular weights when compared to their human counterparts. This is due to the observed lower molecular weight of the ovine equivalent of human p35 (**Figure 3.5C**). An explanation for this difference may be the longer coding sequence of human p35, which is 762 bp, compared to 666 bp for the ovine cDNA. Thus the observed discrepancy in the molecular weights may be due in part to the absence of 32 aa in the ovine p35 subunit protein. Differences in protein glycosylation as a result of the additional N-glycosylation site in the human p35 protein may also account for the molecular weight disparity. In all cases the heterodimer is observed as a doublet (for ovine, human and chimaeric), with the ovine heterodimeric bands having estimated molecular weights of 60 and 66 kDa. This is again likely to result from differential glycosylation of the proteins. In both instances where this is the suggested reason for the size discrepancy, further experimental confirmation is required. Such proof may require the use of deglycosylating agents such as N-glycosidase to remove glycosylated residues. Proteins of a single molecular weight should be generated if the differences in size are due to glycosylation.

The polyclonal antibody was used in the proliferation assays to inhibit the biological function of human, ovine and chimaeric heterodimers. Enhanced proliferation of human PHA-activated or ovine Con A-stimulated PBMNC, using human and chimaeric conditioned medium, was reduced to counts equivalent to that of vector blank medium by addition of antibody. Normal rabbit serum had no effect on the conditioned medium induced proliferation. By comparison, conditioned medium from the ovine co-transfectant was minimally inhibited. This result was

unexpected as this antibody was capable of immunoprecipitating ovine IL-12 proteins. While the anti-human IL-12 polyclonal antibody was able to recognise the individual ovine p40 subunit and the ovine IL-12 heterodimer, it would appear to be unable to effectively block the epitopes involved in the interaction of the ovine heterodimer with the IL-12 receptor. This may account for the minimal inhibition observed in the proliferation assays.

The IL-12 assay allowed the assessment of changes in the ability of IL-12 to induce the proliferation of activated cells. An alternative measure of IL-12 biological activity would have been the assessment of the IFN- γ production from T cells and NK cells, as IL-12 is able to elicit production of this cytokine from these cells (1). However, due to time constraints, this aspect of the study was not pursued.

In conclusion, ovine IL-12 p35 and p40 subunits, and the heterodimer, show both sequence and functional similarity to the human and murine IL-12 subunits and heterodimer. In addition, an assay has been developed for further functional studies described in the following chapters.

Chapter 4

The Antagonistic
Activity of IL-12
p40 in an Ovine
In Vitro Model of
the Alloimmune
Response

Chapter 4

The Antagonistic Activity of IL-12 p40 in an Ovine *In Vitro* Model of the Alloimmune Response

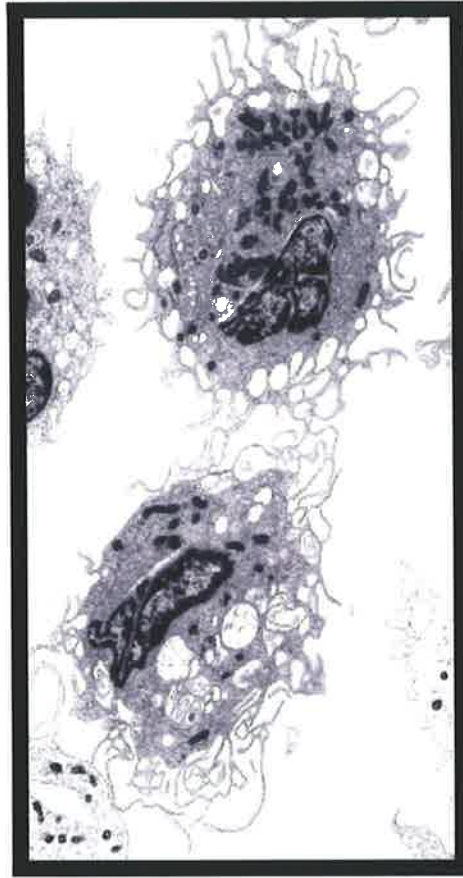
4.1. Introduction

As discussed in the **Literature Review**, IL-12 p40 can inhibit the biological activity of the IL-12 heterodimer (30, 37) and interact with the IL-12 receptor (30, 39). This IL-12 antagonist has been tested in *in vitro* and *in vivo* models of the alloimmune response (116, 117, 119) or using syngeneic tissue (118), with variable success in prolonging graft survival. The antagonistic efficacy of IL-12 p40 may be dependent on the mode of gene product delivery (systemic or localised), or the model in which this antagonist is tested. Delivery of IL-12 p40 via a cell type genetically modified to express IL-12 p40 may be an effective means of administering this antagonist. The work described in this chapter focuses on the dendritic cell (DC) as the cellular vehicle chosen for IL-12 p40 delivery. Dendritic cells are considered the most efficient of the antigen presenting cells (APCs). This reputation stems from several features of DC biology. DCs are able to acquire and process antigen (131) and migrate to lymphoid organs including the lymph node and spleen (132). In addition, DCs are unique amongst antigen presenting cells as they are able to activate naïve T cells (131), which can in turn interact with other APC types (133). DCs have a characteristic cell morphology with long dendrites, which are capable of retraction and extension. The dendrites are suggested to facilitate the selection of antigen-

specific T cells by allowing the DC to survey the surrounding T cell environment (133) (**Figure 4.1**). High level expression of the antigen presenting molecules MHC Class I and Class II can also be detected on the DC cell surface (133). In the mixed lymphocyte reaction (MLR) these cells are far superior in their ability to enhance the proliferation of responder lymphocytes when compared to other APCs such as monocytes (134).

DCs represent a small fraction of the circulating peripheral blood mononuclear cells (< 1%), and isolation of large numbers has been difficult in the past (135, 136). However, DCs can now be derived from myeloid lineage progenitors, including CD34⁺ stem cells (137, 138) or monocytes/macrophages (139, 140), by culturing these cells with cytokines such as granulocyte-macrophage colony stimulating factor (GM-CSF) and IL-4. More recently, another class of DC has been identified. These are of lymphoid origin and express the CD8 α surface marker (141-143). These DCs can suppress T cell responses (144-146), and this is evidenced by the abrogation of *in vivo* priming by peptide-pulsed CD8 α ⁻ DCs by coadministration of only 3% CD8 α ⁺ DCs. However, treatment of the CD8 α ⁻ cells with IL-12 prior to antigen presentation can reverse the inhibitory effect of the CD8 α ⁺ cells (147). CD8 α ⁺ DCs can produce high levels of IL-12 compared to CD8 α ⁻ DCs (143) and this is consistent with the promotion of a Th1-type response when antigen-pulsed CD8 α ⁺ DCs are administered *in vivo* (148). As such, the potential inhibitory effects of these cells in the presence of pro-inflammatory cytokines such as IL-12 should be interpreted with a measure of caution.

A.



B.



Figure 4.1. Ovine afferent lymph dendritic cells. **A.** Transmission electron micrograph at 6000X magnification. **B.** Scanning electron micrograph (dotted line represents 4.3 μm). These micrographs show the typical dendritic cell morphology with the ruffled membrane, or dendrites, from which their name is derived. Transmission electron micrographs of human monocyte-derived DCs have a similar morphology. Pictures courtesy of Dr T Coates.

4.1.1. Dendritic Cell Production of IL-12

DCs are very capable producers of IL-12 (12, 149) with two pathways leading to IL-12 production. The first pathway is initiated when the DCs encounter microbes or microbial products, resulting in rapid production of IL-12. IFN- γ priming of the cells is not required and costimulatory molecule interactions, such as the CD40-CD40L interaction, do not appear to be necessary (150, 151). CD8 α^+ DCs account for the majority of the IL-12 production, however, CD8 α^- DCs can synthesise IL-12 after *in vivo* priming (150).

The second pathway requires two signals for the production of IL-12. Bioactive IL-12 production from DCs is increased upon interaction of CD40 with CD40L (149) and in response to interaction with T cells plus antigen (12). Upregulation of p35 mRNA from macrophages/DCs occurs on contact with antigen/MHC Class II and the T cell receptor (TCR), and p40 mRNA accumulates upon interaction of CD40 with CD40L (152). Bioactive heterodimer formation is significantly increased when both CD40-CD40L and antigen-MHC-TCR interactions occur (153-155). A positive feedback mechanism results as the DCs themselves can respond to IL-12 by upregulation of MHC Class II and increased IL-12 production (16).

4.1.2. Dendritic Cells are able to Prime Naïve T Cells for IFN- γ Production

In the context of transplantation, the ability of DCs to interact with T cells/MHC/antigen and initiate the production of IL-12 provides a mechanism by which a Th1 response can be generated. In the mixed lymphocyte reaction DCs have been used to assess the induction of a Th1 response from CD4 $^+$ T cells. Alloreactive blasts produced IFN- γ upon restimulation, however, addition of anti-IL-12 antibodies

abrogated both IFN- γ production and cell proliferation (12). Similarly, naïve neonatal CD4⁺ T cells in an antigen-specific system incubated with allogeneic DCs resulted in the production of T cells whose phenotype was dependent on the relative levels of IL-4 and IL-12. Neutralising IL-4 during the primary MLR resulted in IFN- γ production from T cells (Th1 phenotype) that was dependent on IL-12, as anti-IL-12 antibodies were able to abrogate this effect. Production of IL-12 also required the CD40-CD40L and CD28-B7 costimulation pathways (156).

4.2. Allograft Rejection and Current Immunosuppressive Therapies

The rejection of organ allografts results from the recognition of allopeptide in the context of allo-MHC molecules by the recipient's immune system (157). The rejection process can be divided into two broad categories, namely acute and chronic rejection. Acute rejection occurs about 10 days after transplantation and characterised by a massive lymphocyte infiltration. In contrast, chronic rejection is mediated by humoral and cell mediated mechanisms, and chronic rejection can occur months or years after transplantation (157). Rejection can be controlled using immunosuppressive drugs which act to prolong allograft survival, however, a significant percentage of grafts are still lost. Current immunosuppressive therapies used to prevent or control allograft rejection are drug-based, and immunosuppressive drugs such as Cyclosporin and FK-506 have many undesirable side effects. Immunosuppression results in systemic depression of the recipient immune system leading to viral and bacterial infections, as well as malignancies (158-160). Neurotoxic and nephrotoxic effects of Cyclosporin and FK-506 have also been

described (161-165). Difficulties also exist with effective oral drug absorption, and metabolic effects such as the onset of insulin-dependent diabetes mellitus (166).

A potential candidate for the replacement of the current drug regime is gene therapy. This improves on conventional methods by allowing localised delivery of an immunomodulatory gene product to the allograft, thereby reducing the risk of systemic side effects. This therapy could still be used in combination with low level standard immunosuppression, if required, without the inherent detrimental effects of drug interactions. Candidate genes for gene therapy include the Th2 cytokines IL-10 (50) and IL-4 (47) or the IL-12 antagonist, IL-12 p40 (30, 37, 39). Costimulatory molecule antagonists (CTLA4-Ig) and negative regulators of gene transcription (for example inhibitors of the NF- κ B transcription factor) are also candidates for transplantation gene therapy.

4.3. Microchimaerism in Transplantation

A small population of donor-derived leukocytes, which can contribute to the immunogenicity of the graft, are present within most solid organ allografts (167). Microchimaerism is the term used to describe the trace population of donor cells that can be detected in an organ recipient, sometimes up to 3 decades posttransplantation (168). The persistence of these donor cells has also been demonstrated within at least one human recipient showing tolerance to the graft after withdrawal of immunosuppressive therapy (169). The existence of these cells in tolerant donors suggests that this cell population may play an integral role in the recipient's ability to remain tolerant to the organ graft (168, 169). This opposes the idea that depletion of the passenger leukocytes should result in prolonged graft survival by removing a source of migrating cells capable of presenting donor alloantigen (170).

DCs are consistently identified as part of the microchimaeric population (171). Evidence to support a role for DCs in allograft tolerance comes from liver transplantation in which spontaneous acceptance of allografts can be demonstrated, despite the high leukocyte content of these organs (172). Indeed, depletion of passenger leukocytes by irradiation of rat liver allografts prior to transplantation can lead to a significant decrease in graft survival time (mean of 16 days compared to untreated of > 100 days) (173). The role of DCs in spontaneous liver allograft acceptance has been extended by the isolation of DC progenitors of donor origin from the bone marrow and spleen of spontaneously accepting MHC-mismatched liver allograft recipients. However, this same cell population was not found in mice that rejected cardiac allografts from the same donor mouse strain (174). Characterisation of these liver-derived DCs revealed them to be relatively immature, with low levels of MHC Class II and the costimulatory molecules CD80 and CD86. These cells also failed to stimulate allogeneic T cells in an MLR when compared to spleen-derived DCs from the same strain that had high level MHC Class II and costimulatory molecule expression (175). Pretreatment of recipient mice with the liver-derived 'immature' DCs was able to extend the survival of pancreatic islet allografts (175). Similarly, bone marrow-derived DCs propagated using GM-CSF, with an MHC Class II⁺, CD80^{dim}, CD86⁻ phenotype, promoted donor-specific unresponsiveness *in vitro*. In contrast, cells cultured in GM-CSF plus IL-4, with upregulated MHC Class II and CD86, were strong inducers of the alloimmune response (176). Administration of these 'immature' DCs to mice receiving cardiac allografts prolonged allograft survival but did not result in long-term graft acceptance. In contrast, administration of DCs with upregulated costimulatory molecules and MHC Class II caused accelerated rejection of the grafts (177).

Although administration of these 'immature' cells alone *in vivo* prolonged graft survival, long-term acceptance was not observed (175, 177). Concomitant administration of anti-CD40L antibody with the costimulatory molecule deficient DCs further improved cardiac graft survival, but again, indefinite allograft acceptance was not observed (178). Cytotoxic T lymphocyte activity was decreased in animals with prolonged allograft acceptance and increased cell apoptosis was observed in the allograft and spleen. In addition, the highest levels of microchimaerism were detected in mice with survival times of greater than 100 days (179). This increase in apoptosis has also been observed in spontaneously accepting liver allograft recipients, where irradiation of the liver prior to transplantation resulted in rejection and reduced apoptosis of cells (180).

Additional manipulation of the DCs may be required to elicit long-term tolerance toward the allograft. Generation of Fas ligand (FasL) expressing DCs, able to kill cells with cell surface Fas expression has been shown to induce alloantigen-specific hyporesponsiveness. Cardiac allograft survival was prolonged by pretreatment of recipients with these cells, however grafts eventually failed (181). As such, there is much scope for the modification of DCs with a gene or gene combination to enhance allograft survival. The specific advantage of modifying the DCs over intragraft gene delivery is the presence of the immunomodulatory gene product at the site of antigen presentation. Antagonists of IL-12 may be especially useful for the prevention of organ allograft rejection as this cytokine has multiple actions that may result in graft damage (**Literature Review** and **Figure 1.3**). The IL-12 p40 subunit is able to inhibit the biological activity of IL-12 heterodimer (30, 37, 39) and it is this property which makes p40 an attractive modulator of immune

function. As an antagonist, IL-12 p40 has the advantage of specifically inhibiting IL-12 biological activity without being immunogenic.

This chapter focuses on the transfection of ovine afferent lymph and human monocyte-derived DCs with an adenoviral vector containing the ovine IL-12 p40 cDNA. The ability of IL-12 p40 to inhibit the proliferation of *in vitro* IL-12 proliferation assays and mixed lymphocyte reaction models is discussed.

Aims

To assess the efficacy of ovine IL-12 p40 inhibition of ovine IL-12 heterodimer biological activity, and determine whether p40 is an effective antagonist of proliferation in an *in vitro* model of the alloimmune response by:

- i. determining the cell surface marker expression on ovine and human DCs to ascertain the cell phenotype, and establishing optimal transfection conditions for the adenoviral vectors;
- ii. demonstrating the expression of ovine IL-12 p40 in cells infected/transfected by the replication-deficient adenoviral construct by immunoprecipitation of the IL-12 p40 protein;
- iii. demonstrating the ability of ovine IL-12 p40 to antagonise IL-12 heterodimer-induced proliferation of activated mononuclear cells, and
- iv. comparing the efficacy of ovine and human DCs transfected with the IL-12 p40 adenoviral construct to for their capacity to inhibit the dendritic cell-mixed lymphocyte reaction (DC-MLR), and the ability of IL-12 p40 conditioned medium to inhibit the ovine DC-MLR and two-way mixed lymphocyte reaction.

Cloning Protocol

Generation of an Ovine IL-12 p40 Expressing Adenoviral Vector

The method used to generate the replication-deficient adenovirus, the adenoviral/shuttle vector plasmid constructs and BJ5183 bacteria were provided by Dr Tong-Chuan He (123). Adenoviral cloning was performed by Dr Sonja Klebe (Department of Ophthalmology, Flinders Medical Centre, Adelaide) from the ovine p40-containing pRc/CMV plasmid derived by S Swinburne described in **Chapter 3**. Svjetlana Kireta performed infection of the 293 packaging cell line, caesium chloride purification and viral titre quantification.

In brief, the ovine p40 cDNA was excised from the pRc/CMV vector using the NotI/XbaI restriction enzymes and subcloned into the pAdTrack-CMV shuttle vector (**Figure 4.2**). The shuttle vector was then linearised with PmeI and mixed with supercoiled GFP-containing adenoviral backbone, pAdEasy-1. Electrocompetent *E. coli* BJ5183 bacteria were then combined with the plasmids and electroporation of the mixture was carried out. Small, recombinant colonies were isolated on kanamycin selective plates and small-scale (5 ml) liquid cultures were obtained. Plasmids were prepared by alkaline lysis (mini-prep) and digested with restriction enzymes to confirm insert presence. *E. coli* DH10B bacteria were transformed with the chosen plasmids for large-scale purification. 293 cells (50-70% confluent) were transfected with adenoviral plasmid linearised with the PacI restriction enzyme. Cells were then harvested at 7-10 days and rapid freeze/thaw lysis was used to generate cell lysate. Large-scale infection of 293 cells was then performed to generate large quantities of virus. Virus was subsequently purified by caesium chloride centrifugation (182) and the viral titre determined (183).

4.4. Methods

4.4.1. Generation of Dendritic Cells from Human Monocytes

Human peripheral blood mononuclear cells were isolated on a Lymphoprep™ density gradient from a buffy coat (courtesy of the South Australian Red Cross, Adelaide) as described in 2.3.17. Cells were resuspended in s10g and cultured for 2 hours with 5×10^7 cells/75 cm² flask in a total volume of 10 ml. Non-adherent T and B cells were then removed by washing with PBS. The adherent monocytes were cultured in s10g supplemented with 400 U/ml IL-4 and 800 U/ml GM-CSF for 5-6 days to derive the DCs (139).

4.4.2. Isolation of Ovine Afferent Lymph Dendritic Cells

A pre-femoral lymph node of a female Merino sheep was surgically removed and the sheep allowed to recover for 6 to 8 weeks. One ml of 1% Patent Blue V dye was injected intradermally to facilitate the identification of the lymphatic vessels, and cannulation of the afferent lymphatics was performed using heparin impregnated catheters. Lymph was collected into a sterile 100 ml bag containing heparin (5000 IU) and gentamycin (40 mg), to prevent clotting and infection, respectively. Heparin (2500 IU) was administered to the sheep on a daily basis to reduce the likelihood of obstruction of the cannula. Dr T Coates and surgeons Burapa Kanachabat and Christine Russell of The Queen Elizabeth Hospital, Adelaide, performed this procedure.

Ovine afferent lymph was obtained from cannulated sheep courtesy of Dr T Coates. Afferent lymph was divided into two 50 ml tubes and the cells were pelleted by centrifugation at 1800 rpm for 10 min. Each cell pellet was resuspended in 2 ml of RPMI and transferred to a 10 ml V-bottom tube. PBS was added to a final volume of

approximately 7 ml and the solution was mixed before underlaying with 2 ml of 14.5% metrizamide. Tubes were centrifuged at 2500 rpm for 15 min and the rotor allowed to come to rest without active braking. The enriched DC population was collected from the interface for further experiments.

4.4.3. Cell Surface Marker Analysis Using Flow Cytometry

DCs were collected and washed with FACS wash buffer (ovine DCs – directly from lymph, human DCs – 5 or 6 day culture in IL-4 and GM-CSF, with or without an additional 18 hours of TNF- α [10 ng/ml] treatment). A minimum of 10^5 cells were used for analysis. Cells were resuspended in 10% normal rabbit serum with 10% EMA (100 μ g/ml) in FACS wash buffer, and 100 μ l was added to each tube. A 25 min incubation on ice in the dark was performed before addition of primary antibody (5 μ l commercial, 50 μ l tissue culture supernatant). The tubes were incubated on ice under fluorescent light for 25 min before the cells were washed in FACS wash buffer to remove unbound primary antibody. Centrifugation of tubes was performed at 1500 rpm for 5 min and the supernatant was then decanted. Secondary FITC-conjugated antibody (sheep anti-mouse Fab₂ fragments, 20 μ l per tube of a 1/50 dilution in FACS wash buffer) was then added for a further 25 min incubation in the dark. One ml of FACS lysing™ solution (1 in 10 dilution) was then added to each tube for 20 min at room temperature (maintaining tubes in the dark). FACS wash buffer was added to each tube and the tubes were centrifuged. The FACS wash buffer was decanted and the cells were resuspended in 200-400 μ l of filtered saline. Cells were acquired using a Becton Dickinson FACScan™ flow cytometer and the results were analysed using CellQuest™ software.

4.4.4. LipofectAMINE™-Mediated Adenoviral Transfection of

Dendritic Cells

Adenovirus (at a multiplicity of infection (MOI) of 1000 or 5000) and 1 μ l of LipofectAMINE™ (1.25 μ g/ μ l) were mixed together and made up to a final volume of 100 μ l with endotoxin- and serum-free MEM. This mixture was incubated at room temperature for 15 min prior to use.

Human monocyte-derived or ovine afferent lymph DCs were collected and resuspended at 5×10^5 cells in 100 μ l of MEM. The adenoviral and DC components were then combined and the tubes placed on a rotating platform for 30 min. Tubes were then placed into to a 37°C incubator for a further 90 min (mixed periodically). Human DCs were then transferred to a 24 well plate and cultured in s10g containing IL-4, GM-CSF and TNF- α (10 ng/ml) for 18-24 hours in a final well volume of 1.2 ml. Ovine DCs were also transferred to a 24 well plate in a final volume of 1.2 ml, with medium containing GM-CSF alone.

4.4.5. Infection of Ovine Fibroblasts with Adenoviral Particles

Fibroblasts were harvested using trypsin/EDTA and resuspended at 3×10^6 cells per 200 μ l of s10g. Cells were then transferred to a 1.5 ml tube containing adenoviral particles (vector blank or IL-12 p40) with a final MOI of 40. An uninfected control was always included. Cells were placed on a rotating platform for 30 min prior to a further 90 min of incubation at 37°C with occasional mixing. After infection, cells were transferred to a 25cm² flask containing 5 ml of s10g and incubated for 48 hours. Conditioned medium (culture supernatant) was collected for use in the MLR. Metabolic labelling of cells and immunoprecipitation was then

performed as described in 2.3.15, and proteins precipitated using the rabbit anti-human IL-12 polyclonal antibody. SDS-PAGE analysis of samples was performed as per 2.3.16. Cells were detached using trypsin/EDTA after labelling and spotted onto slides. Effective adenoviral transfection was confirmed by visualisation of GFP expressing cells using fluorescence microscopy.

4.4.6. Assessment of Adenoviral Transfection Efficiency by Flow Cytometry

DCs (not fewer than 1×10^5 /tube) that had been transfected with GFP expressing adenoviral vectors (and an untransfected control) were pelleted and washed once in FACS wash buffer. Supernatant was then decanted and the cells resuspended in the residual volume to which 10 μ l of EMA (100 μ g/ml) was added. Tubes were incubated on ice in the dark for 25 min, before a further 25 min on ice and exposed to light. Tubes were topped up with FACS wash buffer and centrifuged at 1500 rpm for 5 min. Supernatant was then decanted and FACS lysing™ solution (1 ml into each tube of a 1 in 10 dilution) was then added. A 20 min room temperature incubation was then performed (tubes kept in the dark). Tubes were topped up with FACS wash buffer and centrifuged before resuspension of cells in 200-400 μ l of filtered saline. Cells were then analysed as in 4.4.3.

4.4.7. Dendritic Cell-Mixed Lymphocyte Reaction (DC-MLR)

The mixed lymphocyte reaction is an *in vitro* assay of the alloimmune response (100). In particular, the DC-MLR mimics the response of recipient lymphocytes to donor DCs. Transfected (and untransfected control) DCs were seeded in a 96 well plate at 10^2 , 10^3 or 10^4 cells per well in triplicate for each transfection

treatment. Mononuclear cells (1×10^5) were added to each well in a final volume of 200 μ l. This equated to stimulator:responder ratios of 1:1000, 1:100 and 1:10, DCs to PBMNC. Plates were pulsed on day 4 by addition of 40 μ l of tritiated thymidine per well (25 μ Ci/ml in 10g) and incubated for a further 18 h. Cells were harvested onto filters on day 5 of culture and the filters were counted as per **2.3.18**.

4.4.8. Ovine Two-Way Mixed Lymphocyte Reaction

Mononuclear cells from two unrelated sheep were isolated from peripheral blood as described in **2.3.17**. Cells were plated at 1×10^5 cells/well from each individual. Conditioned medium from adenovirus infected fibroblasts (as described in **4.4.5**) was then added to wells at a final concentration of 10% or 50% in a total well volume of 200 μ l. Plates were pulsed with tritiated thymidine on day 4 (40 μ l of 25 μ Ci/ml in 10g) and cultured for a further 18 hours. Cells were then harvested and the filters counted as per **2.3.18**.

NOTE: Human and ovine IL-12 proliferation assays (using 1.25% CHO cell IL-12 co-transfectant conditioned medium) were set up as described in **2.3.18** and IL-12 p40 fibroblast conditioned medium (10% or 50%) was used. A vector blank virus and untransfected cell control were always included.

4.5. Results

4.5.1. Phenotype of Ovine Dendritic Cells

Scanning and transmission electron micrographs of ovine afferent lymph DCs showed the morphology typical of this cell type with the characteristic dendrites (**Figure 4.1**). Analysis of the markers present on the cell surface revealed high level

expression of the antigen presenting molecules MHC Class I and Class II (**Figure 4.3**). Moderate expression of the costimulatory molecules CD80/CD86 were detected using a soluble form of murine CTLA4 able to interact with the costimulatory molecules for combined detection of both CD80/CD86. This molecule consisted of the extracellular domain of CTLA4 fused to the human IgG1 constant domain (120). Moderate expression of the DC marker CD1a could also be detected. CD14 expression was present, although this may have been due to the small population of contaminating lymphocytes still present after metrizamide enrichment.

4.5.2. Immunoprecipitation of the IL-12 p40 Subunit Protein

The ability of the fibroblasts and DCs to produce IL-12 p40 protein when infected or transfected with the adenoviral construct, respectively, was demonstrated by immunoprecipitation of ³⁵S-labelled p40 proteins from culture supernatants. Within the adenoviral construct separate CMV promoters control the expression of GFP and p40 genes (**Figure 4.2**). DCs were clearly capable of generating GFP protein, as assessed by flow cytometry and fluorescence microscopy, however, this did not ensure expression of the p40 protein from the different cell types. As shown in **Figure 4.4A** and **B**, ovine and human DCs were capable of generating ovine IL-12 p40 protein. The major product immunoprecipitated from the culture supernatant was observed at approximately 40 kDa, with a second, less intense band present at approximately 43 kDa. Under non-reducing conditions a strong band at approximately 80 kDa was apparent from the human DCs (**Figure 4.4A**), with reduction of this protein resulting in the observation of single band on the autoradiograph at approximately 40 kDa (**Figure 4.4B**). As this band was only apparent in the lane of DCs transfected with the p40 adenovirus, this suggested that

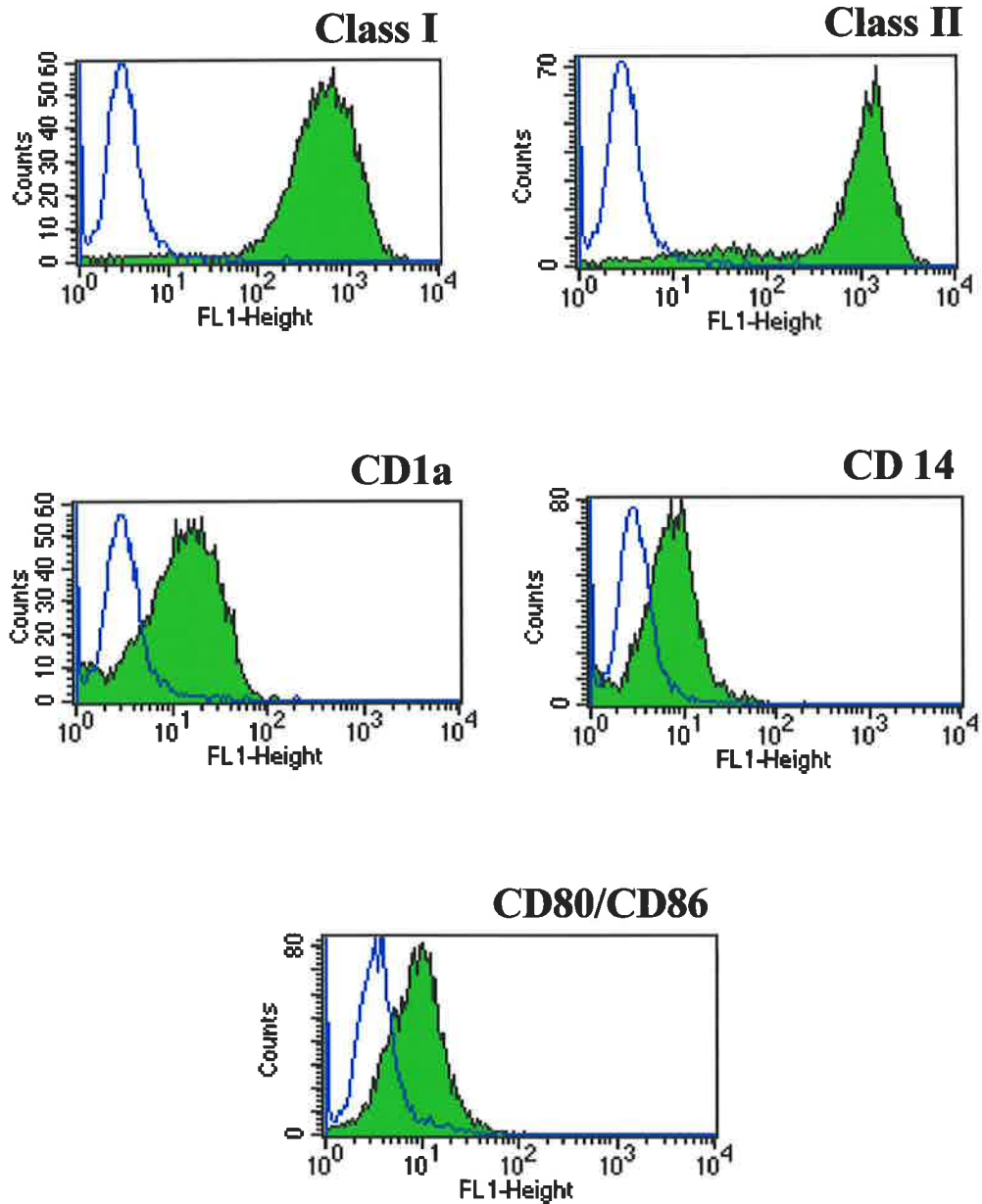


Figure 4.3. Expression of cell surface markers on ovine afferent lymph dendritic cells as assessed by flow cytometry. Solid green histogram indicates degree of marker expression, blue overlay represents an isotype matched negative control antibody. Cell surface marker type is shown in the top right hand corner of each histogram.

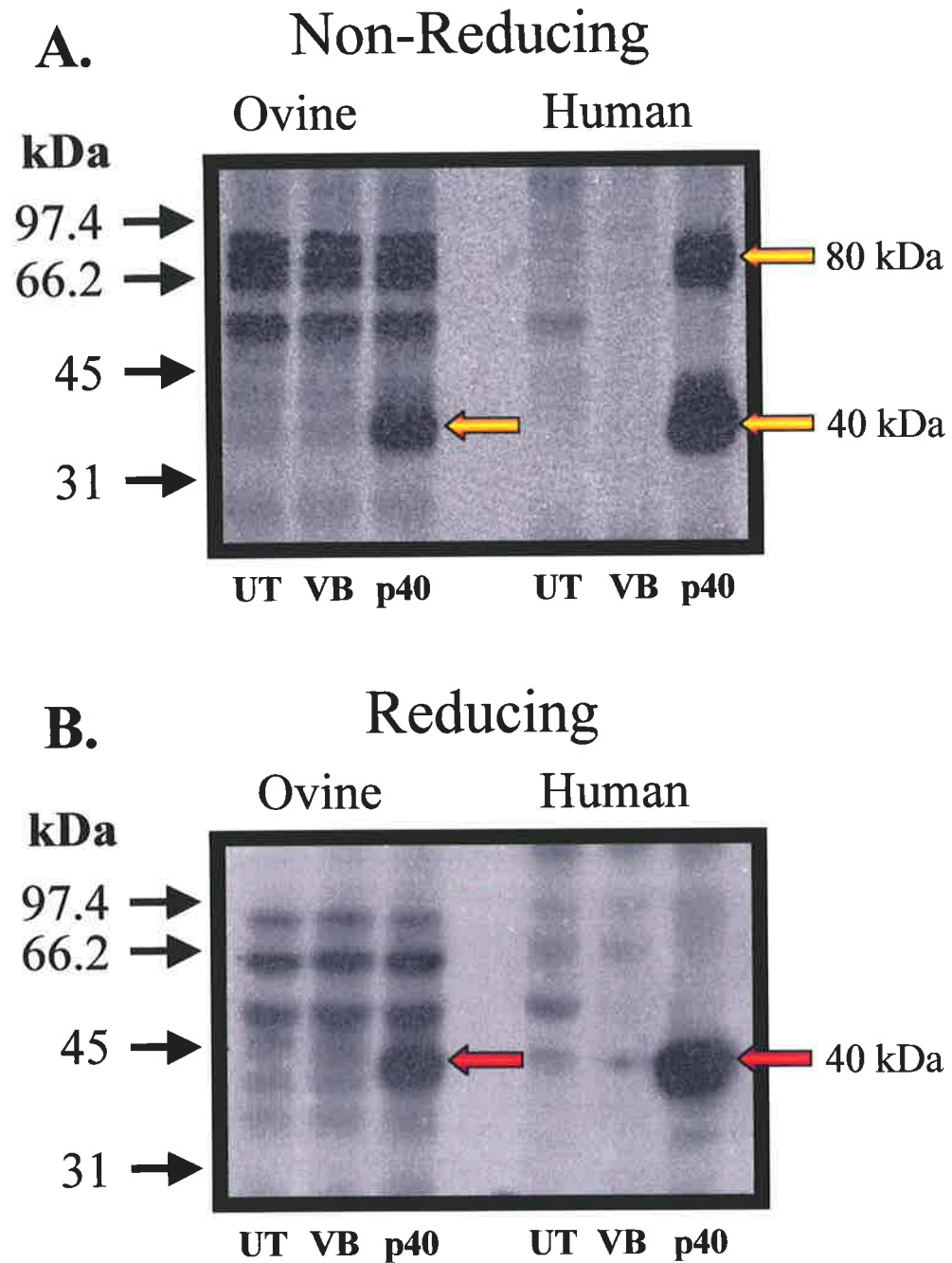


Figure 4.4. An autoradiograph showing immunoprecipitation of proteins from the supernatant of adenovirus-transfected ovine afferent lymph and human monocyte-derived DCs. DCs were transfected with vector blank (VB) or IL-12 p40 (p40) adenovirus, or untreated (UT), metabolically labelled with ^{35}S -methionine/cysteine and the proteins immunoprecipitated using a human anti-IL-12 polyclonal antibody. Samples were run on 10% SDS-PAGE gels under **A.** non-reducing, or **B.** reducing conditions. Coloured arrows indicate the positions of the p40 monomer (approximately 40 kDa) and homodimer (approximately 80 kDa). Ovine fibroblasts (not shown) gave similar results although the band for p40 homodimer was relatively less intense.

the higher molecular weight species was p40 homodimer. This high molecular weight product was not observed for the ovine afferent lymph DCs, although several bands in this molecular weight range were present in all ovine DC treatment lanes (**Figure 4.4A**). However, the higher molecular weight bands in the IL-12 p40 transfected ovine DC lanes were of equivalent intensity to the bands present in the vector blank or untreated lanes. Higher intensity bands from the ovine IL-12 p40 DCs would be expected if p40 homodimer was present. As this was not the case it suggested that there was no p40, or minimal p40, homodimer production from these cells. These high molecular weight bands did not resolve to a single protein of 40 kDa under reducing conditions, suggesting that they were not due to the formation of p40 homodimers, or even IL-12 heterodimer.

Immunoprecipitation of proteins from the culture supernatant of IL-12 p40 infected fibroblasts using the rabbit anti-human IL-12 polyclonal antibody again resulted in detection of 3 bands (not shown). A strong band at approximately 40 kDa was the major product from the infected cells, with a second slightly larger band at 43 kDa also present. This was a consistent observation in all cell types and may result from differential glycosylation of p40. A third, less intense higher molecular weight band at approximately 80 kDa was detected and was suggested to be p40 homodimer (data not shown).

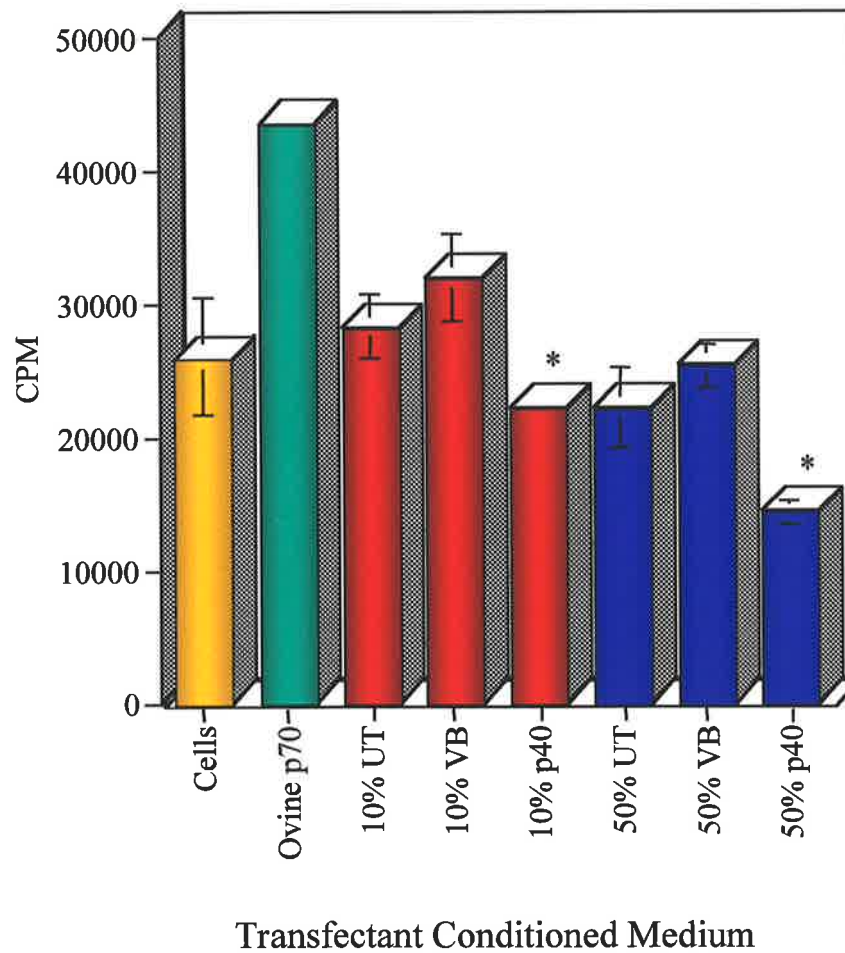
4.5.3. Ovine IL-12 Proliferation Assay with Adenoviral Fibroblast Conditioned Medium

To determine whether ovine p40 was capable of inhibiting IL-12-induced proliferation, the conditioned medium from adenovirus-infected fibroblasts was tested in an ovine Con A proliferation assay. Activated PBMNC were incubated with

ovine IL-12 p70 (from CHO cell co-transfectant supernatant) and adenovirus conditioned medium. IL-12 p40 conditioned medium at either concentration (10% or 50%) inhibited IL-12-induced cellular proliferation (**Figure 4.5**). Incubation with 50% uninfected fibroblast conditioned medium alone resulted in some inhibition of proliferation, however additional inhibition in the wells containing IL-12 p40 was clearly discernible and reproducible. Inhibition was statistically significant with a p value of < 0.05 . This result confirmed that ovine IL-12 p40 had the intrinsic IL-12 heterodimer antagonistic ability previously demonstrated for both mouse and human IL-12 p40 (30, 37).

4.5.4. Adenoviral Transfection Efficiency of Human and Ovine DCs as Assessed by Flow Cytometry

Direct infection of human monocyte-derived DCs using an adenoviral vector alone can be relatively inefficient and this may be due to low level expression of the cell surface molecule(s) required for adenovirus binding and internalisation (184). Enhanced adenovirus delivery can be achieved using liposomal agents (185, 186). In the experiments performed here the liposomal agent chosen was LipofectAMINE™. A typical transfection efficiency, as determined by the percentage of fluorescent positive GFP expressing cells, for both ovine and human DCs, was greater than 50% of live cells. The protocol defined in our laboratory for transfection of human DCs with adenovirus included cell recovery in medium containing IL-4, GM-CSF and TNF- α O/N prior to use in the human DC-MLR. The only detectable difference in cell surface marker expression as a result of TNF- α treatment was a slight upregulation of CD83 marker expression, compared to DCs cultured in IL-4 and GM-CSF alone (**Figure 4.6**). However, GFP gene fluorescence was enhanced in



Yellow bar: cells alone; Green bar: Ovine IL-12 p70 positive control; Red bars: addition of 10% untransfected, vector blank or IL-12 p40 fibroblast conditioned medium; Blue bars: addition of 50% untransfected, vector blank or IL-12 p40 fibroblast conditioned medium.

Figure 4.5. Inhibition of an ovine Con A IL-12 proliferation assay using ovine IL-12 p40 conditioned medium. Activated PBMNC were induced to proliferate in response to 1.25% IL-12 CHO cell conditioned medium and incubated with either 10% or 50% conditioned medium from vector blank (VB), IL-12 p40 (p40) adenovirus-infected or untreated (UT) fibroblasts. Inhibition of IL-12 activity was observed for wells containing IL-12 p40. “*”, $p < 0.05$.

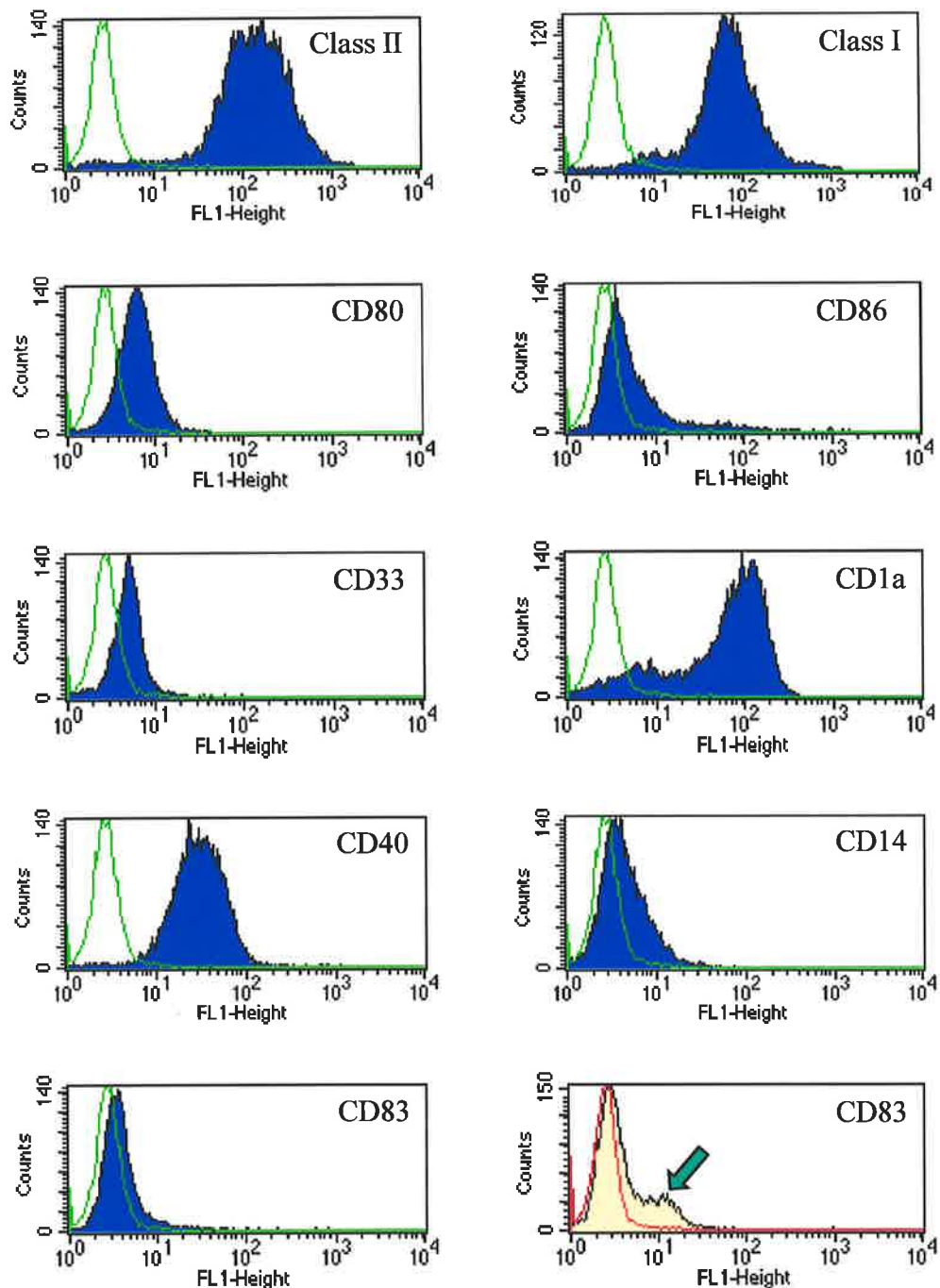


Figure 4.6. Flow cytometric analysis of cell surface markers present on human monocyte-derived DCs. A representative set of histograms shows DCs at day 6 cultured with GM-CSF and IL-4 (blue histogram, green overlay). The pink histogram with red overlay shows DCs at day 6 after treatment with TNF α for the final 24 hours. The green arrow indicates the small population of cells that have acquired the CD83 surface marker. The histogram overlay represents the negative control and the cell surface marker type is indicated in the upper right hand corner of each plot. An isotype matched negative control antibody was used in all cases.

TNF- α -treated cells, as assessed by flow cytometry (**Figure 4.7**). As such, TNF- α was used in the culture medium in which human DCs were allowed to recover after adenoviral transfection.

4.5.5. Ovine DC-MLR with Adenovirus-Transfected DCs

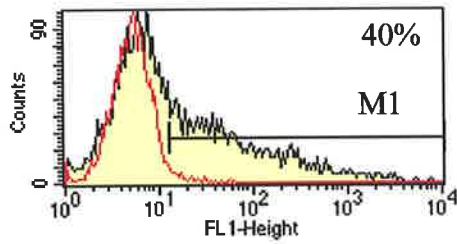
Ovine afferent lymph DCs were transfected with adenovirus (vector blank or IL-12 p40) or left unmodified and plated at different stimulator:responder ratios with ovine PBMNC (**Figure 4.8A**). The presence of unmodified afferent lymph ovine DCs resulted in a dose-dependent increase in the proliferative counts observed, with a stimulator:responder ratio of 1:10 having the highest level of proliferation (**UT 1:10, Figure 4.8A**). Transfection of the ovine DCs with adenovirus (1000 MOI) showed a similar trend, with increased DC number resulting in increased proliferative counts. However, the presence of virus alone resulted in a significant inhibition of proliferation, particularly noticeable when large numbers of transfected DCs were present. Transfection of ovine DCs was initially performed at a MOI of 5000, however, a MOI of 1000 resulted in a similar transfection efficiency, and inhibition due to virus alone was reduced (data not shown). No significant difference in the level of inhibition between vector blank or IL-12 p40 transfected DC wells was observed at any of the stimulator:responder ratios tested.

4.5.6. Ovine DC-MLR with Ovine Adult Fibroblast IL-12 p40

Conditioned Medium

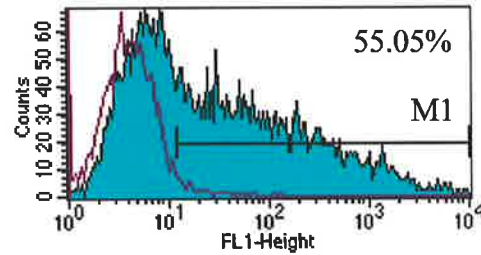
In an effort to resolve the inhibitory effect attributable to virus alone, which may have obscured the observation of inhibition due to IL-12 p40, ovine fibroblasts were infected with adenovirus as described (**4.4.5**). The DC-MLR was performed as

Without TNF α

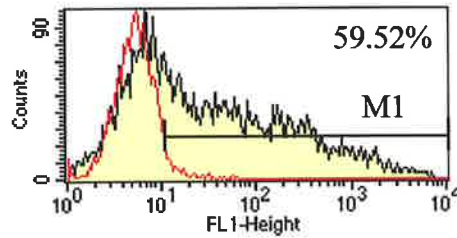


Adv Vector Blank
Dendritic Cells

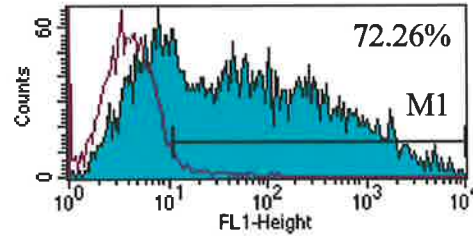
With TNF α



Adv Vector Blank
Dendritic Cells



Adv IL-12 p40
Dendritic Cells



Adv IL-12 p40
Dendritic Cells

Figure 4.7. Adenovirus transfection efficiency of human monocyte-derived dendritic cells, as assessed by flow cytometric analysis of GFP fluorescence. Left panel shows TNF- α -untreated cells with the top histogram indicating vector blank transfected DCs, bottom histogram IL-12 p40 adenovirus. Right panel shows TNF- α -treated DCs with the top histogram indicating vector blank adenovirus and the bottom histogram IL-12 p40 adenovirus. Negative control overlay was untransfected cells with or without TNF- α as appropriate.

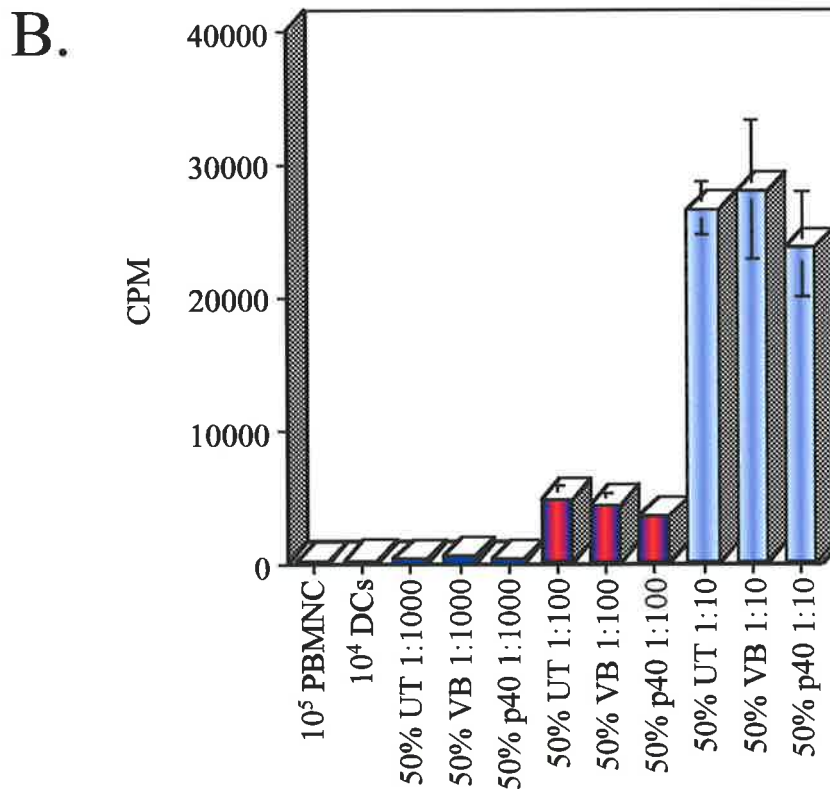
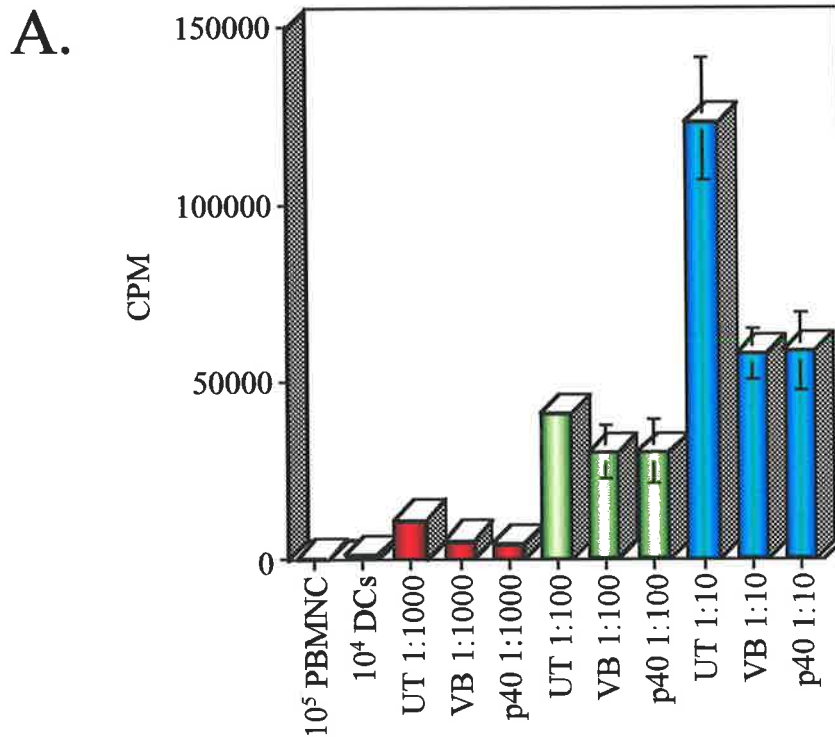


Figure 4.8. Ovine DC-MLR. DCs and PBMNC were plated at different stimulator:responder ratios as shown. A. DCs transfected with adenoviral vectors, vector blank (VB), IL-12 p40 (p40) at MOI 1000, or untransfected (UT). Confirmation of efficient transfection was obtained using flow cytometry. B. A representative graph of adenovirus or untreated conditioned medium from ovine fibroblasts with a final well concentration of 50% in a DC-MLR.

above, with untransfected ovine afferent lymph DCs cultured with PBMNC at stimulator:responder ratios of 1:1000, 1:100 and 1:10. Fibroblast conditioned medium was added to each well with a final concentration of 10% or 50% (**Figure 4.8B**). No additional inhibitory effect was discernible with the addition of p40 conditioned medium, even at concentrations of ovine p40 conditioned medium shown to be inhibitory in the IL-12 proliferation assay.

4.5.7. Ovine Two-Way MLR with Ovine Adult Fibroblast IL-12 p40 Conditioned Medium

The ability of ovine IL-12 p40 to inhibit a standard two-way mixed lymphocyte reaction was tested using the conditioned medium from the infected fibroblasts. Both leukocyte populations are capable of responding to the allogeneic stimulus, without singling out an individual cell type to promote the allogeneic proliferative response. Conditioned medium was used at a final concentration of 10% or 50% and the effects compared to uninfected and vector blank fibroblast conditioned medium. Lower counts were observed for the MLR overall compared to the DC-MLR, however, sufficient proliferation was achieved for the observation of any effect attributable to IL-12 p40 (**Figure 4.9**). No significant difference between vector blank and IL-12 p40 conditioned medium was detected above the inhibition (particularly at 50%) observed for fibroblast culture supernatant alone.

4.5.8. Human IL-12 Proliferation Assay with Ovine Adult Fibroblast IL-12 p40 Conditioned Medium

The production of IL-12 p40 homodimer from human DCs transfected with the IL-12 p40 adenoviral vector suggested that these cells might be more effective at

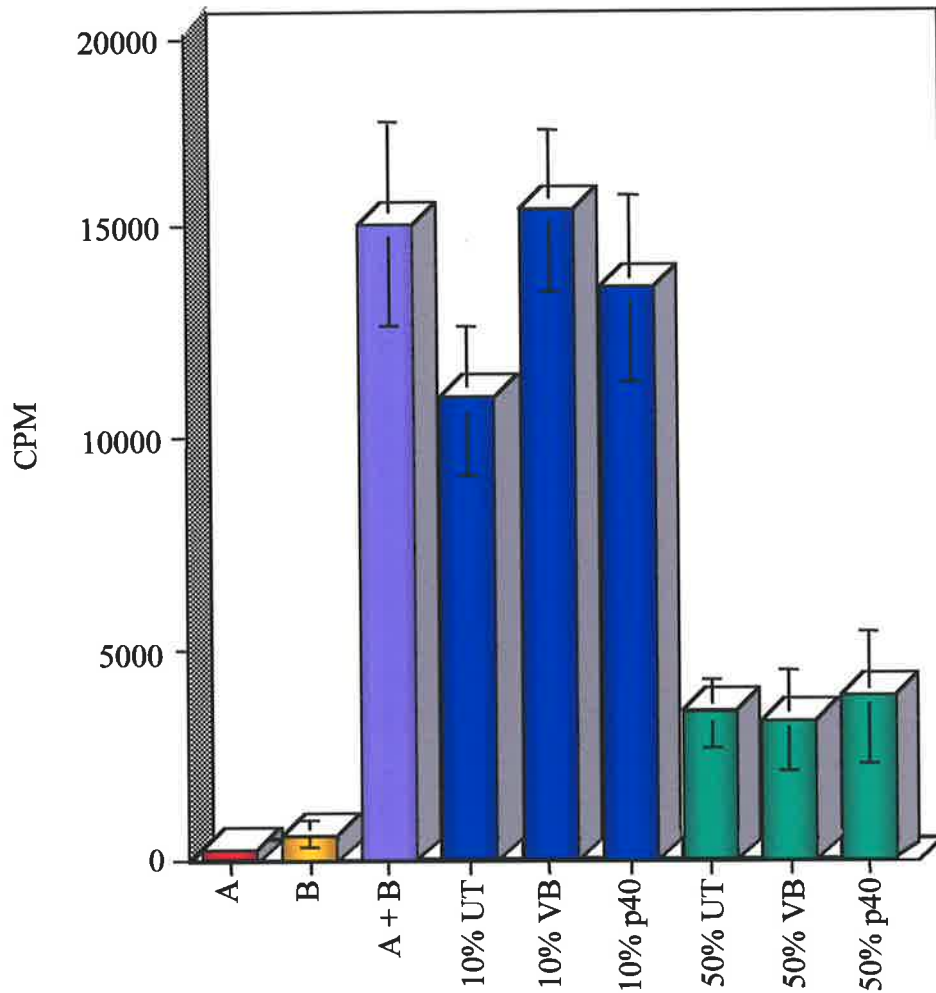


Figure 4.9. Ovine two-way mixed lymphocyte reaction with fibroblast conditioned medium. A and B represent proliferative counts from 2×10^5 PBMNC from a single donor. All other wells contain 1×10^5 PBMNC from each individual (A + B) and fibroblast conditioned medium from vector blank (VB), IL-12 p40 (p40) or uninfected (UT) cells. Fibroblast conditioned medium was tested at 10% and 50% concentrations. No significant difference was observed between vector blank and p40 conditioned medium.

inhibiting the DC-MLR. Although ovine IL-12 heterodimer was able to induce proliferation of activated human PBMNC (**Chapter 3**), most likely due to the high degree of similarity of the individual subunits between species, it could not be assumed that ovine IL-12 p40 would inhibit human IL-12-induced proliferation. To assess this, ovine IL-12 p40 fibroblast conditioned medium was tested in a human IL-12 proliferation assay at a final concentration of 10% or 50%. Inhibition of proliferation was observed for both concentrations of p40 conditioned medium (**Figure 4.10**). Even high level proliferation in the human IL-12 assay was inhibited by the addition of ovine IL-12 p40 conditioned medium (greater than 100,000 cpm – data not shown).

4.5.9. Phenotypic Analysis of Human Dendritic Cells

Human monocyte-derived DC morphology was similar to the morphology of the ovine afferent lymph DCs (**Figure 4.1**). The human monocyte-derived DC phenotype was assessed using flow cytometry and high level expression of MHC Class II and Class I was detected (**Figure 4.6**). Low levels of the costimulatory molecules CD80 and CD86, and the myeloid lineage marker, CD33 (187) were also present. Strong expression of the MHC-like molecule, CD1a, was detectable on the cell surface of the human DCs, and this marker is observed early in the transition from monocyte precursors to the Langerhans cell/DC phenotype (188). Strong expression of the costimulatory molecule CD40 was also detected. Expression of the cell surface markers described above did not differ significantly between TNF- α -treated and untreated cells. However, TNF- α treatment was sufficient to induce expression of CD83, a DC maturational marker (189), which was present on a small population of the DCs (**Figure 4.6**).

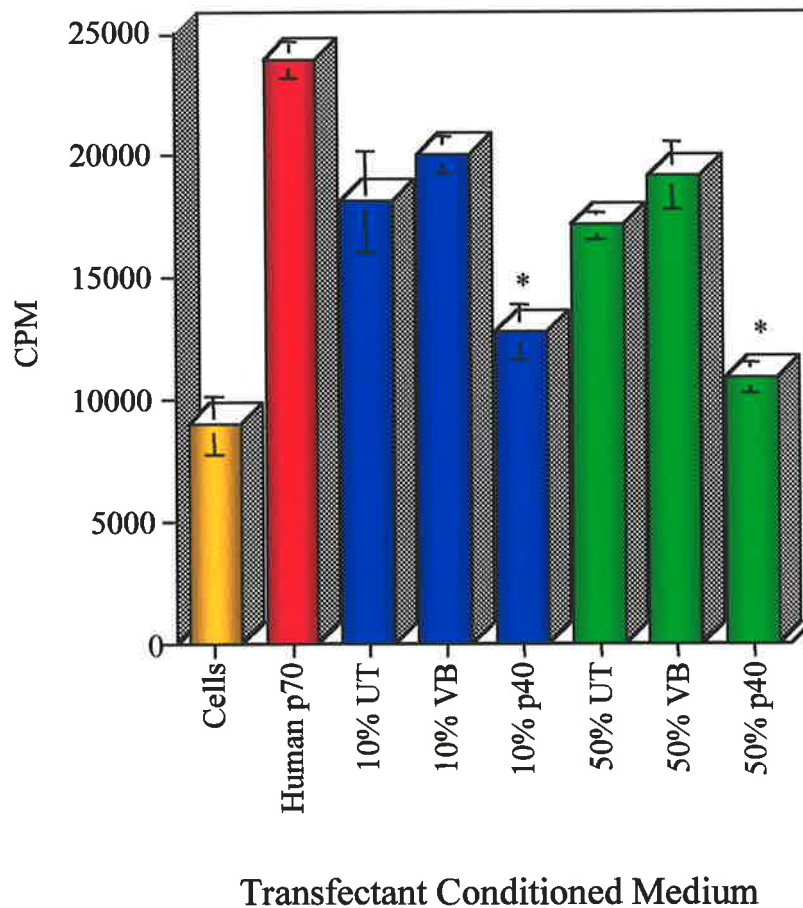


Figure 4.10. Inhibition of a human IL-12 PHA proliferation assay. Activated human PBMNC were induced to proliferate in response to 1.25% IL-12 CHO conditioned medium and incubated with either 10% or 50% conditioned medium from vector blank (VB), IL-12 p40 (p40) adenovirus-infected or untreated (UT) fibroblasts. Inhibition of proliferation with ovine IL-12 p40 conditioned medium was observed. “*”, $p < 0.05$.

4.5.10. Human DC-MLR with IL-12 p40 Adenovirus-Transfected DCs

Human monocyte-derived DCs transfected with adenoviral vector blank, IL-12 p40 or untreated were plated in triplicate at different stimulator:responder ratios (1:1000, 1:100, and 1:10). The presence of unmodified DCs alone resulted in a significant increase in cellular proliferation. This response was DC dose-dependent and occurred at all stimulator:responder ratios (**Figure 4.11**). This effect was further enhanced by transfection of the DCs with either of the adenoviral constructs (vector blank or p40). However, transfection of the DCs with IL-12 p40 did not inhibit DC-MLR proliferation, with the proliferative response comparable to wells containing vector blank adenovirus-transfected DCs.

Discussion

DCs are potent antigen presenting cells capable of processing antigen (131) and migrating to the peripheral lymphoid tissue, including the T dependent areas of the spleen (132), where activation of naïve T cells can occur. Recent evidence suggests that the presence of donor-derived DCs (microchimaerism) within the organ recipient contributes to long term graft survival, in some instances after withdrawal of immunosuppressive therapy (169). Murine DCs isolated from bone marrow and deficient in costimulatory molecule expression have been used to treat recipients prior to transplantation, resulting in prolonged cardiac allograft survival (177). DCs modified to express molecules such as FasL can also facilitate allograft survival (181). However, long term acceptance has not been achieved. Modification of DCs improves on systemic or intragraft gene therapy by providing gene expression at the site of antigen presentation. The candidate gene for DC gene therapy presented here is IL-12 p40.

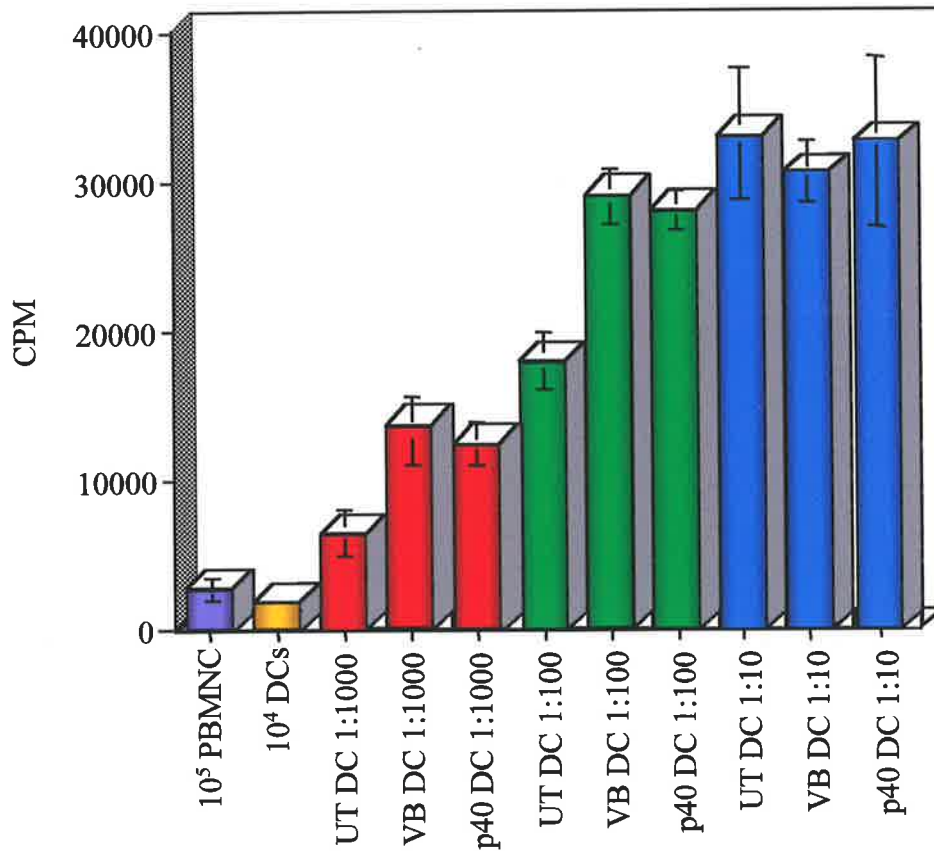


Figure 4.11. Human DC-MLR. PBMNC (10^5) were cultured with monocyte-derived dendritic cells at different stimulator:responder ratios (1:10, 1:100, 1:1000). The dendritic cells included in the assay were transfected with vector blank (VB) or IL-12 p40 (p40) adenovirus at a multiplicity of infection of 5000, or untreated (UT). A DC dose-dependent increase in proliferation was observed, however, no there was no significant difference between vector blank and p40 at any stimulator:responder ratio.

Phenotypic assessment of the ovine afferent lymph DCs using flow cytometry detected high level expression of MHC Class I and Class II antigen presenting molecules and low level CD80/CD86 costimulatory molecule expression (**Figure 4.3**). The presence of the DC marker CD1a was consistent with the DC phenotype (188), however, low level expression of the monocyte marker, CD14, was also detected. Contaminating lymphocytes were present in the cell preparation after metrizamide enrichment for the DC fraction, and this may account for the detection of CD14 expression. The presence of other cell types (without DC morphology) was observed using light microscopy, however, in much reduced numbers when compared to the non-enriched fraction. Alternatively, as the CD14 marker is present on monocytes/macrophages and not present on DCs (190), CD14 marker expression may reflect cells in the enriched population that have not fully differentiated into DCs. Additional characterisation of these cells by flow cytometry was limited by the availability of anti-ovine antibodies. In particular, assessment of the markers CD40, CD33 and the costimulatory molecules CD80 and CD86 (individually as opposed to the combined detection that was available) would have allowed a more direct comparison with the human monocyte-derived DCs. Morphologically, these cells show the characteristic dendrites and were comparable in this regard to the human monocyte-derived DCs (**Figure 4.1**).

Modification of DCs to express a selected gene, or gene combination, can be performed using adenoviral or retroviral vectors, with this type of manipulation becoming increasingly popular. Adenoviral vectors are attractive for this purpose allowing high level transfection without perturbing DC maturation (191) or allostimulatory capacity (192). The gene expressed by the adenoviral vector may also provide some measure of protection for the cells (193) which are likely to induce an

anti-viral immune response due to the expression of adenoviral proteins. One candidate gene is IL-12 p40 due to its intrinsic ability to inhibit the IL-12 heterodimer. Blockade of IL-12 biological activity in allograft transplantation may be effective, for example, by inhibiting the development of a Th1-type response, or the prevention of cytotoxic NK and CD8⁺ T cell activity. An additional advantage of this protein is that it is naturally synthesised and as such is not immunogenic.

An adenoviral construct expressing ovine IL-12 p40 was generated and the capacity of DCs to synthesise this protein upon transfection was assessed. Immunoprecipitation of IL-12 p40 protein was demonstrated from ovine afferent lymph DCs, human monocyte-derived DCs and ovine fibroblasts. Three bands were observed in human DC and ovine fibroblast treatment lanes, with the major species at approximately 40 kDa. An additional 43 kDa species was also present, and may be attributed to a differentially glycosylated form of the p40 protein, with further experiments using deglycosylating agents, such as N-glycosidase required for confirmation. Differentially glycosylated forms of IL-12 p40 from cells transfected with p40 plasmids have been demonstrated using such agents (30). An 80 kDa band could be visualised on the autoradiograph in the lanes of the human DCs transfected with the IL-12 p40 adenovirus. Reduction of this high molecular weight product to a single band of 40 kDa suggested that this species was p40 homodimer. Homodimer was also present in autoradiographs of IL-12 p40-infected fibroblasts (data not shown). The presence of homodimer in lanes of ovine DCs transfected with the IL-12 p40 adenovirus was not clearly discernible, as proteins in this molecular weight range were present in all treatment lanes. Low level expression of homodimer may have been present and not observed due to the higher intensities of the non-specific protein bands. As DCs are capable of IL-12 production (12) these higher molecular

weight proteins may be accounted for by DC expression of IL-12 heterodimer. However, SDS-PAGE analysis of the proteins under reducing conditions did not result in the expected banding pattern. Resolution of the higher molecular weight proteins into two bands of 35 and 40 kDa was not observed, as seen for reduction of ovine IL-12 heterodimer from CHO cells co-transfectants. Based on this analysis the high molecular weight bands do not appear to be related to IL-12. The production of p40 homodimer by the adenovirus-transfected human DCs was the first demonstration that ovine p40 was capable of forming p40 homodimer. Homodimer was not previously identified in CHO cells transfected with the ovine p40 plasmid (**Chapter 3**), and its generation may be dependent on the cell type expressing the p40 gene.

The *in vitro* and *in vivo* inhibitory activity of IL-12 p70 biological activity by the IL-12 p40 subunit has been reported by several groups (37-39). Inhibition of IL-12-induced proliferation by ovine p40 was assessed in this study using the IL-12 proliferation assay described in **Chapter 3**. Conditioned medium from fibroblasts infected with the IL-12 p40 adenovirus was used as a source of p40 protein. Inhibition of IL-12-induced proliferation was observed at 10% and 50% concentrations of IL-12 p40 conditioned medium. This clearly demonstrated that ovine p40 had the IL-12 inhibitory properties ascribed to both human and murine p40 (30, 37, 39). This was important data for studies in which the suppression of IL-12 biological activity was required. Immunoprecipitation data from the fibroblasts showed that p40 monomer was the major p40 species, with a less intense band for the p40 homodimer (data not shown). The monomeric form of p40 has been shown to be less effective than homodimer in binding to the IL-12 receptor and inhibiting IL-12 activity (30, 39). However, effective inhibition of IL-12 activity by the p40

species present in the IL-12 p40 fibroblast conditioned medium was clearly demonstrated.

IL-12 p70 can be detected in the mixed lymphocyte reaction at approximately 48-72 hours of culture (194). IL-12 production in the MLR at this stage would be expected to enhance the proliferation of activated cells expressing IL-12 receptors. As demonstrated by the Con A or PHA assays, activation of cells is a prerequisite for effective IL-12-induced proliferation (1, 2). Extrapolation of these results would suggest that IL-12 produced in the MLR would contribute to the proliferation of activated cells. Therefore, addition of p40 conditioned medium at the 10% or 50% concentrations (shown to be inhibitory in the IL-12 proliferation assay) would be expected to reduce proliferation of the DC-MLR and two-way MLR. In all cases, no additional suppression of the proliferative response using IL-12 p40-transfected DCs or p40 conditioned medium was observed. Inhibition of the allogeneic proliferative response by IL-12 p40 may have been more apparent if DC-induced proliferation of a single T cell population had been assessed. Based on the work of others, the proliferation of the CD4⁺ T cell population would be predicted to be most susceptible to inhibition by p40 (117). This approach was not undertaken, as depletion of a T cell population for *in vivo* treatment is not desirable. Although any *in vitro* assay is limited, where possible the MLR was used to reflect all cell populations.

A DC dose-dependent increase in proliferation was noted for both ovine and human DC-MLR assays, with untransfected DCs having the greatest ability to enhance cell proliferation. Modification of ovine DCs by transfection with vector blank or IL-12 p40 adenovirus actually resulted in decreased proliferation, most apparent at stimulator:responder ratios of 1:10. This was unexpected, as the adenovirus-transfected cells would be predicted to have an increased antigenic

potential compared to unmodified due to the presentation of viral peptides on the DC surface. In contrast, the presence of adenovirus-transfected DCs in the human DC-MLR resulted in increased proliferation, relative to the unmodified control as expected (192). These results may reflect an intrinsic difference between ovine afferent lymph and human monocyte-derived DCs, although both types of DC had a relatively immature phenotype (with low CD80 and CD86, although, high level expression of CD40 was detectable on human cells). The presence of a high viral load may be responsible for the inhibitory effect as transfection with 1000 as opposed to 5000 MOI reproducibly resulted in a slight improvement in proliferation (data not shown). Suppression of immune responses as a result of viral infection has been reported for other virus types (195-198). This includes a replication-deficient herpes simplex virus, where infected DCs were poor stimulators of allogeneic CD4⁺ T cell proliferation (199). Based on the examples above, transfection of ovine DCs with the adenoviral vector may induce production of the inhibitory cytokine IL-10, for example, which is capable of inhibiting alloantigen-specific proliferation (200). Alternatively, the viral presence may affect maturation of the DCs preventing the progression from an immature (antigen uptake and processing (131)) to the mature (T cell stimulation, MHC and costimulatory molecule upregulation (131)) phenotype. The adenoviral presence may downregulate expression of MHC molecules thus limiting antigen presentation. This may inhibit subsequent cell activation and proliferation. Similarly, prevention of costimulatory molecule upregulation may cause the virus to be provided in a tolerogenic manner (presentation without the additional activating signals). Alternatively, overexpression of GFP due to transfection with adenoviral vectors containing this marker gene may have been

toxic. Rounding of cells and apoptosis has been reported in GFP expressing cells (201), with cell death in the DC-MLR likely to result in reduced proliferation.

No additional inhibition of the DC-MLR was observed when IL-12 p40 virus transfected DCs were present. As these cells were effective producers of the p40 protein, as demonstrated by immunoprecipitation, lack of gene expression was unlikely to account for this result. High level expression of the gene product due to efficient transfection and control by a CMV promoter would have provided sufficient p40 in the culture milieu to account for even high level production of IL-12 heterodimer in the DC-MLR. In addition, the p40 protein produced by this adenoviral construct generated IL-12 p40 with IL-12 heterodimer inhibitory activity. Conditioned medium from adenovirus-infected fibroblasts was also used, however, no additional suppression of the proliferative response appeared to be attributable to the presence of p40. The limited availability of ovine-specific reagents prevented direct comparison of IL-12 p40-mediated inhibition with an IL-12 neutralising antibody in the DC-MLR and two-way MLR. As described in **Chapter 3**, the polyclonal anti-human IL-12 antibody was unable to inhibit proliferation of activated cells in response to ovine IL-12 (**Figure 3.6B** and **3.7B**). Direct comparison, although of potential interest, should not ultimately be necessary as the IL-12 inhibitory effect of the p40-conditioned medium used in the MLR was confirmed using the IL-12 proliferation assays.

The strong expression of the homodimer from human monocyte-derived DCs transfected with IL-12 p40 suggested that more effective antagonism of IL-12 activity in the DC-MLR might be achieved. The ability of ovine IL-12 p40 to inhibit human IL-12-induced proliferation was demonstrated using IL-12 p40 fibroblast conditioned medium at 10% and 50% concentrations. However, no significant

difference in proliferation between vector blank and IL-12 p40 transfected DCs was detected in the human DC-MLR.

Assessment of changes in proliferation due to inhibition of IL-12 may not have been a sufficiently sensitive method to determine the effects of IL-12 produced in the MLR. IL-12-driven proliferation of activated cells is but one measure of the biological activity of this cytokine. Culture of allogeneic cells in the mixed lymphocyte reaction is likely to generate cytotoxic effectors as well as the differentiation of CD4⁺ T cells into IFN- γ producers. Comparison of the IFN- γ levels in the culture supernatant between vector blank and IL-12 p40 wells would be expected to show decreased IFN- γ production in the p40 containing wells. Alternatively, the generation of alloantigen-specific CTL could have been assessed, with addition of p40 expected to result in decreased CTL activity. CTL generation in response to IL-4 has been shown to require endogenous IL-12, and specific lysis can be inhibited by anti-IL-12 antibodies or IL-12 p40 (202). Other cytokines produced in the mixed lymphocyte reaction may also promote lymphocyte proliferation, an effect that would not be inhibited by the addition of IL-12 p40. DCs are able to upregulate the expression of high affinity IL-2 receptors on allogeneic T cells and are able to secrete IL-2, promoting T cell proliferation (134). This pathway would not be expected to be inhibited by IL-12 p40 and may compensate for the loss of IL-12-induced proliferation caused by antagonism with IL-12 p40.

As with most *in vitro* models, direct comparison to *in vivo* setting is difficult. A multitude of interactions by soluble factors and cell-cell interactions that cannot be mimicked *in vitro* may influence the final outcome. Effective use of IL-12 p40 in preventing rejection of syngeneic or allogeneic tissue in murine models has been achieved (118, 119). This contrasts with the systemic administration of homodimer

and IL-12 p40 knockout mice (which are also affected systemically by virtue of their genetic background) where graft survival is actually accelerated (116). The therapeutic value of IL-12 p40 may be more effectively assessed in an *in vivo* model. A small animal model of skin transplantation has been developed in our laboratory (Dr G Patrick, Ph.D. Thesis (203)). NOD-SCID (non-obese diabetic severe combined immunodeficiency) mice are deficient in NK cells, mature T and B cells, as well as complement (204). Skin of ovine (or human) origin can be grafted onto the mice and the grafts accepted without rejection. Reconstitution of the mice with allogeneic PBMNC results in a significant infiltration of cells into the graft and the graft is destroyed (Dr G Patrick, Ph.D. Thesis). The injection of autologous DCs simulates *in vivo* the presence of passenger leukocytes migrating from the allograft into the recipient. The administration of unmodified DCs can accelerate the rejection process, however, engineering the DCs to express the cytokine IL-10 has been shown to inhibit the rejection process (205). As with the *in vitro* DC-MLR assay, DCs transfected with IL-12 p40 could be introduced into the grafted mice to assess whether cells engineered to express IL-12 p40 can prevent or reduce graft destruction. Successful inhibition of rejection in this model would then hold promise for the use of this treatment in the pre-clinical ovine model of renal transplantation.

Chapter 5

Characterisation of an IL-12 p35 Subunit mRNA Splice Variant

Chapter 5

Characterisation of an IL-12 p35 Subunit mRNA Splice Variant

5.1. Introduction

Alternative IL-12 p35 mRNA transcripts have been described for both human and murine p35 mRNAs, with these transcripts having different transcription start sites (25, 26). In the course of cloning the human p35 cDNA described in **Chapter 3**, higher molecular weight clones were consistently identified amongst normal p35 clones. These resulted from the inclusion of additional nucleotides corresponding to intron 4 of the p35 gene. Retention of an intron within an mRNA transcript is an unusual event as transcription of eukaryotic genes gives rise to pre-mRNA, composed of exons, which encode for protein, and introns, the intervening non-coding sequence. This pre-mRNA is subsequently processed by the cellular machinery referred to as the 'spliceosome' to remove the intronic sequence (206). The spliceosome is a complex molecule composed of RNA and protein factors, with over 70 different proteins suggested to be involved (207). Under normal circumstances several features serve to identify nucleotide sequence as intronic, and therefore indicate that this sequence should be removed. The ends of the intron are marked by the presence of the invariant GU and AG dinucleotides (208) as shown in **Figure 5.1**. These are the donor and acceptor sites at the 5' and 3' end, respectively. A second, less common, intron class has also been identified with 5' AU and 3' AC as alternative invariant dinucleotides (210). Other features of the intron include the

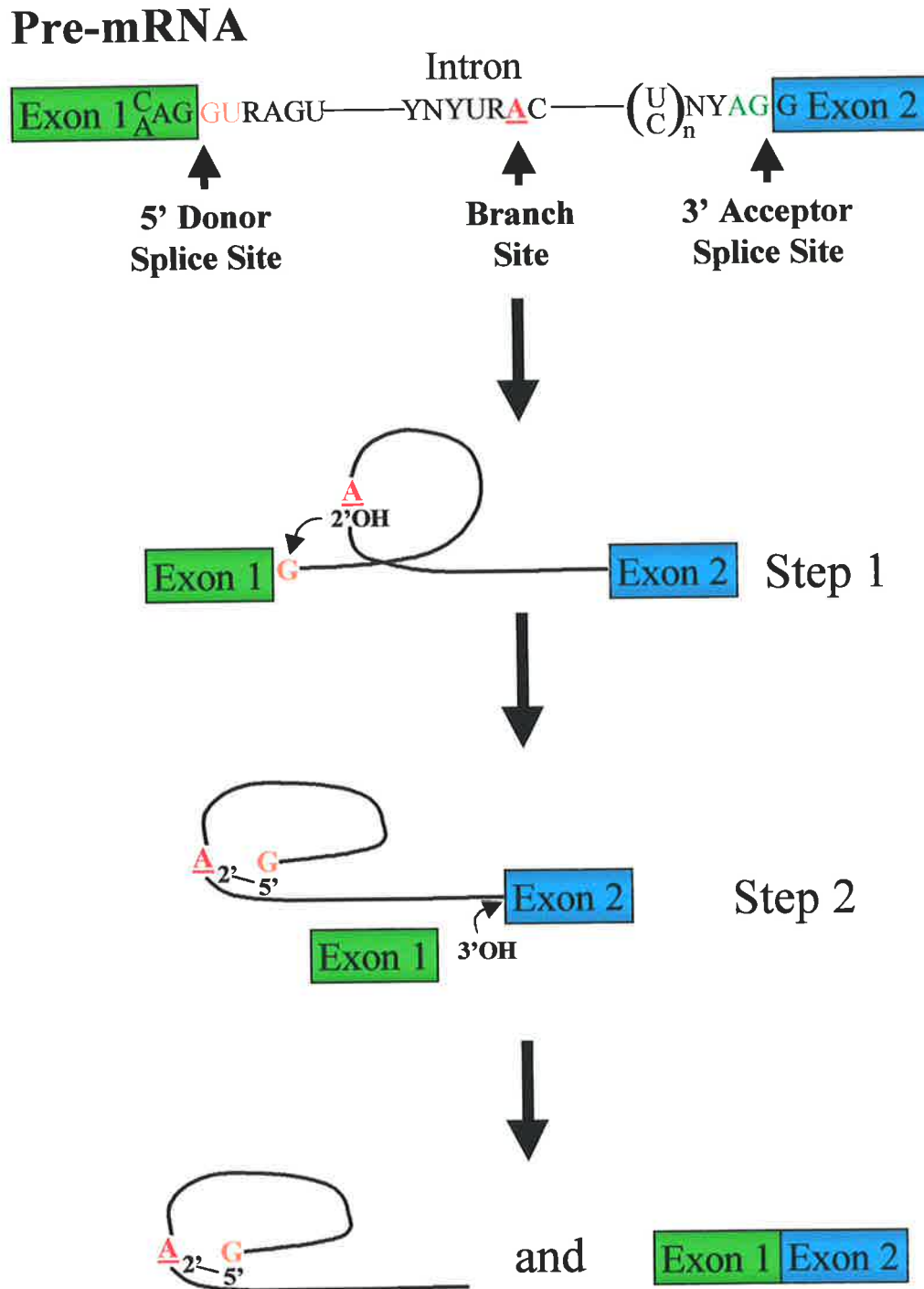


Figure 5.1. Two step transesterification reaction of pre-mRNA splicing. 5' and 3' splice site and branch site consensus sequences shown are for eukaryotic organisms. The invariant nucleotides at the 5' and 3' end of the intron are marked in orange and green respectively. The branch site adenosine residue is indicated in red. R, represents any purine and Y, represents any pyrimidine residue. The polypyrimidine tract is shown by 'n' C or U residues to indicate the variable length of this region. Diagram as modified from Legrain, 1994 (209).

branch site sequence with an adenosine residue (the branch point) located 18-37 bases from the 3' splice site (211, 212), and the polypyrimidine tract, a stretch of C and U residues situated directly upstream of the 3' end of the intron (213). Strong conservation of these sequences is observed in yeast (214), however greater divergence exists in higher eukaryotes.

Once recognition of the intron has occurred, the intron is removed in a two step transesterification reaction (**Figure 5.1**). **Step 1** involves cleavage of the 5' donor splice site to form a 2'-5' phosphodiester bond between the first nucleotide of the intron and an adenosine residue from the intron branch site. This generates a free 3'-hydroxyl group at the exon 1 end, and an intron 1-exon 2 'lariat' structure, with the branch point adenosine involved in 3 phosphodiester bonds. **Step 2** involves cleavage of the 3' acceptor splice site to release the lariat structure and the two exons are then joined (215). A more detailed overview of the splicing mechanism is provided in **Appendix I**. Efficient export of the mature mRNA into the cytoplasm for translation requires the addition of a cap structure to the 5' end (216) and polyadenylation of the transcript 3' end (217). Transport is achieved by the interaction of the mRNA with the nuclear pores (218). The presence of an intron within a pre-mRNA leads to the formation of complexes, as a result of splicing, which actually enhance the transport of mRNA into the cytoplasm (219).

5.2. Intron Retention in mRNA Transcripts

Alternative splicing can generate multiple protein isoforms from a single gene, with potentially different functions. This can be accomplished through the use of mutually exclusive exons (220), exon skipping (221) or less frequently by intron retention. While introns are normally removed, multiple examples of eukaryotic

mRNAs that retain an intron have been reported (222-224). In some instances the translated protein is functionally different to the standard protein isoform. An example of this is the rat vitamin D receptor (rVDR0, standard isoform) which retains intron 8 in the final mRNA transcript (rVDR1) (225). This transcript is expressed at 5-6% of normal transcript levels and appears to be specific to different stages of development. rVDR1 differs from the normal rVDR0 transcript at the C-terminal end due to premature termination of the protein and the inclusion of new amino acids. Consequently, rVDR1 has impaired ligand-binding activity but is still capable of forming homodimers and interacting with the vitamin D response element. This variant protein acts as a negative regulator of the vitamin D signalling pathway (225).

While intron retention can be detected in normal cells due to environmental or developmental changes, retention has also been observed in cancer cell lines (226, 227) and in tumour tissue (226). It has been suggested that deregulation of normal splicing occurs as a result of the transformation to the malignant cell type (227). Antigenic epitopes can also be encoded by introns as a T cell clonoid used to screen an expressed cDNA library identified a transcript which retained intron 4 of *gp100* (*gp100-in4*) (228). The epitope recognised by this clonoid was encoded by intron 4, and in transient transfection assays this intron was inefficiently spliced, as normal gp100 protein was not generated. The 5' splice site showed general consensus, however the polypyrimidine tract contained an unusual number of adenosine residues, affecting the splicing efficiency (228). Similarly, a mRNA transcript retaining intron 2 and part of intron 4 of the tyrosinase-related protein, *TRP-2*, has been identified (229). A cytotoxic T lymphocyte clone was shown to recognise an epitope encoded by *TRP-2* intron 2 (*TRP-2-INT2*). Only melanomas positive for *TRP-2* were shown to have

TRP-2-INT2 mRNA and this mRNA species was absent in melanocyte cell lines derived from normal human individuals (229). Thus, recognition of these cells can be enhanced by the expression of intron-encoded peptides in cells in which the normal function has been disrupted.

The best-described example of intron retention comes from the bovine growth hormone (bGH) (230). Cloning of the complete bovine growth hormone gene into an expression vector resulted in the identification of a mRNA species containing the final intron, intron D. Northern blotting did not reveal mRNA transcripts with the other bGH introns retained, and the intron D-containing transcripts were confirmed by nuclease S1 mapping. Translation of this variant mRNA species was suggested by the detection of the intron D-containing mRNA isolated on polysomes. The intron-encoded sequence was shown to be in-frame with the preceding exon and termination of the transcript predicted to occur 50 nucleotides into the upstream exon. This variant protein contained 125 aa from normal bGH and a further 108 aa encoded by intron D/exon 5, and mRNA expression was detected in normal pituitary tissue (230). Further analysis showed that splicing of intron D was dependent on the presence of an element in exon 5 and deletion of this element resulted in intron D retention in nearly all bGH transcripts (231). This element (termed the 'FP' sequence) bound to a 35 kDa protein which could be cross-linked to this region suggesting that this exon 5 sequence was required for the early steps in spliceosome formation (232). The FP sequence was shown to be rich in purines (and known as a purine-rich exonic splicing enhancer – ESE) and able to bind to the splicing factor, SF2/ASF. Binding of SF2/ASF promoted splicing however this was counteracted by another protein factor involved in splicing, hnRNP A1 (233). Further sequence analysis identified that the 5' (234) and 3' (235) splice sites of bGH intron D

deviated from the consensus sequence, with mutation of the 5' splice site to complete consensus resulting in constitutive intron removal, independent of the FP sequence (234). The branch site and the polypyrimidine tract were also shown to be suboptimal with several purine residues present in the polypyrimidine tract, which has been shown to reduce the efficiency of splicing (236). Dirksen *et al* (235) proposed that the weak splice sites might prevent or reduce the formation of splicing commitment complexes allowing transport of intron-retaining mRNA to the cytoplasm. They also suggested that the splice sites cannot be too weak, while still allowing intron retention in a percentage of transcripts.

Cloning of the p35 cDNA lead to the identification of a previously unreported p35 mRNA variant present in both humans and sheep. It was previously noted (S Swinburne, Honours Thesis) that in PCR analysis of cDNA from ovine renal allograft biopsies that an aberrant molecular weight band was present. This was initially thought to be a PCR artefact, however, its recurrence in RT-PCR amplification, despite increased amplification stringency strongly suggested that further analysis was warranted.

Definitions

Standard p35: complete open reading frame of the p35 subunit of IL-12 generated using primers designed to amplify the human cDNA sequence deposited in the Genbank database (Accession Number M65291).

Variante p35: complete cDNA open reading frame of standard p35 with the inclusion of 75 bp (human) or 76 bp (ovine) of additional intronic nucleotide sequence.

Truncated Variant p35: Variant p35 (human) modified to terminate at the STOP codon encoded by the 75 bp of intronic sequence with all 3' sequence deleted.

Aims

To characterise a p35 mRNA variant identified in both humans and sheep and (a) determine the biological activity of the translated protein, (b) assess the likely utility of this protein as an antagonist for transplantation therapy by:

- i. cloning and sequencing human and ovine standard and variant p35 transcripts and identifying protein motifs;
- ii. determining the pattern of variant mRNA expression in normal human individuals;
- iii. transfecting CHO cells with human and ovine standard and variant p35 cDNA alone or in combination with IL-12 p40, and
- iv. generating constructs of the variant p35 cDNA to elucidate the functional properties of this molecule.

Cloning Protocol

Several different types of clones were generated for the work performed in this chapter and the primer sequences for cloning are provided in **Appendix II**. The 5' end of all forward primers was modified to include the consensus sequence GCCACC (127) to enhance mRNA translation. In all cases sequencing was used to confirm the correct insert type.

pRc/CMV Cloning

Standard p35 and the initial intron-containing p35 variant were generated using primers designed to amplify the complete open reading frame of p35. Products were sequenced and subcloned into the pRc/CMV expression vector. A more detailed description and cloning diagram are provided in **Chapter 3, Figure 3.1**.

Generation of the truncated intron-containing variant p35 utilised the same forward primer as above, however the reverse primer was designed to include a STOP codon, as normally encoded by the intron (**Figure 5.2**). Primer STOP codon sequence was modified from 'TAG' to 'TGA', and PCR products were ligated into the pGEM[®]-T Easy cloning vector. Fragments were excised from the cloning vector using the NotI restriction enzyme and subcloned into the pRc/CMV vector linearised with NotI. Clones were screened for orientation using the PstI restriction enzyme. The PstI restriction enzyme cuts at two sites within the pRc/CMV plasmid, and once within the truncated variant p35 cDNA. However, only the discriminating site within the cDNA is indicated (**Figure 5.2**).

pEGFP-N1 Cloning

Standard and truncated p35 cDNA products were generated using the forward primer as above and terminal primers without the STOP codon sequence, as shown in **Figure 5.3**. PCR products were ligated into the pGEM[®]-T Easy cloning vector. The orientation of the standard p35 cDNA was determined using the restriction enzymes ApaI/BamHI and the truncated variant p35 orientation using ApaI/XbaI. Subcloning was performed by excision of the inserts from the pGEM[®]-T Easy plasmids with ApaI/SacI and ligation of the fragment into the pEGFP-N1 vector cut

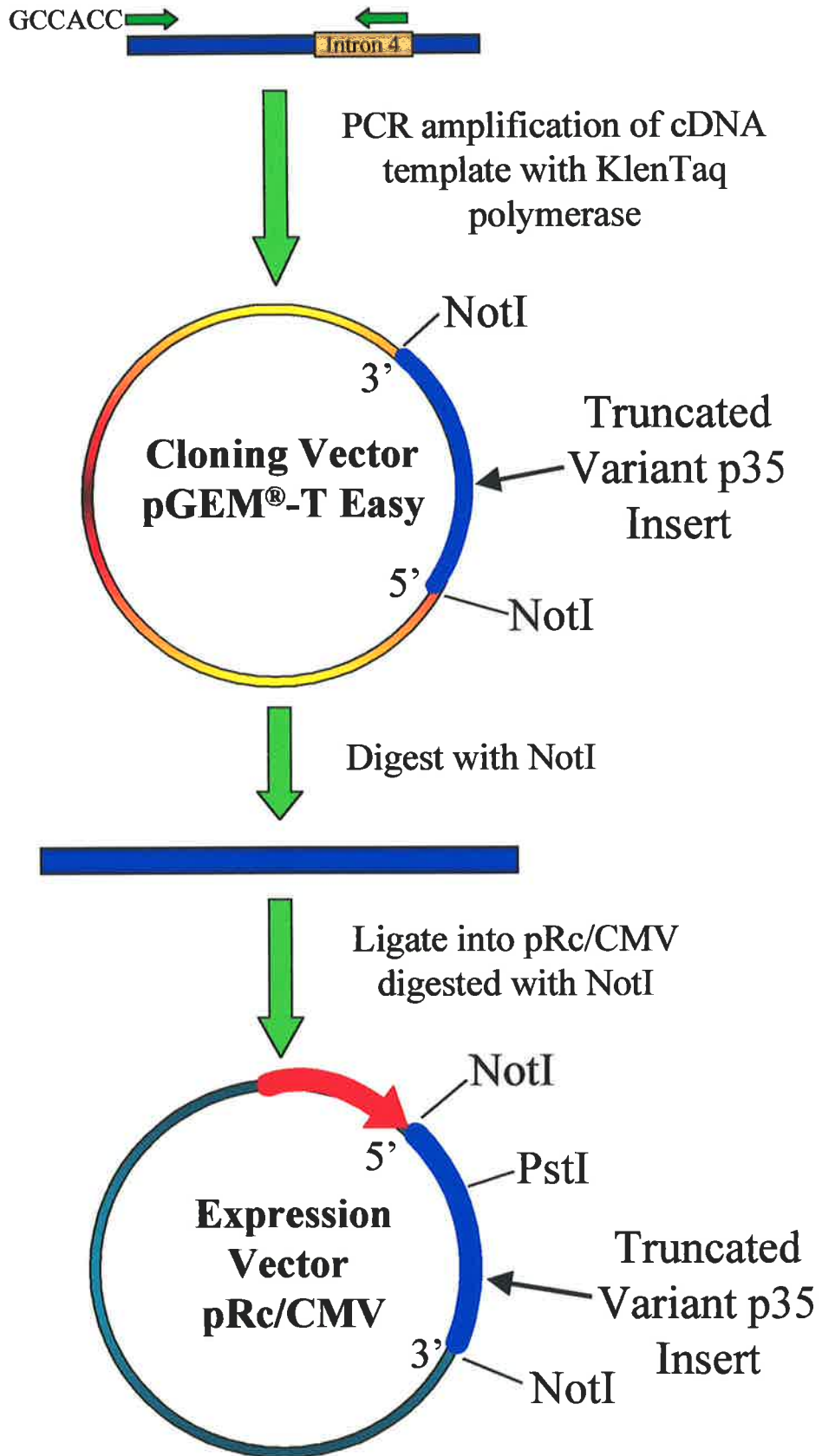


Figure 5.2. Cloning protocol for the generation of truncated variant p35 in the pRc/CMV vector as described in the chapter text under pRc/CMV Cloning.

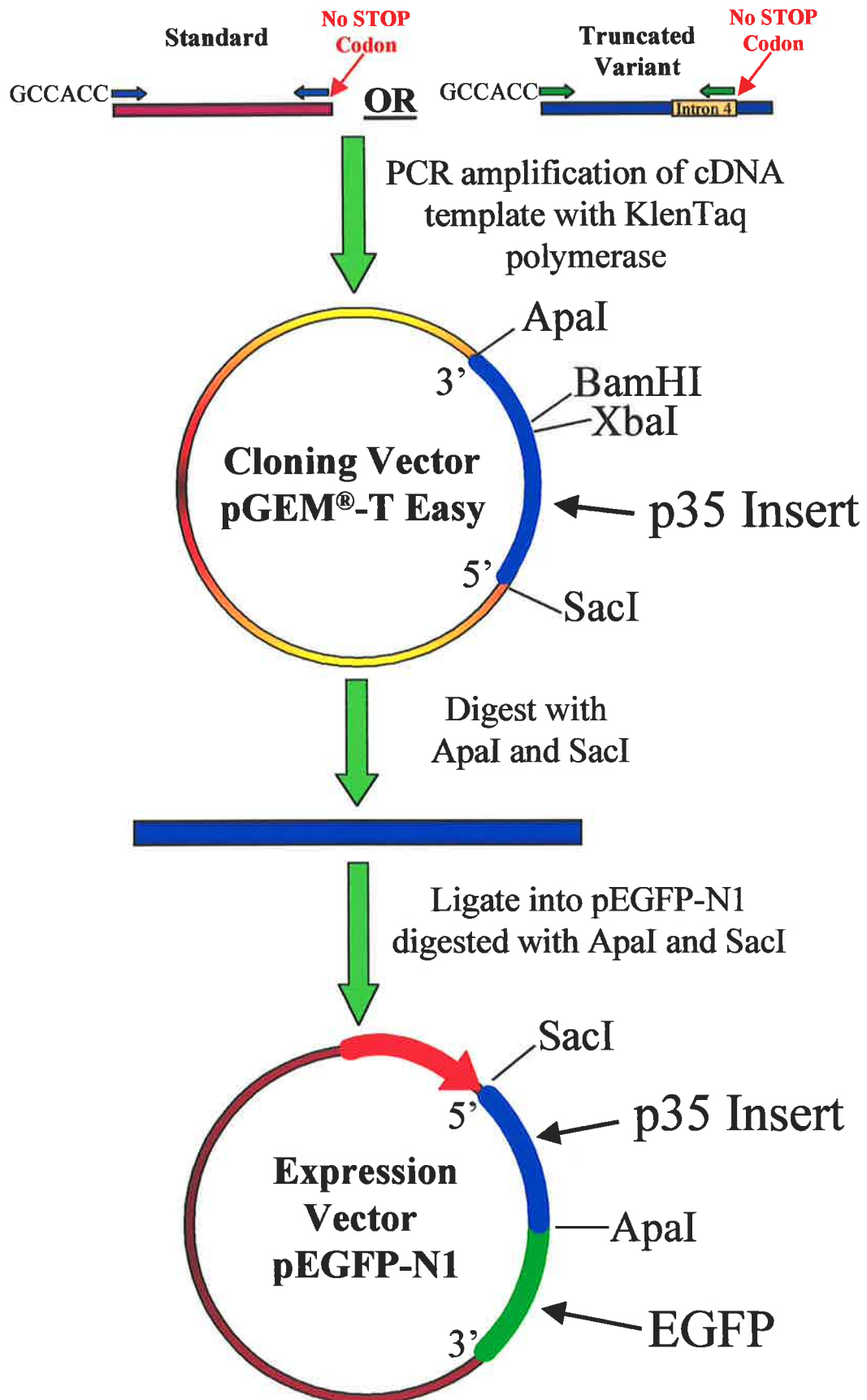


Figure 5.3. Cloning protocol for the generation of in-frame standard and truncated variant p35 EGFP-fusion proteins. Procedure is as outlined in the chapter text under **pEGFP-N1 Cloning**.

with the corresponding enzymes. Sequencing and EGFP fluorescence positive cells confirmed that the cDNA inserts were cloned in-frame.

5.3. Methods

5.3.1. Preparation of Genomic DNA

Human PBMNC (5-20 x 10⁶ cells) were collected and resuspended in 500 µl of TES. Proteinase K (30 µl) was added and mixed before the addition of 30 µl of 20% SDS (in the order cited) and the tubes mixed gently by inversion. Incubation was carried out at 56°C O/N and the protein was precipitated by addition of an equal volume of 3 M NaCl, mixed and incubated on ice for 10 min. Tubes were then microcentrifuged for 10 min and the supernatant added to 2 volumes of ethanol. DNA was precipitated by microfuging for 30 sec at 13,000 rpm. A single wash in 1 ml of 70% ethanol was then performed. DNA was resuspended in Milli-Q water.

NOTE: Resuspension may take some time and tubes can be left O/N or additional water can be added. DO NOT VORTEX! This leads to shearing of the genomic DNA.

5.3.2. Analysis of Enhanced Green Fluorescent Protein in Transfected

CHO Cells

EGFP fluorescent cells were prepared differently for visualisation depending on the final application. For assessment of successful transfection cells were detached and approximately 5 x 10⁵ cells were spotted directly onto a glass slide. A coverslip was placed over the cells and the cells were visualised using fluorescent microscopy.

For confocal microscopy EGFP-transfected cells were washed once in PBS and resuspended in s10g at a density of 1×10^6 cells/ml. Cell suspension (5×10^4 cells in 50 μ l) was added to 950 μ l of s10g in a chambered slide and the cells allowed to adhere O/N. All medium was then removed, the chambered section and seal lifted from the slide base, and a coverslip placed over the cells. Dr Peter Kolesik at the Plant Research Centre of the University of Adelaide's Waite Campus performed the confocal microscopy.

5.3.3. Western Blot of EGFP-Fusion Protein Transfected CHO Cells

CHO cells were transfected with EGFP plasmids using the method described in 2.3.14. Cells were allowed to recover for 48 hours before collection and resuspended at a density of 2×10^6 cells/60 μ l of 2X Laemmli sample buffer. Each sample (30 μ l) was boiled for 10 min before loading onto a SDS-PAGE gel and run as described in 2.3.16. The gel was then equilibrated in cold Western transfer buffer for 15-30 min along with 2 Scotch pads and the nitrocellulose membrane. Two pieces of Whatman filter paper were immersed briefly in transfer buffer and assembled in the cassette as shown in **Figure 5.4**. Transfer was performed at 900 mA for 30 min using a Bio-Rad Mini PROTEAN[®] II apparatus. An ice block was included in the tank to prevent buffer warming and a magnetic stirrer was used to circulate the buffer. When transfer was complete the membrane was washed for 1 min in PBS, followed by a 5 min wash in TBS. Blocking of the membrane was carried out by incubation in 5% Blotto for 2 hours on a rocking platform. TBS washes (2 x 5 min) were performed before incubation of the membrane with the Living Colors[®] peptide anti-EGFP primary antibody (40 μ l in 8 ml of PBS-FT) O/N with rocking. The membrane was washed in TBS (2 x 5 min) and incubated with

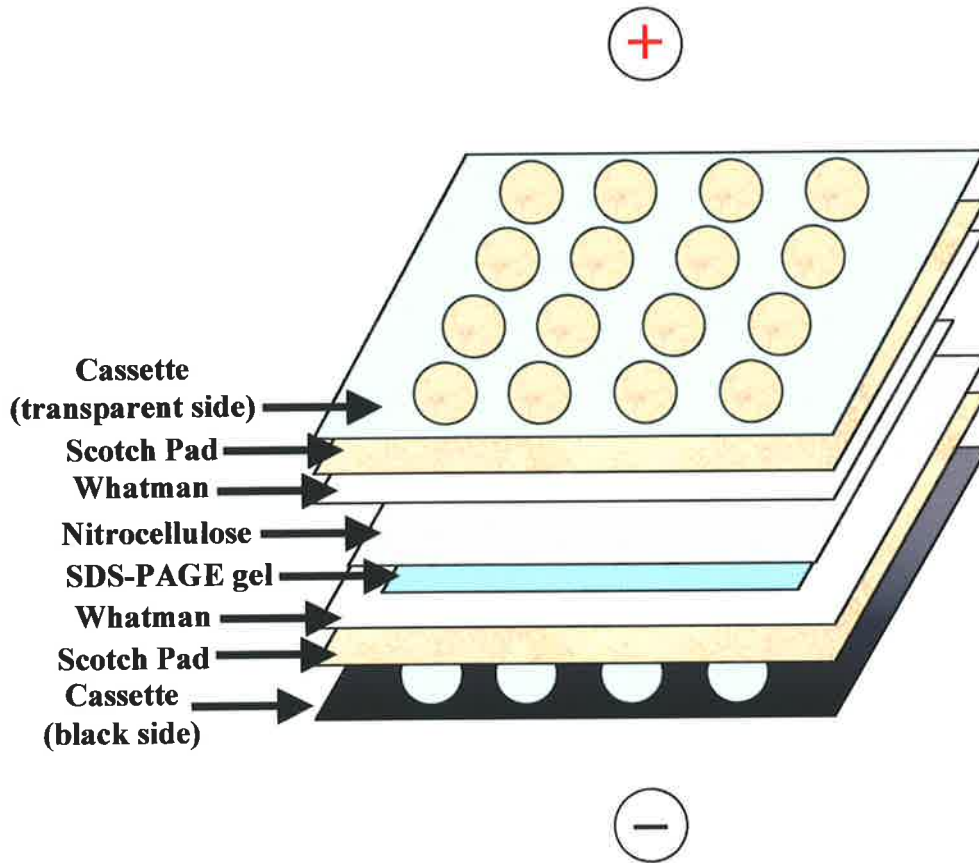


Figure 5.4. Western blot assembly for transfer of proteins to nitrocellulose membrane. All of the above were assembled in a Mini PROTEAN® II cassette as shown, and the cassette was then loaded into the tank. Prestained protein markers present on the nitrocellulose membrane were used as an indicator of effective transfer.

secondary goat anti-rabbit biotinylated antibody (1/8000 dilution in PBS-FT) for 1 hour. Membrane was washed as above and then incubated with streptavidin-AP (AP, alkaline phosphatase) conjugate for a further hour (1/5000 dilution in PBS-FT). The membrane was washed in TBS (2 x 5 min) before a 5 min equilibration step in substrate buffer. The membrane was then incubated in substrate buffer (10 ml) plus 45 μ l NBT and 35 μ l XPO₄ in the dark to allow the colour change reaction to proceed. Reaction was deemed complete when the membrane background became visible and was stopped by washing in water before a final 10 min treatment in 4.5% EDTA. Membranes were then air dried.

5.4. Results

5.4.1. Identification of a p35 mRNA Variant

The variant p35 transcript was initially identified in cDNA from ovine renal transplant biopsies as a larger molecular weight PCR product. Cloning of human IL-12 p35 identified the presence of clones with a higher than expected molecular weight of approximately 100 bp using the pUC19 molecular weight marker as a reference. Several of these clones were selected and sequenced, and this revealed the in-frame insertion of 75 nucleotides within the human p35 coding region.

Cloning of full-length ovine p35 also revealed the presence of clones with a higher than expected molecular weight amongst the standard clones. These too showed the presence of a short sequence of 76 bp within the normal coding sequence (**Figure 5.5**). To confirm that it was this insertion that generated the higher molecular weight band observed in the initial PCRs of ovine renal biopsy cDNA, this band was cloned and sequenced, and revealed the presence of the same 76 bp insert.

				↓ Exon 4 (42 bp)	
	351				400
Human Variant	GGCCTGTTTA	CCATTGGAAT	TAACCAAGAA	TGAGAGTTGC	CTAAATTCCA
Ovine Variant	GGCCTGTTTA	CCACTGGAAT	TAGCCACGAA	TGAGAGTTGC	CTGGCTTCCA
Consensus	GGCCTGTTTA	CCA.TGGAAT	TA.CCA.GAA	TGAGAGTTGC	CT...TTCCA
			Intron 4		
			→		
	401				450
Human Variant	GAGAGACCTC	TTTCATAACT	GTAAGTCAA	AAATGAAAAG	TTTCAGCCTG
Ovine Variant	GAGAGACCTC	TTTAATAACT	GTAAGTCAGA	AAATTGAAAG	TTTCAGCTCA
Consensus	GAGAGACCTC	TTT.ATAACT	<u>GTAAGTCA.A</u>	<u>AAAT..AAAG</u>	<u>TTTCAGC...</u>
					↓ 500
Human Variant	TATGATGAAT	TCATATCACT	GATGTCTGAT	TATTTTTTCC	T.CTAGAATG
Ovine Variant	TATTATGAAT	TCATATCATT	GATATCTCAT	TATTTTTTTC	TTCTAGAATG
Consensus	<u>TAT.ATGAAT</u>	<u>TCATATCA.T</u>	<u>GAT.TCT.AT</u>	<u>TATTTTTT.C</u>	<u>T.CTAGAATG</u>
		Exon 5 (42 bp)		↓ Exon 6	
	501				550
Human Variant	GGAGTTGCCT	GGCCTCCAGA	AAGACCTCTT	TTATGATGGC	CCTGTGCCTT
Ovine Variant	GGCATTGTCT	GTCTTCTGGA	AAGACCTCTT	TTATGACAAC	CCTGTGCCTT
Consensus	GG..TTG.CT	G.C.TC..GA	AAGACCTCTT	TTATGA...C	CCTGTGCCTT

Figure 5.5. Alignment of human and ovine variant p35 nucleotide sequences. Retained intron 4 is shown in bold for human (75 bp) and ovine (76 bp) with the consensus sequence underlined. Nucleotide position of the cDNA is as indicated. The flanking exons (human exons 4 and 5) are marked, and the length of these exons is shown, with the downward arrows marking where introns would be positioned in the genomic DNA. Alignment performed using the MultAlin program (237).

Analysis of the retained sequence identified it as having features consistent with that of an intron. These features included the conserved GU and AG dinucleotides that mark the start and finish of an intron, respectively, as well as the presence of a polypyrimidine tract. Confirmation of this sequence as intronic was obtained upon publication of a paper on human p35 that allowed this sequence to be identified as intron 4 (25).

5.4.2. Exclusion of Genomic DNA

To confirm that genomic DNA (gDNA) was not responsible for the isolated clones, PCR was performed using an intron 4-specific primer and an antisense primer located in exon 6. As expected, a larger band was amplified from the gDNA than for the cDNA control, excluding gDNA as a source of these clones (**Figure 5.6**). Primers spanning a larger region of the p35 gene provided further confirmation that gDNA was not the source of this material (data not shown).

5.4.3. Translation of Human and Ovine Variant p35 Nucleotide Sequence

Translation of the nucleotide sequence would give rise to a truncated p35 protein with new C-terminal amino acids. In both cases the retained sequence is in-frame with the 5' coding sequence. For the human variant a premature termination codon would be encoded by the TAG of the intronic sequence end and generate a truncated p35 protein of 164 amino acids (compared with 253 aa for standard p35, **Figure 5.7**). For the ovine variant protein the termination codon did not occur until 57 bp into the 3' coding sequence, giving rise to a protein of 151 amino acids (compared with 221 aa for standard ovine p35, **Figure 5.8**). This reflects the absence

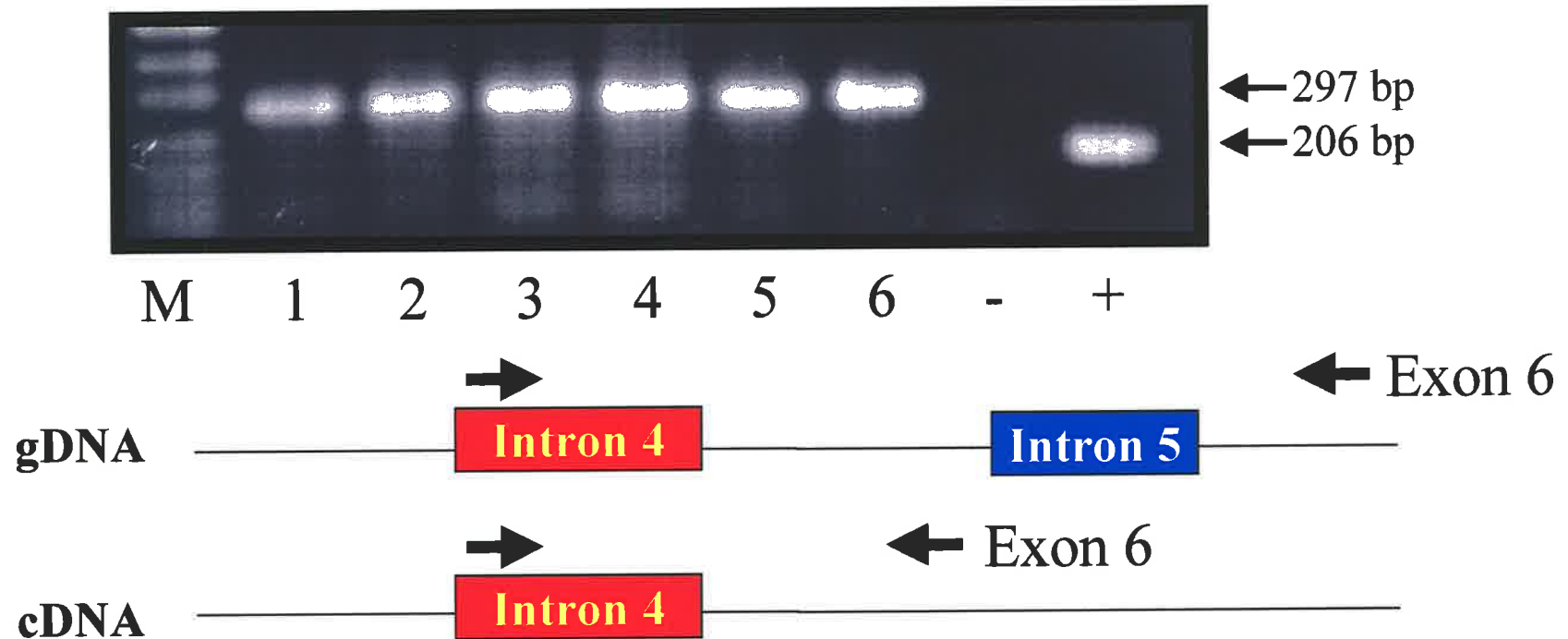


Figure 5.6. Amplification of human genomic DNA using an intron 4-specific primer and an internal human p35 antisense primer located in exon 6. Primers span two p35 introns and clearly demonstrate that the cDNA product does not result from genomic DNA contamination. Primers spanning multiple introns of the p35 gene gave equivalent results (data not shown). M indicates the marker lane, with lanes 1-6 indicating different human gDNA samples. Negative control (-) was PCR without template added, positive control (+) was a dilution of plasmid with the variant p35 cDNA insert.

		10	20	30	40	50	60
Standard p35	MWPPGSASQPPSPAAATGLHPAARPVSLQ	CRLSM	CPARSLLL	VATLVLLD	HLSLARNLP		
Variant p35	MWPPGSASQPPSPAAATGLHPAARPVSLQ	CRLSM	CPARSLLL	VATLVLLD	HLSLARNLP		
		70	80	90	100	110	120
Standard p35	VATPDPGMFPC	LHHSQ	NLLRAVSNML	LQKARQ	TLEFYP	CTSEEIDHEDITKDKTSTVEACL	
Variant p35	VATPDPGMFPC	LHHSQ	NLLRAVSNML	LQKARQ	TLEFYP	CTSEEIDHEDITKDKTSTVEACL	
		130	140	150	160	170	180
Standard p35	PLELTKNES	CLNSRETSFIT	NGSCLAS	RSKTSFMMAL	CLSSIYEDLKMYQVEFKTMNAKLL		
Variant p35	PLELTKNES	CLNSRETSFIT	VSQK	MKSFSL	.YDEFISLMSDYFFL	
		190	200	210	220	230	240
Standard p35	MDPKRQIFLDQ	NMLAVIDELMQALNFNSETVPQKSSLEEPDFYKTKIKL	CILLHAFRIRA				
Variant p35
		250					
Standard p35	VTIDRVMSYLNAS*						
Variant p35						

Figure 5.7. Alignment of human standard and variant p35 amino acid sequences. Amino acid positions are marked by the numbers above the protein sequence. The leucine zipper motif is marked in green, the N-glycosylation site in blue and the protein kinase C phosphorylation sites are marked in yellow. The cysteine residues are indicated in orange and the new amino acids encoded by translation of intron 4 are marked in red. The translated sequence was obtained using ‘The Protein Machine’ and the alignment performed using the MultAlin program (237).

		1							50
Standard	p35	MCPLRSLLLI	STLVLLHHL P	HLSLGRSLPT	TTAGPGTSC L	DYSQNLLRAV			
Variant	p35	MCPLRSLLLI	STLVLLHHL P	HLSLGRSLPT	TTAGPGTSC L	DYSQNLLRAV			
		51							100
Standard	p35	SNTLQKARQT	LEFYSC TSEE	IDHEDITKDK	TSTVEACLPL	ELATNESCLA			
Variant	p35	SNTLQKARQT	LEFYSC TSEE	IDHEDITKDK	TSTVEACLPL	ELATNESCLA			
		101							150
Standard	p35	SRETSLITNG	HCLSSGKTSF	MTTLC LRSIY	KDLKMYHMEF	QAMNAKLLMD			
Variant	p35	SRETSLITVS	QKIESF.SSY	YEFISLISHY	FFLLEWALS.	.VFWKDLFYD			
		151							200
Standard	p35	PKRQVFLDQN	MLAAIAELMQ	ALNFDSETVP	QKPSLEELDF	YKTKVKLCIL			
Variant	p35	NPVP.....			
		201							221
Standard	p35	LHAFRIRAVT	IDRMMSYLSS	S*					
Variant	p35					

Figure 5.8. Alignment of ovine standard and variant p35 amino acid sequences. Amino acid positions are as indicated by the numbers above the protein. The cysteine residues are indicated in orange, the leucine zippers in green and the N-glycosylation site in blue. Protein kinase C phosphorylation sites are shown in yellow and the additional amino acid sequence encoded by intron 4, exon 5 and part of exon 6 in the variant p35 protein is shown in red. Translated using the ‘Protein Machine’ and multiple alignment performed using the MultAlin program (237).

of 113 aa in the human variant p35 protein and the inclusion of 24 new amino acids. In ovine variant p35 113 aa are also absent, however, 43 additional amino acids are included as a result of the translation of intron 4, exon 5 and the first 11 bases of exon 6. The positions of the human and murine p35 introns within the coding sequence are conserved (as assessed by sequence alignment). As such the position of the introns and exons in ovine p35 can be predicted with a high degree of accuracy, allowing the position and length of exon 5 and exon 6 to be estimated.

Analysis of the new human amino acid sequence (variant p35) was performed using a program to search for protein motifs (ScanProsite (128)). An N-glycosylation site at position 141-144 is lost, however, the leucine zipper motif is conserved. A protein kinase C (PKC) phosphorylation site is still present in both the standard and the variant proteins, although, they are positioned differently due to the inclusion of the new amino acids in the variant protein (amino acids 142-144 as opposed to 147-149). Several cysteine residues are also lost as a result of the new amino acid sequence, however, the residue at position 74 involved in intermolecular disulphide-bonding with the p40 subunit is retained (4).

The translated ovine p35 variant protein shows conservation of the single N-glycosylation site at positions 95-98. The first leucine zipper motif at amino acids 40-61 is retained, with the second leucine zipper motif lost due to the inclusion of the new amino acids. The PKC phosphorylation site is also conserved and, as seen for the human protein, the sequence and position are slightly different (standard sequence amino acids SGK, position 115-117; variant sequence SQK, 110-112).

5.4.4. Sequence Similarity of p35 Introns

Alignment of human, ovine and murine intron 4 sequences revealed a higher than expected degree of similarity. As intronic sequence does not normally encode for protein, greater sequence divergence is generally observed between species than for the coding exonic sequence (238). When the intron-containing p35 sequences were aligned, the presence of the intron within the standard p35 backbone did not significantly affect the overall similarity of the nucleotide sequences between species. The similarity between human vs ovine and human vs murine intron 4 sequences was 84.2% and 70.7%, respectively.

As intron 4 was highly conserved, the degree of similarity between other introns of the IL-12 p35 gene was assessed by alignment to determine whether this was a feature of p35 introns. Where sequence information was available, analysis was performed between human and murine sequences. The size of each intron is indicated in **Table 5.1** as published (22, 25). Introns 1, 2, and 6 vary significantly in size between species suggesting that only limited similarity within the intron was likely, and complete human genomic sequence was not available. Comparison of the sequence available for intron 3 (only 316 bp of mouse genomic sequence as compared to complete human intron 3) revealed less than 50% similarity, which was not unexpected considering the difference in size (325 bp compared to 600 bp). Unexpectedly intron 5 showed a higher level of similarity between species (66.7 %).

To assess whether inclusion of intron 4 resulted from a poor splice site consensus, the splice sites were examined. Strong matches to consensus were shown for all constitutively spliced p35 introns at the splice site junctions (**Table 5.1**). Analysis of the splice site flanking intron 4 showed the sequence to be 5' ACT/gtaagt --- tag/A 3'. Compared with the consensus splice sequence the 5' site has a 7 out of 9

match (77%) and the 3' site a 3 out of 4 match (75%). The presence of a 'T' or a 'C' at position -3 of the 3' site has been shown by the analysis of multiple splice sites, with a slight preference for a 'C' nucleotide (213). More recently, a preference for 'C' at position -3 has been shown in primates and mammals (239). The presence of a 'T' nucleotide at this position of intron 4 may contribute to a weakened 3' splice site, as the consensus match was only 50% using these consensus rules.

Other features within the intron may also affect splicing efficiency, for example the polypyrimidine tract (240) and the branch site (241, 242). The identification of a branch site within eukaryotic introns is frequently difficult despite the identification of a consensus sequence YNYURAC (209), as they are generally poorly conserved. The branch point adenosine is usually present 18-37 nucleotides upstream of the 3' splice site (212). The best match in intron 4 using this consensus sequence is at nucleotide positions 47-53 (**Figure 5.9**), with the adenosine residue at nucleotide 52 being designated the branch point adenosine (sequence ⁴⁷CACTGAT⁵³). A cytosine is generally the preferred nucleotide in the 3' position adjacent to branch site adenosine (243). However, within this intron only one 'A' exists with a 'C' in this position (sequence ⁴³ATATCAC⁴⁹), and the rest of the consensus sequence is a much poorer match (4/7 as opposed to 6/7 requirements for consensus).

The polypyrimidine tract of intron 4 is predicted to consist of 11 pyrimidines (with sequence TTATTTTTTCCT) with a single purine insertion. The adenosine may mark the end of the tract or affect polypyrimidine tract function as a result of the presence of the purine residue (236).

5.4.5. Expression of the p35 Variant mRNA Transcript in Normal Human Peripheral Blood Mononuclear Cells

To examine whether this transcript could be identified in normal human individuals RNA was isolated from the PBMNC of normal donors and reverse transcribed. The resulting cDNA was then amplified using a sense intron 4-specific primer and an antisense exon 6 primer. The intron-containing p35 transcript was detected in all individuals as shown in **Figure 5.10**. At 35 cycles the variant p35 transcript was detectable at low levels in all individuals. Extending the cycle number to 50 cycles of amplification more clearly demonstrated the detection of this transcript in normal human PBMNC. All samples were assessed for equivalent loading by amplification of the β -actin mRNA (244) and found to be similar (data not shown).

5.4.6. Functional Aspects of the Intron Containing IL-12 p35 Variant – Formation of Heterodimers with the p40 Subunit

Premature truncation of the protein (in humans) at the end of intron 4 results in the deletion of nearly 50% of the standard p35 coding region. As a result, 3 cysteine residues are absent although cysteine 74, involved in intermolecular disulphide bonding with p40, is retained. As this residue is conserved, the truncated protein may still form intermolecular disulphide bonds with p40. To determine whether the variant p35 alone or in combination with human p40 had a biological function like IL-12 p70, CHO cell transfectants were generated. The conditioned medium was then used in a proliferation assay and the changes in proliferation relative to vector blank control medium were assessed. The conditioned medium obtained from the single transfectant showed no difference in proliferation when

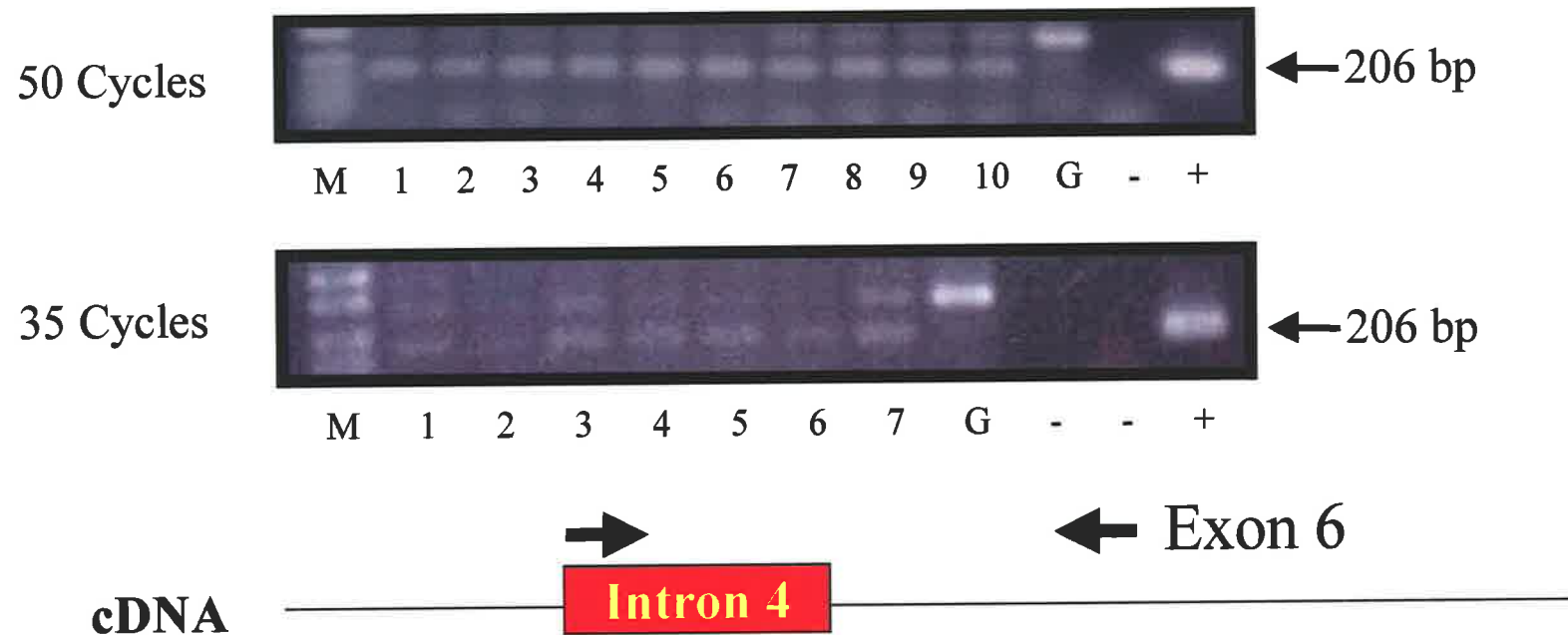


Figure 5.10. Amplification of human cDNA from the peripheral blood mononuclear cells of normal human individuals using an intron 4-specific primer and an internal human p35 antisense primer located in exon 6. The variant p35 mRNA could be detected in all samples. M indicates the marker lane, with lanes 1-7 and 1-10 indicating different human PBMNC samples. G indicates genomic DNA. Negative control (-) was PCR without template added, positive control (+) was a dilution of plasmid with the variant p35 cDNA insert. Loading of samples was equivalent based on β -actin mRNA amplification (data not shown).

compared to the vector blank negative control. However, variant p35 in combination with p40 significantly enhanced proliferation, equivalent to that of the normal p70 heterodimer from standard p35/p40 transfected cells (data not shown).

5.4.7. Immunoprecipitation of Human and Ovine Variant Proteins from CHO Cell Transfectants

Immunoprecipitation of proteins from human and ovine variant p35/p40 transfectants revealed the presence of 2 bands equivalent to the heterodimer generated by co-transfection of standard p35 and p40 (**Figure 5.11**). The expected lower molecular weight heterodimer, which would have been attributed to the variant p35 in combination with p40, was not observed. This suggested that splicing of the intron was occurring within the cell line due to the conditions set up for processing of the mRNA from the cDNA-containing plasmid. This was confirmed by RT-PCR in which standard mRNA transcripts were identified in variant p35 transfectants (data not shown). The activity of the p70 heterodimer generated in these cells may have overwhelmed any biological activity attributable to the variant p35/p40 heterodimer.

5.4.8. Detection of Properties Attributable to the Variant p35 Protein

In light of the difficulties associated with the detection and assessment of biological activity of the variant protein, a modified approach was taken. A truncated version of the variant transcript was generated with the 3' coding region upstream of the intron termination codon removed and the STOP codon modified ('TAG' to 'TGA') (**Figure 5.2**). Transfection of the truncated p35 plasmid alone or in combination with p40 was performed as before and the conditioned medium collected for assessment in the functional assay. No functional IL-12-like activity for

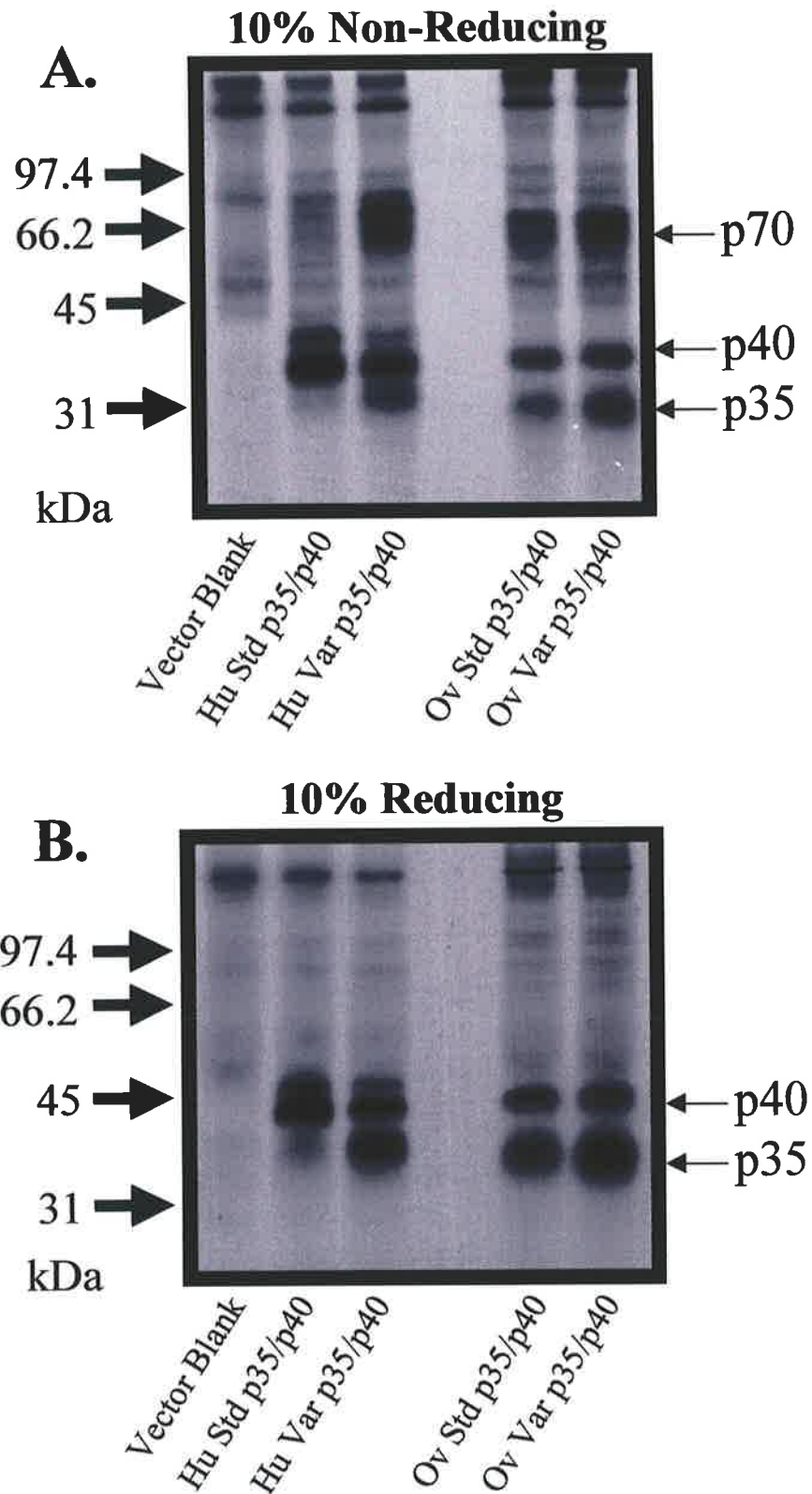


Figure 5.11. Immunoprecipitation of proteins from CHO cells co-transfected with human or ovine standard p35/p40 or variant p35/p40. **A.** Non-reducing gel. **B.** Reducing gel. The autoradiograph reveals the presence of identical banding patterns for both suggesting that the biological activity of the conditioned medium is due to the presence of heterodimeric p70 as a result of intron splicing. Std - standard, Var - variant.

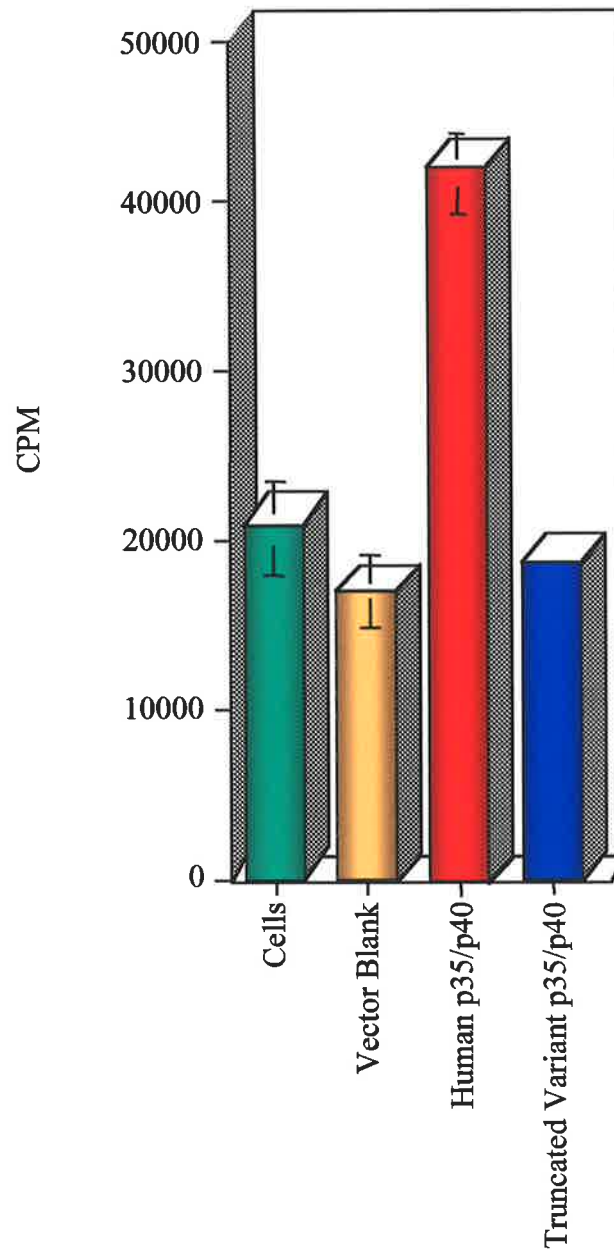
medium from the single (not shown) or double transfectants could be detected in the proliferation assay at any concentration of conditioned medium tested (up to 20%) (Figure 5.12). Proliferation showed no significant enhancement from the vector blank negative control.

5.4.9. Immunoprecipitation of the Truncated Variant p35 Protein Alone and in Combination with p40

Immunoprecipitation of proteins from the CHO cells co-transfected with truncated variant p35 in combination with p40 showed that the only protein present in the double transfectant lane was that attributable to p40 (Figure 5.13). Sequencing data indicated that the truncated variant p35 protein should be expressed, however, the inability to detect the protein by immunoprecipitation made interpretation of the results difficult (data not shown). To address this, another method of detection was used. New clones for standard p35 and the truncated variant p35 were created with the termination codon deleted (Figure 5.3). The resulting clones were then subcloned into the pEGFP-N1 expression vector to fuse the EGFP protein to the C-terminal end of the p35 proteins. This allowed detection without the need for a p35 variant-specific antibody as an anti-EGFP antibody could be used. Correct read-through into the pEGFP-N1 vector was confirmed by sequencing and substantiated by fluorescence microscopy.

5.4.10. Western Blot Assessment of Standard and Truncated Variant p35 EGFP-Fusion Protein Expression

Western blot analysis of lysates from EGFP-fusion protein transfected cells was used to determine the molecular weight of the proteins and assess protein



Transfectant Conditioned Medium

Figure 5.12. Human IL-12 PHA assay proliferation with CHO cell co-transfectant conditioned medium. Standard heterodimer compared with truncated variant p35/p40 conditioned medium, with only normal p70 able to induce proliferation.

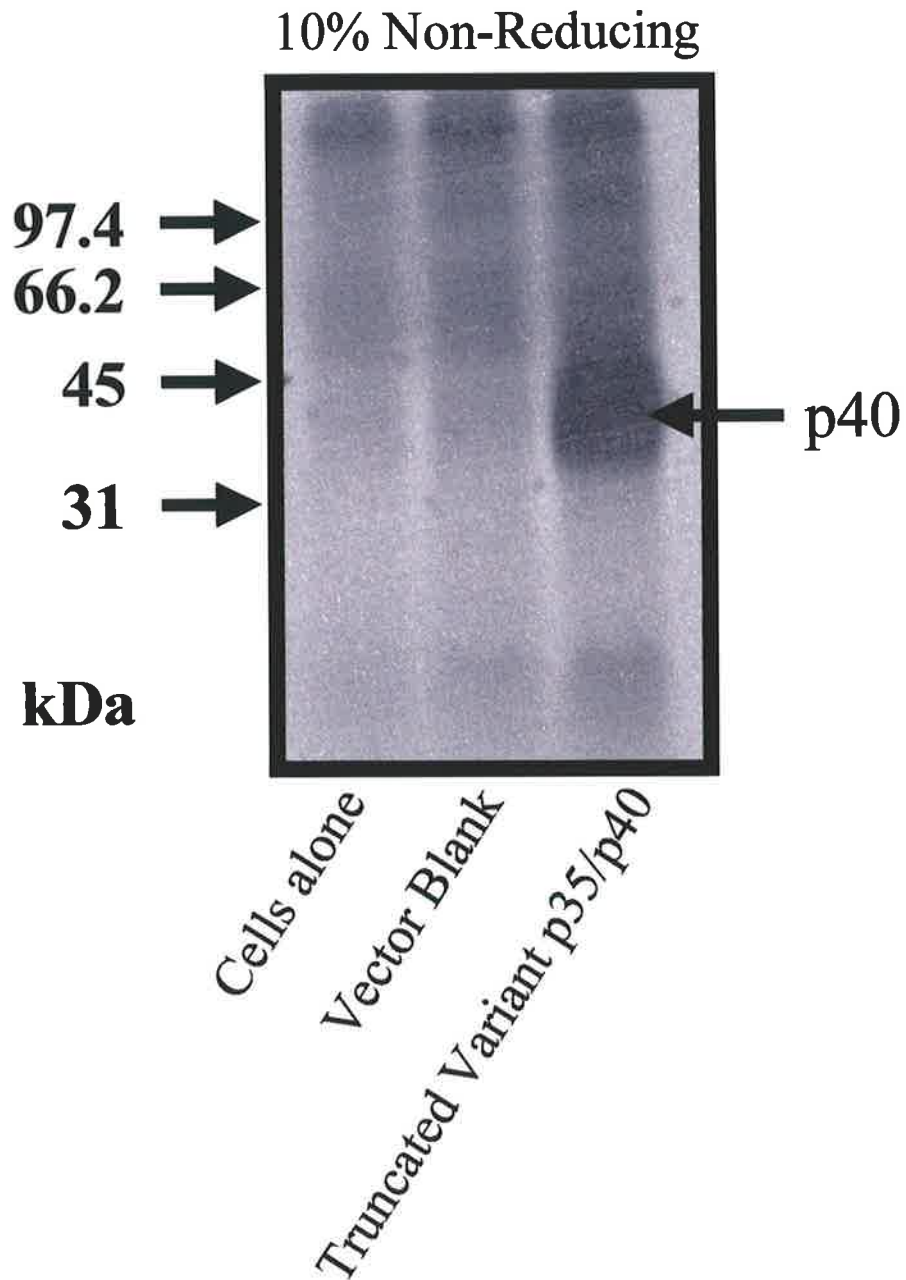


Figure 5.13. Autoradiograph of proteins immunoprecipitated from CHO cells co-transfected with human truncated variant p35 and p40. Proteins were precipitated with an anti-human IL-12 polyclonal antibody and analysed by non-reducing SDS-PAGE on a 10% gel. p40 protein alone was detectable.

production. Under non-reducing conditions high molecular weight bands were present in the lanes of p35 standard and truncated variant fusion proteins. A band at approximately 96 kDa for standard p35 and 70 kDa for the truncated protein were present in some blots (**Figure 5.14A**). Under reducing conditions the higher molecular weight species were resolved and a single band was detected in each of the standard and truncated lanes. The standard EGFP-fusion resulted in an approximately 67 kDa band that was about the predicted size for the 35 kDa protein fused to the approximately 30 kDa EGFP protein. Translation of the truncated p35 transcript was clearly demonstrated by the detection of a 56 kDa protein under reducing conditions (**Figure 5.14B**). The size of this protein without the EGFP would be expected to be about 20-25 kDa. This compares favourably with a predicted molecular weight of 18 kDa, however, this size prediction does not take into account any posttranslational modification.

5.4.11. EGFP-Fusion Protein Cellular Localisation

The presence of a leucine zipper motif within the standard and the truncated p35 suggested a possible role as a DNA transcription factor. As such, the proteins would most likely be located in the nucleus of the cell. The loss of amino acids in the truncated protein and the inclusion of 24 new amino acids may also result in an alternative cellular location for the protein. Using confocal fluorescence microscopy transiently transfected cells were viewed using blue light of approximately 488 nm to excite fluorescence of the EGFP. The distribution of the proteins was assessed by taking images of the cells in 1 μm sections. Cytoplasmic localisation was confirmed by overlaying light microscopy and fluorescent images of the cells in their correct morphology. As an effectively 'neutral' reporter gene, the function and location of

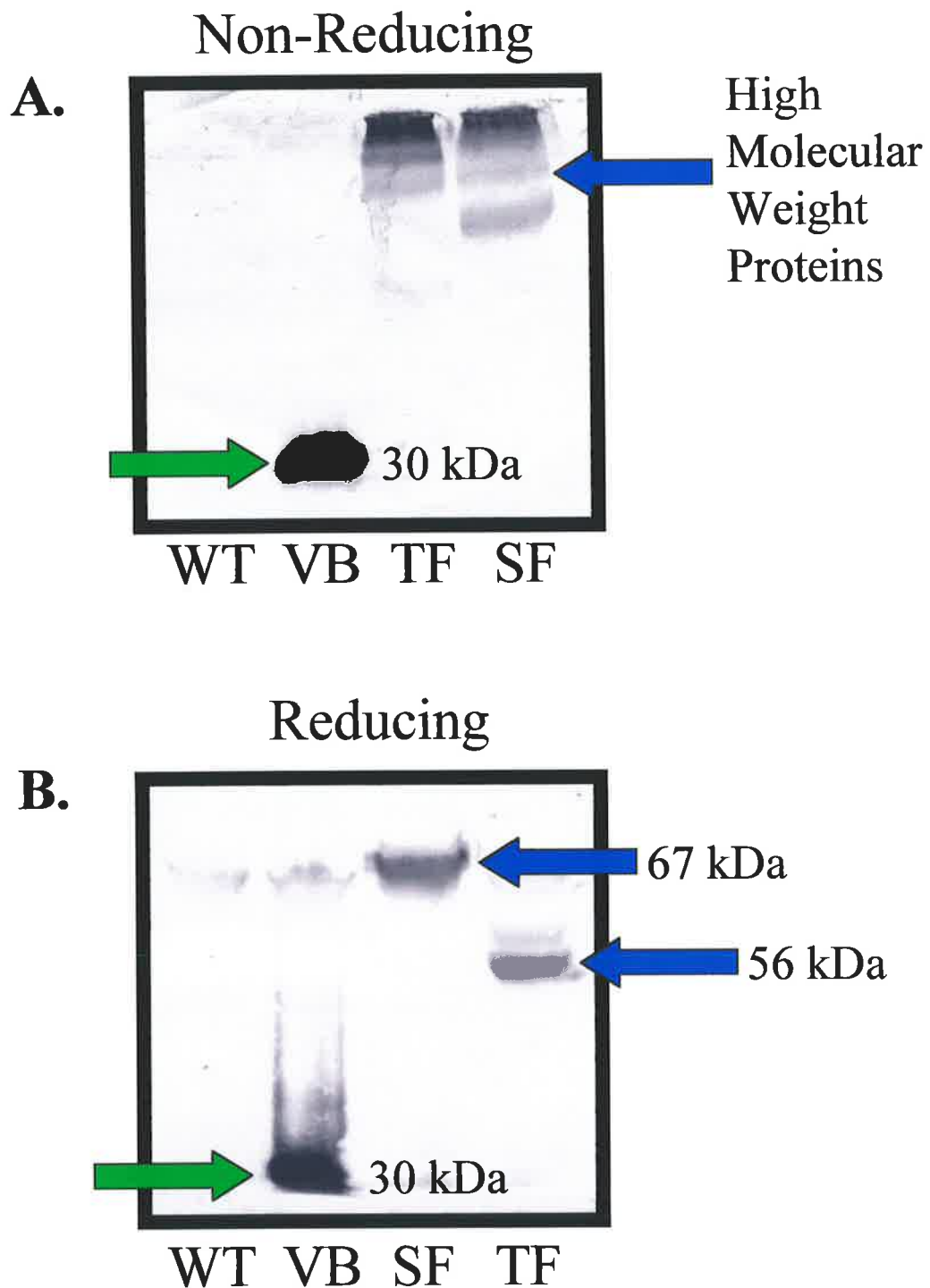


Figure 5.14. Western blots of standard and truncated variant p35 EGFP-fusion proteins from CHO cell transfectant lysates. **A.** Non-reducing and **B.** reducing conditions with wild type cells (WT), vector blank (VB), standard p35 fusion (SF) and truncated variant p35 fusion (TF). Samples were run on 10% SDS-PAGE gels and transferred to nitrocellulose membrane. Blots were probed with a polyclonal anti-EGFP antibody to detect bound proteins. Arrows indicate the proteins of interest and approximate sizes of the individual proteins are given.

the p35 proteins should not be impaired by fusion to EGFP. Wild-type EGFP was distributed throughout the CHO cells, being present in both the nucleus and cytoplasm (**Figure 5.15A**). In the p35 fusion protein transfectants, fluorescence intensity was more varied and on most occasions less intense than for EGFP vector alone transfectants. However, fluorescence was significantly above the autofluorescence of untransfected CHO cells, as assessed by visual inspection. Localisation of the standard (**Figure 5.15B**) and the truncated p35 EGFP-fusion proteins in transfected cells showed fluorescent proteins wholly within the cytoplasm and not nuclear as predicted (**Figure 5.15C**). The nucleus did not appear to contain fluorescent protein and showed up as a distinct, dark region within the cytoplasm. Variable protein distribution in the cell cytoplasm was noted, and on occasion some cells showed a uniform cytoplasmic distribution, whereas others had a more speckled appearance.

5.4.12. Biological Function of EGFP-Fusion/p40 Proteins

Co-transfection of CHO cells was performed using the truncated and standard p35 EGFP-fusion proteins in combination with human p40 (in the pRc/CMV vector). Functionality and ability of standard p35, in particular, to form the biologically active heterodimer was tested using the IL-12 proliferation assay. As shown in **Figure 5.16** the standard p35-fusion/p40 heterodimer was formed and able to enhance the proliferation of activated PBMNC. This suggested that the presence of the EGFP protein did not interfere with p35 protein folding, intermolecular bond formation with p40 or the receptor/cytokine interaction. The conditioned medium from the truncated p35 fusion/p40 transfected cells did not enhance the proliferation of the PHA-activated cells, and was comparable to the vector blank/p40 control.

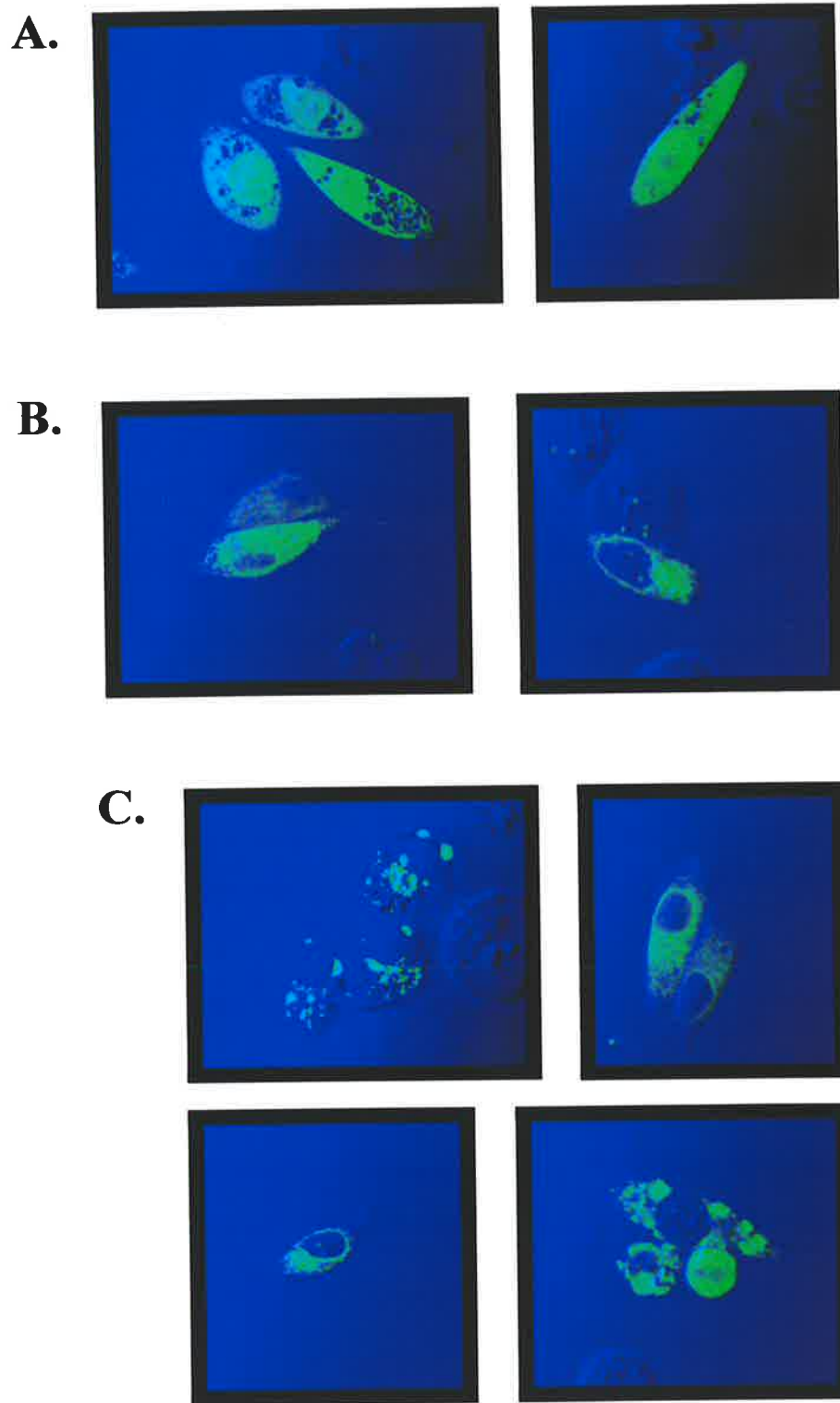


Figure 5.15. Fluorescent confocal microscopy pictures of live CHO cell transfectants expressing p35 EGFP-fusion proteins. A representative 1 μm section of the light microscope image with the fluorescent image overlay, to determine cellular location, is shown in each case. **A.** EGFP vector blank. **B.** Standard p35 fusion protein. **C.** Truncated variant p35 fusion protein. These images provide a representation of the cells visualised and fusion protein images are from a combination of independently isolated clones.

5.4.13. Heterodimerisation of p35 EGFP-Fusion Proteins with p40 as Assessed by Immunoprecipitation

Following Western blotting, which confirmed protein expression, immunoprecipitation was then used to demonstrate the presence or absence of heterodimer formation in the supernatants of truncated variant p35/p40 co-transfectants. In the standard p35/p40 lane the IL-12 antibody precipitated p40, standard p35 EGFP-fusion as well as a higher molecular weight band at approximately 100 kDa (the heterodimer, **Figure 5.17**). Only the p40 protein was precipitated in the truncated variant p35 EGFP-fusion/p40 and vector blank/p40 lanes.

Discussion

Intron retention within a mRNA is an unusual but not unprecedented event. Several mRNAs which retain introns including bovine growth hormone (230) and the vitamin D receptor (225) have been identified. Much work has been performed using the bovine growth hormone as a model to elucidate how this intron escapes removal from the pre-mRNA (231-235). In this chapter, preliminary characterisation of an IL-12 p35 mRNA that retains intron 4 is described. In part the interest in this protein stems from the potential ability of the variant protein to form a bond with p40. If this heterodimer is formed without eliciting p70-like activity, it may be used to inhibit the IL-12 p70 receptor/cytokine interaction or transduce a negative signal. This molecule may then be potentially useful as an IL-12 antagonist for use in transplantation gene therapy.

This intron-containing transcript was identified from clones derived from human peripheral blood mononuclear cells of normal individuals and renal allograft

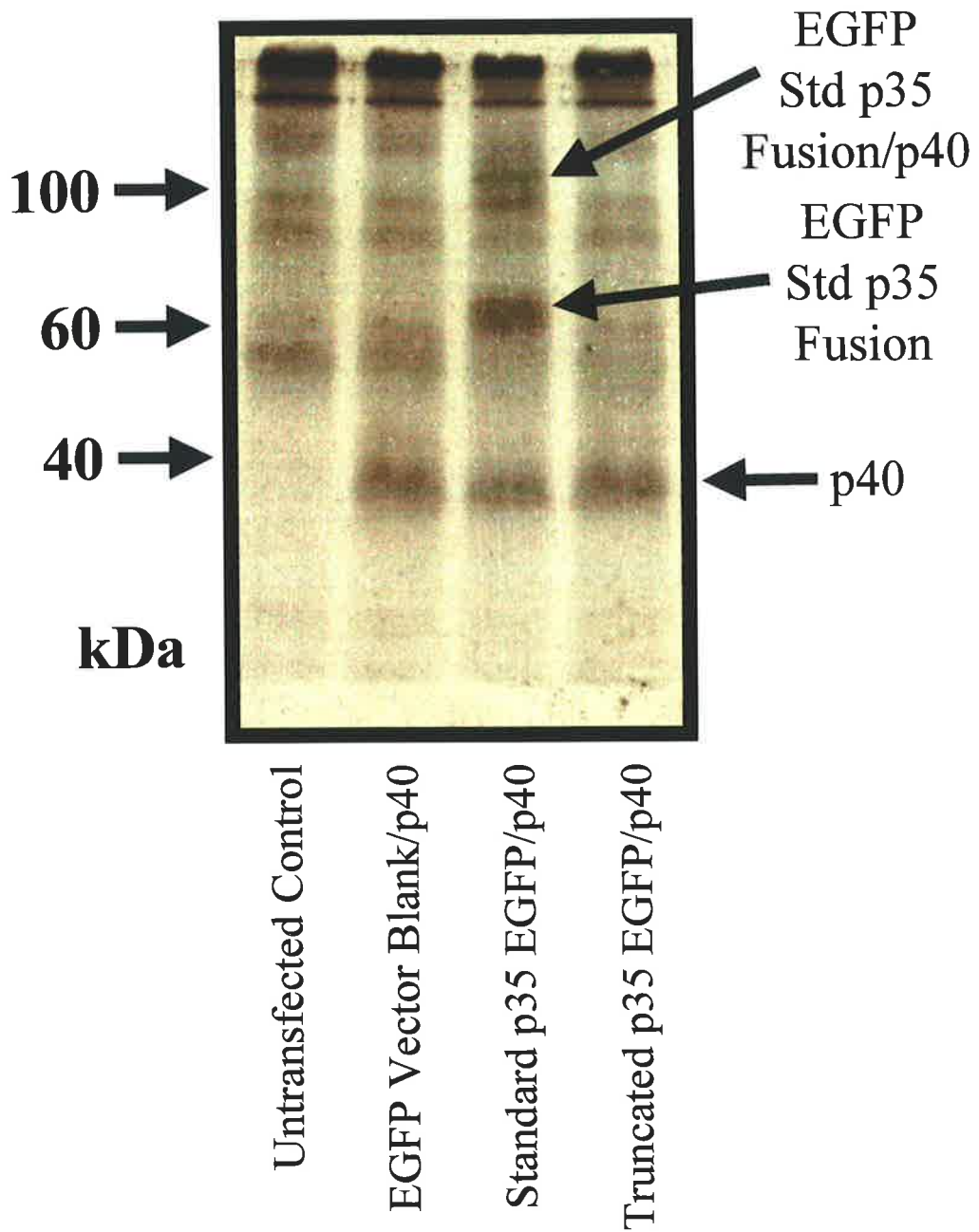


Figure 5.17. Autoradiograph of proteins immunoprecipitated from the supernatant of CHO cells co-transfected with EGFP-fusion proteins and p40. Higher molecular weight bands are present for standard 'p35' and the 'p70' heterodimer as a result of the EGFP protein tag. Only p40 was detected in the vector blank/p40 and truncated variant p35 EGFP-fusion/p40 lanes. Immunoprecipitation was performed using an anti-IL-12 polyclonal antibody.

patients. The cDNA used in the ovine cloning was from renal biopsy tissue. The occurrence of this transcript in both humans and sheep, as well as the high degree of homology between introns of both species (and that of murine intron 4), suggested that the protein translated from the intron-containing transcript may have a physiological function. This situation has also been described for the growth hormone genes where intron D of bovine and human origin show a high degree of conservation and intron D-containing transcripts can be identified in both species (230, 245).

The open reading frame of human variant p35 is in-frame with the coding sequence and terminated by a STOP codon encoded by the intron 3' end. The primers used to detect clones positive for p35 were internal primers capable of detecting all p35 clone types (with or without introns). On occasion, clones shown to be positive for p35 had inserts significantly different in size to standard p35 clones, however these were of variable sizes and a specific size was not consistently observed. Clones retaining intron 5, an intron of comparable size to intron 4 (91 bp compared to 75 bp) were not observed, and these clones would not have been distinguishable until sequenced. No sequenced clones were identified as retaining intron 5. In addition, this intron 4-containing transcript could be identified in normal human peripheral blood mononuclear cells. This suggested that the retention of intron 4 did not result from amplification and cloning of unspliced pre-mRNA. However, this possibility cannot be ruled out completely with the current data, as translation of this transcript in normal cells was not demonstrated.

Translation of the open reading frame of the intron-retaining variant mRNA results in truncation of the human standard p35 and ovine standard p35 protein sequence by approximately 45% and 51%, respectively. This protein sequence is

replaced by the inclusion of 24 intron-encoded amino acids in the human variant p35 protein and 43 intron/exon-encoded amino acids in the ovine variant p35 protein. A single N-linked glycosylation site is lost in the human variant p35 and this may affect secretion of p35 protein as inhibition of glycosylation has been shown to adversely affect the ability of this protein to be secreted (27). Protein kinase C sites were conserved in both the human and ovine variant p35 proteins, although the position of the site was shifted slightly. Conservation of this motif suggests that phosphorylation may be necessary for the function of the p35 subunit. Localisation of standard and variant p35 within the cytoplasm may be a reflection of an inactive state and phosphorylation of the proteins may lead to nuclear translocation. This may be particularly important if the leucine zipper of this protein does predict a role as a transcription factor. An example of such a protein is the nuclear transcription factor NF- κ B which is located in the cytoplasm, and phosphorylation of which is required for nuclear translocation (246). This leucine zipper motif is present in p35 of nearly all species for which the p35 cDNA has been cloned (assessed by analysis of amino acid sequence – data not shown). The leucine zipper motif is present in an amino acid sequence as a repetition of leucine residues every seventh position over eight helical turns of the protein (247). The leucine residues form alpha helices allowing dimers to be generated by interaction with the helix of an opposing molecule (248). The leucine zipper motif has been shown to be present in transcription regulatory proteins including the CCATT-box and enhancer binding protein (C/EBP) (249) and members of the AP1 family of transcription factors, Fos and Jun, which form heterodimers via the leucine zipper interaction (250). The functional significance of this motif in standard p35 and variant p35 has not been demonstrated and may suggest a role in the regulation of gene transcription.

The detection of intron containing mRNA in the cell cytoplasm is a relatively rare event, although several examples have been identified with the best characterised being the bovine growth hormone. Extensive analysis of the bGH mRNA, which retains intron D, revealed the existence of suboptimal 5' (234) and 3' (235) splice sites. The suboptimal sites reduce splicing efficiency, and a purine-rich exonic splicing enhancer is required to promote splicing of intron D (234). Analysis of the splice site sequence flanking intron 4 showed that the splice sites of p35 intron 4 match the consensus (213) with 77% and 75% identity for the 5' and 3' sites, respectively (**Table 5.1**). The presence of a 'T' nucleotide at position -3 of intron 4 may contribute to a weakened 3' splice site, changing consensus for this site to 50%, as mammalian introns show a preference for 'C' at this position (239).

The identification of a branch site within intron 4 was difficult, as complete consensus could not be identified. However a best match using the eukaryotic consensus sequence YNYURAC (209) proposes the branch site at positions 47-53, with the adenosine residue at nucleotide 52 designated as the branch point. An alternative sequence with a much poorer match (4/7 as opposed to 6/7 requirements for consensus) could be identified at positions 43-49 with the adenosine residue followed by the preferred cytosine. Alternatively, the branch site acceptor may not be an adenosine residue, as cytosine has also been shown to act in this role, although an adenosine is the preferred nucleotide (241, 251).

The polypyrimidine tract appeared to be comprised of 11 pyrimidine nucleotides (excludes the 3' splice site sequence) punctuated by the presence of an adenosine nucleotide at the -10 position of the pyrimidine stretch. Preferentially, 11 uninterrupted uridine residues provide the strongest polypyrimidine tracts (252) and purine residues within this region can affect the efficiency of splicing (236).

However, the designation of the polypyrimidine tract length for intron 4 is purely speculative without functional analysis.

Bearing in mind the limitations afforded by sequence analysis, and the examples of intron retention provided in the literature, mechanisms for the inclusion of intron 4 can be proposed. Further analysis such as that performed for the bovine growth hormone (i.e. mutation of sites toward consensus, deletion of the purine element, lengthening of intron or exon sequence and the effect on intron splicing) are required to elucidate the actual mechanism(s). The splice sites, the branch site and potentially the polypyrimidine tract of intron 4 do not achieve complete consensus and each element alone is unlikely to generate retention of the intron. With the exception of the branch site, which was more difficult to match to the consensus sequence, the other components did not show exceptional divergence from consensus. However, this may amount to a sufficient weakening of intron recognition to allow a percentage of transcripts where intron 4 remains unspliced when each component is utilised in concert. With this in mind, additional elements may be required to facilitate intron removal. For the bovine growth hormone an exonic enhancer sequence downstream of intron D facilitates intron removal. A short purine motif (GGAAG) was identified as the core of this enhancing region (234). Furthermore, lengthening of the enhancer by the inclusion of additional purines or repeating the GGAAG motif had variable enhancing effects (235). Analysis of the exon upstream of intron 4 (exon 5) in the p35 gene showed the presence of a palindromic sequence of nucleotides, **CTCCAGAAAGACCTC**. The core region of purines (shown in bold) may act as a binding site for a splicing factor and enhance splicing of this intron. Additional studies are required to assess whether this sequence is capable of acting as an enhancer.

As the splice site and polypyrimidine tract sequences do not show significant divergence from consensus, other mechanisms may generate this intron 4-retaining transcript. The Exon Definition model suggests that splice sites are paired across internal exons (253), or alternatively, across introns if this distance is shorter (254). Additional information on this model is provided in **Appendix I**. Intron 4 is in an unusual position as it is short (only 75 bp) and is flanked by exons 4 and 5, both of which are 42 bp (25), less than the minimum size defined *in vitro* (51 bp) for efficient inclusion (255). As such neither model of intron or exon recognition can easily be applied. Consequently, intron 4 may not be efficiently recognised by the splicing machinery. An alternative scenario for intron inclusion can be proposed, without invoking the requirement of an exonic splicing enhancer or poor splice site consensus. In the case of inefficient intron 4 recognition, and as the Exon Definition model suggests that splice sites are recognised in pairs across exons, (the downstream 5' splice site paired initially with the upstream 3' splice site) the 5' splice site of intron 5 may pair with the 3' splice site of intron 3. The result of this would be that exon 4, intron 4 and exon 5 would be identified as a single 'exon' leading to the inclusion of intron 4 in the final mRNA. This would give a total 'exon' length of 159 bp, slightly larger than the average vertebrate exon size of 137 nucleotides (256), and may be more efficiently spliced as there is greater room for the splicing factors to manoeuvre. As a result, on some occasions the correct pairing would generate standard p35, and on other occasions, variant p35 may be generated.

As discussed in the **Literature Review**, p35 gene expression is complex and several mRNA transcript types have been identified in mouse and human (25, 26). In the mouse only two transcripts are translated into functional protein (26) and the identification of an intron-containing mRNA may have further implications for the

control of p35 gene expression. Translation of this mRNA is expected as it contains the appropriate upstream initiation site. However, if the protein is unable to form functional heterodimers with p40, this may act as a control for heterodimer formation at the translational level by generating p35 protein unable to form bonds with p40. The expression of this transcript may be dependent on the availability of certain splicing factors, for example, which remove the intron more efficiently and allow high level production of p35. Changes in splicing factor levels in antigen presenting cells, such as macrophages and dendritic cells, may occur in response to antigenic challenge and generate functional p35 for heterodimer formation.

An additional consequence of variant p35 protein truncation is the loss of 3 cysteine residues from the C-terminal end of the protein. The intramolecular disulphide bonding of p35 occurs between the 3 cysteines in the N-terminal of the protein partnered with the 3 cysteine residues present in the C-terminal (**Literature Review, Figure 1.1 (4)**). This loss suggests that the variant p35 protein undergoes a radical conformational change. However, the cysteine that participates in the intermolecular disulphide bond with p40 is retained, as is the N-glycosylation site of which it is part. Despite the predicted change in protein shape, this residue may still be capable of interaction with the p40 subunit to generate a heterodimeric protein of potentially modified function.

Immunoprecipitation of the complete p35 variant mRNA (5' region – intron 4 – 3' region) alone or in combination with p40 from CHO cell transfectants failed to detect a protein unique to this variant cDNA using an anti-IL-12 polyclonal antibody. When compared to the standard p35/p40 transfectant the protein banding pattern was shown to be identical, with heterodimer, p35 and p40 all visible on the autoradiograph (**Figure 5.11**). A similar result was obtained from CHO cells into

which the ovine variant p35/p40 and standard p35/p40 had been transfected. RT-PCR of cDNA obtained from these transfectants confirmed the presence of transcripts from which the intron had been spliced, that is, the presence of PCR products attributable to standard p35. These observations were consistent with the enhanced proliferation in human and ovine IL-12 proliferation assays. In other words, the biological activity of the variant p35/p40 co-transfectant was that of the normal IL-12 heterodimer. As only picomolar levels of heterodimer are required to elicit biological activity (1), any activity that may have been observed for the variant p35/p40 heterodimer was potentially obscured. The co-transfection with p40 was aimed at producing a variant p35/p40 heterodimer (as cysteine residue 74 was conserved) that may prove to be either more biologically active or act as an inhibitor of standard heterodimer, for example, by interacting with the IL-12 receptor. If the latter could be demonstrated, the generation of a single transcription unit encoding both proteins (using a linker sequence such as the serine/glycine linker employed by Lieschke *et al* (257)) could be delivered in dendritic cells to compete with naturally formed heterodimer as a means of prolonging allograft survival.

Transfection of this intron-containing cDNA into the CHO cell line generated a situation where splicing of the intron occurred and prevented direct analysis of the variant p35 protein, as standard p35 was regenerated. As each cell line (and species) is likely to have different levels of common splicing factors as well as tissue/development-specific splicing factors, varied levels of spliced versus unspliced product were likely to exist. This has been shown with for bGH intron D where different cell lines had transcripts which retained the intron with variable efficiency (0.1% - 20%) (235). Transfection of COS-7 (monkey kidney) and U937 (human monocytic) cell lines with variant p35 also demonstrated standard p35 mRNA

transcripts, indicating splicing of the intron (data not shown). The relative level of standard p35 versus variant p35 was not assessed, however, in co-transfected cells even a low level of standard p35 protein present with p40 was likely to give rise to the biologically active IL-12 p70 heterodimer.

This prompted the modification of the human variant p35 cDNA. As the 'TAG' at the end of the intron encoded a termination codon, all sequence 3' of this site was superfluous. Removal of this sequence allowed protein truncation in the appropriate position with the C-terminus being intron-encoded, and destroyed the 3' splice site, preventing removal of the intron upon transfection. Immunoprecipitation of proteins from CHO cells transfected with the truncated variant p35 in combination with p40 resulted in the precipitation of p40 alone in the co-transfectants. The truncated variant p35 or a heterodimer of truncated variant p35/p40 were not detected. No detectable biological activity, that is no enhancement of proliferation above vector blank, was observed for conditioned medium from either transfectant type in IL-12 assays. Sequencing confirmed that these cDNA constructs had the correct nucleotide sequence, but detection of protein was limited by the availability of anti-p35 antibodies able to recognise the truncated variant p35 protein. This protein is likely to differ significantly from standard p35 making the commercially available p35 antibodies inapplicable. Alternatively, protein was not being generated from these constructs thus preventing the detection of the protein and its biological function. The polyclonal antibody used in other immunoprecipitations also proved to be ineffective at recognising standard p35 alone. Standard p35 protein was only detected in lanes containing heterodimer, presumably as a result of heterodimer dissociation. To alleviate the problems associated with direct detection of the truncated variant p35, and also the standard p35 protein, these proteins were

generated as in-frame fusions to the EGFP protein. The p35 proteins were fused to the N-terminal end of the EGFP protein by deletion of the STOP codon at the end of the cDNA, allowing transcription to progress across the junction through to the EGFP cDNA, encoding a short region of irrelevant amino acids between the two. The fusion to EGFP could not be performed in the opposite orientation (C-terminal of EGFP to N-terminal of p35) due to the presence of the signal peptide cleavage site in p35. Cleavage at this point would have resulted in the loss of p35 from the fusion. In addition, removal of the signal peptide sequence to allow fusion in the alternative orientation may have adversely affected the behaviour of the protein, potentially by preventing effective secretion or affecting the cellular localisation. The advantage of the EGFP-fusion was the ability to detect the p35 proteins using an antibody directed against the EGFP protein. Analysis of cell lysates under non-reducing conditions using Western blotting techniques revealed the presence of multiple high molecular weight proteins present only in the lanes containing the p35 fusion proteins. More clearly defined bands at approximately 70 or 96 kDa, present in lanes from truncated and standard cell lysates, respectively, were identified on occasion. These high molecular weight species were specific to the fusion protein lanes as vector blank and wild type controls were free of high molecular weight material. Under these conditions, bands corresponding to the predicted molecular weight of single protein molecules were not generally observed. This suggested that the higher molecular weight material might correspond to p35 proteins forming dimers and trimers, as well as other multimeric forms either through the interaction of the leucine zipper present in the N-terminal region of the protein, or via disulphide bonding. Western blots performed under reducing conditions generated a single band in the standard p35 lane corresponding to approximately 67 kDa, and a single band in the truncated

variant p35 lane corresponding to approximately 56 kDa. Analysis of the proteins under reducing conditions resolved almost all of the higher molecular weight species in these lanes. Resolution of the proteins into the individual protein subunits clearly indicates the propensity of p35 to form intermolecular disulphide bonds with other p35 subunit proteins. This property has been alluded to in one of the very early reports on IL-12 (17). The formation of the disulphide linkage would be expected to be mediated via cysteine 74 as this residue has been shown to mediate the intermolecular disulphide linkage with p40 (4). Three other cysteine residues are present in the N-terminal half of the truncated variant p35 that may initiate intermolecular disulphide bonding, although, in the standard p35 these residues would be involved in intramolecular bonds with a partner residue in the C-terminal portion (4). Truncated variant p35, however, does not have these C-terminal cysteines. While the participation of these residues in intermolecular disulphide bonding cannot be ruled out, this protein behaves similarly to the standard p35 suggesting that the disulphide bonding is not mediated in this manner. Resolution by reduction of the proteins also argues against the protein-protein interactions being mediated by the leucine zipper.

The GFP protein (isolated from the jellyfish *Aequorea victoria* (258)) is widely used to aid in the localisation and detection of proteins due to its apparent non-toxicity and stability in a wide variety of cells. The enhanced green fluorescent protein (EGFP), generated by mutagenesis, is up to 35 times brighter than wild type GFP upon excitation with light at a wavelength of 488 nm (259). The presence of the EGFP protein fused to p35 allowed the cellular location of the fusion proteins to be determined. The EGFP protein alone was located in the cell cytoplasm and nucleus, with a relatively even distribution at both sites (**Figure 5.15A**). That is, by visual

inspection the nucleus was not brighter than the cytoplasm or vice versa, with no obvious preference for a particular cellular location in its own right. Confocal microscopy allowed sections to be taken through the cell to clearly identify the location of the fusion proteins. As shown in **Figure 5.15B** and **5.15C** the standard and truncated variant p35 fusion proteins were located wholly within the cytoplasm of the cell, and not in the nucleus as might be expected for a transcription factor (as suggested by the presence of the leucine zipper). Some variation in the pattern of localisation of the fusion proteins was observed on occasion for both the standard and truncated variant fusions (discrete as opposed to a diffuse cytoplasmic location) (**Figure 5.15C**). This may reflect the physiological state of the cell at the time of visualisation, resulting in differences in cytoplasmic expression. The presence of the p35 proteins within the cell cytoplasm was not unexpected based on the observations of Wolf *et al* where minimal secreted protein could be detected (17). However, this is at variance with the presence of a signal peptide, which suggests that the protein is secreted. The p35 protein is, however, processed differently to p40, as the p35 signal peptide is removed in two sequential cleavage reactions with protein glycosylation required for effective secretion (27). The natural partner for the p35 molecule is p40 although a second partner, EBI3, has been described by Devergne *et al* (28). EBI3 shows similarity to the IL-12 p40 protein and can associate with p35 under normal physiological conditions (29). EBI3 is also minimally secreted, however, co-transfection of p35 with EBI3 enhanced the ability of both proteins to exit the cell (29). Co-transfection of standard and truncated variant p35 proteins with p40 was performed, but enhanced movement of p35 fusions from the cytoplasm and the actual cellular location of protein in cells containing both plasmids were not assessed. This was not determined due to the pre-disposition of the CHO cells to lose expression of

EGFP within a week of transfection. Cells retained the plasmid as antibiotic selection using G418 resulted in the generation of stable cell lines, but fluorescence was no longer apparent. Western blotting confirmed the loss of EGFP expression. This prevented the isolation of a clone containing both plasmids (as assessed by PCR for example) to examine changes in protein levels and protein location upon co-transfection with p40 (by immunoprecipitation or Western blot). The loss of GFP expression has been reported in a variety of cell lines, where antibiotic selection generated stable transfectants, but these cells did not maintain their fluorescence. Loss of fluorescence in cells expressing high levels of GFP was associated with cell death (260), although stable fluorescent cell lines have been obtained by cloning out of transfectants (261, 262).

Use of a p40 construct in which the p40 protein is fused to mutants of the GFP protein with different colours (generated by mutagenesis and commercially available) would allow cells containing both plasmids to be identified after transient transfection by overlaying images of each colour fluorophore to identify co-transfectants. The assessment of changes in the levels of p35 protein secretion upon transfection with p40 would then require the selection of clones that maintained EGFP expression. A membrane bound form of IL-12 p70 has been identified in the human U937 monocytic and murine P388D₁ macrophage cell lines using flow cytometry (263). Co-transfection of p35 and p40 EGFP-fusion plasmids into different cell types may reveal which cells are capable of forming the membrane bound heterodimer.

Localisation of fusion proteins within the CHO cells may differ in primary cells capable of producing IL-12, such as dendritic cells. Delivery of the naked plasmid into human monocyte-derived dendritic cells using LipofectAMINE™ was

not efficient, as EGFP positive cells were not observed. A more efficient means of gene delivery would be through the use of an adenoviral vector expressing the fusion gene. Alternatively, this could be assessed by immunohistochemistry using an antibody raised against the truncated variant p35 protein.

An important question to be answered was whether the presence of the EGFP protein interfered with heterodimer formation or the biological activity of the molecule. This was important with regard to determining whether the truncated variant p35 protein was also capable of forming heterodimers with p40. Conditioned medium from co-transfectants of standard or truncated variant p35 fusions in combination with p40 were tested in an IL-12 proliferation assay. The ability of the standard p35 EGFP-fusion/p40 to form a biologically active molecule, as assessed by enhanced proliferation, was clearly demonstrated (**Figure 5.16**). As before, the truncated variant p35 EGFP-fusion/p40 was unable to enhance proliferation. Immunoprecipitation of the proteins from the culture supernatant, as shown on the autoradiograph in **Figure 5.17**, demonstrated the formation of a heterodimer between standard p35 EGFP-fusion and p40, but not between truncated variant p35 EGFP-fusion and p40. Although heterodimer formation was not prevented for standard p35, interference by the EGFP protein in formation of truncated variant p35 EGFP-fusion/p40 heterodimer cannot be completely excluded. However, the results as a whole, with respect to the general behaviour of this protein would suggest this as unlikely. It would appear that the truncated variant p35 protein shows similar cellular localisation, and behaviour with regard to the formation of multimers, but is unable to bond with the p40 subunit of IL-12.

Chapter 6

Final Discussion

Chapter 6

Final Discussion

The development of gene delivery vectors has facilitated the use of both established and novel genes as therapeutic agents to modulate the immune system. For organ transplantation this provides a means by which the rejection process can be regulated utilising specific immunosuppressive cytokines. In particular, the functional division of T helper cells into Th1 and Th2 subsets based on their pattern of cytokine secretion (49), and the subsequent association of a Th2-type response with allograft survival, has prompted the use of the Th2 cytokines, such as IL-4 and IL-10, in transplantation therapy. Mouse and rat cardiac allograft models in which rIL-4 or rIL-10 have been administered systemically have shown that both cytokines can promote graft survival (264, 265), but rIL-10 can also promote graft loss (264, 266). Non-specific immune modulation by administration of recombinant cytokines is comparable to immunosuppressive drug therapy, with potentially toxic side effects generated at the systemic level. In contrast, intragraft gene delivery allows the localisation of immunomodulatory gene expression within the transplanted organ, minimising the likelihood of detrimental systemic effects. The effect of intragraft Th2 cytokine gene expression has been assessed using transgenic mouse models. Transplantation of grafts from IL-4 or IL-10 transgenic mice into allogeneic recipients has both prolonged graft survival (267) or not affected the time frame of allograft rejection (58, 59). Intragraft gene delivery of immunosuppressive genes using viral vectors has also been performed, with the allografts infected prior to transplantation. This has been applied with some success using viral IL-10 (a

homologue of mammalian IL-10 (268, 269)) in adenoviral and retroviral vectors (270-272). Modification of allografts with these vectors has resulted in prolonged graft survival, but not long term acceptance. Allograft survival was prolonged for the duration of gene expression with allograft rejection corresponding to decreased gene expression levels (270). Alternatively, inactivation of gene promoters and anti-viral immunity may attenuate gene expression, thereby preventing inhibition of the alloimmune response resulting in graft rejection (271).

The variable success of Th2 cytokine expression in generating long term allograft acceptance suggests that alternative genes for gene therapy are required. IL-12 p40 is presented as another candidate gene in the studies reported here. IL-12 p40 is able to antagonise the effects of biologically active IL-12, favouring the development of a Th2-type cytokine milieu by prevention of a Th1-type response. In addition, IL-12 blockade could be used to prevent induction of NK cell cytotoxicity, CTL activity and lymphocyte homing all of which may contribute to graft destruction. The ability of IL-12 to enhance the development of CTL responses to viral proteins suggests that inhibition of IL-12 by IL-12 p40 may also reduce the immune response toward cells modified by viral vectors (99).

For the studies performed here a cell type engineered to express IL-12 p40 is provided as an alternative approach to intragraft delivery, with dendritic cells chosen as the cellular delivery vehicle. The advantage of DCs stems from the ability of these cells to both activate naïve T cells and migrate to sites of antigen presentation (131, 132). Modification of this cell type with the immunomodulatory gene may prevent the initiation of the immune response against the organ allograft at the site of antigen presentation. In this case, IL-12 p40 expressed by these modified DCs would be provided at the initial interaction of the DCs with T cells to inhibit the actions of IL-

12. DCs have been genetically modified to express TGF- β or FasL using either adenoviral or phagemid vectors (181, 193), prolonging the survival of DCs *in vivo* (193). However, the inability of FasL expressing DCs to induce long term allograft survival, for example, may be due to increased apoptosis of DCs, as a consequence of FasL expression (181).

One major aim of this study was to assess the potential of ovine IL-12 p40 modified DCs as a therapy in an ovine model of renal transplantation. However, it was first necessary to clone the ovine IL-12 subunits and characterise the biological function of the ovine IL-12 heterodimer. A functional assay was developed in which both ovine IL-12 p40 and heterodimer activity could be tested (**Chapter 3**). As described in **Chapter 4** the proliferation assay was used to demonstrate the ability of ovine IL-12 p40 to act as an IL-12 antagonist. This was evidenced by the inhibition of IL-12-induced cellular proliferation by ovine IL-12 p40. Homodimers of p40 were detected in the culture supernatant of human DCs, and to a lesser extent in ovine fibroblasts, transfected (adenovirus plus LipofectAMINE™) or infected (adenovirus alone) with IL-12 p40 adenovirus, respectively. This result suggested that the ovine p40 subunit would also act as an antagonist *in vivo*, reflecting the *in vivo* antagonistic function of p40 homodimer described in a mouse model of acute endotoxaemia (38).

While IL-12 p40 was capable of inhibiting IL-12-induced proliferation of activated PBMNC (**Chapter 4**) it did not inhibit proliferation of the MLR. Inhibition of proliferation was not observed regardless of whether the cytokine antagonist was added directly to cultures, or whether allostimulatory DCs were transfected with the IL-12 p40 adenoviral construct. Although the *in vitro* studies presented in **Chapter 4** showed limited promise for the use of IL-12 p40, small animal models have been used successfully to demonstrate the ability of IL-12 p40 in prolonging the survival

of allogeneic cells (119) or syngeneic islets (118). By comparison, other *in vitro* and *in vivo* models have failed to show significant inhibition of the alloimmune response using IL-12 p40 homodimer or neutralising IL-12 antibodies (117). However, direct comparison of the *in vitro* DC-MLR and two-way MLR experiments performed in **Chapter 4** to those of Piccotti *et al* was not possible as different end points were assessed. Changes in cellular proliferation were evaluated in the studies present here, whereas Piccotti *et al* assessed the production of IFN- γ . However, optimal proliferation of the MLR and IFN- γ production have been significantly inhibited by addition of neutralising IL-12 antibodies upon restimulation of the alloreactive T cell blasts (12). A more effective means of assessing functional efficacy of IL-12 p40 in the *in vitro* DC-MLR and two-way MLR models may have been the assessment of changes in CTL generation, rather than changes in proliferation or IFN- γ production. In addition, Piccotti *et al* did not trial a range of p40 homodimer doses in the *in vivo* cardiac allograft model system and the recombinant protein was administered systemically (116, 117). The accelerated rejection observed in homodimer treated animals might have been due to the timing or dosage of recombinant p40 homodimer. These factors have influenced the outcome of systemic administration of rIL-10, with prolonged survival or accelerated rejection observed in the same animal model (264, 266). The differential effects of rIL-10 were dependent on the timing of the dose with pretreatment able to prolong survival, with recipients of posttransplant treatment having comparable rejection to untreated animals. In addition, high doses of rIL-10 resulted in accelerated graft rejection (264).

The efficacy of IL-12 p40 modified DCs in the prevention of allograft rejection may be better assessed in a small animal model prior to application in a large animal model. The NOD-SCID mouse model established in our laboratory is a

chimaeric model that allows ovine (or human) reagents to be tested *in vivo* (Dr G Patrick, Ph.D. Thesis). Ovine or human skin can be engrafted onto these mice without subsequent rejection, and graft rejection can then be induced by challenge of the mice with allogeneic lymphocytes, administered by intraperitoneal injection. Moreover, when dendritic cells autologous to the skin are administered concomitantly with allogeneic lymphocytes, aggravated rejection results. Modification of the autologous DCs with ovine IL-10 by transfection with an adenoviral construct can inhibit skin rejection (205). This model could be used in a similar manner to assess the efficacy of IL-12 p40 in the treatment of allograft rejection. If ovine skin allograft rejection can be inhibited in the NOD-SCID model by the administration of ovine DCs expressing IL-12 p40, then this approach can be studied further using the pre-clinical ovine model of renal transplantation.

In **Chapter 5** the identification of a new IL-12 p35 mRNA variant was described and the ability of this molecule to interact with p40 was assessed. This variant was shown to result from the inclusion of intron 4 within the p35 mRNA transcript and was identified in both humans and sheep. The intron showed an unexpectedly high degree of homology across species, suggesting that this protein may have a physiologically relevant function. Translation of the protein would result in premature truncation by virtue of an in-frame STOP codon, with truncation for both species resulting in the loss of 3 cysteine residues involved in intramolecular bonding. The cysteine at position 74 (human) and 73 (ovine) was retained suggesting the ability to form intermolecular disulphide bonds with p40. The formation of this heterodimer may have proved useful for IL-12 antagonism either by competing with the p70 heterodimer for the IL-12R and/or by transducing a negative regulatory signal. All of the available evidence suggested that this variant heterodimer was not

formed in any of the experiments. As such, the therapeutic value of this protein as a gene for use in gene therapy protocols for the treatment of allograft rejection is limited. However, the determination of the biological function of this protein, if any, and the conditions under which this transcript is generated may be of importance for a greater understanding of the biology of IL-12 heterodimer formation. Disulphide-linkage between two or more standard p35 or truncated variant p35 molecules, to form homodimers or multimers, could be demonstrated based on the detection of high molecular weight complexes which could be resolved under reducing conditions to give the predicted molecular weight of a single subunit. An aspect that was not explored was the possibility that the truncated variant p35 protein could interact with other protein subunits to demonstrate a biological function. Expression of this protein in a cell type capable of IL-12 production may identify a molecule with novel functional properties.

In conclusion, this study has provided a useful insight into the biological function of the ovine IL-12 heterodimer, with ovine IL-12 p35 and p40 having sequence similarity to the human and murine subunits. A variant p35 mRNA, generated by the retention of intron 4, was identified in both humans and sheep. Although heterodimer formation with p40 could not be demonstrated, this transcript may provide greater information on the biology of IL-12 heterodimer formation. In addition, ovine IL-12 p40 antagonised the biological function of IL-12 and formed p40 homodimers. The conservation of the antagonistic properties of IL-12 p40, and the existence of both small and large animal transplantation models, will allow gene therapy protocols utilising IL-12 p40-modified dendritic cells to be tested for their ability to prevent allograft rejection in future studies.



Appendices

Appendix I

Pre-mRNA Splicing

The splicing of pre-mRNA is a complex process that involves short RNA species, small nuclear RNAs (snRNAs), which base pair with the pre-mRNA. When coupled to the associated protein factors these particles are referred to as small nuclear ribonucleoproteins (snRNPs). Formation of the catalytic reaction site where the introns are removed and the exons rejoined requires interaction of the snRNAs with the pre-mRNA in the context of snRNP particles. A complicated series of conformational rearrangements involving changes in base pairing of the snRNAs with the pre-mRNA and between the snRNAs themselves takes place over the course of the reaction.

An overview of the splicing mechanism and a description of the Exon Definition model are provided here in addition to the information in **Chapter 5**.

The Splicing Reaction

Introns can number between 0-50 for a given pre-mRNA and are up to 200,000 bp in length (273). While yeast splice site and branch site sequences are highly conserved, few eukaryotic sequences show complete consensus (209). The question that arises is how these sites are recognised consistently and accurately with such sequence variation. Short RNA species called small nuclear RNAs (snRNAs) which are complementary to sequences in the intron, as well as exonic sequence around the splice site junctions, mediate this complicated reaction. A multitude of associated proteins also aid in the splicing reaction (207). These snRNAs (labelled

U1, U2, U4, U5 and U6) are associated with proteins to form small nuclear ribonucleoprotein particles, with the Sm proteins common to each snRNP complex (274). In addition each snRNP is associated with specific proteins integral to its particular function.

The base pairing interactions and conformational rearrangements of splicing are particularly complex. For more detailed information the reader is referred to the following review articles (209, 275). A brief overview of the mechanics of the reaction is provided below.

The early steps of splicing complex assembly are energy-independent and the products of splicing are observed only after the ATP-dependent complexes form (with energy provided in the form of ATP - adenosine triphosphate) (276). The U1 snRNA is complementary to the 5' splice site (277-279) and the interaction of the U1 snRNA is essential for splicing to proceed (280), **Figure A.1 Complex E**. Binding of U1 snRNP to the 5' splice site constitutes the first step in the splicing reaction and is independent of temperature (281) and energy input (282). The U1 snRNP is composed of 9 proteins, 3 of which are specific to this snRNP (U1-70K, A and C), with U1-70K suggested to stabilise base-pairing interactions with the pre-mRNA (283).

The U2 snRNP is involved in pre-mRNA branch point recognition (281, 284) as shown in **Figure A.1 Complex A**. This is an ATP-dependent reaction, as are all subsequent steps in the splicing reaction (282). The U2 snRNP interaction with the branch site is promoted by the U1 snRNP (285) and requires that the splicing factor, U2AF, binds to the 3' region before the U2 snRNP-branch site interaction can take place (286). The preferred branch site consensus sequence in mammals is UACUAAC (287) and the underlined adenosine residue acts as the nucleophile that

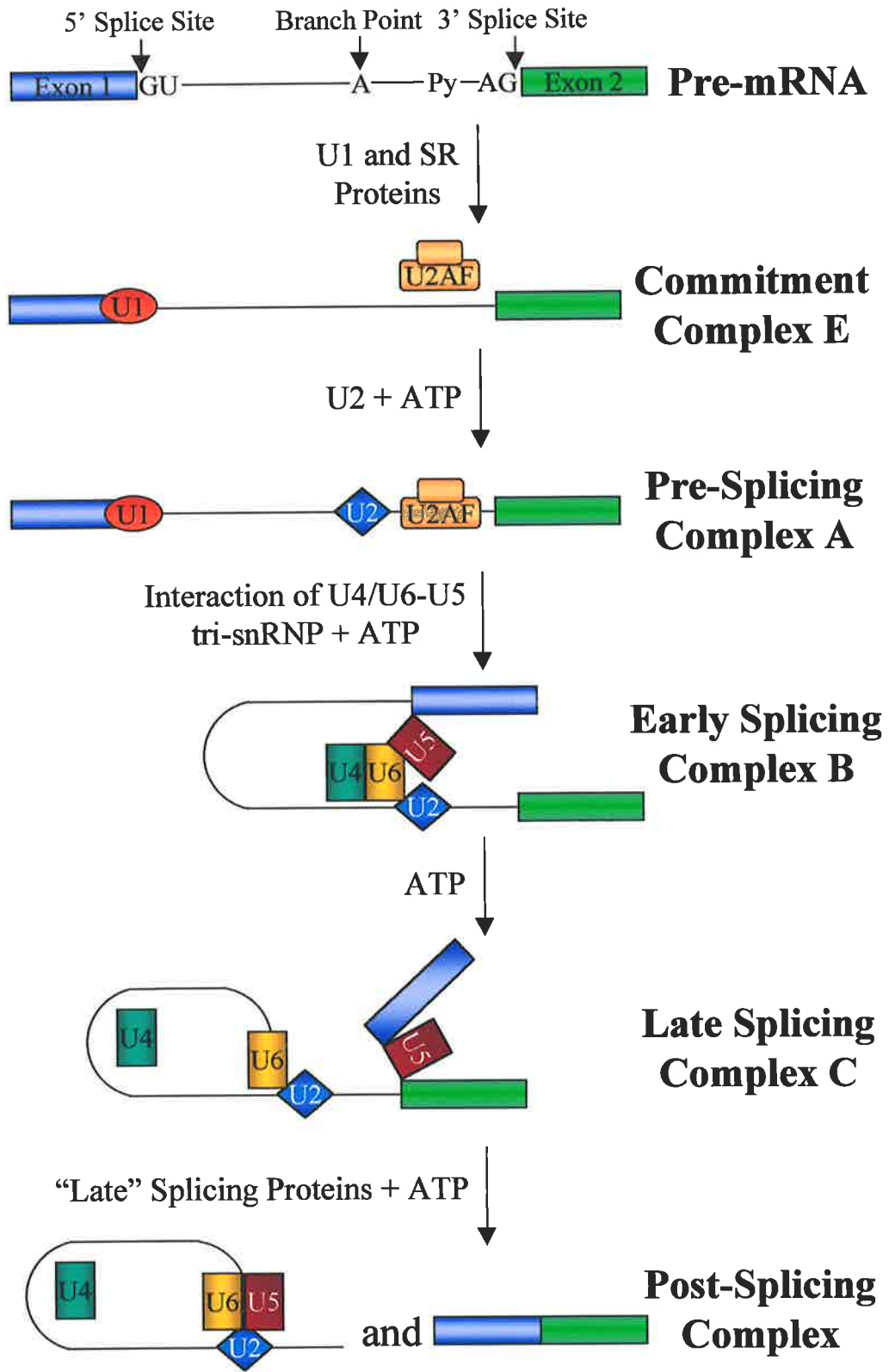


Figure A.1. Assembly of the spliceosome showing snRNP particles, SR proteins and the input of energy in the form of ATP. Modified from Krämer, 1996 (273).

attacks the 5' splice site in the first step of splicing. As a result of U2 snRNA base-pairing to the pre-mRNA the branch site adenosine (the branch point) becomes bulged (288). This has been suggested to be the way in which the adenosine becomes available for the attack on the 5' splice site (288).

U4, U5 and U6 form a triple snRNP particle that interacts with the pre-spliceosome to form the active spliceosome (289) as shown in **Figure A.1 Complex B**. The U6 snRNA is highly conserved between yeast and humans (75%) (290) and is extensively base paired to the U4 snRNA (291, 292). The interaction of the U4 snRNA with U6 snRNA is disrupted prior to the initial cleavage-ligation step (293), and U4 is either released or destabilised from the splicing complex (289, 294, 295). U4 is not required in subsequent steps after the assembly of the active spliceosome and its role appears to be the delivery of U6 into the splicing reaction (289, 293).

The U5 snRNA can be chased through both steps of the splicing reaction (296). A highly conserved sequence within the U5 snRNA (297) forms a loop which interacts with both the 5' (298-300) and 3' splice sites (296, 298) as shown in **Figure A.2**. The exon/U5 snRNA interactions can be explained by non-Watson-Crick base pairing interactions (296, 298) with the multiple uridine residues in the loop able to bond promiscuously to allow base pairing with the variable exonic sequence. As this interaction does not involve specific base pairing, the U5 snRNA is likely to be positioned by other factors such as the U1 snRNP (301). One role of the U5 snRNA appears to be to hold the two exons together during the splicing reaction and subsequent ligation (296) as shown in **Figure A.2**.

Multiple conformational rearrangements generate the catalytically active complex shown in **Figure A.1 Complex C**. The U1 snRNA interaction with the 5' splice site is disrupted (302) and is replaced by the interaction of U6 snRNA with the

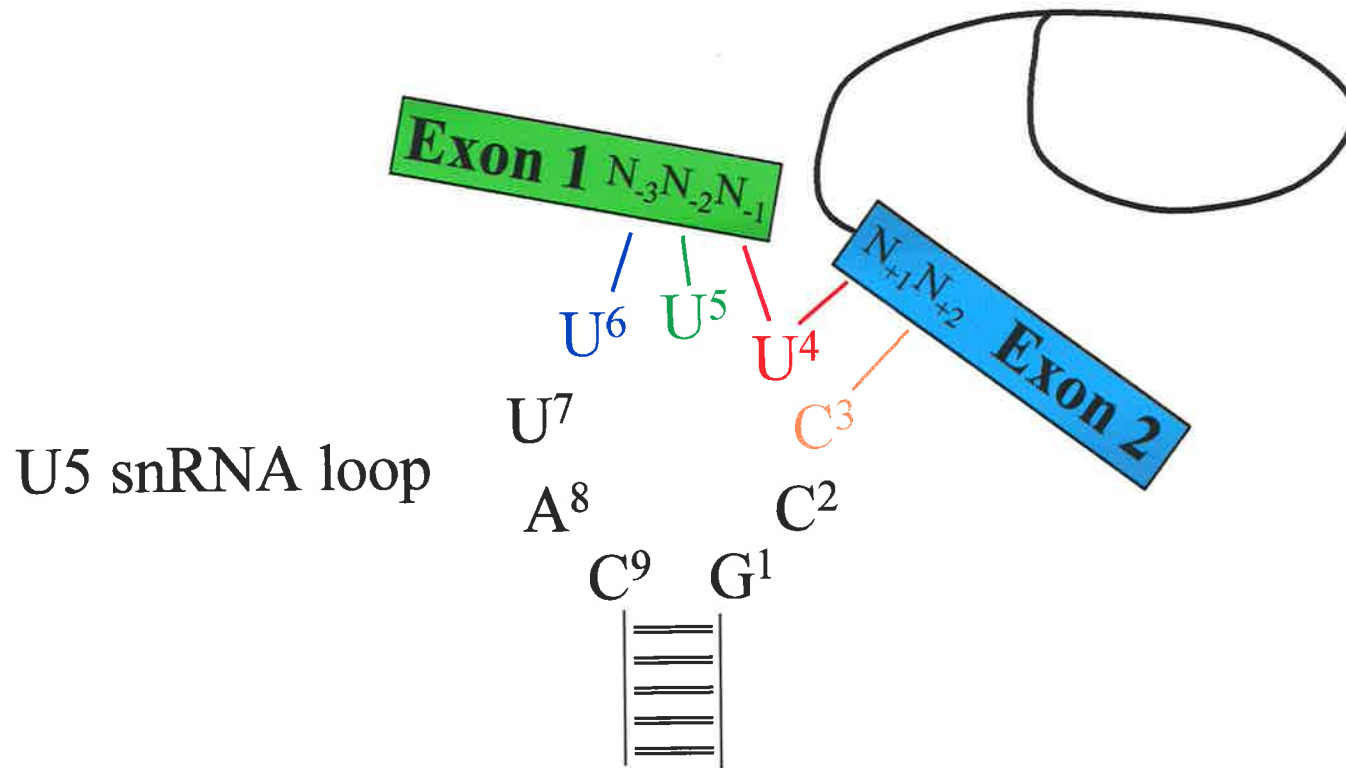


Figure A.2. U5 snRNA invariant loop base pairs with exonic sequence. As described in the chapter text these interactions are not standard Watson-Crick pairings to allow for the nucleotide variation of the exons. The U5 snRNA holds the two exons together during the splicing reaction where the lariat structure is cleaved and the exons are ligated. Diagram modified from Madhani, 1994 (275).

5' splice site (303). U2 snRNA and U6 snRNA become base paired to each other during the reaction and this is mutually exclusive with the U4/U6 base pairing (304). This interaction provides a means by which the branch point adenosine becomes bulged (304), presumably for the first nucleophilic attack. Once catalysis is complete (**Figure A.1 Post-Splicing Complex**) the intron lariat structure is cleaved and the exons are ligated. The discarded lariat structure is ultimately degraded (305) and the process is repeated until all of the introns have been removed from the pre-mRNA.

Protein Splicing Factors

Spliceosomal proteins, or splicing factors, are integral to the formation of splicing complexes and the rearrangement and binding of the snRNAs. Well known splicing factors include SF2/ASF (306), SC35 (307), U1-70K (308, 309) and both subunits of U2AF - U2AF³⁵ and U2AF⁶⁵ (310-312). These are characterised by the presence of an RNA-recognition motif (RRM) (313) and a domain that consists of serine (S) and arginine (R) residues present as variable lengths of either RS or SR dipeptides (314). The RS domains of these proteins, however, can be interchanged with the specificity of each protein being determined by the RRM (315). SR proteins become associated with the pre-mRNA in the first stages of spliceosome assembly (316) and are incorporated into complex E (317), committing the pre-mRNA to the splicing pathway (316). The splicing factor SF2/ASF is thought to stabilise binding of the U1 snRNP to the 5' splice site (318), and the U1 snRNP subsequently promotes the interaction of U2AF⁶⁵ with the 3' splice site (319). The U2AF⁶⁵ subunit is able to bind to the polypyrimidine tract, with the RS domain making contact with the branch point, in turn enabling the U2 snRNA to bind to the pre-mRNA (320). SR

proteins are also necessary for the U4/U6/U5 tri-snRNP particle interaction with complex A to form complex B (321).

The relative levels of splicing factors play an important role in determining how a given transcript is spliced. Two of the splicing factors – SF2/ASF and hnRNP A1 (heterogeneous nuclear ribonucleoprotein A1) – have been shown to affect pre-mRNA splicing. In a model in which an exon may be included in, or excluded from, a pre-mRNA as the situation demands, excess SF2/ASF favours exon inclusion. In contrast, hnRNP A1 promotes exon skipping when this factor is in excess (322). The authors of this study concluded that constitutive splice sites match consensus to avoid skipping of exons, whereas alternative exons splice sites have different relative strengths to allow variable inclusion (322).

The polypyrimidine tract is present at the 3' end of introns and terminates prior to the 3' splice site AG dinucleotide (213, 239). The polypyrimidine tract is involved in the definition of the 3' splice site during the early stages of spliceosome assembly and aids in recognition of the branch point sequence (243). The polypyrimidine tract is bound by hnRNP proteins (323), another group of proteins associated with the pre-mRNA (324), including hnRNP A1, C and D (323). The polypyrimidine tract is also bound by U2AF⁶⁵ (310) and the polypyrimidine tract-binding protein (325, 326), the binding of which is an important step in the early definition of the 3' splice site (327).

Exon Definition in Pre-mRNA Splicing

The Exon Definition model applies to internal exons (i.e. not the first or last exon in a pre-mRNA transcript) and proposes that factors binding to the pre-mRNA 5' splice site interact with the preceding 3' splice site to define the exon for assembly

of the spliceosome (253) (**Figure A.3**). The exon is then defined by the binding of U1 and U2 snRNPs and associated protein factors such as U2AF and SF2/ASF (329). The Exon Definition model is supported by *in vitro* testing, where the 5' splice site of exon 2/intron 2 of a test mRNA was mutated, exon 1 was ligated directly to exon 3. Exon 2 was skipped as mutation of the site prohibited the recognition of the exon, removing all of the sequence between the upstream and downstream exons as if intronic (330). Further evidence for this model comes from the analysis of diseases that result from mutation of either of the splice sites, where exon skipping is the most common phenomenon observed (51%) (331). The formation of cryptic splice sites (sites within an intron or exon that have sequence similar to the true splice site, are located close to the original, and are used when the true site has been mutated or lost [30%]) and intron retention (6%) are also observed (331).

The average size of vertebrate exons is 137 nucleotides (256). The observation that exon length is kept within certain limits lends further credence to this model, suggesting that the imposition of a maximum size reflects a function. In primates the analysis of 1600 internal exons revealed only 3.5% were larger than 300 bp and less than 1% greater than 400 bp (329). A minimum size for efficient inclusion is also apparent with the observation that artificially shortened exons (less than 51 nucleotides) are skipped *in vitro* and *in vivo* (255). Increasing 5' splice site strength and/or increasing branch site consensus relieves this problem (332), as does increasing the exon length (255, 333). Under these circumstances, short exons may require additional help from enhancers which may be present in the neighbouring intron and act as binding sites for splicing factors (334). In the event that the intron is the shorter of the two distances, pairing across introns may occur, and both exon and intron definition may occur within an individual pre-mRNA (254).

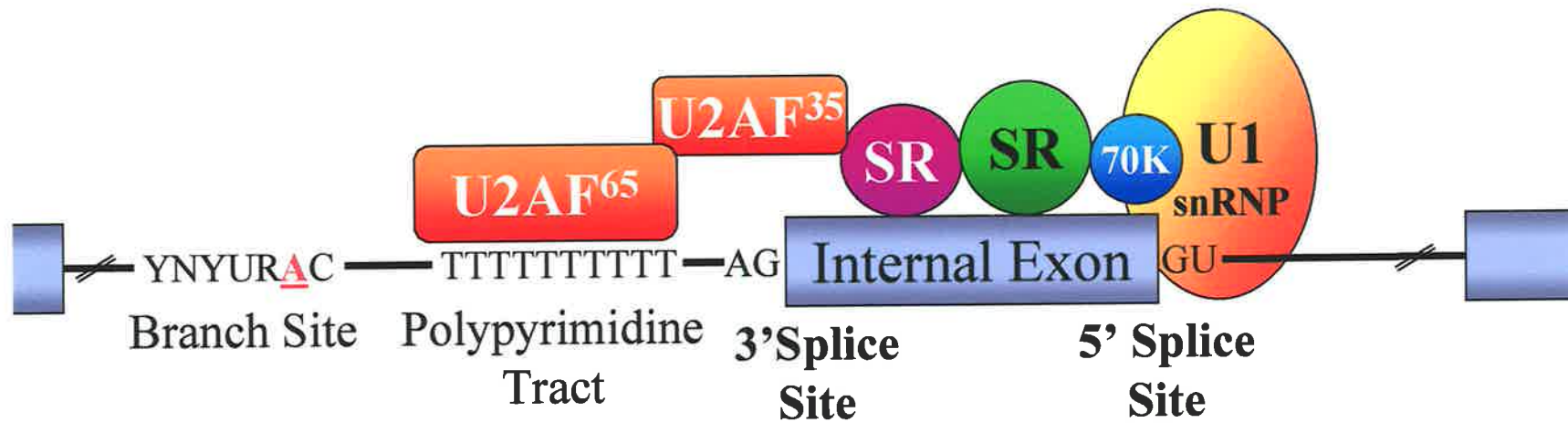


Figure A.3. Exon definition model of splice site selection. In this model, splice sites are determined by the downstream 5' splice site pairing with the upstream 3' splice site across the exon via multiple protein interactions and the binding of the U1 snRNP. Diagram modified from Will *et al.*, 1997 (207) and Reed, 1996 (328).

This model also requires that additional help be provided to the first and last introns that do not have a partnering splice site. For the first intron this is provided by the 7-methylguanosine cap present on the 5' end of most eukaryotic mRNA transcripts (335). The presence of the cap structure promotes splicing of the proximal intron (336). Similarly, polyadenylation of the pre-mRNA, which is enhanced by the presence of an intact terminal 3' splice site (337) assists in the removal of the final intron (338).

Appendix II

Cloning Primers

Primer Name	Primer Sequence	Species	Gene	Product Size
p35riboF	gccaccatgtggccccctgggtcagcc	human	p35	768 bp
p35TAAR	ttaggaagcattcagatagctc	human	p35	768 bp
p40riboF	gccaccatgtgtcaccagcagttggtc	human	p40	999 bp
p40XbaR	tctagactaactgcagggcacagatgcc	human	p40	999 bp
shp40riboF	gccaccatgcaccctcagcagttgg	ovine	p40	996 bp
shp40XbaR	tctagactaactgcaggacacagatgc	ovine	p40	996 bp
shCDSF	gccaccatgtgcccgcttcgMagcctcc	ovine	p35	672 bp
shCDSR	ctaggaagaactcagatagctc	ovine	p35	672 bp
Intron 4 spliceR	tcagaggaaaaaataatcagacatcagtg	human	p35 intron 4	501 bp
Intron 4 STOP deleted EGFP	gaggaaaaaataatcagacatcagtgatg	human	p35 intron 4	498 bp

Primer sequences for cloning human and ovine p35 and p40. Primer sequences are also provided for cloning truncated variant p35, with and without the STOP codon. Primers are listed in pairs except for those specific for intron 4 which are to be matched with the p35riboF primer. F indicates forward primer; R indicates the reverse complement. The degenerate base in the shCDSF primer is indicated by M, which represents bases A or C.

Appendix III

General Purpose Primers

Primer Name	Primer Sequence	Species	Gene	Primer Location
BOV35F	gcaacacgcttcagaaggcca	human/ovine	p35	307 bp (h) or 307 bp (o)
BOV35R	cctcttaggatccatcagaagc	human/ovine	p35	307 bp (h) or 307 bp (o)
BOSF	tttgagatgctgggcagtaca	human/ovine	p40	455 bp (h) or 458 bp (o)
BOSR	gatgatgtccctgatgaagaagc	human/ovine	p40	455 bp (h) or 458 bp (o)
p18F	gtcaaaaaatgaaaagtttcagcc	human	p35 intron 4	Nucleotide 1 of intron 4
β -actinF*	atcatgtttgagacctca	multiple species	β -actin	318 bp
β -actinR*	catctcttgctcgaagtcca	multiple species	β -actin	318 bp
M13F	gtaaacgacggccagtgaat	pUC19 plasmid	T7 promoter	Nucleotide 2961
M13R	cagctatgaccatgattacg	pUC19 plasmid	SP6 promoter	Nucleotide 151

Primers are listed in pairs for use in PCR. Product size is shown as either human (h) or ovine (o) sequence as applicable. All primers have an internal location except where stated otherwise. The p18F primer was used to amplify p35 intron 4-specific transcripts. *Primer sequences as per Fuqua *et al*, 1990 (244).

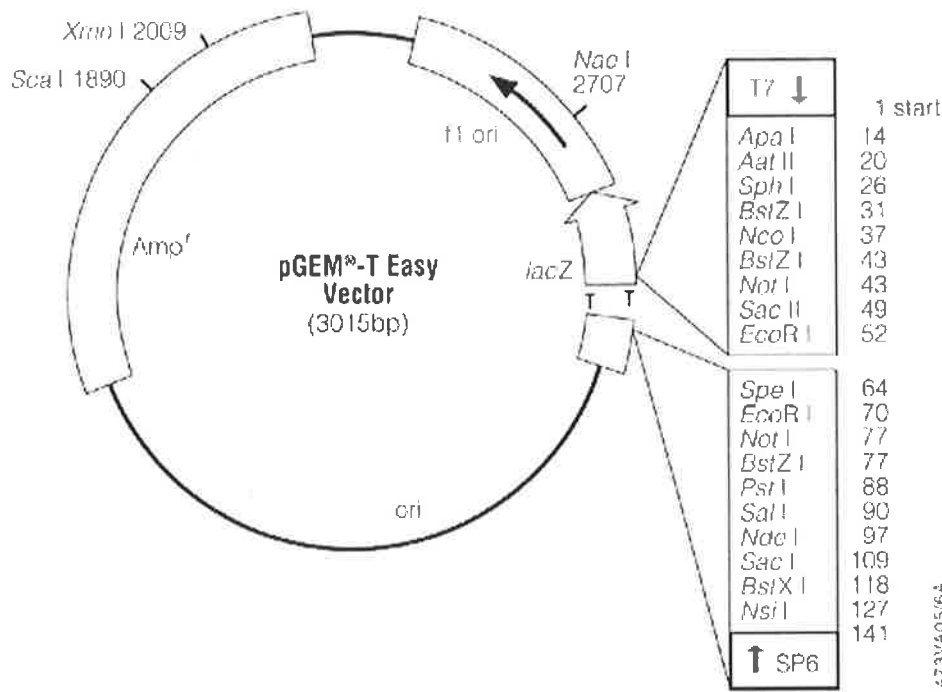
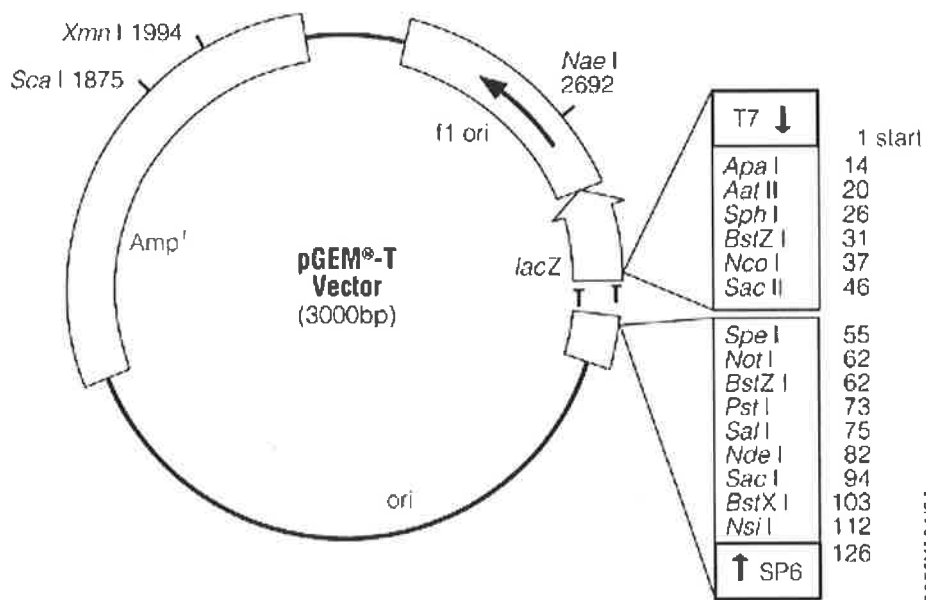
Appendix IV

PCR Conditions

PCR Type	Initial Denaturation	Cycling Parameters			Final Extension	Cycle Number
		<i>Denaturation</i>	<i>Annealing</i>	<i>Extension</i>		
Cytokine	94°C/5 min	94°C/1 min	55°C/30 sec	72°C/30 sec	72°C/7 min	35
KlenTaq	94°C/1 min	94°C/30 sec	68°C/3 min		72°C/7 min	35
β-actin	94°C/5 min	94°C/1 min	55°C/1 min	72°C/1 min	72°C/7 min	23
Sequencing	94°C/1 min	96°C/30 sec	50°C/15 sec	68°C/4 min	-	25

Appendix V

Cloning and Expression Plasmids



Diagrams of the pGEM[®]-T cloning vectors courtesy of the Promega website.

Appendix VI

Plasmids Used in this Thesis

Plasmid Name	Insert Type	Plasmid Backbone	Species
X.4.1B	p40 CDS with XbaI restriction enzyme site on 3' end	pGEM-T	Human
CMV-n3B	insert from X.4.1B	pRc/CMV	Human
pG35.1.1A	p35 CDS (full length cDNA)	pGEM-T	Human
RIA.3B	insert from pG35.1.1A	pRc/CMV	Human
pGΔ2.1B	p35 CDS with intron 4 retained	pGEM-T	Human
RA.14A	insert from pGΔ2.1B	pRc/CMV	Human
pGJay.4A	p35 CDS with intron 4 retained	pGEM-T	Human
pGLawlor.23B	p35 CDS with intron 4 retained	pGEM-T	Human
RLawlor.5B	insert from pGLawlor.23B	pRc/CMV	Human
pGOVp18.1.6B	p35 retains intron 4 amplified using Bov35F/Bov35R primers	pGEM-T	Ovine
pGShCDS2.1B	p35 CDS (**dud clone as assessed by sequencing)	pGEM-T	Ovine
pGShCDS1.9B	p35 CDS	pGEM-T	Ovine
RSp35.7B	insert from pGShCDS1.9B	pRc/CMV	Ovine
pGShCDS1.10A	p35 CDS with intron 4 retained	pGEM-T	Ovine

RShCDS18.4A	insert from pGShCDS1.10A (intron 4 retained)	pRc/CMV	Ovine
pGShCDS2.7A	p35 CDS with intron 4 retained	pGEM-T	Ovine
SHB19.2A	p40 CDS with XbaI restriction enzyme site on 3' end	pGEM-T	Ovine
RB19.1A	insert from SHB19.2A	pRc/CMV	Ovine
SHB23.3B	p40 CDS with XbaI restriction site on 3' end	pGEM-T	Ovine
pGERC9.3B	p35 CDS with intron 4 retained and truncated at intron end	pGEM-T Easy	Human
pRRC9.3xA	insert from pGERC9.3B	pRc/CMV	Human
pGED4.9A	p35 CDS with intron 4 retained and truncated at intron end	pGEM-T Easy	Human
pRD4.5A	insert from pGED4.9A	pRc/CMV	Human
pGZΔ35.13A	p35 CDS with STOP codon removed	pGEM-T Easy	Human
GFP35A.4B	insert from pGZΔ35.13A	pEGFP-N1	Human
pGZΔ18.4A	p35 CDS with intron 4 retained and STOP codon removed	pGEM-T Easy	Human
GFPtrunc.33A	insert from pGZΔ18.4A	pEGFP-N1	Human
pGH35.20A	p35 CDS with STOP codon removed	pGEM-T Easy	Human
GFP20A.4A	insert from pGH35.20A	pEGFP-N1	Human
pGZΔ18.9B	p35 CDS with intron 4 retained and STOP codon removed	pGEM-T Easy	Human
GFP9B.10B	insert from pGZΔ18.9B	pEGFP-N1	Human
GFP(3).3A	no insert (vector blank)	pEGFP-N1	N/A



Bibliography

Bibliography*

1. Kobayashi, M., L. Fitz, M. Ryan, R. M. Hewick, S. C. Clark, S. Chan, R. Loudon, F. Sherman, B. Perussia, and G. Trinchieri. 1989. Identification and purification of natural killer cell stimulatory factor (NKSF), a cytokine with multiple biologic effects on human lymphocytes. *J Exp Med* 170:827.
2. Stern, A., F. Podlaski, J. Hulmes, Y. Pan, P. Quinn, A. Wolitzky, P. Familletti, D. Stremlo, T. Truitt, R. Chizzonite, and M. Gately. 1990. Purification to homogeneity and partial characterization of cytotoxic lymphocyte maturation factor from human B-lymphoblastoid cells. *Proc Natl Acad Sci USA* 87:6808.
3. Robertson, M. J., R. J. Soiffer, S. F. Wolf, T. J. Manley, C. Donahue, D. Young, S. H. Herrmann, and J. Ritz. 1992. Response of human natural killer (NK) cells to NK cell stimulatory factor (NKSF): cytolytic activity and proliferation of NK cells are differentially regulated by NKSF. *J Exp Med* 175:779.
4. Tangarone, B., Poster 501-T, Ninth Symposium of the Protein Society. As cited in Lotze, M. T. 1996. Interleukin 12: cellular and molecular immunology of an important regulatory cytokine. *Ann N Y Acad Sci* 795:xiii.
5. Gubler, U., A. O. Chua, D. S. Schoenhaut, C. M. Dwyer, W. McComas, R. Motyka, N. Nabavi, A. G. Wolitzky, P. M. Quinn, P. C. Familletti, and M. K. Gately. 1991. Coexpression of two distinct genes is required to generate secreted bioactive cytotoxic lymphocyte maturation factor. *Proc Natl Acad Sci USA* 88:4143.

* Article titles are presented as they appear in the journal. As such spelling may differ from that used in the chapter text.

6. D'Andrea, A., M. Rengaraju, N. Valiante, J. Chehimi, M. Kubin, M. Aste, S. Chan, M. Kobayashi, D. Young, E. Nickbarg, R. Chizzonite, S. Wolf, and G. Trinchieri. 1992. Production of natural killer cell stimulatory factor (interleukin 12) by peripheral blood mononuclear cells. *J Exp Med* 176:1387.
7. Hsieh, C. S., S. E. Macatonia, C. S. Tripp, S. F. Wolf, A. O'Garra, and K. M. Murphy. 1993. Development of Th1 CD4⁺ T cells through IL-12 produced by *Listeria*-induced macrophages. *Science* 260:547.
8. Hayes, M. P., J. Wang, and M. A. Norcross. 1995. Regulation of interleukin-12 expression in human monocytes: selective priming by interferon- γ of lipopolysaccharide-inducible p35 and p40 genes. *Blood* 86:646.
9. Müller, G., J. Saloga, T. Germann, I. Bellinghausen, M. Mohamadzadeh, J. Knop, and A. Enk. 1994. Identification and induction of human keratinocyte-derived IL-12. *J Clin Invest* 94:1799.
10. Cassatella, M., L. Meda, S. Gasperini, A. D'Andrea, X. Ma, and G. Trinchieri. 1995. Interleukin-12 production by human polymorphonuclear leukocytes. *Eur J Immunol* 25:1.
11. Takahashi, M., K. Ogasawara, K. Takeda, W. Hashimoto, H. Sakihara, K. Kumagai, R. Anzai, M. Satoh, and S. Seki. 1996. LPS induces NK1.1⁺ $\alpha\beta$ T cells with potent cytotoxicity in the liver of mice via production of IL-12 from Kupffer cells. *J Immunol* 156:2436.
12. Heufler, C., F. Koch, U. Stanzl, G. Topar, M. Wysocka, G. Trinchieri, A. Enk, R. M. Steinman, N. Romani, and G. Schuler. 1996. Interleukin-12 is produced by dendritic cells and mediates T helper 1 development as well as interferon- γ production by T helper 1 cells. *Eur J Immunol* 26:659.

13. Aste-Amezaga, M., A. D'Andrea, M. Kubin, and G. Trinchieri. 1994. Cooperation of natural killer cell stimulatory factor/interleukin-12 with other stimuli in the induction of cytokines and cytotoxic cell-associated molecules in human T and NK cells. *Cell Immunol* 156:480.
14. Chan, S. H., B. Perussia, J. W. Gupta, M. Kobayashi, M. Pospíšil, H. A. Young, S. F. Wolf, D. Young, S. C. Clark, and G. Trinchieri. 1991. Induction of interferon γ production by natural killer cell stimulatory factor: characterization of the responder cells and synergy with other inducers. *J Exp Med* 173:869.
15. Desai, B. B., P. M. Quinn, A. G. Wolitzky, P. K. Mongini, R. Chizzonite, and M. K. Gately. 1992. IL-12 receptor. II. Distribution and regulation of receptor expression. *J Immunol* 148:3125.
16. Grohmann, U., M. L. Belladonna, R. Bianchi, C. Orabona, E. Ayroldi, M. C. Fioretti, and P. Puccetti. 1998. IL-12 acts directly on DC to promote nuclear localization of NF- κ B and primes DC for IL-12 production. *Immunity* 9:315.
17. Wolf, S. F., P. A. Temple, M. Kobayashi, D. Young, M. Dicig, L. Lowe, R. Dzialo, L. Fitz, C. Ferenz, R. M. Hewick, K. Kelleher, S. H. Herrmann, S. C. Clark, L. Azzoni, S. H. Chan, G. Trinchieri, and B. Perussia. 1991. Cloning of cDNA for natural killer cell stimulatory factor, a heterodimeric cytokine with multiple biologic effects on T and natural killer cells. *J Immunol* 146:3074.
18. Schoenhaut, D. S., A. O. Chua, A. G. Wolitzky, P. M. Quinn, C. M. Dwyer, W. McComas, P. C. Familletti, M. K. Gately, and U. Gubler. 1992. Cloning and expression of murine IL-12. *J Immunol* 148:3433.
19. Sieburth, D., E. Jabs, J. Warrington, X. Li, J. Lasota, S. LaForgia, K. Kelleher, K. Huebner, J. Wasmuth, and S. Wolf. 1992. Assignment of genes encoding a unique cytokine (IL12) composed of two unrelated subunits to chromosomes 3 and 5. *Genomics* 14:59.

20. Yoshimoto, T., K. Kojima, T. Funakoshi, Y. Endo, T. Fujita, and H. Nariuchi. 1996. Molecular cloning and characterization of murine IL-12 genes. *J Immunol* 156:1082.
21. Noben-Trauth, N., P. A. Schweitzer, K. R. Johnson, S. F. Wolf, B. B. Knowles, and L. D. Shultz. 1996. The interleukin-12 beta subunit (p40) maps to mouse chromosome 11. *Mamm Genome* 7:392.
22. Tone, Y., S. Thompson, J. Babik, K. Nolan, M. Tone, C. Raven, and H. Waldmann. 1996. Structure and chromosomal location of the mouse interleukin-12 p35 and p40 subunit genes. *Eur J Immunol* 26:1222.
23. D'Andrea, A., M. Aste-Amezaga, N. M. Valiante, X. Ma, M. Kubin, and G. Trinchieri. 1993. Interleukin 10 (IL-10) inhibits human lymphocyte interferon γ -production by suppressing natural killer cell stimulatory factor/IL-12 synthesis in accessory cells. *J Exp Med* 178:1041.
24. Snijders, A., C. M. Hilkens, T. C. van der Pouw Kraan, M. Engel, L. A. Aarden, and M. L. Kapsenberg. 1996. Regulation of bioactive IL-12 production in lipopolysaccharide-stimulated human monocytes is determined by the expression of the p35 subunit. *J Immunol* 156:1207.
25. Hayes, M. P., F. J. Murphy, and P. R. Burd. 1998. Interferon- γ -dependent inducible expression of the human interleukin-12 p35 gene in monocytes initiates from a TATA-containing promoter distinct from the CpG-rich promoter active in Epstein-Barr virus-transformed lymphoblastoid cells. *Blood* 91:4645.
26. Babik, J. M., E. Adams, Y. Tone, P. J. Fairchild, M. Tone, and H. Waldmann. 1999. Expression of murine IL-12 is regulated by translational control of the p35 subunit. *J Immunol* 162:4069.

27. Murphy, F. J., M. P. Hayes, and P. R. Burd. 2000. Disparate intracellular processing of human IL-12 preprotein subunits: atypical processing of the p35 signal peptide. *J Immunol* 164:839.
28. Devergne, O., M. Hummel, H. Koeppen, M. M. Le Beau, E. C. Nathanson, E. Kieff, and M. Birkenbach. 1996. A novel interleukin-12 p40-related protein induced by latent Epstein-Barr virus infection in B lymphocytes. *J Virol* 70:1143.
29. Devergne, O., M. Birkenbach, and E. Kieff. 1997. Epstein-Barr virus-induced gene 3 and the p35 subunit of interleukin 12 form a novel heterodimeric hematopoietin. *Proc Natl Acad Sci USA* 94:12041.
30. Ling, P., M. K. Gately, U. Gubler, A. S. Stern, P. Lin, K. Hollfelder, C. Su, Y. C. Pan, and J. Hakimi. 1995. Human IL-12 p40 homodimer binds to the IL-12 receptor but does not mediate biologic activity. *J Immunol* 154:116.
31. Doucey, M. A., D. Hess, M. J. Blommers, and J. Hofsteenge. 1999. Recombinant human interleukin-12 is the second example of a C-mannosylated protein. *Glycobiology* 9:435.
32. Murphy, T. C., MG; Kulesza, P; Magram, J and Murphy, KM. 1995. Regulation of interleukin 12 p40 expression through an NF- κ B half-site. *Mol Cell Biol* 15:5258.
33. Ma, X., J. M. Chow, G. Gri, G. Carra, F. Gerosa, S. F. Wolf, R. Dzialo, and G. Trinchieri. 1996. The interleukin 12 p40 gene promoter is primed by interferon γ in monocytic cells. *J Exp Med* 183:147.
34. Wedel, A., and H. W. Ziegler-Heitbrock. 1995. The C/EBP family of transcription factors. *Immunobiology* 193:171.

35. Plevy, S. E., J. H. Gemberling, S. Hsu, A. J. Dorner, and S. T. Smale. 1997. Multiple control elements mediate activation of the murine and human interleukin 12 p40 promoters: evidence of functional synergy between C/EBP and Rel proteins. *Mol Cell Biol* 17:4572.
36. Gri, G., D. Savio, G. Trinchieri, and X. Ma. 1998. Synergistic regulation of the human interleukin-12 p40 promoter by NF κ B and Ets transcription factors in Epstein-Barr virus-transformed B cells and macrophages. *J Biol Chem* 273:6431.
37. Mattner, F., S. Fischer, S. Guckes, S. Jin, H. Kaulen, E. Schmitt, E. Rüde, and T. Germann. 1993. The interleukin-12 subunit p40 specifically inhibits effects of the interleukin-12 heterodimer. *Eur J Immunol* 23:2202.
38. Heinzl, F., A. Hujer, F. Ahmed, and R. Rerko. 1997. *In vivo* production and function of IL-12 p40 homodimers. *J Immunol* 158:4381.
39. Gillessen, S., D. Carvajal, P. Ling, F. J. Podlaski, D. L. Stremlo, P. C. Familletti, U. Gubler, D. H. Presky, A. S. Stern, and M. K. Gately. 1995. Mouse interleukin-12 (IL-12) p40 homodimer: a potent IL-12 antagonist. *Eur J Immunol* 25:200.
40. Nickbarg, E. B., J. E. Vath, D. D. Pittman, J. E. Leonard, K. E. Waldburger, and M. D. Bond. 1995. Structural characterization of the recombinant p40 heavy chain subunit monomer and homodimer of murine IL-12. *Bioorg Chem* 23:380.
41. Ha, S. J., C. H. Lee, S. B. Lee, C. M. Kim, K. L. Jang, H. S. Shin, and Y. C. Sung. 1999. A novel function of IL-12 p40 as a chemotactic molecule for macrophages. *J Immunol* 163:2902.

42. Chua, A. O., R. Chizzonite, B. B. Desai, T. P. Truitt, P. Nunes, L. J. Minetti, R. R. Warriar, D. H. Presky, J. F. Levine, M. K. Gately, and U. Gubler. 1994. Expression cloning of a human IL-12 receptor component. A new member of the cytokine receptor superfamily with strong homology to gp130. *J Immunol* 153:128.
43. Presky, D. M., LJ; Gillessen, S; Gubler, U; Chizzonite, R; Stern, AS and Gately, M. 1996. Evidence for multiple sites of interaction between IL-12 and its receptor. *Ann N Y Acad Sci* 795:390.
44. Presky, D. H., H. Yang, L. J. Minetti, A. O. Chua, N. Nabavi, C.-Y. Wu, M. K. Gately, and U. Gubler. 1996. A functional interleukin 12 receptor complex is composed of two β -type cytokine receptor subunits. *Proc Natl Acad Sci USA* 93:14002.
45. Zou, J., D. H. Presky, C.-Y. Wu, and U. Gubler. 1997. Differential associations between the cytoplasmic regions of the interleukin-12 receptor subunits β 1 and β 2 and JAK kinases. *J Biol Chem* 272:6073.
46. Kawashima, T., H. Kawasaki, T. Kitamura, Y. Nojima, and C. Morimoto. 1998. Interleukin-12 induces tyrosine phosphorylation of an 85-kDa protein associated with the interleukin-12 receptor β 1 subunit. *Cell Immunol* 186:39.
47. Mosmann, T. R., H. Cherwinski, M. W. Bond, M. A. Giedlin, and R. L. Coffman. 1986. Two types of murine helper T cell clone. I. Definition according to profiles of lymphokine activities and secreted proteins. *J Immunol* 136:2348.

48. Del Prete, G. F., M. De Carli, C. Mastromauro, R. Biagiotti, D. Macchia, P. Falagiani, M. Ricci, and S. Romagnani. 1991. Purified protein derivative of *Mycobacterium tuberculosis* and excretory-secretory antigen(s) of *Toxocara canis* expand *in vitro* human T cells with stable and opposite (Type 1 T helper or Type 2 T helper) profile of cytokine production. *J Clin Invest* 88:346.
49. Mosmann, T. R., and R. L. Coffman. 1989. Th1 and Th2 cells: different patterns of lymphokine secretion lead to different functional properties. *Annu Rev Immunol* 7:145.
50. Fiorentino, D. F., M. W. Bond, and T. R. Mosmann. 1989. Two types of mouse T helper cell. IV. Th2 clones secrete a factor that inhibits cytokine production by Th1 clones. *J Exp Med* 170:2081.
51. Mosmann, T. R., and S. Sad. 1996. The expanding universe of T-cell subsets: Th1, Th2 and more. *Immunol Today* 17:138.
52. Chen, Y., V. K. Kuchroo, J. Inobe, D. A. Hafler, and H. L. Weiner. 1994. Regulatory T cell clones induced by oral tolerance: suppression of autoimmune encephalomyelitis. *Science* 265:1237.
53. Nickerson, P., W. Steurer, J. Steiger, X. Zheng, A. W. Steele, and T. B. Strom. 1994. Cytokines and the Th1/Th2 paradigm in transplantation. *Curr Opin Immunol* 6:757.
54. Kelso, A. 1995. Th1 and Th2 subsets: paradigms lost? *Immunol Today* 16:374.
55. Mottram, P. L., W. R. Han, L. J. Purcell, I. F. McKenzie, and W. W. Hancock. 1995. Increased expression of IL-4 and IL-10 and decreased expression of IL-2 and interferon- γ in long-surviving mouse heart allografts after brief CD4-monoclonal antibody therapy. *Transplantation* 59:559.

56. Sayegh, M. H., E. Akalin, W. W. Hancock, M. E. Russell, C. B. Carpenter, P. S. Linsley, and L. A. Turka. 1995. CD28-B7 blockade after alloantigenic challenge *in vivo* inhibits Th1 cytokines but spares Th2. *J Exp Med* 181:1869.
57. Takeuchi, T., R. P. Lowry, and B. Konieczny. 1992. Heart allografts in murine systems. The differential activation of Th2-like effector cells in peripheral tolerance. *Transplantation* 53:1281.
58. Lee, M.-S., L. Wogensen, J. Shizuru, M. B. Oldstone, and N. Sarvetnick. 1994. Pancreatic islet production of murine interleukin-10 does not inhibit immune-mediated tissue destruction. *J Clin Invest* 93:1332.
59. Mueller, R., J. D. Davies, T. Krahl, and N. Sarvetnick. 1997. IL-4 expression by grafts from transgenic mice fails to prevent allograft rejection. *J Immunol* 159:1599.
60. Quan, D., D. R. Grant, R. Z. Zhong, Z. Zhang, B. M. Garcia, and A. M. Jevnikar. 1994. Altered gene expression of cytokine, ICAM-1, and class II molecules precedes mouse intestinal allograft rejection. *Transplantation* 58:808.
61. Thai, N. L., F. Fu, S. Qian, H. Sun, L. Gao, S. C. Wang, A. J. Demetris, J. Woo, A. W. Thomson, R. J. Duquesnoy, and J. J. Fung. 1995. Cytokine mRNA profiles in mouse orthotopic liver transplantation. Graft rejection is associated with augmented Th1 function. *Transplantation* 59:274.
62. Chen, N., Q. Gao, and E. H. Field. 1996. Prevention of Th1 response is critical for tolerance. *Transplantation* 61:1076.
63. Macatonia, S. E., N. A. Hosken, M. Litton, P. Vieira, C. S. Hsieh, J. A. Culpepper, M. Wysocka, G. Trinchieri, K. M. Murphy, and A. O'Garra. 1995. Dendritic cells produce IL-12 and direct the development of Th1 cells from naive CD4⁺ T cells. *J Immunol* 154:5071.

64. O'Garra, A., and K. Murphy. 1994. Role of cytokines in determining T-lymphocyte function. *Curr Opin Immunol* 6:458.
65. Kopf, M., G. Le Gros, M. Bachmann, M. C. Lamers, H. Bluethmann, and G. Köhler. 1993. Disruption of the murine IL-4 gene blocks Th2 cytokine responses. *Nature* 362:245.
66. Manetti, R., P. Parronchi, M. G. Giudizi, M. P. Piccinni, E. Maggi, G. Trinchieri, and S. Romagnani. 1993. Natural killer cell stimulatory factor (interleukin 12 [IL-12]) induces T helper type 1 (Th1)-specific immune responses and inhibits the development of IL-4-producing Th cells. *J Exp Med* 177:1199.
67. Rogge, L., L. Barberis-Maino, M. Biffi, N. Passini, D. H. Presky, U. Gubler, and F. Sinigaglia. 1997. Selective expression of an interleukin-12 receptor component by human T helper 1 cells. *J Exp Med* 185:825.
68. Szabo, S. J., A. S. Dighe, U. Gubler, and K. M. Murphy. 1997. Regulation of the interleukin (IL)-12R β 2 subunit expression in developing T helper 1 (Th1) and Th2 cells. *J Exp Med* 185:817.
69. Gollob, J. A., H. Kawasaki, and J. Ritz. 1997. Interferon- γ and interleukin-4 regulate T cell interleukin-12 responsiveness through the differential modulation of high-affinity interleukin-12 receptor expression. *Eur J Immunol* 27:647.
70. Heinzl, F. P., M. D. Sadick, B. J. Holaday, R. L. Coffman, and R. M. Locksley. 1989. Reciprocal expression of interferon γ or interleukin 4 during the resolution or progression of murine leishmaniasis. Evidence for expansion of distinct helper T cell subsets. *J Exp Med* 169:59.

71. Sypek, J. P., C. L. Chung, S. E. Mayor, J. M. Subramanyam, S. J. Goldman, D. S. Sieburth, S. F. Wolf, and R. G. Schaub. 1993. Resolution of cutaneous leishmaniasis: interleukin 12 initiates a protective T helper type 1 immune response. *J Exp Med* 177:1797.
72. Decken, K., G. Köhler, K. Palmer-Lehmann, A. Wunderlin, F. Mattner, J. Magram, M. K. Gately, and G. Alber. 1998. Interleukin-12 is essential for a protective Th1 response in mice infected with *Cryptococcus neoformans*. *Infect Immun* 66:4994.
73. Carr, J. A., J. A. Rogerson, M. J. Mulqueen, N. A. Roberts, and A. A. Nash. 1999. The role of endogenous interleukin-12 in resistance to murine cytomegalovirus (MCMV) infection and a novel action for endogenous IL-12 p40. *J Interferon Cytokine Res* 19:1145.
74. Cooper, A. M., J. Magram, J. Ferrante, and I. M. Orme. 1997. Interleukin 12 (IL-12) is crucial to the development of protective immunity in mice intravenously infected with *Mycobacterium tuberculosis*. *J Exp Med* 186:39.
75. Stamm, L. M., A. A. Satoskar, S. K. Ghosh, J. R. David, and A. R. Satoskar. 1999. STAT-4 mediated IL-12 signaling pathway is critical for the development of protective immunity in cutaneous leishmaniasis. *Eur J Immunol* 29:2524.
76. Mattner, F., K. Di Padova, and G. Alber. 1997. Interleukin-12 is indispensable for protective immunity against *Leishmania major*. *Infect Immun* 65:4378.
77. Altare, F., D. Lammas, P. Revy, E. Jouanguy, R. Dörfinger, S. Lamhamedi, P. Drysdale, D. Scheel-Toellner, J. Girdlestone, P. Darbyshire, M. Wadhwa, H. Dockrell, M. Salmon, A. Fischer, A. Durandy, J. L. Casanova, and D. S. Kumararatne. 1998. Inherited interleukin 12 deficiency in a child with Bacille Calmette-Guérin and *Salmonella enteritidis* disseminated infection. *J Clin Invest* 102:2035.

78. Bancroft, A. J., K. J. Else, J. P. Sypek, and R. K. Grencis. 1997. Interleukin-12 promotes a chronic intestinal nematode infection. *Eur J Immunol* 27:866.
79. Binder, J., E. Graser, W. W. Hancock, B. Wasowska, M. H. Sayegh, H. D. Volk, and J. W. Kupiec-Weglinski. 1995. Downregulation of intragraft IFN- γ expression correlates with increased IgG1 alloantibody response following intrathymic immunomodulation of sensitized rat recipients. *Transplantation* 60:1516.
80. Hancock, W. W., M. H. Sayegh, X.-G. Zheng, R. Peach, P. S. Linsley, and L. A. Turka. 1996. Costimulatory function and expression of CD40 ligand, CD80, and CD86 in vascularized murine cardiac allograft rejection. *Proc Natl Acad Sci USA* 93:13967.
81. Wasowska, B., K. J. Wieder, W. W. Hancock, X. X. Zheng, B. Berse, J. Binder, T. B. Strom, and J. W. Kupiec-Weglinski. 1996. Cytokine and alloantibody networks in long term cardiac allografts in rat recipients treated with rapamycin. *J Immunol* 156:395.
82. Thai, N. L., Y. Li, F. Fu, S. Qian, A. J. Demetris, R. J. Duquesnoy, and J. J. Fung. 1997. Interleukin-2 and interleukin-12 mediate distinct effector mechanisms of liver allograft rejection. *Liver Transpl Surg* 3:118.
83. Li, X. C., M. S. Zand, Y. Li, X. X. Zheng, and T. B. Strom. 1998. On histocompatibility barriers, Th1 to Th2 immune deviation, and the nature of the allograft responses. *J Immunol* 161:2241.
84. Ar'Rajab, A., I. Dawidson, and R. Fabia. 1996. Reperfusion injury. *New Horiz* 4:224.
85. Daemen, M. A., C. van't Veer, T. G. Wolfs, and W. A. Buurman. 1999. Ischemia/reperfusion-induced IFN- γ up-regulation: involvement of IL-12 and IL-18. *J Immunol* 162:5506.

86. Lentsch, A. B., H. Yoshidome, A. Kato, R. L. Warner, W. G. Cheadle, P. A. Ward, and M. J. Edwards. 1999. Requirement for interleukin-12 in the pathogenesis of warm hepatic ischemia/reperfusion injury in mice. *Hepatology* 30:1448.
87. Trinchieri, G. 1994. Interleukin-12: a cytokine produced by antigen-presenting cells with immunoregulatory functions in the generation of T-helper cells type 1 and cytotoxic lymphocytes. *Blood* 84:4008.
88. Chehimi, J., S. E. Starr, I. Frank, M. Rengaraju, S. J. Jackson, C. Llanes, M. Kobayashi, B. Perussia, D. Young, E. Nickbarg, S. F. Wolf, and G. Trinchieri. 1992. Natural killer (NK) cell stimulatory factor increases the cytotoxic activity of NK cells from both healthy donors and human immunodeficiency virus-infected patients. *J Exp Med* 175:789.
89. Naume, B., M. Gately, and T. Espevik. 1992. A comparative study of IL-12 (cytotoxic lymphocyte maturation factor)-, IL-2-, and IL-7-induced effects on immunomagnetically purified CD56⁺ NK cells. *J Immunol* 148:2429.
90. Tan, J., C. A. Newton, J. Y. Djeu, D. E. Gutsch, A. E. Chang, N. S. Yang, T. W. Klein, and Y. Hua. 1996. Injection of complementary DNA encoding interleukin-12 inhibits tumor establishment at a distant site in a murine renal carcinoma model. *Cancer Res* 56:3399.
91. Masson, D., M. Nabholz, C. Estrade, and J. Tschopp. 1986. Granules of cytolytic T-lymphocytes contain two serine esterases. *EMBO J* 5:1595.
92. Masson, D., and J. Tschopp. 1985. Isolation of a lytic, pore-forming protein (perforin) from cytolytic T-lymphocytes. *J Biol Chem* 260:9069.
93. Lipman, M. L., A. C. Stevens, and T. B. Strom. 1994. Heightened intragraft CTL gene expression in acutely rejecting renal allografts. *J Immunol* 152:5120.

94. Allavena, P., C. Paganin, D. Zhou, G. Bianchi, S. Sozzani, and A. Mantovani. 1994. Interleukin-12 is chemotactic for natural killer cells and stimulates their interaction with vascular endothelium. *Blood* 84:2261.
95. Mehrotra, P. T., D. Wu, J. A. Crim, H. S. Mostowski, and J. P. Siegel. 1993. Effects of IL-12 on the generation of cytotoxic activity in human CD8⁺ T lymphocytes. *J Immunol* 151:2444.
96. Bhardwaj, N., R. A. Seder, A. Reddy, and M. V. Feldman. 1996. IL-12 in conjunction with dendritic cells enhances antiviral CD8⁺ CTL responses *in vitro*. *J Clin Invest* 98:715.
97. Tannenbaum, C. S., N. Wicker, D. Armstrong, R. Tubbs, J. Finke, R. M. Bukowski, and T. A. Hamilton. 1996. Cytokine and chemokine expression in tumors of mice receiving systemic therapy with IL-12. *J Immunol* 156:693.
98. Rakhmilevich, A. L., K. Janssen, J. Turner, J. Culp, and N. S. Yang. 1997. Cytokine gene therapy of cancer using gene gun technology: superior antitumor activity of interleukin-12. *Hum Gene Ther* 8:1303.
99. Iwasaki, A., B. J. Stiernholm, A. K. Chan, N. L. Berinstein, and B. H. Barber. 1997. Enhanced CTL responses mediated by plasmid DNA immunogens encoding costimulatory molecules and cytokines. *J Immunol* 158:4591.
100. Häyry, P., and V. Defendi. 1970. Mixed lymphocyte cultures produce effector cells: model *in vitro* for allograft rejection. *Science* 168:133.
101. Chouaib, S., J. Chehimi, L. Bani, N. Genetet, T. Tursz, F. Gay, G. Trinchieri, and F. Mami-Chouaib. 1994. Interleukin 12 induces the differentiation of major histocompatibility complex class I-primed cytotoxic T-lymphocyte precursors into allospecific cytotoxic effectors. *Proc Natl Acad Sci USA* 91:12659.

102. Bloom, E. T., and J. A. Horvath. 1994. Cellular and molecular mechanisms of the IL-12-induced increase in allospecific murine cytolytic T cell activity. Implications for the age-related decline in CTL. *J Immunol* 152:4242.
103. Gately, M. K., R. R. Warriar, S. Honasoge, D. M. Carvajal, D. A. Faherty, S. E. Connaughton, T. D. Anderson, U. Sarmiento, B. R. Hubbard, and M. Murphy. 1994. Administration of recombinant IL-12 to normal mice enhances cytolytic lymphocyte activity and induces production of IFN- γ *in vivo*. *Int Immunol* 6:157.
104. Herrmann, S., and K. Abdi. 1996. Both IL-2 and IL-4 synergize with IL-12 to induce a CTL response, a response completely blocked by TGF- β . *Ann N Y Acad Sci* 795:168.
105. Kos, F. J., and E. G. Engleman. 1995. Requirement for natural killer cells in the induction of cytotoxic T cells. *J Immunol* 155:578.
106. Su, H. C., R. Ishikawa, and C. A. Biron. 1993. Transforming growth factor- β expression and natural killer cell responses during virus infection of normal, nude, and SCID mice. *J Immunol* 151:4874.
107. Su, H. C., J. S. Orange, L. D. Fast, A. T. Chan, S. J. Simpson, C. Terhorst, and C. A. Biron. 1994. IL-2-dependent NK cell responses discovered in virus-infected β 2-microglobulin-deficient mice. *J Immunol* 153:5674.
108. Bradley, L. M., S. R. Watson, and S. L. Swain. 1994. Entry of naïve CD4 T cells into peripheral lymph nodes requires L-selectin. *J Exp Med* 180:2401.
109. Van Wely, C. A., P. C. Beverley, S. J. Brett, C. J. Britten, and J. P. Tite. 1999. Expression of L-selectin on Th1 cells is regulated by IL-12. *J Immunol* 163:1214.

110. Xie, H., Y. C. Lim, F. W. Luscinskas, and A. H. Lichtman. 1999. Acquisition of selectin binding and peripheral homing properties by CD4⁺ and CD8⁺ T cells. *J Exp Med* 189:1765.
111. Marth, T., W. Strober, and B. L. Kelsall. 1996. High dose oral tolerance in ovalbumin TCR-transgenic mice. Systemic neutralization of IL-12 augments TGF- β secretion and T cell apoptosis. *J Immunol* 157:2348.
112. Marth, T., M. Zeitz, B. R. Ludviksson, W. Strober, and B. L. Kelsall. 1999. Extinction of IL-12 signaling promotes Fas-mediated apoptosis of antigen-specific T cells. *J Immunol* 162:7233.
113. Grohmann, U., R. Bianchi, E. Ayroldi, M. L. Belladonna, D. Surace, M. C. Fioretti, and P. Puccetti. 1997. A tumor-associated and self antigen peptide presented by dendritic cells may induce T cell anergy *in vivo*, but IL-12 can prevent or revert the anergic state. *J Immunol* 158:3593.
114. Ushio, H., R. F. Tsuji, M. Szczepanik, K. Kawamoto, H. Matsuda, and P. W. Askenase. 1998. IL-12 reverses established antigen-specific tolerance of contact sensitivity by affecting costimulatory molecules B7-1 (CD80) and B7-2 (CD86). *J Immunol* 160:2080.
115. Van Parijs, L., V. L. Perez, A. Biuckians, R. G. Maki, C. A. London, and A. K. Abbas. 1997. Role of interleukin-12 and costimulators in T cell anergy *in vivo*. *J Exp Med* 186:1119.
116. Piccotti, J. R., S. Y. Chan, R. E. Goodman, J. Magram, E. J. Eichwald, and D. K. Bishop. 1996. IL-12 antagonism induces T helper 2 responses, yet exacerbates cardiac allograft rejection. Evidence against a dominant protective role for T helper 2 cytokines in alloimmunity. *J Immunol* 157:1951.

117. Piccotti, J. R., S. Y. Chan, K. Li, E. J. Eichwald, and D. K. Bishop. 1997. Differential effects of IL-12 receptor blockade with IL-12 p40 homodimer on the induction of CD4⁺ and CD8⁺ IFN- γ -producing cells. *J Immunol* 158:643.
118. Yasuda, H., M. Nagata, K. Arisawa, R. Yoshida, K. Fujihira, N. Okamoto, H. Moriyama, M. Miki, I. Saito, H. Hamada, K. Yokono, and M. Kasuga. 1998. Local expression of immunoregulatory IL-12p40 gene prolonged syngeneic islet graft survival in diabetic NOD mice. *J Clin Invest* 102:1807.
119. Kato, K., O. Shimozato, K. Hoshi, H. Wakimoto, H. Hamada, H. Yagita, and K. Okumura. 1996. Local production of the p40 subunit of interleukin 12 suppresses T-helper 1-mediated immune responses and prevents allogeneic myoblast rejection. *Proc Natl Acad Sci USA* 93:9085.
120. Lane, P., T. Brocker, S. Hubele, E. Padovan, A. Lanzavecchia, and F. McConnell. 1993. Soluble CD40 ligand can replace the normal T cell-derived CD40 ligand signal to B cells in T cell-dependent activation. *J Exp Med* 177:1209.
121. Graham, F. L., J. Smiley, W. C. Russell, and R. Nairn. 1977. Characteristics of a human cell line transformed by DNA from human adenovirus type 5. *J Gen Virol* 36:59.
122. 1988. *ATCC Catalogue of Cell Lines and Hybridomas, 6th Edition*.
123. He, T.-C., S. Zhou, L. T. da Costa, J. Yu, K. W. Kinzler, and B. Vogelstein. 1998. A simplified system for generating recombinant adenoviruses. *Proc Natl Acad Sci USA* 95:2509.
124. Chomczynski, P., and N. Sacchi. 1987. Single-step method of RNA isolation by acid guanidinium thiocyanate-phenol-chloroform extraction. *Anal Biochem* 162:156.

125. Laemmli, U. K. 1970. Cleavage of structural proteins during the assembly of the head of bacteriophage T4. *Nature* 227:680.
126. Zou, J. J., D. S. Schoenhaut, D. M. Carvajal, R. R. Warriar, D. H. Presky, M. K. Gately, and U. Gubler. 1995. Structure-function analysis of the p35 subunit of mouse interleukin 12. *J Biol Chem* 270:5864.
127. Kozak, M. 1987. An analysis of 5'-noncoding sequences from 699 vertebrate messenger RNAs. *Nucleic Acids Res* 15:8125.
128. Appel, R. D., A. Bairoch, and D. F. Hochstrasser. 1994. A new generation of information retrieval tools for biologists: the example of the ExPASy WWW server. *Trends Biochem Sci* 19:258.
129. Nielsen, H., J. Engelbrecht, S. Brunak, and G. Von Heinje. 1997. Identification of prokaryotic and eukaryotic signal peptides and prediction of their cleavage sites. *Prot Engin* 10:1.
130. Hein, W. R. 1995. Sheep as experimental animals for immunological research. *The Immunologist* 3:12.
131. Banchereau, J., and R. M. Steinman. 1998. Dendritic cells and the control of immunity. *Nature* 392:245.
132. Steinman, R. M., M. Pack, and K. Inaba. 1997. Dendritic cells in the T-cell areas of lymphoid organs. *Immunol Rev* 156:25.
133. Steinman, R. M. 1991. The dendritic cell system and its role in immunogenicity. *Annu Rev Immunol* 9:271.
134. Vakkila, J., and M. Hurme. 1990. Both dendritic cells and monocytes induce autologous and allogeneic T cells receptive to interleukin 2. *Scand J Immunol* 31:75.

135. Freudenthal, P. S., and R. M. Steinman. 1990. The distinct surface of human blood dendritic cells, as observed after an improved isolation method. *Proc Natl Acad Sci USA* 87:7698.
136. O'Doherty, U., R. M. Steinman, M. Peng, P. U. Cameron, S. Gezelter, I. Kopeloff, W. J. Swiggard, M. Pope, and N. Bhardwaj. 1993. Dendritic cells freshly isolated from human blood express CD4 and mature into typical immunostimulatory dendritic cells after culture in monocyte-conditioned medium. *J Exp Med* 178:1067.
137. Santiago-Schwarz, F., E. Belilos, B. Diamond, and S. E. Carsons. 1992. TNF in combination with GM-CSF enhances the differentiation of neonatal cord blood stem cells into dendritic cells and macrophages. *J Leukoc Biol* 52:274.
138. Caux, C., C. Dezutter-Dambuyant, D. Schmitt, and J. Banchereau. 1992. GM-CSF and TNF- α cooperate in the generation of dendritic Langerhans cells. *Nature* 360:258.
139. Romani, N., S. Gruner, D. Brang, E. Kämpgen, A. Lenz, B. Trockenbacher, G. Konwalinka, P. O. Fritsch, R. M. Steinman, and G. Schuler. 1994. Proliferating dendritic cell progenitors in human blood. *J Exp Med* 180:83.
140. Sallusto, F., and A. Lanzavecchia. 1994. Efficient presentation of soluble antigen by cultured human dendritic cells is maintained by granulocyte/macrophage colony-stimulating factor plus interleukin 4 and downregulated by tumor necrosis factor α . *J Exp Med* 179:1109.
141. Ardavin, C., L. Wu, C.-L. Li, and K. Shortman. 1993. Thymic dendritic cells and T cells develop simultaneously in the thymus from a common precursor population. *Nature* 362:761.
142. Wu, L., C.-L. Li, and K. Shortman. 1996. Thymic dendritic cell precursors: relationship to the T lymphocyte lineage and phenotype of the dendritic cell progeny. *J Exp Med* 184:903.

143. Pulendran, B., J. Lingappa, M. K. Kennedy, J. Smith, M. Teepe, A. Rudensky, C. R. Maliszewski, and E. Maraskovsky. 1997. Developmental pathways of dendritic cells *in vivo*: distinct function, phenotype, and localization of dendritic cell subsets in FLT3 ligand-treated mice. *J Immunol* 159:2222.
144. Inaba, K., M. Pack, M. Inaba, H. Sakuta, F. Isdell, and R. M. Steinman. 1997. High levels of a major histocompatibility complex II-self peptide complex on dendritic cells from the T cell areas of lymph nodes. *J Exp Med* 186:665.
145. Süss, G., and K. Shortman. 1996. A subclass of dendritic cells kills CD4 T cells via Fas/Fas-ligand-induced apoptosis. *J Exp Med* 183:1789.
146. Kronin, V., K. Winkel, G. Süss, A. Kelso, W. Heath, J. Kirberg, H. Von Boehmer, and K. Shortman. 1996. A subclass of dendritic cells regulates the response of naive CD8 T cells by limiting their IL-2 production. *J Immunol* 157:3819.
147. Grohmann, U., R. Bianchi, M. L. Belladonna, C. Vacca, S. Silla, E. Ayroldi, M. C. Fioretti, and P. Puccetti. 1999. IL-12 acts selectively on CD8 α -dendritic cells to enhance presentation of a tumor peptide *in vivo*. *J Immunol* 163:3100.
148. Maldonado-López, R., T. De Smedt, P. Michel, J. Godfroid, B. Pajak, C. Heirman, K. Thielemans, O. Leo, J. Urbain, and M. Moser. 1999. CD8 α ⁺ and CD8 α - subclasses of dendritic cells direct the development of distinct T helper cells *in vivo*. *J Exp Med* 189:587.
149. Cella, M., D. Scheidegger, K. Palmer-Lehmann, P. Lane, A. Lanzavecchia, and G. Alber. 1996. Ligation of CD40 on dendritic cells triggers production of high levels of interleukin-12 and enhances T cell stimulatory capacity: T-T help via APC activation. *J Exp Med* 184:747.

150. Reis e Sousa, C., S. Hieny, T. Scharton-Kersten, D. Jankovic, H. Charest, R. N. Germain, and A. Sher. 1997. *In vivo* microbial stimulation induces rapid CD40 ligand-independent production of interleukin 12 by dendritic cells and their redistribution to T cell areas. *J Exp Med* 186:1819.
151. Sher, A., and C. Reis e Sousa. 1998. Ignition of the type 1 response to intracellular infection by dendritic cell-derived interleukin-12. *Eur Cytokine Netw* 9:65.
152. Kato, T., R. Hakamada, H. Yamane, and H. Nariuchi. 1996. Induction of IL-12 p40 messenger RNA expression and IL-12 production of macrophages via CD40-CD40 ligand interaction. *J Immunol* 156:3932.
153. Yamane, H., T. Kato, and H. Nariuchi. 1999. Effective stimulation for IL-12 p35 mRNA accumulation and bioactive IL-12 production of antigen-presenting cells interacted with Th cells. *J Immunol* 162:6433.
154. Ria, F., G. Penna, and L. Adorini. 1998. Th1 cells induce and Th2 inhibit antigen-dependent IL-12 secretion by dendritic cells. *Eur J Immunol* 28:2003.
155. Guéry, J.-C., F. Ria, F. Galbiati, and L. Adorini. 1997. Normal B cells fail to secrete interleukin-12. *Eur J Immunol* 27:1632.
156. Ohshima, Y., and G. Delespesse. 1997. T cell-derived IL-4 and dendritic cell-derived IL-12 regulate the lymphokine-producing phenotype of alloantigen-primed naive human CD4 T cells. *J Immunol* 158:629.
157. Kuby, J. 1994. *Immunology*. W.H. Freeman and Company.
158. Murphy, J. F., F. D. McDonald, M. Dawson, A. Reite, J. Turcotte, and F. R. Fekety, Jr. 1976. Factors affecting the frequency of infection in renal transplant recipients. *Arch Intern Med* 136:670.

159. Wiecek, A., M. Nowicki, F. Kokot, and E. Ritz. 1996. Acute failure of the transplanted kidney-pathophysiology, diagnosis and prevention. *Ann Transplant* 1:5.
160. Rigg, K. M. 1995. Renal transplantation: current status, complications and prevention. *J Antimicrob Chemother* 36:51.
161. Klintmalm, G. B., S. Iwatsuki, and T. E. Starzl. 1981. Nephrotoxicity of cyclosporin A in liver and kidney transplant patients. *Lancet* 1:470.
162. Hows, J. M., P. M. Chipping, S. Fairhead, J. Smith, A. Baughan, and E. C. Gordon-Smith. 1983. Nephrotoxicity in bone marrow transplant recipients treated with cyclosporin A. *Br J Haematol* 54:69.
163. Porayko, M. K., S. C. Textor, R. A. Krom, J. E. Hay, G. J. Gores, T. M. Richards, P. H. Crotty, S. J. Beaver, J. L. Steers, and R. H. Wiesner. 1994. Nephrotoxic effects of primary immunosuppression with FK-506 and cyclosporine regimens after liver transplantation. *Mayo Clin Proc* 69:105.
164. Starzl, T. E., J. Fung, M. Jordan, R. Shapiro, A. Tzakis, J. McCauley, J. Johnston, Y. Iwaki, A. Jain, M. Alessiani, and S. Todo. 1990. Kidney transplantation under FK 506. *JAMA* 264:63.
165. Bäckman, L., M. Nicari, M. Levy, D. Distant, C. Eisenstein, T. Renard, R. Goldstein, B. Husberg, T. A. Gonwa, and G. Klintmalm. 1994. FK506 trough levels in whole blood and plasma in liver transplant recipients. Correlation with clinical events and side effects. *Transplantation* 57:519.
166. Jain, A. B., and J. J. Fung. 1996. Cyclosporin and tacrolimus in clinical transplantation: a comparative review. *Clin Immunother* 5:351.
167. Billingham, R. E. 1971. The passenger cell concept in transplantation immunology. *Cell Immunol* 2:1.

168. Starzl, T. E., A. J. Demetris, M. Trucco, A. Zeevi, H. Ramos, P. Terasaki, W. A. Rudert, M. Kocova, C. Riccordi, S. Ildstad, and N. Murase. 1993. Chimerism and donor-specific nonreactivity 27 to 29 years after kidney allotransplantation. *Transplantation* 55:1272.
169. Burlingham, W. J., A. P. Grailer, J. H. Fechner, Jr., S. Kusaka, M. Trucco, M. Kocova, F. O. Belzer, and H. W. Sollinger. 1995. Microchimerism linked to cytotoxic T lymphocyte functional unresponsiveness (clonal anergy) in a tolerant renal transplant recipient. *Transplantation* 59:1147.
170. McKenzie, J. L., M. E. Beard, and D. N. Hart. 1984. The effect of donor pretreatment on interstitial dendritic cell content and rat cardiac allograft survival. *Transplantation* 38:371.
171. Bonham, A. C., L. Lu, and A. W. Thomson. 1997. Is chimerism necessary for tolerance and how? *Curr Opin Organ Trans* 2:23.
172. Qian, S., A. J. Demetris, N. Murase, A. S. Rao, J. J. Fung, and T. E. Starzl. 1994. Murine liver allograft transplantation: tolerance and donor cell chimerism. *Hepatology* 19:916.
173. Sun, J., G. W. McCaughan, N. D. Gallagher, A. G. Sheil, and G. A. Bishop. 1995. Deletion of spontaneous rat liver allograft acceptance by donor irradiation. *Transplantation* 60:233.
174. Lu, L., W. A. Rudert, S. Qian, D. McCaslin, F. Fu, A. S. Rao, M. Trucco, J. J. Fung, T. E. Starzl, and A. W. Thomson. 1995. Growth of donor-derived dendritic cells from the bone marrow of murine liver allograft recipients in response to granulocyte/macrophage colony-stimulating factor. *J Exp Med* 182:379.

175. Rastellini, C., L. Lu, C. Ricordi, T. E. Starzl, A. S. Rao, and A. W. Thomson. 1995. Granulocyte/macrophage colony-stimulating factor-stimulated hepatic dendritic cell progenitors prolong pancreatic islet allograft survival. *Transplantation* 60:1366.
176. Lu, L., D. McCaslin, T. E. Starzl, and A. W. Thomson. 1995. Bone marrow-derived dendritic cell progenitors (NLDC 145⁺, MHC class II⁺, B7-1^{dim}, B7-2⁻) induce alloantigen-specific hyporesponsiveness in murine T lymphocytes. *Transplantation* 60:1539.
177. Fu, F., Y. Li, S. Qian, L. Lu, F. Chambers, T. E. Starzl, J. J. Fung, and A. W. Thomson. 1996. Costimulatory molecule-deficient dendritic cell progenitors (MHC class II⁺, CD80^{dim}, CD86⁻) prolong cardiac allograft survival in nonimmunosuppressed recipients. *Transplantation* 62:659.
178. Lu, L., W. Li, F. Fu, F. G. Chambers, S. Qian, J. J. Fung, and A. W. Thomson. 1997. Blockade of the CD40-CD40 ligand pathway potentiates the capacity of donor-derived dendritic cell progenitors to induce long-term cardiac allograft survival. *Transplantation* 64:1808.
179. Lu, L., W. Li, C. Zhong, S. Qian, J. J. Fung, A. W. Thomson, and T. E. Starzl. 1999. Increased apoptosis of immunoreactive host cells and augmented donor leukocyte chimerism, not sustained inhibition of B7 molecule expression are associated with prolonged cardiac allograft survival in mice preconditioned with immature donor dendritic cells plus anti-CD40L mAb. *Transplantation* 68:747.
180. Sharland, A., Y. Yan, C. Wang, D. G. Bowen, J. Sun, A. G. Sheil, G. W. McCaughan, and G. A. Bishop. 1999. Evidence that apoptosis of activated T cells occurs in spontaneous tolerance of liver allografts and is blocked by manipulations which break tolerance. *Transplantation* 68:1736.

181. Min, W. P., R. Gorczynski, X.-Y. Huang, M. Kushida, P. Kim, M. Obataki, J. Lei, R. M. Suri, and M. S. Cattral. 2000. Dendritic cells genetically engineered to express fas ligand induce donor-specific hyporesponsiveness and prolong allograft survival. *J Immunol* 164:161.
182. Kanegae, Y., M. Makimura, and I. Saito. 1994. A simple and efficient method for purification of infectious recombinant adenovirus. *Jpn J Med Sci Biol* 47:157.
183. Nyberg-Hoffman, C., P. Shabram, W. Li, D. Giroux, and E. Aguilar-Cordova. 1997. Sensitivity and reproducibility in adenoviral infectious titer determination. *Nat Med* 3:808.
184. Rea, D., F. H. Schagen, R. C. Hoeben, M. Mehtali, M. J. Havenga, R. E. Toes, C. J. Melief, and R. Offringa. 1999. Adenoviruses activate human dendritic cells without polarization toward a T-helper type 1-inducing subset. *J Virol* 73:10245.
185. Arthur, J. F., L. H. Butterfield, M. D. Roth, L. A. Bui, S. M. Kiertscher, R. Lau, S. Dubinett, J. Glaspy, W. H. McBride, and J. S. Economou. 1997. A comparison of gene transfer methods in human dendritic cells. *Cancer Gene Ther* 4:17.
186. Dietz, A. B., and S. Vuk-Pavlovic. 1998. High efficiency adenovirus-mediated gene transfer to human dendritic cells. *Blood* 91:392.
187. Thomas, R., and P. E. Lipsky. 1994. Human peripheral blood dendritic cell subsets. Isolation and characterization of precursor and mature antigen-presenting cells. *J Immunol* 153:4016.
188. Rossi, G., N. Heveker, B. Thiele, H. Gelderblom, and F. Steinbach. 1992. Development of a Langerhans cell phenotype from peripheral blood monocytes. *Immunol Lett* 31:189.

189. Zhou, L.-J., and T. F. Tedder. 1996. CD14⁺ blood monocytes can differentiate into functionally mature CD83⁺ dendritic cells. *Proc Natl Acad Sci USA* 93:2588.
190. Peters, J. H., J. Ruppert, R. K. Gieseler, H. M. Najjar, and H. Xu. 1991. Differentiation of human monocytes into CD14 negative accessory cells: do dendritic cells derive from the monocytic lineage? *Pathobiology* 59:122.
191. Zhong, L., A. Granelli-Piperno, Y. Choi, and R. M. Steinman. 1999. Recombinant adenovirus is an efficient and non-perturbing genetic vector for human dendritic cells. *Eur J Immunol* 29:964.
192. Sonderbye, L., S. Feng, S. Yacoubian, H. Buehler, N. Ahsan, R. Mulligan, and E. Langhoff. 1998. In vivo and *in vitro* modulation of immune stimulatory capacity of primary dendritic cells by adenovirus-mediated gene transduction. *Exp Clin Immunogenet* 15:100.
193. Lee, W.-C., C. Zhong, S. Qian, Y. Wan, J. Gauldie, Z. Mi, P. D. Robbins, A. W. Thomson, and L. Lu. 1998. Phenotype, function, and *in vivo* migration and survival of allogeneic dendritic cell progenitors genetically engineered to express TGF- β . *Transplantation* 66:1810.
194. Kohka, H., H. Iwagaki, T. Yoshino, K. Kobashi, N. Urushihara, T. Yagi, T. Tanimoto, M. Kurimoto, T. Akagi, and N. Tanaka. 1999. Involvement of interleukin-18 (IL-18) in mixed lymphocyte reactions (MLR). *J Interferon Cytokine Res* 19:1053.
195. Redpath, S., A. Angulo, N. R. Gascoigne, and P. Ghazal. 1999. Murine cytomegalovirus infection down-regulates MHC class II expression on macrophages by induction of IL-10. *J Immunol* 162:6701.
196. Gabilovich, D. I., S. Patterson, J. J. Harvey, G. M. Woods, W. Elsley, and S. C. Knight. 1994. Murine retrovirus induces defects in the function of dendritic cells at early stages of infection. *Cell Immunol* 158:167.

197. Fugier-Vivier, I., C. Servet-Delprat, P. Rivaller, M.-C. Rissoan, Y.-J. Liu, and C. Roubourdin-Combe. 1997. Measles virus suppresses cell-mediated immunity by interfering with the survival and functions of dendritic and T cells. *J Exp Med* 186:813.
198. Engelmayer, J., M. Larsson, M. Subklewe, A. Chahroudi, W. I. Cox, R. M. Steinman, and N. Bhardwaj. 1999. Vaccinia virus inhibits the maturation of human dendritic cells: a novel mechanism of immune evasion. *J Immunol* 163:6762.
199. Salio, M., M. Cella, M. Suter, and A. Lanzavecchia. 1999. Inhibition of dendritic cell maturation by herpes simplex virus. *Eur J Immunol* 29:3245.
200. Bejarano, M. T., R. de Waal Malefyt, J. S. Abrams, M. Bigler, R. Bacchetta, J. E. de Vries, and M. G. Roncarolo. 1992. Interleukin 10 inhibits allogeneic proliferative and cytotoxic T cell responses generated in primary mixed lymphocyte cultures. *Int Immunol* 4:1389.
201. Liu, H. S., M. S. Jan, C. K. Chou, P. H. Chen, and N. J. Ke. 1999. Is green fluorescent protein toxic to the living cells? *Biochem Biophys Res Commun* 260:712.
202. Abdi, K., and S. H. Herrmann. 1997. CTL generation in the presence of IL-4 is inhibited by free p40: evidence for early and late IL-12 function. *J Immunol* 159:3148.
203. Patrick, G. M. 1998. Studies of cytokines in alloimmune responses. *Ph.D. Thesis*.
204. Shultz, L. D., P. A. Schweitzer, S. W. Christianson, B. Gott, I. B. Schweitzer, B. Tennent, S. McKenna, L. Mobraaten, T. V. Rajan, D. L. Greiner, and E. H. Leiter. 1995. Multiple defects in innate and adaptive immunologic function in NOD/LtSz-*scid* mice. *J Immunol* 154:180.

205. Coates, T., R. Krishnan, S. Kireta, J. Johnston, and G. R. Russ. 1999. Human myeloid dendritic cells transfected with an adenoviral interleukin 10 gene construct inhibit human skin graft rejection in a chimeric human-NOD/SCID mouse transplant model. *Immunol Cell Biol* 77:3, A11.
206. Brody, E., and J. Abelson. 1985. The "spliceosome": yeast pre-messenger RNA associates with a 40S complex in a splicing-dependent reaction. *Science* 228:963.
207. Will, C. L., and R. Lührmann. 1997. Protein functions in pre-mRNA splicing. *Curr Opin Cell Biol* 9:320.
208. Breathnach, R., C. Benoist, K. O'Hare, F. Gannon, and P. Chambon. 1978. Ovalbumin gene: evidence for a leader sequence in mRNA and DNA sequences at the exon-intron boundaries. *Proc Natl Acad Sci USA* 75:4853.
209. Legrain, P., and G. Chanfreau. 1994. Pre-mRNA splicing: from intron recognition to catalysis. *Bull Inst Pasteur* 92:153.
210. Jackson, I. J. 1991. A reappraisal of non-consensus mRNA splice sites. *Nucleic Acids Res* 19:3795.
211. Ruskin, B., J. M. Greene, and M. R. Green. 1985. Cryptic branch point activation allows accurate *in vitro* splicing of human β -globin intron mutants. *Cell* 41:833.
212. Reed, R., and T. Maniatis. 1985. Intron sequences involved in lariat formation during pre-mRNA splicing. *Cell* 41:95.
213. Mount, S. M. 1982. A catalogue of splice junction sequences. *Nucleic Acids Res* 10:459.
214. Green, M. R. 1991. Biochemical mechanisms of constitutive and regulated pre-mRNA splicing. *Annu Rev Cell Biol* 7:559.

215. Padgett, R. A., M. M. Konarska, P. J. Grabowski, S. F. Hardy, and P. A. Sharp. 1984. Lariat RNA's as intermediates and products in the splicing of messenger RNA precursors. *Science* 225:898.
216. Hamm, J., and I. W. Mattaj. 1990. Monomethylated cap structures facilitate RNA export from the nucleus. *Cell* 63:109.
217. Wickens, M. P., and J. B. Gurdon. 1983. Post-transcriptional processing of simian virus 40 late transcripts in injected frog oocytes. *J Mol Biol* 163:1.
218. Huang, S., T. J. Deerinck, M. H. Ellisman, and D. L. Spector. 1994. *In vivo* analysis of the stability and transport of nuclear poly(A)⁺ RNA. *J Cell Biol* 126:877.
219. Luo, M.-J., and R. Reed. 1999. Splicing is required for rapid and efficient mRNA export in metazoans. *Proc Natl Acad Sci USA* 96:14937.
220. Southby, J., C. Gooding, and C. W. Smith. 1999. Polypyrimidine tract binding protein functions as a repressor to regulate alternative splicing of α -actinin mutually exclusive exons. *Mol Cell Biol* 19:2699.
221. Porter, S., and B. Mintz. 1991. Multiple alternatively spliced transcripts of the mouse tyrosinase-encoding gene. *Gene* 97:277.
222. Riegman, P. H., R. J. Vlietstra, J. A. Van Der Korput, J. C. Romijn, and J. Trapman. 1989. Characterization of the prostate-specific antigen gene: a novel human kallikrein-like gene. *Biochem Biophys Res Commun* 159:95.
223. Okano, K., H. Heng, S. Trevisanato, M. Tyers, and S. Varmuza. 1997. Genomic organization and functional analysis of the murine protein phosphatase 1c γ (*Ppp1cc*) gene. *Genomics* 45:211.

224. Dytrych, L., D. L. Sherman, C. S. Gillespie, and P. J. Brophy. 1998. Two PDZ domain proteins encoded by the murine periaxin gene are the result of alternative intron retention and are differentially targeted in Schwann cells. *J Biol Chem* 273:5794.
225. Ebihara, K., Y. Masuhiro, T. Kitamoto, M. Suzawa, Y. Uematsu, T. Yoshizawa, T. Ono, H. Harada, K. Matsuda, T. Hasegawa, S. Masushige, and S. Kato. 1996. Intron retention generates a novel isoform of the murine vitamin D receptor that acts in a dominant negative way on the vitamin D signaling pathway. *Mol Cell Biol* 16:3393.
226. Yoshida, K., J. Bolodeoku, T. Sugino, S. Goodison, Y. Matsumura, B. F. Warren, T. Toge, E. Tahara, and D. Tarin. 1995. Abnormal retention of intron 9 in CD44 gene transcripts in human gastrointestinal tumors. *Cancer Res* 55:4273.
227. Stickeler, E., V. J. Möbus, D. G. Kieback, P. Kohlberger, I. B. Runnebaum, and R. Kreienberg. 1997. Intron 9 retention in gene transcripts suggests involvement of CD44 in the tumorigenesis of ovarian cancer. *Anticancer Res* 17:4395.
228. Robbins, P. F., M. El-Gamil, Y. F. Li, E. B. Fitzgerald, Y. Kawakami, and S. A. Rosenberg. 1997. The intronic region of an incompletely spliced *gp100* gene transcript encodes an epitope recognized by melanoma-reactive tumor-infiltrating lymphocytes. *J Immunol* 159:303.
229. Lupetti, R., P. Pisarra, A. Verrecchia, C. Farina, G. Nicolini, A. Anichini, C. Bordignon, M. Sensi, G. Parmiani, and C. Traversari. 1998. Translation of a retained intron in tyrosinase-related protein (TRP) 2 mRNA generates a new cytotoxic T lymphocyte (CTL)-defined and shared human melanoma antigen not expressed in normal cells of the melanocytic lineage. *J Exp Med* 188:1005.

230. Hampson, R., and F. M. Rottman. 1987. Alternative processing of bovine growth hormone mRNA: nonsplicing of the final intron predicts a high molecular weight variant of bovine growth hormone. *Proc Natl Acad Sci USA* 84:2673.
231. Hampson, R. K., L. La Follette, and F. M. Rottman. 1989. Alternative processing of bovine growth hormone mRNA is influenced by downstream exon sequences. *Mol Cell Biol* 9:1604.
232. Sun, Q., R. K. Hampson, and F. M. Rottman. 1993. *In vitro* analysis of bovine growth hormone pre-mRNA alternative splicing. Involvement of exon sequences and trans-acting factor(s). *J Biol Chem* 268:15659.
233. Sun, Q., A. Mayeda, R. K. Hampson, A. R. Krainer, and F. M. Rottman. 1993. General splicing factor SF2/ASF promotes alternative splicing by binding to an exonic splicing enhancer. *Genes Dev* 7:2598.
234. Dirksen, W. P., R. K. Hampson, Q. Sun, and F. M. Rottman. 1994. A purine-rich exon sequence enhances alternative splicing of bovine growth hormone pre-mRNA. *J Biol Chem* 269:6431.
235. Dirksen, W. P., Q. Sun, and F. M. Rottman. 1995. Multiple splicing signals control alternative intron retention of bovine growth hormone pre-mRNA. *J Biol Chem* 270:5346.
236. Hoshijima, K., K. Inoue, I. Higuchi, H. Sakamoto, and Y. Shimura. 1991. Control of *doublesex* alternative splicing by *transformer* and *transformer-2* in *Drosophila*. *Science* 252:833.
237. Corpet, F. 1988. Multiple sequence alignment with hierarchical clustering. *Nucleic Acids Res* 16:10881.
238. Sharp, P. A. 1994. Split genes and RNA splicing. *Cell* 77:805.

239. Shapiro, M. B., and P. Senapathy. 1987. RNA splice junctions of different classes of eukaryotes: sequence statistics and functional implications in gene expression. *Nucleic Acids Res* 15:7155.
240. Roscigno, R. F., M. Weiner, and M. A. Garcia-Blanco. 1993. A mutational analysis of the polypyrimidine tract of introns. Effects of sequence differences in pyrimidine tracts on splicing. *J Biol Chem* 268:11222.
241. Hornig, H., M. Aebi, and C. Weissmann. 1986. Effect of mutations at the lariat branch acceptor site on β -globin pre-mRNA splicing *in vitro*. *Nature* 324:589.
242. Wu, J., and J. L. Manley. 1989. Mammalian pre-mRNA branch site selection by U2 snRNP involves base pairing. *Genes Dev* 3:1553.
243. Reed, R., and T. Maniatis. 1988. The role of the mammalian branchpoint sequence in pre-mRNA splicing. *Genes Dev* 2:1268.
244. Fuqua, S. A., S. D. Fitzgerald, and W. L. McGuire. 1990. A simple polymerase chain reaction method for detection and cloning of low-abundance transcripts. *BioTechniques* 9:206.
245. Gordon, D. F., D. P. Quick, C. R. Erwin, J. E. Donelson, and R. A. Maurer. 1983. Nucleotide sequence of the bovine growth hormone chromosomal gene. *Mol Cell Endocrinol* 33:81.
246. Naumann, M., and C. Scheidereit. 1994. Activation of NF- κ B *in vivo* is regulated by multiple phosphorylations. *EMBO J* 13:4597.
247. Landschulz, W. H., P. F. Johnson, and S. L. McKnight. 1988. The leucine zipper: a hypothetical structure common to a new class of DNA binding proteins. *Science* 240:1759.

248. O'Shea, E. K., R. Rutkowski, and P. S. Kim. 1989. Evidence that the leucine zipper is a coiled coil. *Science* 243:538.
249. Landschulz, W. H., P. F. Johnson, and S. L. McKnight. 1989. The DNA binding domain of the rat liver nuclear protein C/EBP is bipartite. *Science* 243:1681.
250. Gentz, R., F. J. Rauscher III, C. Abate, and T. Curran. 1989. Parallel association of Fos and Jun leucine zippers juxtaposes DNA binding domains. *Science* 243:1695.
251. Hartmuth, K., and A. Barta. 1988. Unusual branch point selection in processing of human growth hormone pre-mRNA. *Mol Cell Biol* 8:2011.
252. Coolidge, C. J., R. J. Seely, and J. G. Patton. 1997. Functional analysis of the polypyrimidine tract in pre-mRNA splicing. *Nucleic Acids Res* 25:888.
253. Robberson, B. L., G. J. Cote, and S. M. Berget. 1990. Exon definition may facilitate splice site selection in RNAs with multiple exons. *Mol Cell Biol* 10:84.
254. Talerico, M., and S. M. Berget. 1994. Intron definition in splicing of small *Drosophila* introns. *Mol Cell Biol* 14:3434.
255. Dominski, Z., and R. Kole. 1991. Selection of splice sites in pre-mRNAs with short internal exons. *Mol Cell Biol* 11:6075.
256. Hawkins, J. D. 1988. A survey on intron and exon lengths. *Nucleic Acids Res* 16:9893.
257. Lieschke, G. J., P. K. Rao, M. K. Gately, and R. C. Mulligan. 1997. Bioactive murine and human interleukin-12 fusion proteins which retain antitumour activity *in vivo*. *Nat Biotech* 15:35.

258. Shimomura, O., F. H. Johnson, and Y. Saiga. 1962. Extraction, purification and properties of aequorin, a bioluminescent protein from the luminous hydromedusan, *Aequorea*. *J Cell Comp Physiol* 59:223.
259. Cormack, B. P., R. H. Valdivia, and S. Falkow. 1996. FACS-optimized mutants of the green fluorescent protein (GFP). *Gene* 173:33.
260. Hanazono, Y., J.-M. Yu, C. E. Dunbar, and R. V. Emmons. 1997. Green fluorescent protein retroviral vectors: low titer and high recombination frequency suggest a selective disadvantage. *Hum Gene Ther* 8:1313.
261. Gubin, A. N., S. Koduru, J. M. Njoroge, R. Bhatnagar, and J. L. Miller. 1999. Stable expression of green fluorescent protein after liposomal transfection of K562 cells without selective growth conditions. *BioTechniques* 27:1162.
262. Gubin, A. N., B. Reddy, J. M. Njoroge, and J. L. Miller. 1997. Long-term, stable expression of green fluorescent protein in mammalian cells. *Biochem Biophys Res Commun* 236:347.
263. Fan, X., V. Sibalic, E. Niederer, and R. P. Wüthrich. 1996. The proinflammatory cytokine interleukin-12 occurs as a cell membrane-bound form on macrophages. *Biochem Biophys Res Commun* 225:1063.
264. Li, W., F. Fu, L. Lu, S. K. Narula, J. J. Fung, A. W. Thomson, and S. Qian. 1999. Recipient pretreatment with mammalian IL-10 prolongs mouse cardiac allograft survival by inhibition of anti-donor T cell responses. *Transplant Proc* 31:115.
265. He, X. Y., J. Chen, N. Verma, K. Plain, G. Tran, and B. M. Hall. 1998. Treatment with interleukin-4 prolongs allogeneic neonatal heart graft survival by inducing T helper 2 responses. *Transplantation* 65:1145.

266. Qian, S., W. Li, Y. Li, F. Fu, L. Lu, J. J. Fung, and A. W. Thomson. 1996. Systemic administration of cellular interleukin-10 can exacerbate cardiac allograft rejection in mice. *Transplantation* 62:1709.
267. Takeuchi, T., T. Ueki, S. Sunaga, K. Ikuta, Y. Sasaki, B. Li, N. Moriyama, J. Miyazaki, and K. Kawabe. 1997. Murine interleukin 4 transgenic heart allograft survival prolonged with down-regulation of the Th1 cytokine mRNA in grafts. *Transplantation* 64:152.
268. Vieira, P., R. de Waal-Malefyt, M. N. Dang, K. E. Johnson, R. Kastelein, D. F. Fiorentino, J. E. deVries, M.-G. Roncarolo, T. R. Mosmann, and K. W. Moore. 1991. Isolation and expression of human cytokine synthesis inhibitory factor cDNA clones: homology to Epstein-Barr virus open reading frame BCRFI. *Proc Natl Acad Sci USA* 88:1172.
269. Moore, K. W., P. Vieira, D. F. Fiorentino, M. L. Trounstein, T. A. Khan, and T. R. Mosmann. 1990. Homology of cytokine synthesis inhibitory factor (IL-10) to the Epstein-Barr virus gene BCRFI. *Science* 248:1230. [Published erratum appears in *Science* 1990, 250:494].
270. Brauner, R., M. Nonoyama, H. Laks, D. C. Drinkwater, Jr., S. McCaffery, T. Drake, A. J. Berk, L. Sen, and L. Wu. 1997. Intracoronary adenovirus-mediated transfer of immunosuppressive cytokine genes prolongs allograft survival. *J Thorac Cardiovasc Surg* 114:923.
271. Qin, L., K. D. Chavin, Y. Ding, J. P. Favaro, J. E. Woodward, J. Lin, H. Tahara, P. Robbins, A. Shaked, D. Y. Ho, R. M. Sapolsky, M. T. Lotze, and J. S. Bromberg. 1995. Multiple vectors effectively achieve gene transfer in a murine cardiac transplantation model. Immunosuppression with TGF- β 1 or vIL-10. *Transplantation* 59:809.

272. Qin, L., K. D. Chavin, Y. Ding, H. Tahara, J. P. Favaro, J. E. Woodward, T. Suzuki, P. D. Robbins, M. T. Lotze, and J. S. Bromberg. 1996. Retrovirus-mediated transfer of viral IL-10 gene prolongs murine cardiac allograft survival. *J Immunol* 156:2316.
273. Krämer, A. 1996. The structure and function of proteins involved in mammalian pre-mRNA splicing. *Annu Rev Biochem* 65:367.
274. Bringmann, P., J. Rinke, B. Appel, R. Reuter, and R. Lührmann. 1983. Purification of snRNPs U1, U2, U4, U5 and U6 with 2,2,7-trimethylguanosine-specific antibody and definition of their constituent proteins reacting with anti-Sm and anti-(U1)RNP antisera. *EMBO J* 2:1129.
275. Madhani, H. D., and C. Guthrie. 1994. Dynamic RNA-RNA interactions in the spliceosome. *Annu Rev Genet* 28:1.
276. Friendewey, D., and W. Keller. 1985. Stepwise assembly of a pre-mRNA splicing complex requires U-snRNPs and specific intron sequences. *Cell* 42:355.
277. Lerner, M. R., J. A. Boyle, S. M. Mount, S. L. Wolin, and J. A. Steitz. 1980. Are snRNPs involved in splicing? *Nature* 283:220.
278. Rogers, J., and R. Wall. 1980. A mechanism for RNA splicing. *Proc Natl Acad Sci USA* 77:1877.
279. Zhuang, Y., and A. M. Weiner. 1986. A compensatory base change in U1 snRNA suppresses a 5' splice site mutation. *Cell* 46:827.
280. Krämer, A., W. Keller, B. Appel, and R. Lührmann. 1984. The 5' terminus of the RNA moiety of U1 small nuclear ribonucleoprotein particles is required for the splicing of messenger RNA precursors. *Cell* 38:299.

281. Black, D. L., B. Chabot, and J. A. Steitz. 1985. U2 as well as U1 small nuclear ribonucleoproteins are involved in premessenger RNA splicing. *Cell* 42:737.
282. Bindereif, A., and M. R. Green. 1987. An ordered pathway of snRNP binding during mammalian pre-mRNA splicing complex assembly. *EMBO J* 6:2415.
283. Patton, J. R., and T. Pederson. 1988. The Mr 70,000 protein of the U1 small nuclear ribonucleoprotein particle binds to the 5' stem-loop of U1 RNA and interacts with Sm domain proteins. *Proc Natl Acad Sci USA* 85:747.
284. Keller, E. B., and W. A. Noon. 1984. Intron splicing: a conserved internal signal in introns of animal pre-mRNAs. *Proc Natl Acad Sci USA* 81:7417.
285. Barabino, S. M., B. J. Blencowe, U. Ryder, B. S. Sproat, and A. I. Lamond. 1990. Targeted snRNP depletion reveals an additional role for mammalian U1 snRNP in spliceosome assembly. *Cell* 63:293.
286. Ruskin, B., P. D. Zamore, and M. R. Green. 1988. A factor, U2AF, is required for U2 snRNP binding and splicing complex assembly. *Cell* 52:207.
287. Zhuang, Y. A., A. M. Goldstein, and A. M. Weiner. 1989. UACUAAC is the preferred branch site for mammalian mRNA splicing. *Proc Natl Acad Sci USA* 86:2752.
288. Query, C. C., M. J. Moore, and P. A. Sharp. 1994. Branch nucleophile selection in pre-mRNA splicing: evidence for the bulged duplex model. *Genes Dev* 8:587.
289. Konarska, M. M., and P. A. Sharp. 1987. Interactions between small nuclear ribonucleoprotein particles in formation of spliceosomes. *Cell* 49:763.
290. Brow, D. A., and C. Guthrie. 1988. Spliceosomal RNA U6 is remarkably conserved from yeast to mammals. *Nature* 334:213.

291. Hashimoto, C., and J. A. Steitz. 1984. U4 and U6 RNAs coexist in a single small nuclear ribonucleoprotein particle. *Nucleic Acids Res* 12:3283.
292. Rinke, J., B. Appel, M. Digweed, and R. Lührmann. 1985. Localization of a base-paired interaction between small nuclear RNAs U4 and U6 in intact U4/U6 ribonucleoprotein particles by psoralen cross-linking. *J Mol Biol* 185:721.
293. Yean, S. L., and R.-J. Lin. 1991. U4 small nuclear RNA dissociates from a yeast spliceosome and does not participate in the subsequent splicing reaction. *Mol Cell Biol* 11:5571.
294. Blencowe, B. J., B. S. Sproat, U. Ryder, S. Barabino, and A. I. Lamond. 1989. Antisense probing of the human U4/U6 snRNP with biotinylated 2'-OMe RNA oligonucleotides. *Cell* 59:531.
295. Lamond, A. I., M. M. Konarska, P. J. Grabowski, and P. A. Sharp. 1988. Spliceosome assembly involves the binding and release of U4 small nuclear ribonucleoprotein. *Proc Natl Acad Sci USA* 85:411.
296. Sontheimer, E. J., and J. A. Steitz. 1993. The U5 and U6 small nuclear RNAs as active site components of the spliceosome. *Science* 262:1989. [Published erratum appears in *Science* 1994, 263:739].
297. Patterson, B., and C. Guthrie. 1987. An essential yeast snRNA with a U5-like domain is required for splicing *in vivo*. *Cell* 49:613.
298. Newman, A. J., and C. Norman. 1992. U5 snRNA interacts with exon sequences at 5' and 3' splice sites. *Cell* 68:743.
299. Wyatt, J. R., E. J. Sontheimer, and J. A. Steitz. 1992. Site-specific cross-linking of mammalian U5 snRNP to the 5' splice site before the first step of pre-mRNA splicing. *Genes Dev* 6:2542.

300. Newman, A. J. 1997. The role of U5 snRNP in pre-mRNA splicing. *EMBO J* 16:5797.
301. Ast, G., and A. M. Weiner. 1997. A novel U1/U5 interaction indicates proximity between U1 and U5 snRNAs during an early step of mRNA splicing. *RNA* 3:371.
302. Konforti, B. B., M. J. Koziolkiewicz, and M. M. Konarska. 1993. Disruption of base pairing between the 5' splice site and the 5' end of U1 snRNA is required for spliceosome assembly. *Cell* 75:863.
303. Staley, J. P., and C. Guthrie. 1999. An RNA switch at the 5' splice site requires ATP and the DEAD box protein Prp28p. *Mol Cell* 3:55.
304. Madhani, H. D., and C. Guthrie. 1992. A novel base-pairing interaction between U2 and U6 snRNAs suggests a mechanism for the catalytic activation of the spliceosome. *Cell* 71:803.
305. Sittler, A., H. Gallinaro, L. Kister, and M. Jacob. 1987. *In-vivo* degradation pathway of an excised intervening sequence. *J Mol Biol* 197:737.
306. Krainer, A. R., A. Mayeda, D. Kozak, and G. Binns. 1991. Functional expression of cloned human splicing factor SF2: homology to RNA-binding proteins, U1 70K, and *Drosophila* splicing regulators. *Cell* 66:383.
307. Fu, X.-D., and T. Maniatis. 1990. Factor required for mammalian spliceosome assembly is localized to discrete regions in the nucleus. *Nature* 343:437.
308. Theissen, H., M. Etzerodt, R. Reuter, C. Schneider, F. Lottspeich, P. Argos, R. Lührmann, and L. Philipson. 1986. Cloning of the human cDNA for the U1 RNA-associated 70K protein. *EMBO J* 5:3209.

309. Query, C. C., R. C. Bentley, and J. D. Keene. 1989. A common RNA recognition motif identified within a defined U1 RNA binding domain of the 70K U1 snRNP protein. *Cell* 57:89.
310. Zamore, P. D., and M. R. Green. 1989. Identification, purification, and biochemical characterization of U2 small nuclear ribonucleoprotein auxiliary factor. *Proc Natl Acad Sci USA* 86:9243.
311. Zamore, P. D., J. G. Patton, and M. R. Green. 1992. Cloning and domain structure of the mammalian splicing factor U2AF. *Nature* 355:609.
312. Zhang, M., P. D. Zamore, M. Carmo-Fonseca, A. I. Lamond, and M. R. Green. 1992. Cloning and intracellular localization of the U2 small nuclear ribonucleoprotein auxiliary factor small subunit. *Proc Natl Acad Sci USA* 89:8769.
313. Birney, E., S. Kumar, and A. R. Krainer. 1993. Analysis of the RNA-recognition motif and RS and RGG domains: conservation in metazoan pre-mRNA splicing factors. *Nucleic Acids Res* 21:5803.
314. Zahler, A. M., W. S. Lane, J. A. Stolk, and M. B. Roth. 1992. SR proteins: a conserved family of pre-mRNA splicing factors. *Genes Dev* 6:837.
315. Chandler, S. D., A. Mayeda, J. M. Yeakley, A. R. Krainer, and X.-D. Fu. 1997. RNA splicing specificity determined by the coordinated action of RNA recognition motifs in SR proteins. *Proc Natl Acad Sci USA* 94:3596.
316. Fu, X.-D. 1993. Specific commitment of different pre-mRNAs to splicing by single SR proteins. *Nature* 365:82.
317. Staknis, D., and R. Reed. 1994. SR proteins promote the first specific recognition of pre-mRNA and are present together with the U1 small nuclear ribonucleoprotein particle in a general splicing enhancer complex. *Mol Cell Biol* 14:7670.

318. Eperon, I. C., D. C. Ireland, R. A. Smith, A. Mayeda, and A. R. Krainer. 1993. Pathways for selection of 5' splice sites by U1 snRNPs and SF2/ASF. *EMBO J* 12:3607.
319. Hoffman, B. E., and P. J. Grabowski. 1992. U1 snRNP targets an essential splicing factor, U2AF65, to the 3' splice site by a network of interactions spanning the exon. *Genes Dev* 6:2554.
320. Valcárcel, J., R. K. Gaur, R. Singh, and M. R. Green. 1996. Interaction of U2AF65 RS region with pre-mRNA branch point and promotion of base pairing with U2 snRNA *Science* 273:1706. [Published erratum appears in *Science* 1996 274:21].
321. Roscigno, R. F., and M. A. Garcia-Blanco. 1995. SR proteins escort the U4/U6.U5 tri-snRNP to the spliceosome. *RNA* 1:692.
322. Mayeda, A., D. M. Helfman, and A. R. Krainer. 1993. Modulation of exon skipping and inclusion by heterogeneous nuclear ribonucleoprotein A1 and pre-mRNA splicing factor SF2/ASF *Mol Cell Biol* 13:2993. [Published erratum appears in *Mol Cell Biol* 1993 13:4458].
323. Swanson, M. S., and G. Dreyfuss. 1988. RNA binding specificity of hnRNP proteins: a subset bind to the 3' end of introns. *EMBO J* 7:3519.
324. Piñol-Roma, S., Y. D. Choi, M. J. Matunis, and G. Dreyfuss. 1988. Immunopurification of heterogeneous nuclear ribonucleoprotein particles reveals an assortment of RNA-binding proteins *Genes Dev* 2:215. [Published erratum appears in *Genes Dev* 1988, 2:490].
325. Gil, A., P. A. Sharp, S. F. Jamison, and M. A. Garcia-Blanco. 1991. Characterization of cDNAs encoding the polypyrimidine tract-binding protein. *Genes Dev* 5:1224.

326. Patton, J. G., S. A. Mayer, P. Tempst, and B. Nadal-Ginard. 1991. Characterization and molecular cloning of polypyrimidine tract-binding protein: a component of a complex necessary for pre-mRNA splicing. *Genes Dev* 5:1237.
327. Mullen, M. P., C. W. Smith, J. G. Patton, and B. Nadal-Ginard. 1991. α -tropomyosin mutually exclusive exon selection: competition between branchpoint/polypyrimidine tracts determines default exon choice. *Genes Dev* 5:642.
328. Reed, R. 1996. Initial splice-site recognition and pairing during pre-mRNA splicing. *Curr Opin Genet Dev* 6:215.
329. Berget, S. M. 1995. Exon recognition in vertebrate splicing. *J Biol Chem* 270:2411.
330. Talerico, M., and S. M. Berget. 1990. Effect of 5' splice site mutations on splicing of the preceding intron. *Mol Cell Biol* 10:6299.
331. Nakai, K., and H. Sakamoto. 1994. Construction of a novel database containing aberrant splicing mutations of mammalian genes. *Gene* 141:171.
332. Dominski, Z., and R. Kole. 1992. Cooperation of pre-mRNA sequence elements in splice site selection. *Mol Cell Biol* 12:2108.
333. Black, D. L. 1991. Does steric interference between splice sites block the splicing of a short *c-src* neuron-specific exon in non-neuronal cells? *Genes Dev* 5:389.
334. Black, D. L. 1992. Activation of *c-src* neuron-specific splicing by an unusual RNA element *in vivo* and *in vitro*. *Cell* 69:795.
335. Shatkin, A. J. 1976. Capping of eucaryotic mRNAs. *Cell* 9:645.

336. Ohno, M., H. Sakamoto, and Y. Shimura. 1987. Preferential excision of the 5' proximal intron from mRNA precursors with two introns as mediated by the cap structure. *Proc Natl Acad Sci USA* 84:5187.
337. Niwa, M., S. D. Rose, and S. M. Berget. 1990. *In vitro* polyadenylation is stimulated by the presence of an upstream intron. *Genes Dev* 4:1552.
338. Niwa, M., and S. M. Berget. 1991. Mutation of the AAUAAA polyadenylation signal depresses *in vitro* splicing of proximal but not distal introns. *Genes Dev* 5:2086.

Amendments

Page 34, Line 24 – “resulting a” to read “resulting in a”

Page 58, s10g Culture Medium; Page 73, Line 24; Page 74, Line 2 – L-glutamine final concentration is 2 mM. Manufacturer is cited on Page 50, Line 14.

Page 59, 2X Laemmli Sample Buffer, and Page 74, Line 3 - 10X Protease Inhibitor consists of AEBSF: 4 mg/ml, EDTA-Na₂: 10 mg/ml, Leupeptin: 10 µg/ml, Pepstatin A: 10 µg/ml.

Page 62, Line 10 – 13,000 rpm \equiv 12,000 x g

Section 2.3.3 – Modified from manufacturers instructions.

Page 64, Line 3 – “Main laboratory” refers to a different room in which the cDNA/gDNA was added to prevent nucleic acid contamination of reagents.

Page 64, Line 26 – “Main laboratory” refers to a different room in which the cDNA/gDNA was added to prevent nucleic acid contamination of reagents.

Section 2.3.4 – Modified from manufacturers instructions.

Section 2.3.5 – Modified from manufacturers instructions.

Page 66, Line 24 – “re-dissolving” to read “re-melting”

Page 67, Line 9 – “according instructions” to read “according to the instructions”

Page 67, Line 22 – “Main laboratory” refers to a different room in which the cDNA/gDNA was added to prevent nucleic acid contamination of reagents.

Section 2.3.8 – Modified from manufacturers instructions.

Page 68, Line 1 – “PC2” refers to a different room in which all PCR product and plasmid manipulations were performed to prevent nucleic acid contamination of reagents.

Section 2.3.10 to 2.3.12 – Modified from “Molecular cloning: a laboratory manual” J. Sambrook, E.F. Fritsch, T. Maniatis, 2nd Edition. Cold Spring Harbor, N.Y. Cold Spring Harbor Laboratory Press, 1989.

Page 69, Line 9 – 5000 rpm \equiv 3000 x g

Page 69, Line 24 – “before exposed” to read “before being exposed”

Page 71, Line 10 – 13,000 rpm \equiv 12,000 x g

Section 2.3.13 – Modified from manufacturers instructions

Section 2.3.14 – Conditions determined within the laboratory

Page 72, Line 3 – 13,000 rpm \equiv 12,000 x g

Page 72, Line 25 – 13,000 rpm \equiv 12,000 x g

Page 73, Line 15 – “The cells were aspirated from the cuvettes gently” to read “The cells were gently aspirated from the cuvettes”

Section 2.3.15 – Method modified from “Evolutionary conservation of the biochemical properties of p53: Specific interaction of *Xenopus laevis* p53 with Simian Virus 40 large T antigen and mammalian heat shock protein 70” T. Soussi, C. C. de Fromentel, H. W. Stürzbecher, S. Ullrich, J. Jenkins and P. May. 1989. *J. Virol.* 63:3894-901.

Page 74, Line 14 – 6,500 rpm \equiv 3000 x g

Page 75, Line 20 – 600 rpm \equiv 70 x g

Page 75, Line 20 – 1000 rpm \equiv 200 x g

Page 75, Line 23 – 2000 rpm \equiv 800 x g

Page 75, Line 24 – 2400 rpm \equiv 1100 x g

Page 75 Line 25/Page 76, Line 1 – 1800 rpm \equiv 650 x g

Page 76, Line 2 – 1800 rpm \equiv 650 x g

Page 93, Line 14 – “after transplantation and characterised” to read “after transplantation and is characterised”

Page 97, Line 21 – “to for” to read “for”

Page 99, Line 24 – 1800 rpm \equiv 650 x g

Page 100 – With regard to the suggestion that the preparation of the human DCs is insufficiently clear, and the method not outlined or referenced. These details are already provided in the thesis in Section 4.4.1.

Page 100, Line 2 – 2500 rpm \equiv 1200 x g

Page 100, Line 16 – 1500 rpm \equiv 400 x g

Page 101, Line 10 – “into to” to read “into”

Page 102, Line 15 – 1500 rpm \equiv 400 x g

Page 103/104, Discussed Page 111 – The leukocyte subpopulations contaminating the metrizamide enriched ovine DC preparation were not defined. As such the degree of contamination was not calculated. This observation was made by observation of cells other than those with the typical DC morphology.

Page 107 and Figure 4.7 – The reader is directed to Figure 4.2, which indicates the presence of the GFP gene in the pAdTrack-CMV plasmid. As such, when combined with pAdEasy-1, with or without the p40 gene, the resulting virus is capable of expressing the GFP protein. Figure 4.7 demonstrates fluorescence as due to the GFP protein in both vector blank and p40 transfected cells, and is not due to cell autofluorescence as suggested.

Figure 4.11, Line 7 – “no there” to read “there”

Page 115, Line 6 – An alternative possibility for the low level of CD80/CD86 expression on the ovine DCs may reflect poor recognition of the ovine costimulatory molecules as the CTLA4 is of murine origin.

Page 118, Line 2 – “graft survival is actually accelerated” to read “graft rejection is actually accelerated”

Page 126, Line 12 – 13,000 rpm \equiv 12,000 x g

Page 142, Line 21 - “upstream” to read “downstream”

Page 145, Line 22 - “with for” to read “for”